Peptidomimetic ligands for the tandem SH2 domain of Syk kinase

Joeri Kuil

Peptidomimetic ligands for the tandem SH2 domain of Syk kinase

Joeri Kuil

PhD thesis with summary in Dutch

Department of Medicinal Chemistry and Chemical Biology,
Utrecht University, Utrecht, The Netherlands

November 2009

ISBN: 978-90-902-4696-3

Cover design: Frouke Kuijer and Joeri Kuil

Printing: Ipskamp Drukkers

The research described in this thesis was financially supported by the Division of Chemical Sciences (CW) of The Netherlands Organisation for Scientific Research (NWO).

Peptidomimetic ligands for the tandem SH2 domain of Syk kinase

Peptidomimetische liganden voor het tandem SH2 domein van Syk kinase

(met samenvatting in het Nederlands)

Proefschrift

ter verkrijging van de graad van doctor
aan de Universiteit Utrecht
op gezag van de rector magnificus, prof. dr. J.C. Stoof,
ingevolge het besluit van het college voor promoties
in het openbaar te verdedigen
op woensdag 18 november 2009 des middags te 2.30 uur

door

Joeri Kuil

geboren op 28 november 1980, te Amersfoort

Promotor: Prof. dr. R.M.J. Liskamp

Co-promotor: Dr. N.J. de Mol

Contents

Chapter 1

General introduction

1. Protein tyrosine kinase Syk and its role in human pathologies

The Spleen tyrosine kinase (Syk) is a 72 kDa cytosolic protein.[1] It is a member of the non-receptor protein tyrosine kinases (PTKs) that associate with activated antigen receptors at the cytosolic side of the plasma membrane. More than 10 families of non-receptor PTKs exist including the Src, Csk, Abl and Syk families. The Syk family consists of Syk and the closely related cytosolic 70 kDa zeta-associated protein (Zap-70). Syk and Zap-70 comprise two tandemly arranged SH2 domains (tSH2) in addition to a kinase domain. Syk is expressed in most hematopoietic cells such as basophiles, mast cells and lymphocytes.[2-4] In those cells Syk functions in immunoreceptor signaling events that mediate cellular processes such as proliferation, differentiation and phagocytosis. Syk is also widely expressed in non-hematopoietic cells like fibroblasts, epithelial cells, breast tissue, hepatocytes, neuronal cells and vascular endothelial cells.[3,4]

Because of its presence in a large variety of cell types, Syk is involved in many different diseases.[2,3] It plays a role in inflammatory and autoimmune disorders such as allergic rhinitis, asthma, rheumatoid arthritis, multiple sclerosis and systemic lupus erythematosus. Furthermore, Syk is also linked to leukemia and breast cancer, i.e. Syk is absent in malignant breast cancer cells.[2-4]

In this introducing chapter some background information is given on the studies described in this thesis. First, the role of Syk in immunoreceptor signaling cascades is described, after which SH2 domains are described in more detail. Then, the structure and function of Syk family kinases are reviewed and our hypothesis for the activation mechanism of Syk is introduced. Next, some reported Syk kinase inhibitors and tSH2 ligands are described and the approaches used for studying Syk are explained. Finally, the outline of this thesis is given.

2. The role of Syk in FcεRI-mediated mast cell degranulation

Syk plays a role in several signaling pathways, including B-cell receptor signaling, cell-cell adhesion and immunoreceptor signaling.[5-7] Here, the focus is on the high affinity IgE receptor (FcεRI) signaling pathway, in which Syk is essential. A schematic

overview of initial events after IgE receptor activation is given in Figure 1.[3,4,8-29] FcεRI is a multimeric cell-surface receptor that binds immunoglobulin E (IgE) with high affinity. The receptor consists of an α-, β- and two disulfide-linked γ-chains.[20,21,30] This tetrameric receptor is present in mast cells and basophils. A trimeric form, lacking the β-chain, is also found in human antigen presenting cells such as dendritic cells and macrophages.[21]

The Fc fragment of IgE binds to the extracellular domain of the α-chain of FcεRI. When the receptor-bound IgE is cross linked by antigen, FcεRI is stimulated. This stimulation occurs in cholesterol rich micro domains in the cell membrane, which are called lipid rafts.[31,32] After IgE and antigen mediated receptor aggregation, intercellular Immunoreceptor Tyrosine based Activation Motifs (ITAMs) on the β- and γ-chains are phosphorylated. The ITAM sequence consists of Tyr-Xxx-Xxx-(Leu/Ile)-$(Xxx)_{n=6-8}$-Tyr-Xxx-Xxx-(Leu/Ile), in which Xxx can be any amino acid.[33,34] The underlined residues comprise the binding epitopes for SH2 domains, when tyrosine is phosphorylated. The ITAM motif was first described by Reth in 1989 and in 1995 Cambier et al. introduced the name ITAM.[35,36] In FcεRI the β-ITAM (sequence: YEELHVYSPIYSAL) is not essential for activation of signaling events, but it amplifies the intensity of cell activation signals mediated by γ-ITAM.[37] The Src family kinases Lyn and Fyn bind through their SH2 domains to the FcεRI β-ITAM.[21] The γ-ITAM (sequence: YTGLNTRSQETYETL) functions as an autonomous activation module and is responsible for the primary onset of signal.[20,21,37]

After receptor stimulation, Lyn phosphorylates both the β-ITAM and the γ-ITAMs. Phosphorylation of both tyrosine residues in ITAM results in the recruitment of Syk to the diphosphorylated γ-ITAM (γ-dpITAM). Syk binds γ-ITAM with 18-fold higher affinity than β-ITAM, indicating the preference of Syk for γ-ITAM.[38] Phosphorylation of the ITAMs activates two complementary signaling pathways,[19-21] which both require Syk kinase activity (Figure 1).[25] Furthermore, permeabilized cells incubated with Syk lacking the kinase domain (i.e. tSH2) were unable to degranulate.[39]

The primary or principle signaling pathway is crucial for Ca^{2+} signaling and is initiated by ITAM-mediated Syk activation.[19-21] The divalent binding of Syk tSH2 to γ-dpITAM is necessary for Syk activation, since the localization of Syk in the lipid raft alone is not sufficient to generate or enhance signaling events.[10] ITAM binding leads to transphosphorylation of Syk by Lyn and Syk itself. In addition, autophosphorylation of the catalytic domain of Syk as well as autophosphorylation of its linker between tSH2

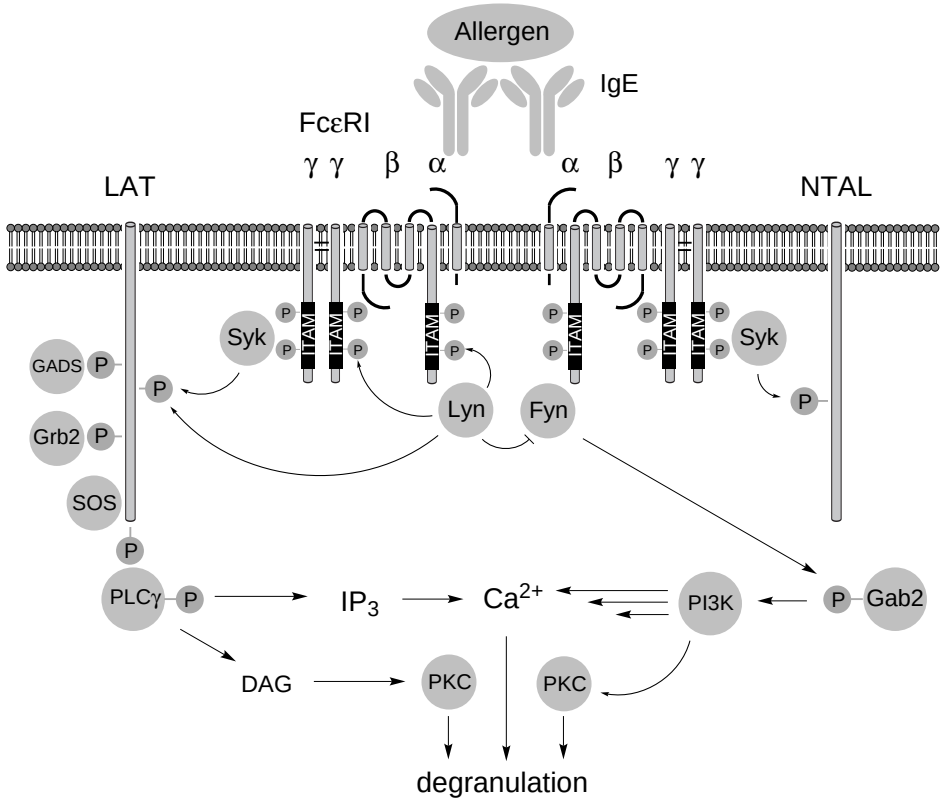

Figure 1. Simplified model of initial FcεRI signaling events. On the left side the Lyn-mediated primary pathway is shown and on the right side the Fyn-mediated complementary pathway. The grey circles represent cellular proteins and abbreviations without a circle represent small second messenger molecules. The dark grey circles labeled with 'P' represent pTyr.

and the kinase domain result in activation of the kinase domain.[20-22] Then a protein called 'linker for activation of T cells' (LAT) is phosphorylated by Syk, which leads to binding of SH2 domain containing proteins like Grb2, GADS, and PLCγ (Figure 1). Activated PLCγ generates diacylglycerol (DAG) and inositol-1,4,5-triphosphate (IP_3), which are responsible for degranulation through both PKC activation and an increase of the cytosolic calcium (Ca^{2+}) concentration.

In addition to this primary pathway, there is also a complementary pathway[19-21], which has a more direct effect on degranulation and is important for maintenance and/or amplification of the Ca^{2+} signal. Where in the primary pathway signaling is through Lyn, the complementary pathway is initiated by the Src-kinase Fyn. In Lyn deficient

cells, the Fyn mediated degranulation is substantially increased and Ca^{2+}-influx decreased (Figure 1).[21] The underlying mechanism is not clear yet. Also the complementary pathway requires Syk activation. As a result Syk phosphorylates a protein called 'non T cell activation linker' (NTAL) and Fyn phosphorylates the Grb2-associated binding protein 2 (Gab2). After several other steps, this cascade also leads to an increase of the cytosolic calcium (Ca^{2+}) concentration and cell degranulation.

Overstimulation of the FcεRI signaling cascades leads to allergic responses and is responsible for diseases like asthma and hay-fever.[26,27] The modulation and inhibition of this cascade could therefore be a good strategy for reducing the symptoms of allergic diseases.

3. SH2 domains in signal transduction

Syk is an intriguing example of how different structural domains cooperate within one protein. In fact, many proteins possess several domains and the cooperation and interaction of those domains can yield a great variety of functions.[40,41] Two major groups of domains are the catalytic – and the binding domains. Examples of binding domains are the Src homology-2 (SH2) domain [42,43] and the Src homology-3 (SH3) domain, which are named after the Src kinase. Src also possesses a kinase domain (SH1) and a membrane binding domain (SH4).[44-46] SH2 binds phosphotyrosine peptides and SH3 binds polyproline motifs.[47]

SH2 domains specifically function in protein tyrosine kinase (PTK) and protein tyrosine phosphatase (PTPase) pathways, due to their ability of binding to phosphorylated tyrosines.[43,48-58] SH2 domains consist of ~100 amino acid residues with two α-helixes and seven β-strands (their 3D structure is shown in Figure 2A). Eck et al. introduced a notation for these secondary structure elements which is in general use: βA-αA- βB-βC-βD-βE-βF-αB-βG.[59] The central β-sheet (Figure 2A) consists of three antiparallel strands (βD, βC and βB, augmented by βA and βG).[59] There are more than 100 different SH2 domains found in the human genome.

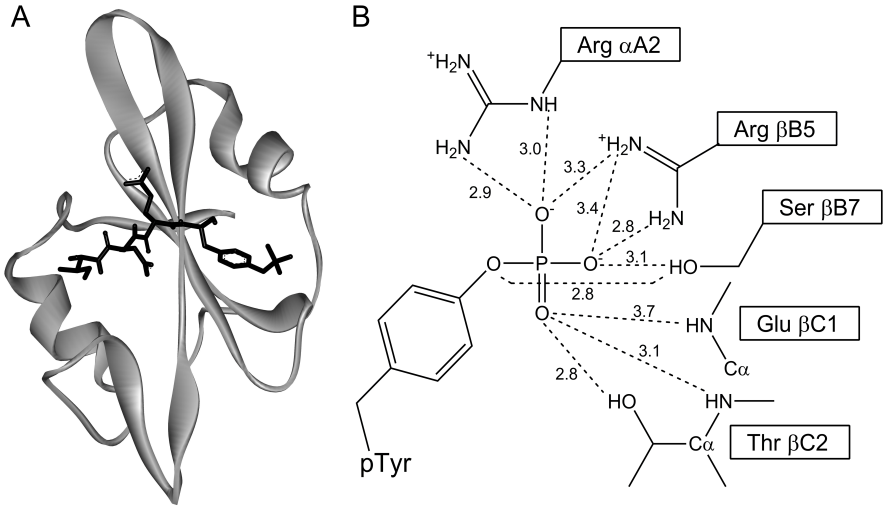

Figure 2. Crystal structure of the Src SH2 domain complexed with the pYEEI peptide (PDB entry code 1sps).[50] A: Ribbon diagram of the SH2 domain with the pYEEI ligand in black. On the left the specificity determining region is located and on the right is the phosphotyrosine (pTyr) binding region with the phosphorylated tyrosine in the centre. B: Schematic diagram showing all interactions of the phosphotyrosine residue with the Src-SH2 domain. Notation of the position of residues according to Eck.[59]

The binding of phosphotyrosine (pTyr) containing peptides to most SH2 domains is the result of binding to two key regions at each side of the central β-sheet (Figure 2A).[60,61] The first one is the 'pTyr binding region', which contributes substantially more to binding than interactions with the rest of the binding interface.[62,63] The pTyr residue is surrounded by a dense network of hydrogen bonds, in which a universally conserved arginine residue (βB5) has an ionic interaction with two oxygen atoms of the phosphate group (Figure 2B). Electrostatic interactions play an important role in pTyr binding, since the interaction affinity of the doubly negatively charged phosphate group and the SH2 domain is dependent on the salt concentration and pH.[64,65]

The second site of interaction is called the 'specificity determining region' (Figure 2A). Here the SH2 domain interacts with at least one of the amino acids located three to five residues C-terminal to pTyr in the interacting phosphopeptide. This part of an SH2 domain has the function to differentiate between various phosphopeptidic ligands. In the SH2 domains of the Src and Syk families hydrophobic residues like leucine and isoleucine in the ligand generally bind to the specificity determining region.

The function of SH2 domains is often relocalization of proteins, which is very important for PTK signal propagation, because many SH2 domain containing proteins can only be active at specific locations in the cell. Upon recruitment of an SH2 domain containing protein to a tyrosine phosphorylated protein, another domain within the SH2 domain containing protein, e.g. a kinase domain, is often activated.

Besides relocalization, pTyr – SH2 interactions play a role in internal regulation. An SH2 domain can bind to a phosphotyrosine in the same protein, whereby it regulates the activity of the protein. The SH2 domains of the Src and Abl kinases, for example, maintain their kinase domains in an inactive state by binding to a phosphorylated tyrosine present in the protein.[66]

3.1 Tandem SH2 domains

A number of SH2 domain containing proteins have two SH2 domains located in tandem. Those tandem SH2 domains (tSH2) bind diphosphorylated peptides with high affinity.[67] Examples of proteins containing a tSH2 domain are SHP-1, SHP-2, Syk, Zap-70, PLCγ and PI3K.[43] Single SH2 domain – phosphopeptide interactions are often around 100 nM and a monophosphorylated peptide has even much lower affinity for Syk tSH2, i.e. 20 μM. Divalent tSH2 – diphosphorylated peptide interactions have considerable higher affinities, which are in the low nanomolar range (Table 1). Moreover, the binding specificity of tSH2 domains is significantly higher compared to individual SH2 domains. Tandem SH2 domains bind with 1000 to >10000 fold higher affinity to their native phosphopeptidic ligand compared with diphosphorylated peptides with randomized sequences, while this level of specificity for individual SH2 domains is only ~20-50 fold.[67]

The arrangement of the two SH2 domains within a tSH2 differs significantly from protein to protein. Only the crystal structures of the tSH2 domains of the two members of the Syk family, Syk and Zap-70, can be relatively well superimposed, while the structures of other tSH2 domains are rather different.

Table 1. Binding affinities of tandem SH2 domains for native ligands.[67]

tSH2 containing protein	tSH2 ligand	$K_{D\,(app)}$ (nM)
SHP-2	SHPS-1 425-458	1.3 ± 0.4
Syk	FcεRIγ ITAM	2.6 ± 0.2
Zap-70	TCRζ ITAM 1	2.0 ± 0.5
PI3K	PGFRβ 738-757	0.58 ± 0.08
PLCγ1	PGFRβ 1006-1029	2.2 ± 0.6 and 0.65 ± 0.06

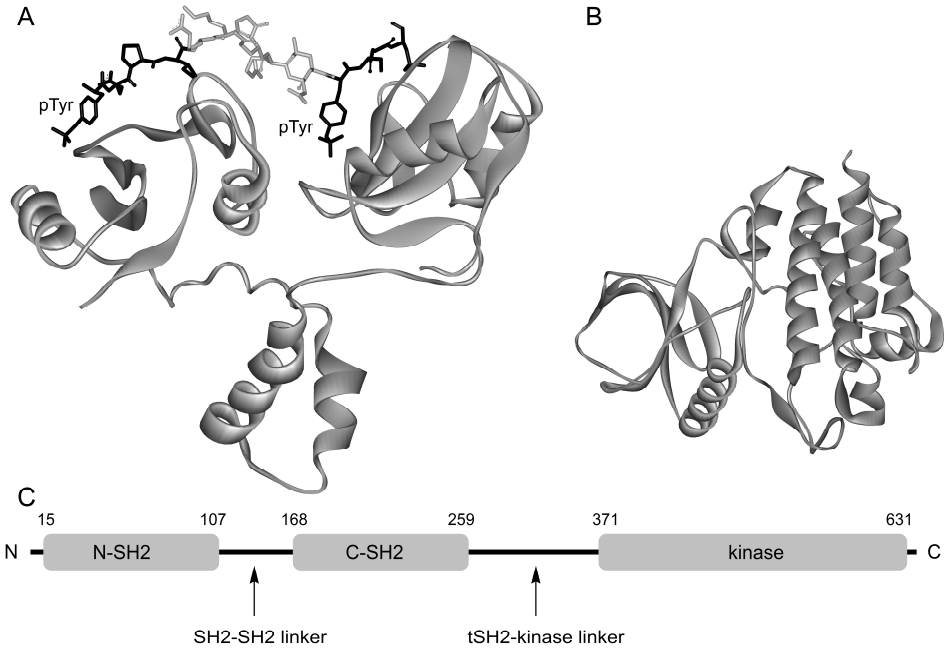

Figure 3. The structure of Syk. A: Crystal structure of Syk tSH2 complexed with ITAM (PDB entry code 1a81).[68] The C-SH2 domain is shown left, the N-SH2 domain right and the SH2-SH2 linker at the bottom. B: Crystal structure of the kinase domain of Syk (PDB entry code 1xba).[69] C: Schematic representation of human Syk.

4. The Syk family of tyrosine kinases

The Syk family of non-receptor tyrosine kinases consists of two proteins often found in immune cells: Syk and Zap-70. Both proteins exist of a tandem SH2 domain (tSH2) and a kinase domain (Figure 3). Furthermore, there is an SH2-SH2 linker (also called interdomain A) and a tSH2-kinase linker (interdomain B).[70] Unfortunately, there is no high resolution structure of full length Syk available. There are more structures of Zap-70 known, among which a crystal structure of the full-length protein.[34]

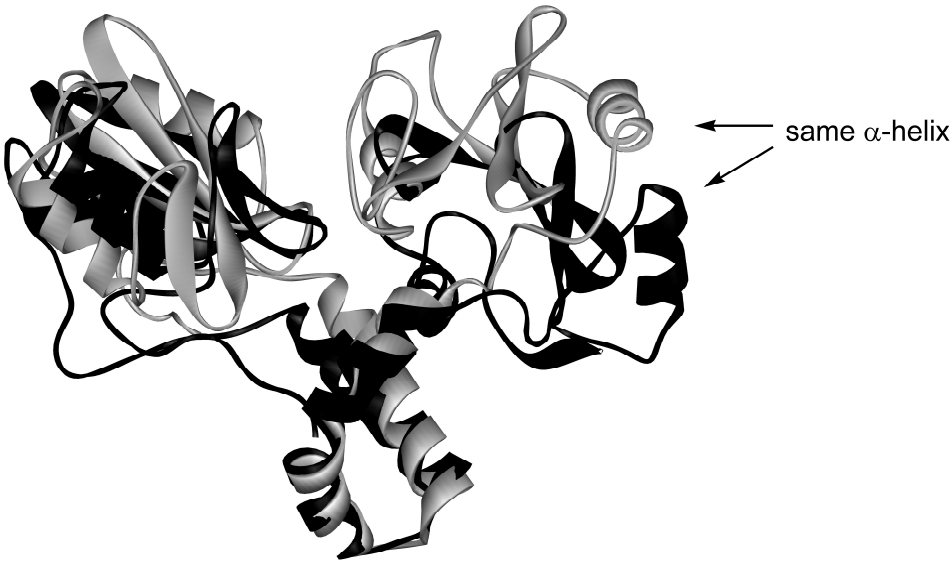

Figure 4. Zap-70 tSH2. Comparison of the complexed (grey, PDB entry code 2oq1[71], ITAM is omitted for clarity) and uncomplexed (black, PDB entry code 1m61[72]) Zap-70 tSH2. The residues in the SH2-SH2 linker were superimposed on each other. In particular the C-SH2 domains in the complexed and uncomplexed structures, shown right, are completely differently orientated.

4.1 The structure and function of Zap-70

In 1995 the crystal structure of Zap-70 tSH2 complexed with ITAM was reported.[71] In this structure the SH2 domains are in very close proximity. In contrast, the SH2 domains in the uncomplexed Zap-70 tSH2 structure are further apart from each other (Figure 4).[72] The character of the SH2 domains in both structures is very similar and features the common fold observed in most SH2 domains.

The bound and unbound structures differ mostly in the orientation of the SH2 domains with respect to each other. Also the α-helixes in the SH2-SH2 linker are altered and differently oriented, which is responsible for the difference in inter-SH2 domain distance (Figure 4).

Zap-70 binds ITAM 'antiparallel': C-SH2 binds the N-terminal pTyr of ITAM and N-SH2 binds the C-terminal pTyr of ITAM. However, residues from the C-SH2 domain are also crucial for binding of the C-terminal pTyr of ITAM.[60] In other words, N-SH2 itself is incomplete and can only be fully functional in the context of C-SH2.

For Zap-70 also a crystal structure of the kinase domain complexed with the staurosporine inhibitor has been reported.[73] Most interestingly, the crystal structure of full-length Zap-70 in the inactive state has been elucidated recently.[34] This structure showed that tSH2 is accessible for ITAM binding in the inactive, unbound state (Figure 5). Some residues in the SH2-SH2 linker dock onto two helices of the kinase C-terminal lobe and the tSH2-kinase linker is packed between the kinase domain and the SH2-SH2 linker. This region is referred to as the 'linker-kinase sandwich'. At the heart of this region is a set of closely packed aromatic-aromatic interactions between the side chains of Tyr315 and Tyr319 in the tSH2-kinase linker and Trp131 in the SH2-SH2 linker.

The structure of tSH2 in the full-length inactive, uncomplexed Zap-70 is very similar to the structure of the uncomplexed tSH2, with the two SH2 domains apart from each other as shown in Figure 4.[34,72,74] It is likely that binding of Zap-70 to ITAM promotes disassembly of the linker-kinase sandwich, due to a decrease in inter SH2 domain distance and conformational changes in the SH2-SH2 linker. This disassembly could facilitate access to phosphorylation sites such as Tyr126 in the SH2-SH2 linker, Tyr292, Tyr315 and Tyr319 in the tSH2-kinase linker and Tyr492 and Tyr 493 in the activation loop of the kinase domain (Figure 5). Phosphorylation of Tyr292, Tyr315 and Tyr319 is only important for recruitment of other proteins, since mutation of those residues into phenylalanine does not affect kinase activity.[75-77] Phosphorylation of Tyr492 and Tyr493 promotes removal of the activation loop from the catalytic cavity and thus activation of the kinase domain.[34]

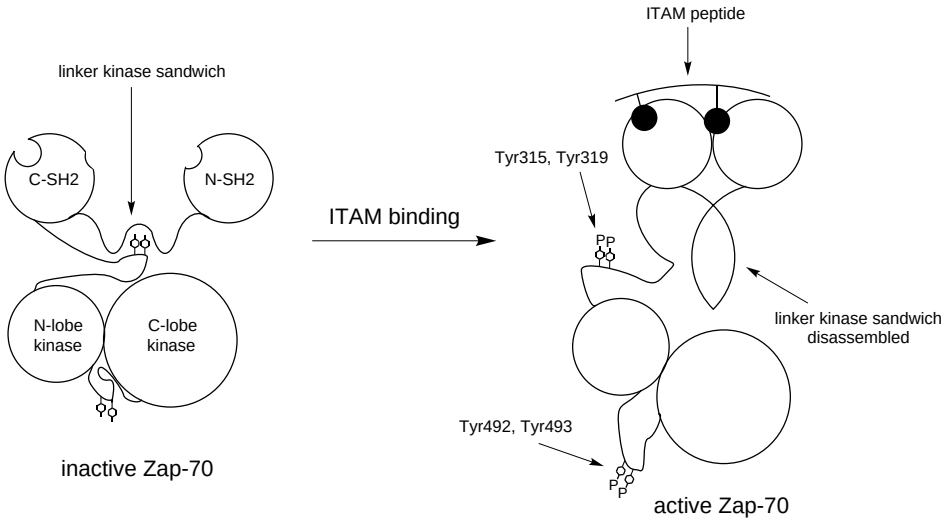

Figure 5. Schematic diagram of Zap-70 activation upon ITAM binding proposed by Deindl et al.[34]

4.2 The structure and function of Syk

In 1995 the first high resolution (NMR) structure of a Syk domain was reported involving the complex of the C-SH2 domain and a phosphopentapeptide.[78] Three years later a crystal structure of Syk tSH2 complexed with ITAM was elucidated (Figure 3A).[68] Unfortunately, there is not yet a high resolution structure of Syk tSH2 without an ITAM ligand available and, therefore, it has not been established if the conformational change in tSH2 caused by ITAM binding is similar as observed for Zap-70 tSH2.

The crystal structure of Syk tSH2 complexed with a diphosphorylated ITAM peptide derived from the CDε chain of the T cell receptor distinctly shows that the interaction is divalent (Figure 3A).[68] The CDε chain ITAM peptide pTyr-Glu-Pro-Ile-Arg-Lys-Gly-Gln-Arg-Asp-Leu-pTyr-Ser-Gly-Leu binds in an antiparallel manner to Syk tSH2. The four underlined N-terminal residues of ITAM contact the C-SH2 domain and the four underlined C-terminal residues of ITAM contact the N-SH2 domain. The seven intervening residues make little contact with Syk tSH2. The pTyr binding region of N-SH2 is in close proximity with C-SH2. However, in Syk the C-SH2 and the N-SH2 function each as a complete SH2 domain, in contrast to Zap-70, as explained above.

The six different ITAM – tSH2 complexes in the crystallographic asymmetric unit of Syk tSH2 revealed a substantial variability in the relative orientation of the two SH2

domains.[68] The two most extreme snap shots in the unit cell differ by 18° in rotation and 2.0 Å in translation of C-SH2 with respect to N-SH2. Hence, even bound to ITAM, Syk tSH2 demonstrates a considerable conformational flexibility. The free tSH2 is probably even more flexible, although this is not yet confirmed by high resolution structures. Nevertheless, the flexible nature of Syk tSH2 was demonstrated by Grucza et al., who found evidence for two conformers.[79] Furthermore, De Mol et al. inferred from SPR and MS measurements that unbound Syk tSH2 probably possesses significantly more flexibility than ITAM-bound tSH2.[80,81]

Another indication of the degree of flexibility of tSH2 is the observation that it bound with the same affinity as for γ-ITAM to an ITAM peptide derived from the single chain Fc receptor class IIA (FcRIIA), which has 5 residues more between the two SH2 binding epitopes compared to γ-ITAM derived from FcεRIγ.[64,82] Reduction of the flexibility of tSH2 by the introduction of a disulfide bridge between the two SH2 domains locked tSH2 into a conformation with the SH2 domains in close proximity, leading to a 62-fold less affinity for the larger ITAM derived from FcRIIA.[82]

A high resolution crystal structure of the kinase domain of Syk is also available in the protein data bank (PDB entry code 1xba, Figure 3B).[69] Furthermore, an electron microscopy (EM) structure of full length Syk, as a GST construct, with a resolution of 24 Å has been reported recently (Figure 6).[70] This EM structure is without ITAM and probably shows Syk in the 'resting state'. According to the EM reconstruction, the GST-Syk displays a square-shaped conformation. Two mayor regions could be defined: a bulky, massive region, which consisted of the kinase – and GST domain and a two-lobule domain, comprising tSH2. Into this EM structure, the crystal structures of Syk tSH2 and the Syk kinase domain were fitted (Figure 6B). This fitting suggested that the SH2 domains are, as in Zap-70, accessible for ITAM binding. The 3D reconstruction of resting Syk revealed a slightly more open conformation than Zap-70, suggesting that the SH2-SH2 linker in Syk is in less close contact with the kinase domain (compare Figures 6A and 6B). It is possible that this difference can be ascribed to the low resolution of the EM structure. However, it is also possible that the observed difference is not an artefact, and, therefore, it could explain the striking difference in kinase activity. The kinase activity of Syk is intrinsically 100-fold higher than that of Zap-70. This may be caused by the less intimate interactions of the SH2-SH2 linker with the Syk kinase domain.[70] These interactions are proposed to inhibit the protein, similar as in Zap-70 (Figure 5). However, also in Syk close contacts between the tSH2 domain and the

kinase domain seem to exist. As indicated above, so far there is no unbound Syk tSH2 structure available for a better understanding of the structure of the resting state.

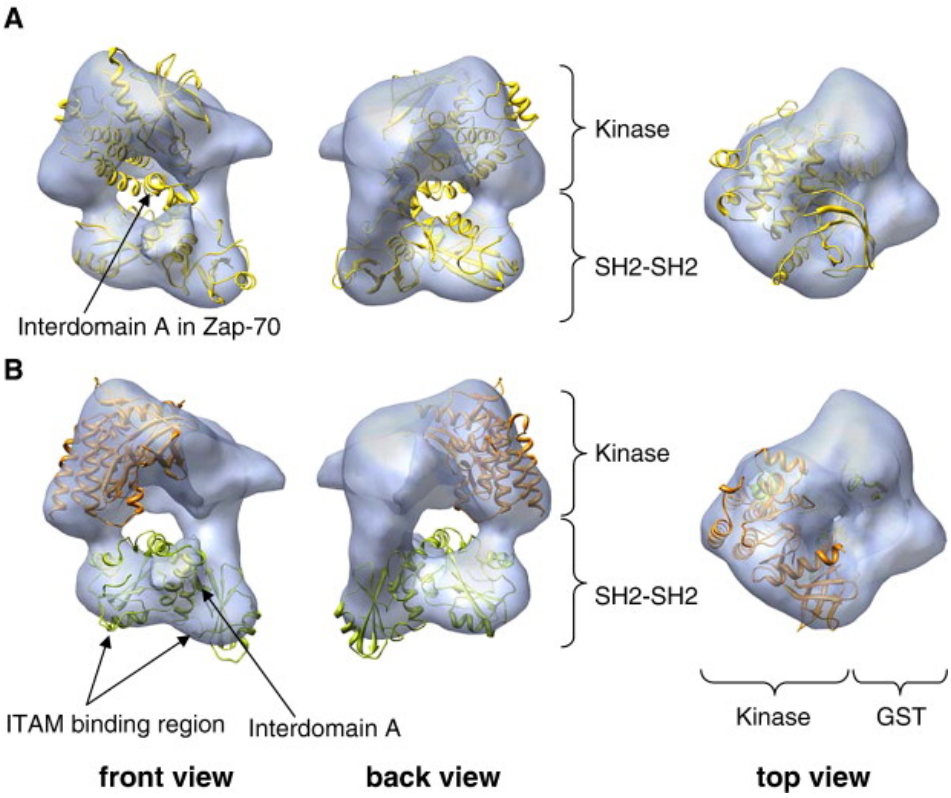

Figure 6. Fits of crystal structures of Syk and Zap-70 into the EM map of GST-Syk.[70] A: Fits of the crystal structure of the full-length Zap-70[34] into the EM map of Syk. B: Fits of the crystal structures of Syk tSH2[68] (bound to ITAM) and the Syk kinase domain[69] into the EM map of Syk (Figure taken from Arias-Palomo[70]).

Tyrosine phosphorylation in the tSH2-kinase linker and in the kinase domain is important for Syk activation.[69,83-85] However, Syk *in vitro* kinase activity did not depend on phosphorylation of Tyr519 and Tyr520 present in the activation loop within the kinase domain. Syk mutant Y519F and Y520F were still capable of phosphorylating proteins after IgE stimulation of FcεRI, but were incapable of transducing FcεRI signaling.[86]

Some interesting information on phosphorylation of Tyr130 in Syk, which is part of the SH2-SH2 linker and is the equivalent of Tyr126 in Zap-70, is available. As Tyr126 in Zap-70,[87] also Syk Tyr130 is autophosphorylated, resulting in decreased affinity for dpITAM to that of a single pTyr-SH2 interaction (1.8 μM). As a consequence, Syk is dissociated from ITAM on the B cell receptor for antigen (BCR).[88,89] Phosphorylation of Tyr130 is proposed to destabilize the α-helices in the SH2-SH2 linker, causing an altered, more extended SH2-SH2 orientation, which is less compatible with divalent ITAM binding. The function of phosphorylation of Tyr130 is probably to further disrupt the linker-kinase sandwich, which may result in a larger accessibility of the other phosphorylation sites. Hence, phosphorylation of Tyr130 may increase kinase activity.

4.3 Hypothesis for mode of Syk activation

The SH2-SH2 linker is remarkably conserved between Syk and Zap-70.[90] The homology between the SH2-SH2 linker of murine Syk and murine Zap-70 is larger than either of the two SH2 domains (65% and 50-57%, respectively). Furthermore, the SH2-SH2 linker in Syk is more conserved among different species than the SH2 domains and a mutant of Syk carrying a deletion of 20 residues in the SH2-SH2 linker fails to mediate B cell antigen receptor (BCR) signaling.[90] These data confirm the importance of the linker in tSH2, which was also clear from the crystal structure of Zap-70, as indicated above.[34]

There is no high resolution structure of uncomplexed Syk tSH2 and of full-length Syk available as yet. As a consequence, ITAM binding and the effect on kinase activation is not yet fully understood. However, several aspects of ITAM binding are known. Based on SPR measurements and MS H/D exchange experiments De Mol et al. proposed a two step binding model (Figure 7).[80] In this model, the SH2 domains are apart from each other when tSH2 is not bound to ITAM. In this extended conformation, the residues in the SH2-SH2 linker displayed a large conformational flexibility, which was demonstrated by H/D exchange experiments.[81] When association with ITAM occured, first one SH2 domain (most likely C-SH2) bound one pTyr of ITAM. This step was rapidly followed by binding of the second N-SH2 domain to the second pTyr of ITAM, which locked tSH2 in a closed conformation. During the second binding step, a large conformational change occured within the SH2-SH2 linker. When tSH2 was complexed to ITAM, the dynamics of the backbone of the linker was largely reduced.[81]

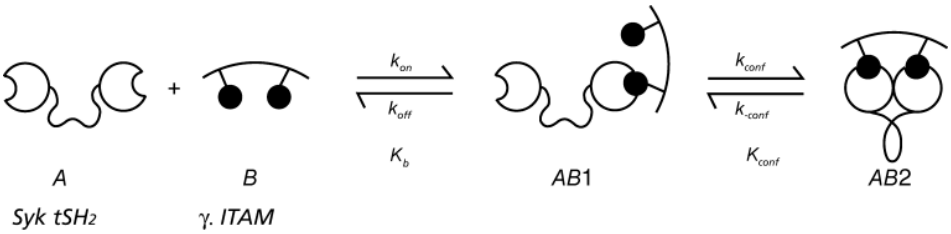

Figure 7. Mechanism of diphosphorylated ITAM binding to Syk tSH2 proposed by De Mol et al. (Figure taken from De Mol[80]).

This two step binding model was the basis for the hypothesis for the mode of Syk activation: ITAM binding brings the SH2 domains together, resulting in a conformational change in the SH2-SH2 linker. This change initiates activation of the kinase domain. This hypothesis is supported by the full length Zap-70 structure, and is also compatible with the less resolved Syk EM structure, as was discussed above. Selective Syk inhibitors might be obtained by designing ITAM mimics, which can prevent Syk from binding to native ITAM and recruitment to the receptor.

This SH2-SH2 distance hypothesis is a main research line in the research described in this thesis, concerning the design and synthesis of ITAM mimics in which the SH2 binding epitopes are forced at shorter or longer distance.

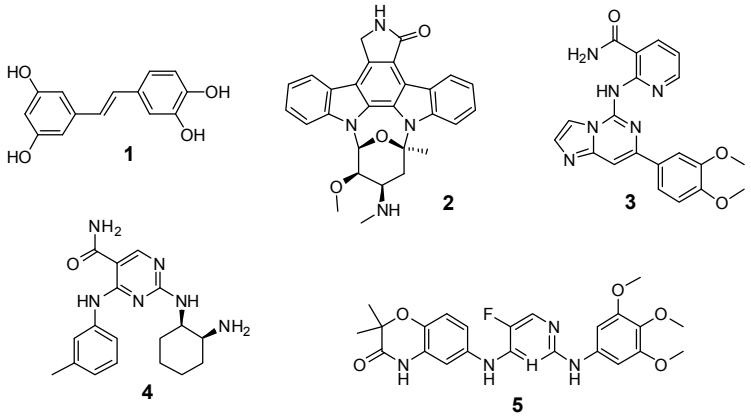

Figure 8. The Syk kinase inhibitors piceatannol[91] (**1**), staurosporine[69] (**2**), BAY 61-3606[92] (**3**), YM193306[93] (**4**) and R406[94] (**5**).

4.4 Inhibitors of Syk and Zap-70

The importance of Syk as a target for anti-allergic therapy was demonstrated by the large number of kinase inhibitors which have been developed (Figure 8).[2,91,92,94-97] Two archetypical, non selective inhibitors are piceatannol and staurosporine (compounds **1** and **2** in Figure 8).[69,91] For example, the orally available BAY 61-3606 (**3**) is a potent Syk inhibitor (K_i = 7.5 nM) and is also reasonably selective.[92] However, this Syk kinase inhibitor showed not a completely adequate pharmacokinetic profile. Generally, these kinase inhibitors bind to the ATP-binding site in the kinase domain, which makes the development of selective inhibitors very difficult. In potential, tSH2 ligands may be more selective Syk and Zap-70 inhibitors than these inhibitors binding to the kinase domain.

4.4.1 Ligands for Zap-70 tSH2

An ITAM peptide in which two difluorophosphonomethyl phenylalanyl (F_2Pmp) residues replaced the phosphotyrosines was the first reported non-native tSH2 domain ligand for a protein from the Syk family.[33] This peptide was protein tyrosine phosphatase (PTPase)-resistant and was able to inhibit the binding of Zap-70 tSH2 to the ITAM motif of the T cell antigen receptor (TCR) in permeabilized T cells. By inhibiting this association the kinase activity of Zap-70 was reduced to basal levels.[33] However, permeabilization of the cells with tetanolysin could have resulted in artifacts, and therefore, these results are not indisputable.

Revesz et al. showed that a monovalent tetrapeptoid binds approximately 1000 times weaker to Zap-70 tSH2 compared to the divalent full-length ITAM peptide (Figure 9, compound **6**).[98] In addition to this, they stated that the correct distance between the two phosphate groups is more important for obtaining high affinity than the intervening peptide sequence, although they did not test different diphosphorylated ITAM mimics with varying distances between the phosphate groups/mimics.[99] Only one scaffold was used between two PTPase-resistant phosphotyrosine mimics, i.e. the non-peptidic ITAM mimic **8**.[99] The relative rigid and hydrophobic linker between the phosphate mimics was responsible for maintaining the optimal distance between the two phosphate mimics. The IC_{50} value (0.25 μM) for binding of this mimic was 10 times higher compared to the native ITAM peptide (0.03 μM). The monovalent form of the non-peptidic ligand (**7**) was still reasonably active, displaying an IC_{50} value (1.9 μM) of 10 times higher than the divalent ligand **8**.[99]

Vu et al. synthesized a library of 1,2,4-oxadiazole analogues (**9**) and tested them for Syk, Zap-70 and Src SH2 domain binding (Figure 9).[100,101] More than ten compounds were selective for Zap-70 and had IC_{50} values lower than 10 μM. For Syk all compounds had IC_{50} values of 250 μM or higher. Some compounds were more than 150-fold more potent Zap-70 ligands than the native phosphotetrapeptide.

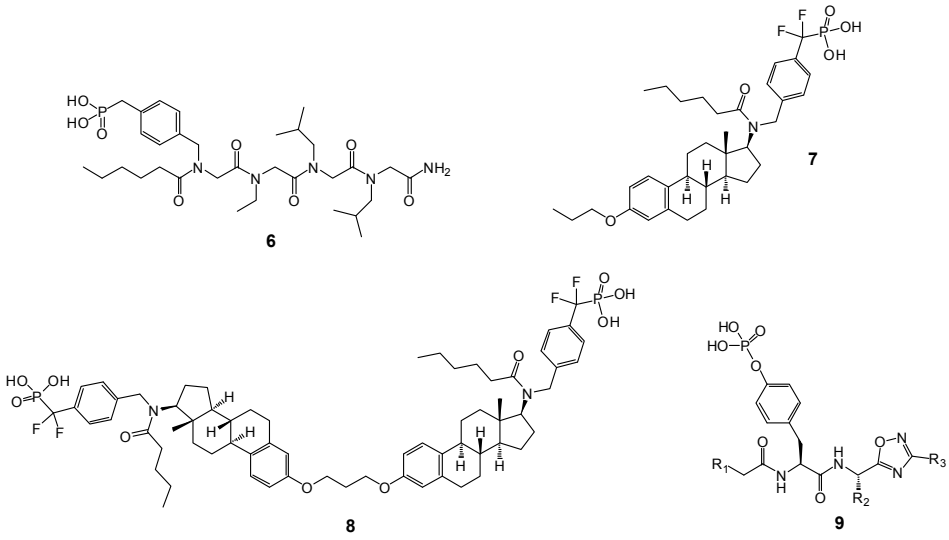

Figure 9. Ligands for Zap-70 tSH2 from the literature. The tetrapeptoid **6** has 1000 fold less affinity for Zap-70 tSH2 compared to native ITAM.[98] Monovalent **7** and divalent **8** non-peptidic ligands were developed by Revesz et al.[99] Compound **9** represents a series of Zap-70 tSH2 domain ligands with higher binding affinity ($IC_{50} \geq 1$ μM) than the monovalent native Ac-pTyr-Asp-Val-Leu-NH_2 peptide ($IC_{50} = 328$ μM).[100,101]

4.4.2 Ligands for Syk tSH2

The interaction between the full-length ITAM peptide or ITAM mimics and Syk tSH2 has been studied in detail.[67,80-82,102,103] Some compounds discussed below are shown in Figure 10. The binding affinity of the divalent native γ-ITAM peptide **13** was 1000 fold higher compared to a monovalent phosphotetrapeptide, which indicates that for high affinity the two phosphotyrosine residues are essential. A series of non-peptidic ligands for Syk C-SH2 has been prepared.[104] These ligands, directed towards binding of Syk C-SH2, were designed using structure-based *in silico* screening. The best

compound, **10**, exhibited an IC_{50} value of 38 μM, which is comparable to a monophosphorylated tetrapeptide.

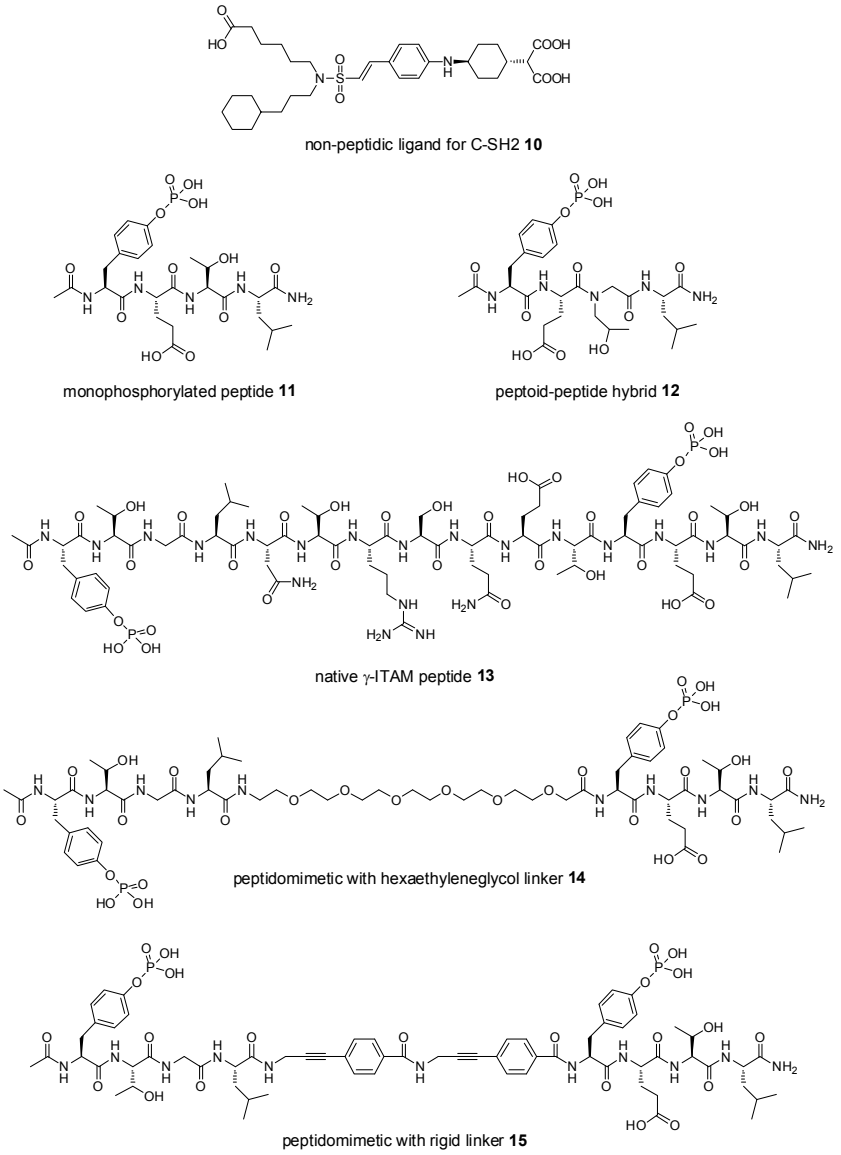

Figure 10. Ligands for Syk tSH2. Compound **10** is a member of the only known non-peptidic library of tSH2 ligands.[104] The monophosphorylated peptide **11** and the peptoid-peptide hybrid **12** are ligands for N-SH2.[105] The seven intervening residues in native ligand **13** can be replaced by a flexible – (**14**) or a rigid (**15**) linker without substantial loss of affinity.[106,107]

In our group the ITAM – Syk tSH2 interaction has been studied extensively. Ruijtenbeek et al. synthesized and assayed a monovalent peptidic ligand (**11**) derived from the part of γ-ITAM that binds N-SH2. Furthermore, a set of corresponding peptoids was prepared (e.g. **12**) (Figure 10).[105] The IC_{50} values of some peptide-peptoid hydrids were five to eight times higher than the IC_{50} value of the native phosphotetrapeptide.

Later, Dekker et al. prepared several ITAM peptidomimetics. In these compounds the seven intervening residues in ITAM were replaced by unnatural linkers. An ITAM mimic with a hexaethyleneglycol linker (compound **14** in Figure 10) had only a 5-fold less affinity for Syk tSH2 than the native peptide (IC_{50} values are 1.8 μM and 0.38 μM, respectively).[107] The development of ITAM mimics was further expanded to the design of a mimic containing a rigid linker. This rigid ITAM mimic (compound **15** in Figure 10) even had a similar affinity for Syk tSH2 as native ITAM.[106] The development of this high-affinity rigid ITAM mimic was the starting point of the research described in this thesis.

5. Approaches to interfere in the ITAM – Syk tSH2 interaction: photoswitches, dendrimers and cell penetrating peptides

In this thesis several approaches are described which were used for studying the ITAM – Syk tSH2 interaction and the effect of ITAM binding on Syk kinase activity. Photoswitches were incorporated into the ITAM sequence, dendrimers were functionalized with ITAM-derived phosphopeptides and ITAM mimics were conjugated to cell penetrating peptides. The obtained compounds were subsequently used in different assays. Because of the considerable role of photoswitches, dendrimers and cell penetrating peptides in this research, they will be briefly discussed below.

5.1 Photoswitches in regulation of peptides

Being able to regulate the structure and/or function of peptides during (biological) experiments is important for studying the effect of conformational changes. Such a regulation can be achieved with photoswitches, which are molecules that can change their structure and/or configuration upon irradiation with light of a certain wavelength.[108] Azobenzene, mainly as part of (4-aminomethyl)phenylazobenzoic acid

(AMBP), is the most used photoswitch in peptide chemistry, because the synthesis is well established, its incorporation into a peptide is straightforward and the isomerization process is fast and fully reversible (Figure 11).[109-113]

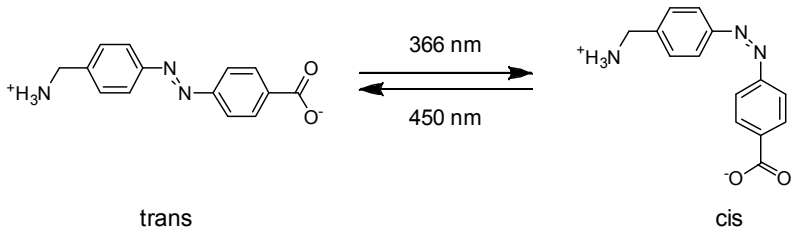

Figure 11. Photoisomerization of azobenzene derivative (4-aminomethyl)phenylazobenzoic acid (AMBP).

Azobenzene isomerization can be achieved with visible light (450 nm) from the cis – to the trans isomer and with UV light (366 nm) for conversion of the trans – to the cis isomer (Figure 11). 100% trans azobenzene cannot be obtained by light irradiation, due to partial overlap of the n-π^* and π-π^* transitions.[113,114] Nonetheless, because the trans isomer is thermodynamically the most stable isomer, 100% trans can be reached by thermal relaxation in the dark, which is unfortunately a relative slow process. Therefore, instead of thermal relaxation, almost 100% of the trans isomer is often used, which can be rapidly obtained by irradiation with visible light of 450 nm. The cis isomer is only accessible via irradiation with UV light of approximately 366 nm. A maximal cis isomer content of 60-80% can be reached, resulting in a significant amount of trans isomer still present after UV irradiation.[113] This trans 'contamination' present after UV irradiation can hamper the study of the effect of the pure cis isomer.

Another disadvantage of the use of the azobenzene moiety as a photoswitch for biological applications is that thermal relaxation from cis to trans can be fast when the aromatic rings are substituted with electron-donating groups. Furthermore, intracellular modification (e.g. reduction) of the azo compound could lead to loss of photoswitching ability.[115] Both these disadvantages can be overcome by ortho-amino-substitution of the two aromatic rings.[116] However, synthesis of (unsymmetrical) ring-substituted azobenzene derivatives is considerably more time-consuming.

Despite these disadvantages, numerous examples of the incorporation of azobenzene into peptides have been described in the literature.[113] For instance, the azobenzene

moiety has been incorporated as a turn element into an amino acid sequence known to fold into a β-hairpin structure.[117] In the trans configuration the structure of the peptide could not be determined, whereas the peptide had a β-hairpin structure when the azobenzene moiety was in the cis configuration. In another study the azobenzene moiety was used to constrain a peptide into an α-helical structure.[118]

In contrast to the large amount of structure elucidation, which has been performed on azobenzene containing peptides, examples of the effect of isomerization on biological activity (e.g. binding affinity) are very rare. An interesting example is that of a cyclic RGD peptide, which possessed different binding affinities for the $\alpha_v\beta_3$ integrin in the cis – and trans configuration.[119]

Other photoswitches, which are able to switch from 100% state A to 100% state B and vice versa, have been prepared.[120,121] However, incorporation of these photoswitches into a peptide is far from standard. Most likely, this will change in the near future, considering the disadvantages of azobenzene.

5.2 Dendrimers as multivalent ligands

The divalent ITAM – Syk tSH2 interaction, which is a 1000-fold stronger than the monovalent interaction, is a good example of a multivalent interaction. Multivalency is used to enhance binding affinity of especially weakly interacting ligands and can be defined as the simultaneous binding of multiple ligands which are part of one biological entity (a molecule, a surface) to multiple receptors which also form an entity.[122,123] An outstanding example of a scaffold that can be functionalized in a multivalent way is a dendrimer.[124]

Dendrimers can be functionalized with peptides. These peptide-dendrimers can be used as artificial enzymes and – receptors and as drug-delivery agents.[125] Furthermore, peptide-dendrimers can be applied in diagnostics, as vaccines, as anticancer agents and as inhibitors of enzymes and protein-protein interactions.[126,127]

In general, peptide-dendrimers possess, besides higher binding affinity, also higher selectivity, compared to monomeric peptides. These two properties are responsible for the fact that dendrimers are becoming increasingly important in the design of a variety of therapeutics. In the field of anticancer agents and cancer diagnostics dendrimers can have superior tumor targeting properties. A promising application is described by Dijkgraaf et al.[128] They prepared DOTA-conjugated cyclic RGD peptide dendrimers and

showed that the tetravalent dendrimer was relatively more potent *in vivo* than the monomeric compound.

5.3 Delivery of bioactive compounds: cell penetrating peptides

Whereas small, lipophilic molecules can enter cells by passive diffusion, larger compounds like peptides, proteins and nucleic acids are unable to cross cell membranes. Besides that, the pTyr residues in ITAM sequences are negatively charged, which hampers cellular uptake. Therefore, a delivery method is required to be able to study the intracellular effect of those large compounds. Several delivery methods are in principle available, including microinjection, cell membrane permeabilization, viral delivery, a prodrug approach and attachment of a carrier to the compound of interest.[129,130]

Microinjection is the only method which allows a nearly 100% transduction efficiency.[129] Further advantages include the well-defined dose and timing of the delivery and low cytotoxicity. However, a major drawback of manual injection is that this method is limited to a small number of cells. In most experiments the read-out is limited to one cell and therefore microinjection cannot be used in combination with cellular assays, which require large amounts of cells.

The delivery of non-permeable substances into cells can also be achieved by temporary permeabilization of the cell membrane. Electroporation, i.e. permeabilization by a rapid, high-voltage electric pulse, is a commonly used method.[129] The transduction efficiency is lower than for microinjection and electroporation cannot be used in a high-throughput manner as well.

Cells can also be made permeable by chemical treatment. Treatment of cells with streptolysin O, which forms pores in the plasma membrane by binding to cholesterol, allows the delivery of proteins into the cytosol.[39] Advantages of this method are the high efficiency and the possibility to use 96-wells plates. However, this method weakens the cells considerably and can give artifacts during cellular assays.

Viruses are efficient in the delivery for DNA.[129] However, the type of biomolecule which can be delivered this way is limited. This method is time consuming and often toxicity problems occur. Therefore, viruses are by far not the first choice for cellular assays.

Delivery of charged compounds, such as phosphotyrosine containing peptides, can also be accomplished by masking the negatively charged phosphate group.[130] In such a prodrug strategy, the phosphate group is protected with an esterase cleavable group, making the compound less hydrophilic, which should result in better membrane permeability. Recently, Mandal et al. reported that two tetrapeptidomimetics, which possessed both a doubly protected phosphate mimic, could enter MD-AMB-468 cells.[131] However, the chances of successful delivery of ITAM mimics using this prodrug approach is questionable, because ITAM is a relatively large molecule and the ITAM mimics also possess a negatively charged glutamic acid residue, which should probably also be masked.

Delivery can be achieved by attachment of a carrier to a compound of interest. The type of carriers can be divided in cell penetrating peptides and lipophilic carriers. Lipophilic carriers are often fatty acid chains which are covalently bound to the cargo molecule.[132] Such a construct can insert into a cell membrane and deliver the compound intracellularly by means of a 'flip-flop' mechanism.[133]

Cell penetrating peptides (also called protein transduction domains) are frequently used as delivery vehicle.[134-137] Cell penetrating peptides (CPPs) can be defined as small peptides (< 30 amino acids) capable of translocating across cell membranes. The first two CPPs discovered were an 11-residue containing peptide derived from HIV-1 Tat and a peptide derived from Drosophila antennapedia homeodomain (penetratin).[138,139] The discovery of these two CPPs initiated the search for other CPPs. Since then many CPPs, such as the chimeric transportan[140] and polyarginines,[141] have been described.

The mechanism of membrane translocation is still a subject of debate.[134,135] The main discussion involves the question whether an energy-independent or energy-dependent (endocytosis) pathway is followed. Initially, the membrane translocation was considered to be energy-independent by direct permeation.[142,143] Nowadays, the majority of papers report that endocytosis is the mechanism of uptake and that the previously found energy-independent mechanism could be explained by experimental artifacts. However, in the presence of endocytosis inhibitors high concentrations of Tat(48-58) and nona-arginine were still able to enter cells.[143] Furthermore, there are some CPPs which translocate by pore formation via a similar mechanism as antimicrobial peptides (AMPs).[144] Mastoparan X is an example of such a pore-forming CPP.[145]

For energy-dependent cell penetration the interaction with heparin sulfate proteoglycans (HSPGs) on the cell surface is important.[146,147] After binding of the CPP to HSPGs, cellular uptake by endocytosis can take place via macropinocytosis, clathrin-mediated endocytosis, caveolae/lipid raft-mediated endocytosis or (most likely) a combination thereof.[142,143,148] It is very likely that different CPPs utilize different mechanisms of translocation. Moreover, the cargo, the cell type and the experimental settings (concentration, temperature, etc.) can also influence the endocytotic pathway.

CPPs can be attached to a cargo in a covalent or non-covalent way. Covalent attachment has been studied extensively, but attachment through non-covalent interactions is gaining increasing attention. A well-studied example of a 'non-covalent' carrier is Pep-1 (Chariot^{TM}).[149] This commercial available peptide forms small aggregates with the cargo and these aggregates can translocate into cells. The advantages of non-covalently linked CPPs, such as Pep-1, are that the preparation is less time consuming and more convenient. However, far more than stoichiometric amounts of CPP are required for non-covalently attached CPPs, which can give rise to experimental artifacts. Recently, it has been shown that, besides the known non-covalent carriers, also established 'covalent carriers' such as octa-arginine can be used to deliver cargo in a non-covalent way.[150,151]

For the delivery of ITAM mimics we have chosen for carrier-mediated delivery, also in view of the aim to design deliverable compounds that can be eventually developed further.

6. Outline of this thesis

The ITAM – Syk tSH2 interaction is the main theme of this thesis. Several approaches, such as the azobenzene photoswitch and CPPs, were used to study this interaction.

In **chapter 2** and **3** the synthesis and evaluation of azobenzene-containing photoswitchable ITAM mimics is described. The azobenzene moiety replaced the linker residues between the SH2 binding epitopes in ITAM, allowing to change the orientation of the two SH2 binding epitopes with respect to each other upon irradiation. Four different photoswitchable ITAM mimics were prepared. To three of these peptidomimetics also additional units were placed on each side of the azobenzene moiety AMPB in the linker, to generate a series of ITAM mimics with different

distances between the two phosphotyrosine containing epitopes in the cis – and trans configuration. The affinity of the cis – and trans isomers of the ITAM mimics for Syk tSH2 was assayed with SPR. The effect of isomerization upon light irradiation on tSH2 binding could be monitored in real time.

In **chapter 4** the possibility of the use of dendrimers as high-affinity ligands for Syk tSH2 is explored. One phosphotyrosine-containing tetrapeptidic SH2 binding epitope was selected to be conjugated to dendrimers. This tetrapeptide was coupled via 'click' chemistry to create a series of functional phosphopeptide containing dendrimers ranging from a monovalent to an octavalent dendrimer. The affinity of the functionalized dendrimers for Syk tSH2 has been assayed in SPR competition experiments.

In **Chapter 5** the rigid ITAM mimic, which was reported by Dekker et al. (compound **15** in Figure 10), was used in affinity pull-down experiments. An adapted synthesis route for the preparation of the rigid building block is reported in this chapter. Furthermore, the synthesis of native ITAM as well as the synthesis of a nonphosphorylated, two monophosphorylated and a diphosphorylated rigid ITAM mimic is described. Those five ITAM peptides were used for affinity pull-down experiments. For this, the peptides needed a reactive thiol group for immobilization and therefore the peptides were functionalized with a cysteine residue, which was coupled to ITAMs possessing an N-terminal ethyleneglycol spacer. A synthesis route for the Fmoc-protected ethyleneglycol spacer is also described. All five ITAM peptides were immobilized on agarose beads for the pull-down experiments. In preliminary experiments the beads were incubated with a cell lysate and the proteins binding to the immobilized peptides were analyzed with gel electrophoresis.

In **chapter 6** the effect of the diphosphorylated rigid ITAM mimic, provided with different carriers, on mediator release in mast cells was investigated. To explore which cell penetrating peptide (CPP) could best be used, several CPPs and a liphophilic alkyl chain were conjugated to the ITAM mimic. Carrier-ITAM constructs with fluorescent labels were prepared to be able to quantify cell labeling using flow cytometry. Constructs without fluorescent labels were prepared for assaying the bioactivity in living cells. Furthermore, the constructs were tested for cytotoxicity and affinity for Syk tSH2. One of the constructs was able to penetrate into cells and to affect exocytosis.

In **chapter 7** the effect of native ITAM and two rigid ITAM mimics possessing linkers with different distances between the SH2 binding epitopes on Syk kinase activity is described. First, the affinity of the rigid ITAM mimics for Syk tSH2 was

established with SPR experiments. The effect of native ITAM and the ITAM mimics on Syk kinase activity was evaluated with a dynamic microarray technique. Native ITAM and one rigid mimic with a linker with approximately the same length as in native ITAM displayed moderate effects on kinase activity. The ITAM mimic with a longer linker, however, inhibited kinase activity to a large extent.

In **chapter 8** a summary of this thesis is given. Some perspectives for further research are also presented.

References

1. Taniguchi, T., Kobayashi, T., Kondo, J., Takahashi, K., Nakamura, H., Suzuki, J., Nagai, K., Yamada, T., Nakamura, S., Yamamura, H., Molecular-cloning of a porcine gene Syk that encodes a 72-kDa protein-tyrosine kinase showing high susceptibility to proteolysis, *J. Biol. Chem.*, **1991**, 266, 15790-15796.
2. Navara, C.S., The spleen tyrosine kinase (Syk) in human disease, implications for design of tyrosine kinase inhibitor based therapy, *Curr. Pharm. Design*, **2004**, 10, 1739-1744.
3. Singh, R., Masuda, E.S., Spleen tyrosine kinase (Syk) biology, inhibitors and therapeutic applications, *Annu. Rep. Med. Chem.*, **2007**, 42, 379-391.
4. Yanagi, S., Inatome, R., Takano, T., Yamamura, H., Syk expression and novel function in a wide variety of tissues, *Biochem. Biophys. Res. Commun.*, **2001**, 288, 495-498.
5. Carsetti, L., Laurenti, L., Gobessi, S., Longo, P.G., Leone, G., Efremov, D.G., Phosphorylation of the activation loop tyrosines is required for sustained Syk signaling and growth factor-independent B-cell proliferation, *Cell. Signal.*, **2009**, 21, 1187-1194.
6. Larive, R.M., Urbach, S., Poncet, J., Jouin, P., Mascre, G., Sahuquet, A., Mangeat, P.H., Coopman, P.J., Bettache, N., Phosphoproteomic analysis of Syk kinase signaling in human cancer cells reveals its role in cell-cell adhesion, *Oncogene*, **2009**, 28, 2337-2347.
7. Denyer, J., Patel, V., Syk kinase inhibitors in allergic diseases, *Drug News Perspect.*, **2009**, 22, 146-150.
8. Geahlen, R.L., Burg, D.L., The role of Syk in cell signaling, *Adv. Exp. Med. Biol.*, **1994**, 365, 103-109.
9. Nimmerjahn, F., Ravetch, J.V., Fc-receptors as regulators of immunity, *Advances in Immunology*, **2007**, 96, 179-204.
10. Sada, K., Zhang, J., Siraganian, R.P., SH2 domain-mediated targeting, but not localization, of Syk in the plasma membrane is critical for FcεRI signaling, *Blood*, **2001**, 97, 1352-1359.
11. Pawson, T., Specificity in signal transduction: From phosphotyrosine-SH2 domain interactions to complex cellular systems, *Cell*, **2004**, 116, 191-203.
12. Bradding, P., Novel approaches to the inhibition of mast cells in allergic disease, *Clin. Exp. Allergy*, **2008**, 38, 704-708.
13. Chan, A.C., Syk family of protein tyrosine kinases, *Encyclopedia Biol. Chem.*, **2004**, 4, 139-145.
14. Wong, B.R., Grossbard, E.B., Payan, D.G., Masuda, E.S., Targeting Syk as a treatment for allergic and autoimmune disorders, *Exp. Opin. Inv. Drugs*, **2004**, 13, 743-762.
15. Ulanova, M., Duta, F., Puttagunta, L., Schreiber, A.D., Befus, A.D., Spleen tyrosine kinase (Syk) as a novel target for allergic asthma and rhinitis, *Exp. Opin. Ther. Tar.*, **2005**, 9, 901-921.

16. Turner, M., Schweighoffer, E., Colucci, F., Di Santo, J.P., Tybulewicz, V.L., Tyrosine kinase SYK: essential functions for immunoreceptor signaling, *Immunol. Today*, **2000**, 21, 148-154.
17. Rivera, J., Gilfillan, A.M., Molecular regulation of mast cell activation, *J. Allergy Clin. Immunol.*, **2006**, 117, 1214-1225.
18. Zhang, J., Swaim, W.D., Berenstein, E.H., Siraganian, R.P., Syk protein tyrosine kinase is essential for the high affinity IgE receptor-induced morphological changes in mast cells., *J. Allergy Clin. Immunol.*, **1997**, 99, 379-379.
19. Parravicini, V., Gadina, M., Kovarova, M., Odom, S., Gonzalez-Espinosa, C., Furumoto, Y., Saitoh, S., Samelson, L.E., O'Shea, J.J., Rivera, J., Fyn kinase initiates complementary signals required for IgE-dependent mast cell degranulation, *Nat. Immunol.*, **2002**, 3, 741-748.
20. Gilfillan, A.M., Tkaczyk, C., Integrated signalling pathways for mast-cell activation, *Nat. Rev. Immunol.*, **2006**, 6, 218-230.
21. Kraft, S., Kinet, J.-P., New developments in FcεRI regulation, function and inhibition, *Nat. Rev. Immunol.*, **2007**, 7, 365-378.
22. Siraganian, R.P., Zhang, J., Suzuki, K., Sada, K., Protein tyrosine kinase Syk in mast cell signaling, *Mol. Immunol.*, **2001**, 38, 1229-1233.
23. Blank, U., Rivera, J., The ins and outs of IgE-dependent mast-cell exocytosis, *Trends Immunol.*, **2004**, 25, 266-273.
24. Siraganian, R.P., Mast cell signal transduction from the high-affinity IgE receptor, *Curr. Opin. Immunol.*, **2003**, 15, 639-646.
25. Zhang, J., Berenstein, E.H., Evans, R.L., Siraganian, R.P., Transfection of Syk protein tyrosine kinase reconstitutes high affinity IgE receptor-mediated degranulation in a Syk-negative variant of rat basophilic leukemia RBL-2H3 cells, *J. Exp. Med.*, **1996**, 184, 71-79.
26. Galli, S.J., Tsai, M., Piliponsky, A.M., The development of allergic inflammation, *Nature*, **2008**, 454, 445-454.
27. Barnes, P.J., Therapeutic strategies for allergic diseases, *Nature*, **1999**, 402, B31-B38.
28. Rivera, J., Olivera, A., A current understanding of FcεRI-dependent mast cell activation, *Curr. Allergy Asthm. Rep.*, **2008**, 8, 14-20.
29. Minoguchi, K., Benhamou, M., Swaim, W.D., Kawakami, Y., Kawakami, T., Siraganian, R.P., Activation of protein-tyrosine kinase $p72^{syk}$ by FcεRI aggregation in rat basophilic leukemia-cells. $p72^{syk}$ is a minor component but the major protein-tyrosine kinase of pp72, *J. Biol. Chem.*, **1994**, 269, 16902-16908.
30. Gonzalez-Espinosa, C., Medina-Tamayo, J., Sanchez-Miranda, E., Benitez-Garrido, J.P., Avila-Hernandez, A.M., Padilla, A., Garcia-Roman, J., Signaling through the high affinity IgE receptor and conditions able to modify IgE-antigen responsiveness of mast cells, *Sign. Transd.*, **2007**, 7, 402-414.
31. Draber, P., Draberova, L., Lipid rafts in mast cell signaling, *Mol. Immunol.*, **2001**, 38, 1247-1252.
32. Field, K.A., Holowka, D., Baird, B., Compartmentalized activation of the high affinity immunoglobulin E receptor within membrane domains, *J. Biol. Chem.*, **1997**, 272, 4276-4280.
33. Wange, R.L., Isakov, N., Burke, T.R., Otaka, A., Roller, P.P., Watts, J.D., Aebersold, R., Samelson, L.E., $F_2(Pmp)_2$-TAMζ_3, a novel competitive inhibitor of the binding of ZAP-70 to the T cell antigen receptor, blocks early T cell signaling, *J. Biol. Chem.*, **1995**, 270, 944-948.
34. Deindl, S., Kadlecek, T.A., Brdicka, T., Cao, X., Weiss, A., Kuriyan, J., Structural basis for the inhibition of tyrosine kinase activity of ZAP-70, *Cell*, **2007**, 129, 735-746.
35. Reth, M., Antigen receptor tail clue, *Nature*, **1989**, 338, 383-384.
36. Cambier, J.C., Daeron, M., Fridman, W., Gergely, J., Kinet, J.P., Klausner, R., Lynch, R., Malissen, B., Pecht, I., Reinherz, E., Ravetch, J., Reth, M., Samelson, L., Sandor, M.,

Schreiber, A., Seed, B., Terhorst, C., Vandewinkel, J., Weiss, A., New nomenclature for the Reth motif (or ARH1/TAM/ARAM/YXXL), *Immunol. Today*, **1995**, 16, 110-110.
37. Lin, S.Q., Cicala, C., Scharenberg, A.M., Kinet, J.P., The FcεRIβ subunit functions as an amplifier of FcεRIγ-mediated cell activation signals, *Cell*, **1996**, 85, 985-995.
38. Shiue, L., Zoller, M.J., Brugge, J.S., Syk is activated by phosphotyrosine-containing peptides representing the tyrosine-based activation motifs of the high-affinity receptor for IgE, *J. Biol. Chem.*, **1995**, 270, 10498-10502.
39. Taylor, J.A., Karas, J.L., Ram, M.K., Green, O.M., Seideldugan, C., Activation of the High-Affinity Immunoglobulin-E receptor FcεRI in RBL-2H3 cells is inhibited by Syk SH2 domains, *Mol. Cell. Biol.*, **1995**, 15, 4149-4157.
40. Copley, R.R., Ponting, C.P., Schultz, J., Bork, P., Sequence analysis of multidomain proteins: Past perspectives and future directions, *Advances in Protein Chemistry*, **2003**, 61, 75-98.
41. Itoh, M., Nacher, J.C., Kuma, K., Goto, S., Kanehisa, M., Evolutionary history and functional implications of protein domains and their combinations in eukaryotes, *Genome Biol.*, **2007**, 8, R121.
42. Sadowski, I., Stone, J.C., Pawson, T., A noncatalytic domain conserved among cytoplasmic protein-tyrosine kinases modifies the kinase function and transforming activity of Fujinami Sarcoma virus $P130^{gag\text{-}fps}$, *Mol. Cell. Biol.*, **1986**, 6, 4396-4408.
43. Machida, K., Mayer, B.J., The SH2 domain: versatile signaling module and pharmaceutical target, *Biochim. Biophys. Acta - Proteins and Proteomics*, **2005**, 1747, 1-25.
44. Parsons, S.J., Parsons, J.T., Src family kinases, key regulators of signal transduction, *Oncogene*, **2004**, 23, 7906-7909.
45. Roskoski, R., Src protein-tyrosine kinase structure and regulation, *Biochem. Biophys. Res. Commun.*, **2004**, 324, 1155-1164.
46. Mandine, E., Jean-Baptiste, V., Vayssière, B., Gofflo, D., Bénard, D., Sarubbi, E., Deprez, P., Baron, R., Superti-Furga, G., Lesuisse, D., High-affinity Src-SH2 ligands which do not activate Tyr^{527}-phosphorylated Src in an experimental in vivo system, *Biochem. Biophys. Res. Commun.*, **2002**, 298, 185–192.
47. Musacchio, A., Noble, M., Pauptit, R., Wierenga, R., Saraste, M., Crystal-structure of a Src-homology-3 (SH3) domain, *Nature*, **1992**, 359, 851-855.
48. Koch, C.A., Anderson, D., Moran, M.F., Ellis, C., Pawson, T., SH2 and SH3 domains - Elements that control interactions of cytoplasmic signaling proteins, *Science*, **1991**, 252, 668-674.
49. Waksman, G., Kominos, D., Robertson, S.C., Pant, N., Baltimore, D., Birge, R.B., Cowburn, D., Hanafusa, H., Mayer, B.J., Overduin, M., Resh, M.D., Rios, C.B., Silverman, L., Kuriyan, J., Crystal-structure of the phosphotyrosine recognition domain SH2 of v-src complexed with tyrosine-phosphorylated peptides, *Nature*, **1992**, 358, 646-653.
50. Waksman, G., Shoelson, S.E., Pant, N., Cowburn, D., Kuriyan, J., Binding of a high affinity phosphotyrosyl peptide to the Src SH2 domain: crystal structures of the complexed and peptide-free forms, *Cell*, **1993**, 72, 779-790.
51. Brugge, J.S., New intracellular targets for therapeutic drug design, *Science*, **1993**, 260, 918-919.
52. Birge, R.B., Hanafusa, H., Closing in on SH2 specificity, *Science*, **1993**, 262, 1522-1523.
53. Cohen, G.B., Ren, R.B., Baltimore, D., Modular binding domains in signal-transduction proteins, *Cell*, **1995**, 80, 237-248.
54. Pawson, T., Protein modules and signaling networks, *Nature*, **1995**, 373, 573-580.
55. Pawson, T., Scott, J.D., Signaling through scaffold, anchoring, and adaptor proteins, *Science*, **1997**, 278, 2075-2080.
56. Sawyer, T.K., Src homology-2 domains: Structure, mechanisms, and drug discovery, *Biopolymers*, **1998**, 47, 243-261.
57. Vidal, M., Gigoux, V., Garbay, C., SH2 and SH3 domains as targets for anti-proliferative agents, *Crit. Rev. Oncol. Hemat.*, **2001**, 40, 175–186.

58. Pawson, T., Gish, G.D., Nash, P., SH2 domains, interaction modules and cellular wiring, *Trends Cell Biol.*, **2001**, 11, 504-511.
59. Eck, M.J., Shoelson, S.E., Harrison, S.C., Recognition of a high-affinity phosphotyrosyl peptide by the Src homology-2 domain of $p56^{lck}$, *Nature*, **1993**, 362, 87-91.
60. Bradshaw, J.M., Waksman, G., Molecular recognition by SH2 domains, *Advances in Protein Chemistry*, **2003**, 61, 161-210.
61. Grucza, R.A., Bradshaw, J.M., Futterer, K., Waksman, G., SH2 domains: From structure to energetics, a dual approach to the study of structure-function relationships, *Med. Res. Rev.*, **1999**, 19, 273-293.
62. Bradshaw, J.M., Waksman, G., Calorimetric examination of high-affinity Src SH2 domain-tyrosyl phosphopeptide binding: Dissection of the phosphopeptide sequence specificity and coupling energetics, *Biochemistry*, **1999**, 38, 5147-5154.
63. Bradshaw, J.M., Mitaxov, V., Waksman, G., Investigation of phosphotyrosine recognition by the SH2 domain of the Src kinase, *J. Mol. Biol.*, **1999**, 293, 971-985.
64. Grucza, R.A., Bradshaw, J.M., Mitaxov, V., Waksman, G., Role of electrostatic interactions in SH2 domain recognition: Salt-dependence of tyrosyl-phosphorylated peptide binding to the tandem SH2 domain of the Syk kinase and the single SH2 domain of the Src kinase, *Biochemistry*, **2000**, 39, 10072-10081.
65. De Mol, N.J., Gillies, M.B., Fischer, M.J.E., Experimental and calculated shift in pK_a upon binding of phosphotyrosine peptide to the SH2 domain of $p56^{lck}$, *Bioorg. Med. Chem.*, **2002**, 10, 1477-1482.
66. Hubbard, S.R., Mohammadi, M., Schlessinger, J., Autoregulatory mechanisms in protein-tyrosine kinases, *J. Biol. Chem.*, **1998**, 273, 11987-11990.
67. Ottinger, E.A., Botfield, M.C., Shoelson, S.E., Tandem SH2 domains confer high specificity in tyrosine kinase signaling, *J. Biol. Chem.*, **1998**, 273, 729-735.
68. Futterer, K., Wong, J., Grucza, R.A., Chan, A.C., Waksman, G., Structural basis for Syk tyrosine kinase ubiquity in signal transduction pathways revealed by the crystal structure of its regulatory SH2 domains bound to a dually phosphorylated ITAM peptide, *J. Mol. Biol.*, **1998**, 281, 523-537.
69. Atwell, S., Adams, J.M., Badger, J., Buchanan, M.D., Feil, I.K., Froning, K.J., Gao, X., Hendle, J., Keegan, K., Leon, B.C., Muller-Dieckmann, H.J., Nienaber, V.L., Noland, B.W., Post, K., Rajashankar, K.R., Ramos, A., Russell, M., Burley, S.K., Buchanan, S.G., A novel mode of Gleevec binding is revealed by the structure of spleen tyrosine kinase, *J. Biol. Chem.*, **2004**, 279, 55827-55832.
70. Arias-Palomo, E., Recuero-Checa, M.A., Bustelo, X.R., Llorca, O., 3D structure of Syk kinase determined by single-particle electron microscopy, *Biochim. Biophys. Acta - Proteins and Proteomics*, **2007**, 1774, 1493-1499.
71. Hatada, M.H., Lu, X.D., Laird, E.R., Green, J., Morgenstern, J.P., Lou, M.Z., Marr, C.S., Phillips, T.B., Ram, M.K., Theriault, K., Zoller, M.J., Karas, J.L., Molecular basis for interaction of the protein tyrosine kinase Zap-70 with the T-cell receptor, *Nature*, **1995**, 377, 32-38.
72. Folmer, R.H.A., Geschwindner, S., Xue, Y., Crystal structure and NMR studies of the apo SH2 domains of ZAP-70: two bikes rather than a tandem, *Biochemistry*, **2002**, 41, 14176-14184.
73. Jin, L., Pluskey, S., Petrella, E.C., Cantin, S.M., Gora, J.C., Rynkiewicz, M.J., Pandey, P., Strickler, J.E., Babine, R.E., Weaver, D.T., Seidl, K.J., The three-dimensional structure of the ZAP-70 kinase domain in complex with staurosporine. Implications for the design of selective inhibitors, *J. Biol. Chem.*, **2004**, 279, 42818-42825.
74. Au-Yeung, B.B., Deindl, S., Hsu, L.Y., Palacios, E.H., Levin, S.E., Kuriyan, J., Weiss, A., The structure, regulation, and function of ZAP-70, *Immunol. Rev.*, **2009**, 228, 41-57.
75. Brdicka, T., Kadlecek, T.A., Roose, J.P., Pastuszak, A.W., Weiss, A., Intramolecular regulatory switch in ZAP-70: Analogy with receptor tyrosine kinases, *Mol. Cell. Biol.*, **2005**, 25, 4924-4933.

76. Magistrelli, G., Bosotti, R., Valsasina, B., Visco, C., Perego, R., Toma, S., Acuto, O., Isacchi, A., Role of the src homology 2 domains and interdomain regions in ZAP-70 phosphorylation and enzymatic activity, *Eur. J. Biochem.*, **1999**, 266, 1166-1173.
77. Visco, C., Magistrelli, G., Bosotti, R., Perego, R., Rusconi, L., Toma, S., Zamai, M., Acuto, O., Isacchi, A., Activation of Zap-70 tyrosine kinase due to a structural rearrangement induced by tyrosine phosphorylation and/or ITAM binding, *Biochemistry*, **2000**, 39, 2784-2791.
78. Narula, S.S., Yuan, R.W., Adams, S.E., Green, O.M., Green, J., Philips, T.B., Zydowskyt, L.D., Botfield, M.C., Hatada, M., Laird, E.R., Zoller, M.J., Karas, J.L., Dalgarnol, D.C., Solution structure of the C-terminal SH2 domain of the human tyrosine kinase Syk complexed with a phosphotyrosine pentapeptide, *Structure*, **1995**, 3, 1061-1073.
79. Grucza, R.A., Fütterer, K., Chan, A.C., Waksman, G., Thermodynamic study of the binding of the tandem-SH2 domain of the Syk kinase to a dually phosphorylated ITAM peptide: evidence for two conformers, *Biochemistry*, **1999**, 38, 5024-5033.
80. De Mol, N.J., Catalina, M.I., Dekker, F.J., Fischer, M.J.E., Heck, A.J., Liskamp, R.M.J., Protein flexibility and ligand rigidity: a thermodynamic and kinetic study of ITAM-based ligand binding to Syk tandem SH2, *ChemBioChem*, **2005**, 6, 2261-2270.
81. Catalina, I., Fischer, M.J.E., Dekker, F.J., Liskamp, R.M.J., Heck, A.J.R., Binding of a diphosphorylated-ITAM peptide to spleen tyrosine kinase (Syk) induces distal conformational changes: a hydrogen exchange mass spectrometry study, *J. Am. Soc. Mass. Spectrom.*, **2005**, 16, 1039–1051.
82. Kumaran, S., Grucza, R.A., Waksman, G., The tandem Src homology 2 domain of the Syk kinase: a molecular device that adapts to interphosphotyrosine distances, *Proc. Natl. Acad. Sci. U.S.A.*, **2003**, 100, 14828–14833.
83. Couture, C., Williams, S., Gauthier, N., Tailor, P., Mustelin, T., Role of Tyr518 and Tyr519 in the regulation of catalytic activity and substrate phosphorylation by Syk protein-tyrosine kinase, *Eur. J. Biochem.*, **1997**, 246, 447-451.
84. Zhang, J., Billingsley, M.L., Kincaid, R.L., Siraganian, R.P., Phosphorylation of Syk activation loop tyrosines is essential for Syk function. An in vivo study using a specific anti-Syk activation loop phosphotyrosine antibody, *J. Biol. Chem.*, **2000**, 275, 35442-35447.
85. Sada, K., Takano, T., Yanagi, S., Yamamura, H., Structure and function of Syk protein-tyrosine kinase, *J. Biochem.*, **2001**, 130, 177-186.
86. Zhang, J., Kimura, T., Siraganian, R.P., Mutations in the activation loop tyrosines of protein tyrosine kinase Syk abrogate intracellular signaling but not kinase activity, *J. Immunol.*, **1998**, 161, 4366-4374.
87. Watts, J.D., Affolter, M., Krebs, D.L., Wange, R.L., Samelson, L.E., Aebersold, R., Identification by electrospray-ionization mass-spectrometry of the sites of tyrosine phosphorylation-induced in activated jurkat T-cells on the protein-tyrosine kinase Zap-70, *J. Biol. Chem.*, **1994**, 269, 29520-29529.
88. Zhang, Y.J., Oh, H., Burton, R.A., Burgner, J.W., Geahlen, R.L., Post, C.B., Tyr130 phosphorylation triggers Syk release from antigen receptor by long-distance conformational uncoupling, *Proc. Natl. Acad. Sci. U.S.A.*, **2008**, 105, 11760-11765.
89. Keshvara, L.M., Isaacson, C., Harrison, M.L., Geahlen, R.L., Syk activation and dissociation from the B-cell antigen receptor is mediated by phosphorylation of tyrosine 130, *J. Biol. Chem.*, **1997**, 272, 10377-10381.
90. Adachi, T., Wienands, J., Tsubata, T., Kurosaki, T., Interdomain A is crucial for ITAM-dependent and -independent regulation of Syk, *Biochem. Biophys. Res. Commun.*, **2007**, 364, 111-117.
91. Oliver, J.M., Burg, D.L., Wilson, B.S., Mclaughlin, J.L., Geahlen, R.L., Inhibition of Mast-Cell FcεRI-mediated signaling and effector function by the Syk-selective inhibitor, piceatannol, *J. Biol. Chem.*, **1994**, 269, 29697-29703.

92. Yamamoto, N., Takeshita, K., Shichijo, M., Kokubo, T., Sato, M., Nakashima, K., Ishimori, M., Nagai, H., Li, Y.F., Yura, T., Bacon, K.B., The orally available spleen tyrosine kinase inhibitor 2-[7-(3,4-dimethoxyphenyl)-imidazo[1,2-c]pyrimidin-5-ylamino]-nicotinamide dihydrochloride (BAY 61-3606) blocks antigen-induced airway inflammation in rodents, *J. Pharmacol. Exp. Ther.*, **2003**, 306, 1174-1181.
93. Villasenor, A.G., Kondru, R., Ho, H., Wang, S., Papp, E., Shaw, D., Barnett, J.W., Browner, M.F., Kuglstatter, A., Structural insights for design of potent Spleen tyrosine kinase inhibitors from crystallographic analysis of three inhibitor complexes, *Chem. Biol. Drug Des.*, **2009**, 73, 466-470.
94. Braselmann, S., Taylor, V., Zhao, H.R., Wang, S., Sylvain, C., Baluom, M., Qu, K.B., Herlaar, E., Lau, A., Young, C., Wong, B.R., Lovell, S., Sun, T., Park, G., Argade, A., Jurcevic, S., Pine, P., Singh, R., Grossbard, E.B., Payan, D.G., Masuda, E.S., R406, an orally available spleen tyrosine kinase inhibitor blocks Fc receptor signaling and reduces immune complex-mediated inflammation, *J. Pharmacol. Exp. Ther.*, **2006**, 319, 998-1008.
95. Hisamichi, H., Naito, R., Toyoshima, A., Kawano, N., Ichikawa, A., Orita, A., Orita, M., Hamada, N., Takeuchi, M., Ohta, M., Tsukamoto, S.I., Synthetic studies on novel Syk inhibitors. Part 1: Synthesis and structure-activity relationships of pyrimidine-5-carboxamide derivatives, *Bioorg. Med. Chem.*, **2005**, 13, 4936-4951.
96. Rossi, A.B., Herlaar, E., Braselmann, S., Huynh, S., Taylor, V., Frances, R., Issakani, S.D., Argade, A., Singh, R., Payan, D.G., Masuda, E.S., Identification of the Syk kinase inhibitor R112 by a human mast cell screen, *J. Allergy Clin. Immunol.*, **2006**, 118, 749-755.
97. Hirabayashi, A., Mukaiyama, H., Kobayashi, H., Shiohara, H., Nakayama, S., Ozawa, M., Miyazawa, K., Misawa, K., Ohnota, H., Isaji, M., A novel Syk family kinase inhibitor: Design, synthesis, and structure–activity relationship of 1,2,4-triazolo[4,3-c]pyrimidine and 1,2,4-triazolo[1,5-c]pyrimidine derivatives, *Bioorg. Med. Chem.*, **2008**, 16, 7347–7357.
98. Revesz, L., Bonne, F., Manning, U., Zuber, J.F., Solid phase synthesis of a biased mini tetrapeptoid-library for the discovery of monodentate ITAM mimics as ZAP-70 inhibitors, *Bioorg. Med. Chem. Lett.*, **1998**, 8, 405-408.
99. Revesz, L., Blum, E., Manning, U., Demange, J., Widmer, A., Zuber, J., Non-peptide ITAM mimics as ZAP-70 antagonists, *Bioorg. Med. Chem. Lett.*, **1997**, 7, 2875-2878.
100. Vu, C.B., Corpuz, E.G., Merry, T.J., Pradeepan, S.G., Bartlett, C., Bohacek, R.S., Botfield, M.C., Eyermann, C.J., Lynch, B.A., MacNeil, I.A., Ram, M.K., Van Schravendijk, M.R., Violette, S., Sawyer, T.K., Discovery of potent and selective SH2 inhibitors of the tyrosine kinase ZAP-70, *J. Med. Chem.*, **1999**, 42, 4088-4098.
101. Vu, C.B., Corpuz, E.G., Pradeepan, S.G., Violette, S., Bartlett, C., Sawyer, T.K., Nonpeptidic SH2 inhibitors of the tyrosine kinase ZAP-70, *Bioorg. Med. Chem. Lett.*, **1999**, 9, 3009-3014.
102. Bu, J.Y., Shaw, A.S., Chan, A.C., Analysis of the interaction of ZAP-70 and syk protein-tyrosine kinases with the T-cell antigen receptor by plasmon resonance, *Proc. Natl. Acad. Sci. U.S.A.*, **1995**, 92, 5106-5110.
103. Chen, T., Repetto, B., Chizzonite, R., Pullar, C., Burghardt, C., Dharm, E., Zhao, A.C., Carroll, R., Nunes, P., Basu, M., Danho, W., Visnick, M., Kochan, J., Waugh, D., Gilfillan, A.M., Interaction of phosphorylated FcεRIγ immunoglobulin receptor tyrosine activation motif-based peptides with dual and single SH2 domains of $p72^{syk}$. Assessment of binding parameters and real, time binding kinetics, *J. Biol. Chem.*, **1996**, 271, 25308-25315.
104. Niimi, T., Orita, M., Okazawa-Igarashi, M., Sakashita, H., Kikuchi, K., Ball, E., Ichikawa, A., Yamagiwa, Y., Sakamoto, S., Tanaka, A., Tsukamoto, S., Fujita, S., Tatsuta, K., Maeda, Y., Chikauchi, K., Design and synthesis of non-peptidic inhibitors for the Syk C-terminal SH2 domain based on structure-based in-silico screening, *J. Med. Chem.*, **2001**, 44, 4737-4740.
105. Ruijtenbeek, R., Kruijtzer, J.A.W., van de Wiel, W., Fischer, M.J.E., Fluck, M., Redegeld, F.A.M., Liskamp, R.M.J., Nijkamp, F.P., Peptoid-peptide hybrids that bind Syk SH2 domains involved in signal transduction, *ChemBioChem*, **2001**, 2, 171-179.

106. Dekker, F.J., de Mol, N.J., Fischer, M.J.E., Liskamp, R.M.J., Amino propynyl benzoic acid building block in rigid spacers of divalent ligands binding to the Syk SH2 domains with equally high affinity as the natural ligand, *Bioorg. Med. Chem. Lett.*, **2003**, 13, 1241-1244.
107. Dekker, F.J., de Mol, N.J., van Ameijde, J., Fischer, M.J.E., Ruijtenbeek, R., Redegeld, F.A.M., Liskamp, R.M.J., Replacement of the intervening amino acid sequence of a Syk-binding diphosphopeptide by a nonpeptide spacer with preservation of high affinity, *ChemBioChem*, **2002**, 3, 238-242.
108. Mayer, G., Heckel, A., Biologically active molecules with a "light switch", *Angew. Chem. Int. Ed.*, **2006**, 45, 4900-4921.
109. Ulysse, L., Cubillos, J., Chmielewski, J., Photoregulation of cyclic peptide conformation, *J. Am. Chem. Soc.*, **1995**, 117, 8466-8467.
110. Ulysse, L., Chmielewski, J., The synthesis of a light-switchable amino acid for inclusion into conformationally mobile peptides, *Bioorg. Med. Chem. Lett.*, **1994**, 4, 2145-2146.
111. Gorostiza, P., Isacoff, E.Y., Optical switches for remote and noninvasive control of cell signaling, *Science*, **2008**, 322, 395-399.
112. Renner, C., Kusebauch, U., Loeweneck, M., Milbradt, A.G., Moroder, L., Azobenzene as photoresponsive conformational switch in cyclic peptides, *J. Pept. Res.*, **2005**, 65, 4-14.
113. Renner, C., Moroder, L., Azobenzene as conformational switch in model peptides, *ChemBioChem*, **2006**, 7, 868-878.
114. Rau, H., Azo compounds, in *Studies in organic chemistry 40: Photochromism, molecules and systems*, Bouas-Laurent, H., Editor, **1990**, Elsevier: Amsterdam, 165-192.
115. Boulegue, C., Loweneck, M., Renner, C., Moroder, L., Redox potential of azobenzene as an amino acid residue in peptides, *ChemBioChem*, **2007**, 8, 591-594.
116. Sadovski, O., Beharry, A.A., Zhang, F., Woolley, G.A., Spectral tuning of azobenzene photoswitches for biological applications, *Angew. Chem. Int. Ed.*, **2009**, 48, 1484-1486.
117. Aemissegger, A., Krautler, V., van Gunsteren, W.F., Hilvert, D., A photoinducible beta-hairpin, *J. Am. Chem. Soc.*, **2005**, 127, 2929-2936.
118. Beharry, A.A., Sadovski, O., Woolley, G.A., Photo-control of peptide conformation on a timescale of seconds with a conformationally constrained, blue-absorbing, photo-switchable linker, *Org. Biomol. Chem.*, **2008**, 6, 4323-4332.
119. Schutt, M., Krupka Simone, S., Milbradt Alexander, G., Deindl, S., Sinner Eva, K., Oesterhelt, D., Renner, C., Moroder, L., Photocontrol of cell adhesion processes: model studies with cyclic azobenzene-RGD peptides, *Chem. Biol.*, **2003**, 10, 487-490.
120. Feringa, B.L., The art of building small: From molecular switches to molecular motors, *J. Org. Chem.*, **2007**, 72, 6635-6652.
121. Tian, H., Wang, S., Photochromic bisthienylethene as multi-function switches, *Chem. Commun.*, **2007**, 781-792.
122. Mammen, M., Choi, S.K., Whitesides, G.M., Polyvalent interactions in biological systems: Implications for design and use of multivalent ligands and inhibitors, *Angew. Chem. Int. Ed.*, **1998**, 37, 2755-2794.
123. Pieters, R.J., Maximising multivalency effects in protein-carbohydrate interactions, *Org. Biomol. Chem.*, **2009**, 7, 2013-2025.
124. Pieters, R.J., Rijkers, D.T.S., Liskamp, R.M.J., Application of the 1,3-dipolar cycloaddition reaction in chemical biology: Approaches toward multivalent carbohydrates and peptides and peptide-based polymers, *QSAR Comb. Sci.*, **2007**, 26, 1181-1190.
125. Darbre, T., Reymond, J.L., Peptide dendrimers as artificial enzymes, receptors, and drug-delivery agents, *Acc. Chem. Res.*, **2006**, 39, 925-934.
126. Niederhafner, P., Sebestik, J., Jezek, J., Peptide dendrimers, *J. Pept. Sci.*, **2005**, 11, 757-788.
127. Sadler, K., Tam, J.P., Peptide dendrimers: applications and synthesis, *Rev. Mol. Biotechnol.*, **2002**, 90, 195-229.
128. Dijkgraaf, I., Rijnders, A.Y., Soede, A., Dechesne, A.C., van Esse, G.W., Brouwer, A.J., Corstens, F.H.M., Boerman, O.C., Rijkers, D.T.S., Liskamp, R.M.J., Synthesis of DOTA-

conjugated multivalent cyclic-RGD peptide dendrimers via 1,3-dipolar cycloaddition and their biological evaluation: implications for tumor targeting and tumor imaging purposes, *Org. Biomol. Chem.*, **2007**, 5, 935-944.
129. Zhang, Y., Yu, L.C., Microinjection as a tool of mechanical delivery, *Curr. Opin. Biotechnol.*, **2008**, 19, 506-510.
130. Hecker, S.J., Erion, M.D., Prodrugs of phosphates and phosphonates, *J. Med. Chem.*, **2008**, 51, 2328-2345.
131. Mandal, P.K., Liao, W.S.L., McMurray, J.S., Synthesis of Phosphatase-Stable, Cell-Permeable Peptidomimetic Prodrugs That Target the SH2 Domain of Stat3, *Org. Lett.*, **2009**, 11, 3394-3397.
132. Gras-Masse, M., Lipid vector for the delivery of peptides towards intracellular pharmacological targets, *J. Mol. Recog.*, **2003**, 16, 234-239.
133. Kol, M.A., de Kroon, A.I.P.M., Killian, J.A., de Kruijff, B., Transbilayer movement of phospholipids in biogenic membranes, *Biochemistry*, **2004**, 43, 2673-2681.
134. Fischer, R., Fotin-Mleczek, M., Hufnagel, H., Brock, R., Break on through to the other side - Biophysics and cell biology shed light on cell-penetrating peptides, *ChemBioChem*, **2005**, 6, 2126 – 2142.
135. Herce, H.D., Garcia, A.E., Cell penetrating peptides: How do they do it?, *J. Biol. Phys.*, **2007**, 33, 345-356.
136. Vivès, E., Schmidt, J., Pèlegrin, A., Cell-penetrating and cell-targeting peptides in drug delivery, *Biochim. Biophys. Acta - Rev. Cancer*, **2008**, 1786, 126–138.
137. Howl, J., Nicholl, I.D., Jones, S., The many futures for cell-penetrating peptides: how soon is now?, *Biochem. Soc. Trans.*, **2007**, 35, 767-769.
138. Vives, E., Brodin, P., Lebleu, B., A truncated HIV-1 Tat protein basic domain rapidly translocates through the plasma membrane and accumulates in the cell nucleus, *J. Biol. Chem.*, **1997**, 272, 16010-16017.
139. Derossi, D., Joliot, A.H., Chassaing, G., Prochiantz, A., The third helix of the Antennapedia homeodomain translocates through biological-membranes, *J. Biol. Chem.*, **1994**, 269, 10444-10450.
140. Pooga, M., Hallbrink, M., Zorko, M., Langel, U., Cell penetration by transportan, *FASEB J.*, **1998**, 12, 67-77.
141. Mitchell, D.J., Kim, D.T., Steinman, L., Fathman, C.G., Rothbard, J.B., Polyarginine enters cells more efficiently than other polycationic homopolymers, *J. Pept. Res.*, **2000**, 56, 318-325.
142. Lundin, P., Johansson, H., Guterstam, P., Holm, T., Hansen, M., Langel, U., El Andaloussi, S., Distinct uptake routes of cell-penetrating peptide conjugates, *Bioconjugate Chem.*, **2008**, 19, 2535-2542.
143. Duchardt, F., Fotin-Mleczek, M., Schwarz, H., Fischer, R., Brock, R., A comprehensive model for the cellular uptake of cationic cell-penetrating peptides, *Traffic*, **2007**, 8, 848-866.
144. Henriques, S.T., Melo, M.N., Castanho, M.A.R.B., Cell-penetrating peptides and antimicrobial peptides: how different are they?, *Biochem. J.*, **2006**, 399, 1-7.
145. Matsuzaki, K., Yoneyama, S., Murase, O., Miyajima, K., Transbilayer transport of ions and lipids coupled with mastoparan X translocation, *Biochemistry*, **1996**, 35, 8450-8456.
146. Nakase, I., Tadokoro, A., Kawabata, N., Takeuchi, T., Katoh, H., Hiramoto, K., Negishi, M., Nomizu, M., Sugiura, Y., Futaki, S., Interaction of arginine-rich peptides with membrane-associated proteoglycans is crucial for induction of actin organization and macropinocytosis, *Biochemistry*, **2007**, 46, 492-501.
147. Poon, G.M.K., Gariepy, J., Cell-surface proteoglycans as molecular portals for cationic peptide and polymer entry into cells, *Biochem. Soc. Trans.*, **2007**, 35, 788-793.
148. Mueller, J., Kretzschmar, I., Volkmer, R., Boisguerin, P., Comparison of cellular uptake using 22 cell-penetrating peptides in 4 different cell lines, *Bioconjugate Chem.*, **2008**, 19, 2363-2374.

149. Morris, M.C., Depollier, J., Mery, J., Heitz, F., Divita, G., A peptide carrier for the delivery of biologically active proteins into mammalian cells, *Nat. Biotechnol.*, **2001**, 19, 1173-1176.
150. Loudet, A., Han, J., Barhoumi, R., Pellois, J.P., Burghardt, R.C., Burgess, K., Non-covalent delivery of proteins into mammalian cells, *Org. Biomol. Chem.*, **2008**, 6, 4516-4522.
151. Lundberg, P., El-Andaloussi, S., Sutlu, T., Johansson, H., Langel, U., Delivery of short interfering RNA using endosomolytic cell-penetrating peptides, *FASEB J.*, **2007**, 21, 2664-2671.

Chapter 2

A photoswitchable ITAM peptidomimetic: Synthesis and real time surface plasmon resonance (SPR) analysis of the effects of cis-trans isomerization on binding

Parts of this chapter have been published:

Kuil, J., van Wandelen, L.T.M., de Mol, N.J., Liskamp, R.M.J., A photoswitchable ITAM peptidomimetic: Synthesis and real time surface plasmon resonance (SPR) analysis of the effects of cis-trans isomerization on binding, *Bioorg. Med. Chem.*, **2008**, 16, 1393-1399

Abstract

The Syk protein plays an important role in immune receptor signaling. The Syk tandem SH2 domain (tSH2) – ITAM interaction is important for recruiting Syk to the receptor complex and for Syk kinase activation. A peptidomimetic ligand for tSH2 was synthesized in which a photoswitchable azobenzene moiety was incorporated. Such a photoswitchable moiety may regulate the distance between the two phosphotyrosine-containing ITAM sequences, which bind to tSH2. Different affinities of the cis – and trans isomer of the ligand were found by surface plasmon resonance (SPR). By *in situ* irradiation during SPR measurements the effect of the cis – trans isomerization on binding could be monitored in real time.

Introduction

The Spleen tyrosine kinase (Syk) protein takes part in a number of receptor signaling cascades.[1-6] It is involved in early events after activation of, for example, the IgE-, T-cell-, and B-cell receptors. Furthermore, it is involved in IL-15-receptor and integrin signaling. The role of Syk in the high affinity IgE receptor (FcεRI) signaling in mast cells and basophils is shown in Figure 1. FcεRI consists of an α-, β- and two γ-chains. The β- and γ-chains contain a specific intracellular sequence called the Immunoreceptor Tyrosine based Activation Motif (ITAM). The ITAM sequence consists of Tyr-Xxx-Xxx-(Leu/Ile)-$(Xxx)_{n=6-8}$-Tyr-Xxx-Xxx-(Leu/Ile), in which Xxx can be any amino acid. The underlined residues comprise the binding epitopes for the tandem SH2 (tSH2) domain of Syk, when tyrosine is phosphorylated. We have found that the intervening residues $(Xxx)_{n=6-8}$ (in FcεRIγ n = 7) were not essential for binding.[7,8]

Upon IgE stimulation of the receptor, the ITAM motif is diphosphorylated (γ-dpITAM). After this, Syk is recruited to the membrane by binding to γ-dpITAM (Figure 1). This results in a conformational change and Syk activation.[5] Further events involved in activation of the kinase domain are still subject of investigation. They include phosphorylation of tyrosine residues in the linker region between the tSH2 and kinase domains of Syk, and in the kinase domain itself.[5] Syk activation eventually leads to cell degranulation and release of mediators. Overstimulation of this pathway leads to allergic responses and therefore Syk is an interesting target for potential anti-allergic therapy.

The relative orientation of the SH2 domains in tSH2 displays remarkable conformational flexibility. Recently, we have found that binding of Syk tSH2 to an ITAM peptide causes a significant change in the dynamics of tSH2.[1,9] This change could imply that a fixation in the inter SH2 distance is necessary for Syk activation by ITAM binding. To gain more insight into the functioning of Syk tSH2, we decided to take advantage of a photoswitchable building block and incorporate this into the ITAM sequence.

Azobenzene as part of (4-aminomethyl)phenylazobenzoic acid (AMPB) is the most widely used photoswitch because of its fast and fully reversible photoisomerization.[10-12] Moreover, the synthesis of AMPB is well described and the cis isomer is relatively

stable in solution, when not exposed to light. AMPB is compatible with solid phase peptide synthesis and can easily be incorporated into a peptide sequence.

Binding of the cis – and trans isomers of the photoswitch containing ITAM mimic was determined using surface plasmon resonance (SPR). In a convenient approach, the cis – trans transition and its effect on binding could be monitored in real time using *in situ* irradiation in the SPR measuring cell.

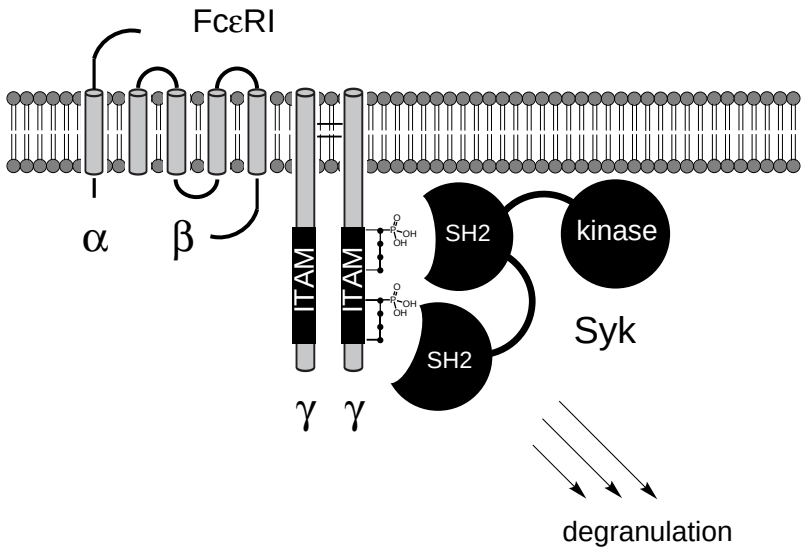

Figure 1. Recruitment of Syk to the diphosphorylated γ-ITAM of FcεRI results in activation of its kinase domain and ultimately degranulation.

Results and discussion

The length of the seven intervening amino acids in γ-ITAM, which are not essential for binding, is 14.1-16.4 Å, according to the X-ray structure.[13] The photoswitch AMPB is only 6.2 Å in the cis – and 12.0 Å in the trans configuration.[14,15] Therefore, an extra glycine residue was added to each side of AMPB and in this way a linker of 18.6 Å in the trans configuration was obtained. The linker length, including the two glycine residues, is only 7.2 Å in the cis configuration.

For synthesis of the Fmoc protected azobenzene containing building block **9** (Scheme 1) a literature procedure was adapted.[12,16,17] First, (4-amino)benzylamine was selectively protected using Fmoc-OSu to yield the Fmoc protected amine **3**. Initially, it was attempted to synthesize AMPB from 4-nitrobenzoic acid tert-butyl protected as is described in the literature.[12,17] After the tert-butyl protection, the nitro group was converted into a hydroxylamine using activated zinc dust. However, in our hands under these conditions also the tert-butyl ester was removed, possibly due to traces of HCl left in the zinc after activation, resulting in the undesired 4-hydroxylaminebenzoic acid. Therefore, 4-nitrobenzoic acid (**4**) was instead allyl protected and now the preparation of hydroxylamine allylester **6** went smoothly. Next, hydroxylamine **6** was treated with $FeCl_3$ to produce the corresponding nitroso compound **7**. Due to the instability of this compound, it was immediately used in the condensation reaction with Fmoc-protected amine **3**. The allyl group was easily removed afterwards with $Pd(PPh_3)_4$ and phenylsilane as scavenger, which gave no undesired reduction of the azo group.

NMR spectra of 100% trans azobenzene moiety **9** and mixtures with cis and trans conformers revealed that a maximum cis content of 78% could be obtained for **9** upon irradiation with 366 nm light.

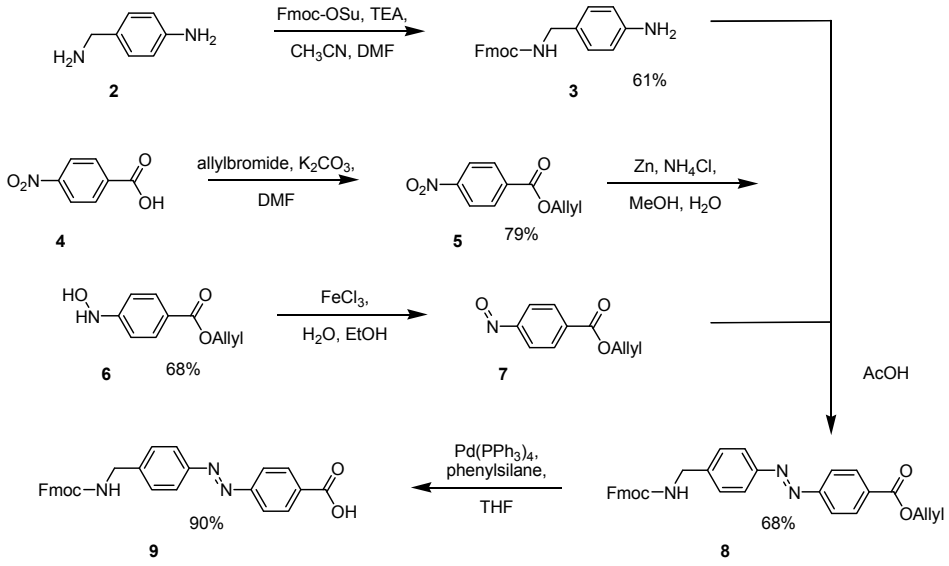

Scheme 1. Synthesis of the photoswitchable building block **9** (Fmoc-AMPB-OH).

The photoswitchable peptidomimetics **1a-b** (Figure 2) were synthesized using standard Fmoc/tBu chemistry including **9** as a building block. A small amount of TIS could be used in the cleavage cocktail without reducing the azobenzene. This was also recently observed by Hilvert et al.[18]

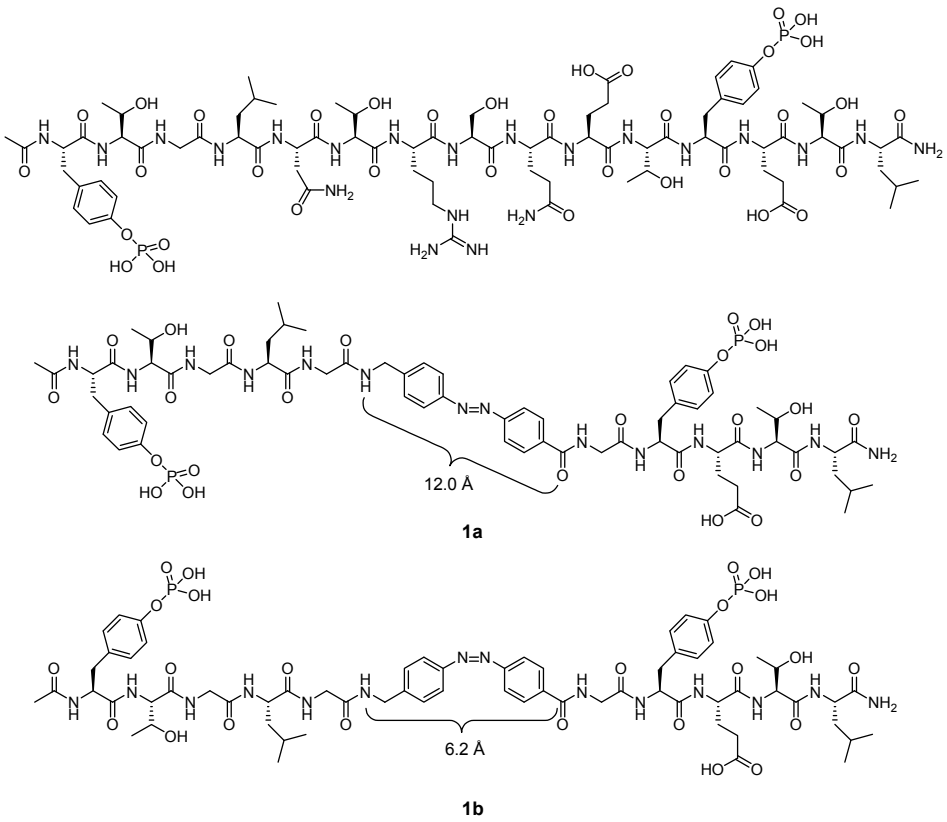

Figure 2. The native γ-ITAM peptide (derived from FcεRI) and the photoswitchable ITAM mimics **1a** and **1b**. The indicated distances are between the SH2 binding epitopes.[14,15]

After preparative RP-HPLC, a small amount of the peptide was dissolved in water to record UV-VIS spectra. First, the sample was irradiated with visible light to obtain trans isomer **1a**. NMR spectra of compounds **8** and **9** showed that the amount of trans isomer after irradiation with visible light was nearly 100%. This 100% trans isomer cannot be obtained by irradiation alone, due to partial overlap of the n-π* and π-π* transitions.[11] To reach 100% trans also thermal isomerization has to occur. After the spectrum of **1a** was measured, the sample was irradiated with 366 nm light for several time intervals

and spectra were recorded (Figure 3). This was repeated until no further change in the spectrum was observed after 120 s. The spectra showed three isosbestic points at 240, 286, and 403 nm.

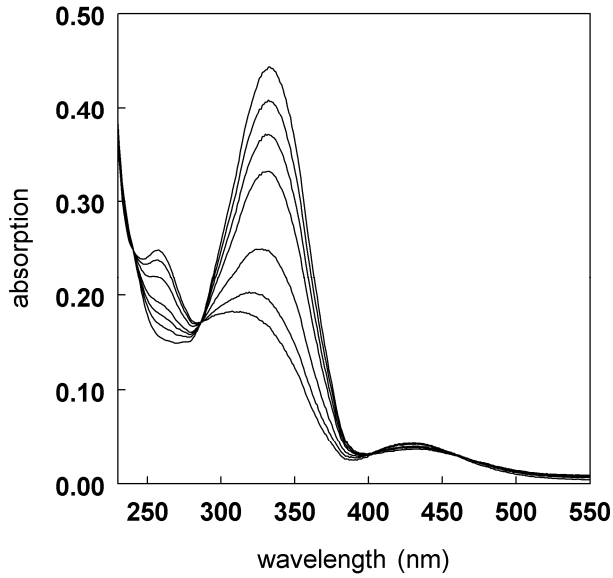

Figure 3. UV-absorption spectra of trans isomer **1a** (t = 0) upon increasing time of irradiation with 366 nm light. From top (335 nm) spectrum: t = 0 s, then t = 10, 20, 30, 60, 90 and 120 s.

Integration of the signals from NMR spectra of trans isomer **1a** (8.61 and 8.95 ppm) and cis isomer **1b** (8.49 and 8.79 ppm) revealed that a maximum cis isomer percentage of 60% could be reached upon irradiation with 366 nm light. The lower maximal cis percentage for the peptide as compared with its building block **9** has also been observed in other peptides and might be due to a higher degree of steric hindrance.[19]

The interaction between the two isomers and the Syk tSH2 protein was measured with SPR. Competition experiments were performed with the native ITAM peptide immobilized on the SPR chip as previously described.[1,7,8] Prior to addition, the competing ligand **1** was irradiated with UV light (366 nm) or visible light to give 60% cis isomer or 100% trans isomer, respectively. The tSH2 and the irradiated cis – or trans isomer in different concentrations were injected into the SPR cuvette and the binding of the tSH2 to the sensor chip was measured. From these measurements the dissociation

constants (K_D) could be calculated as described previously (Figure 4).[20] The K_D value of the trans isomer was 65 ± 8 nM and the observed K_D of the mixture containing 60% cis isomer was 146 ± 11 nM. Since the mixture still contained 40% trans isomer **1a**, the actual $K_{D,cis}$ can be calculated with Equation 1 (see Experimental section) and amounts to 860 nM.

Although the difference in affinity is more than 10-fold, these numbers show that the cis isomer, in which the SH2 domains are forced to be much closer to each other than in the complex with native ITAM, still has an affinity that is significantly higher than for a monovalent interaction, which has a K_D of 27 μM.[21] Syk tSH2 has a very flexible coiled-coil linker which connects the two SH2 domains.[1] Therefore, it accommodates fairly easy ITAM sequences containing different linker lengths. Furthermore, the glycine residues also have a moderate degree of flexibility, which can result in a somewhat larger linker length in the cis isomer **1b**, when bound to tSH2 compared with the free linker, which was used for initial modeling.

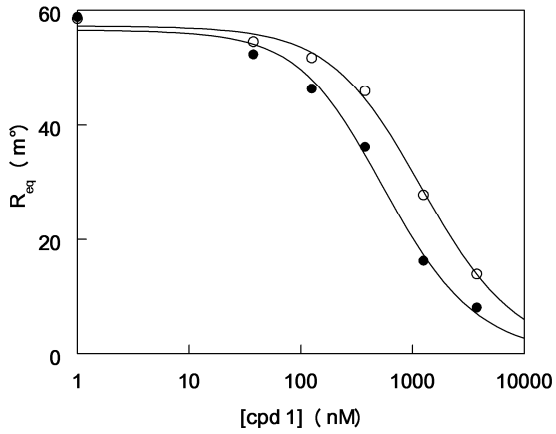

Figure 4. SPR competition experiments with Syk tSH2 (50 nM) in the presence of various concentrations of peptide **1** in cis (○) – or trans (●) configuration. The data are fitted and K_D derived as described.[20]

Now that different affinities for cis isomer **1b** and trans isomer **1a** have been established, it is interesting to monitor the conversion from cis to trans, and the effect on binding in real time with SPR. For this, an experiment was performed, making use of the convenient cuvette design of the IBISII SPR instrument, which makes it possible to

irradiate the sample during the SPR binding assay. First, the sensograms of only tSH2 and tSH2 with **1a** were recorded (Figure 5, top – and bottom curve). Then the mixture containing 60% **1b** with tSH2 was injected into the cuvette and after 800 s a steady state situation was almost reached (Figure 5, middle curve). Then the sample in the SPR cuvette was irradiated with visible light with the SPR instrument in the measuring mode. This resulted in a decrease of SPR signal, as the weaker binding **1b** was transformed to the stronger binding **1a**, displacing more Syk tSH2 from the sensor surface in the competition experiment. Within 500 s the signal reached the level of binding of only the trans isomer (bottom curve), showing that a 100% trans state could be obtained in reasonably short time. The cis – trans isomerization could be perfectly fitted by a mono-exponential function (not shown), showing pseudo first order kinetics, as was expected for a photochemical process with constant irradiation intensity.

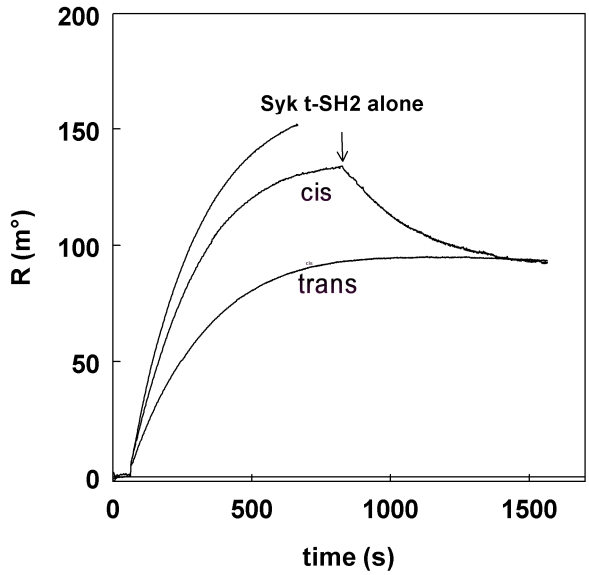

Figure 5. Effect of conversion of cis isomer **1b** to trans isomer **1a** in a SPR competition experiment with *in situ* irradiation with visible light. Top curve: Real time SPR signal for binding of 50 nM Syk tSH2 to immobilized native diphosphorylated γ-ITAM peptide on the SPR sensor surface. Bottom curve: SPR signal of 50 nM Syk tSH2 in the presence of 375 nM **1a**. Middle curve: 50 nM Syk tSH2 in the presence of 375 nM 60% **1b**, after 800 s the sample in the SPR cuvette was irradiated with visible light as indicated by the arrow.

Conclusions

In conclusion, we have shown that we can design and synthesize an ITAM peptidomimetic with significant difference in binding affinity between the cis – and trans isomer for Syk tSH2. Using SPR the change in binding affinity due to photoisomerization could be studied in real time. To our knowledge, this is the first report on the effect of isomerization of a photoswitchable ligand on binding to a protein that is monitored during an SPR binding assay. In the near future we aim to design a photoswitchable Syk tSH2 ligand, which can enter cells, having a larger difference in affinity between cis – and trans isomers. Such a ligand might be an interesting tool to study the possibility of instantaneously switching intracellular processes on and off by irradiation.

Experimental section

All chemicals were obtained from commercial sources and used without further purification. Solvents, which were used for the solid phase peptide synthesis, were stored over 4 Å molecular sieves, except for MeOH, which was stored over 3 Å molecular sieves. Prior to use, zinc was activated by stirring in 2% HCl for 30 min. The zinc was filtered, washed with water, ethanol and diethyl ether and dried under reduced pressure. The reactions were performed at room temperature unless stated otherwise. The reactions were monitored and the Rf values were determined by thin layer chromatography (TLC). The TLC plates were obtained from Merck and were coated with silica gel 60 F-254 (0.25 mm). The spots were visualized by UV light and ninhydrin staining. Solvents were removed under reduced pressure at a temperature of 40 °C. Column chromatography was performed with Silicycle UltraPure silica gels, SiliaFlash (pore size 60 Å, particle size distribution 40-63 μm). Photoisomerization was performed using a visible light emitting lamp (Schott/Paes KL-1500) in combination with a glass plate to filter the UV light or a 6 W 366 nm handheld TLC lamp (Konrad Benda).[14]

^{1}H NMR spectra were measured on a Varian Mercury plus 300 MHz spectrometer and the chemical shifts are given in ppm (δ) relative to TMS. ^{13}C NMR spectra were measured on a Varian Mercury plus 75 MHz spectrometer and the chemical shifts are given in ppm (δ) relative to $CDCl_3$ or DMSO-d_6. The ^{13}C NMR spectra were measured

using the attached proton test (APT). NMR spectra of peptide **1** were recorded on a Varian Inova 500 MHz spectrometer in H_2O/D_2O 9:1 and were calibrated on dioxane. UV-VIS spectra were recorded with a UV1 spectrophotometer (Thermo Electron Corporation). Analytical HPLC was measured on a Shimadzu HPLC system with a UV detector operating at 220 and 254 nm using an Alltech Adsorbosphere XL C8 90 Å 5 μm (250 × 4.6 mm) column. For the analytical HPLC a gradient from 100% buffer A (15 mM TEA in H_2O titrated at pH 6 with 85% H_3PO_4) to 100% buffer B (buffer A/CH_3CN 1:9) in 20 min was used. For the preparative HPLC a Gilson system with a UV detector operating at 220 and 254 nm equipped with an Alltech Adsorbosphere XL C8 90 Å 10 μm (250 × 22 mm) column was used. A gradient of 100% buffer A (0.1% TFA in H_2O/CH_3CN) to 100% buffer B (0.1% TFA in H_2O/CH_3CN) was used. For the use in HPLC buffers TEA was distilled over ninhydrin and KOH.

SPR measurements were performed on a double channel IBISII SPR instrument (Eco Chemie, Utrecht, The Netherlands) equipped with a CM 5 sensor chip (BIAcore AB, Uppsala, Sweden).

Molecular simulations

For all calculations YASARA (http://www.yasara.org) was used. PDB files of the linkers of compounds **1**a and **1b** were made using ChemDraw and Chem3D. These files were loaded in YASARA and a simulation cell, in which each axis was extended 5.0 Å from the molecule, was defined. The Amber99 forcefield was used and the temperature control was step-10 annealing, starting from 298 K and every 10 simulation steps the velocity of all atoms was reduced to 90%. Within approximately 2500 fs the temperature of 0 K was reached and the atoms almost did not move anymore. To be sure, the simulation was continued until 10000 fs was reached. All linkers were modeled as their N-terminal acetamide and C-terminal amide derivatives. All distances were measured from the N-terminal nitrogen atom to the C-terminal carbon atom after completion of the simulation of 10000 fs.

N-Fmoc(4-amino)benzylamine (3)

Compound **3** was synthesized according to a procedure described in the literature.[16] Yield: 10.47 g (30.42 mmol, 61%) of a white solid.

Allyl 4-nitrobenzoate (5)

Allylbromide (2.50 mL, 30 mmol) and K_2CO_3 (4.15 g, 30 mmol) were added to a solution of 4-nitrobenzoic acid (3.36 g, 20 mmol) in DMF (100 mL). After 5 min of stirring the solvent was removed under reduced pressure. The resulting solid was dissolved in CH_2Cl_2 and water. The organic layer was washed with 5% $NaHCO_3$ (2 ×), 1 M $KHSO_4$ and brine, dried over Na_2SO_4, filtered, and concentrated, yielding 3.30 g (15.9 mmol, 79%) of **5** as a brown solid. R_f = 0.61 (hexane/EtOAc 5:1) ^{1}H NMR ($CDCl_3$, 300 MHz) δ = 4.87–4.89 (d, 2H, OCH_2), 5.32–5.48 (2dd, 2H, CH_2), 6.00–6.12 (m, 1H, CH), 8.22-8.30 (m, 4H, Ar.) ^{13}C NMR ($CDCl_3$, 75 MHz) δ = 66.6 (OCH_2), 119.3 (CH*C*H_2), 123.7, 130.9, 135.7 and 150.7 (C_6H_4), 131.70 (*C*HCH$_2$), 164.5 (COO).

Allyl 4-hydroxylaminebenzoate (6)

Compound **6** was synthesized according to a procedure described in the literature.[22] Yield: 524 mg (2.71 mmol, 68%) of **6** as an orange solid. R_f = 0.35 (CH_2Cl_2/MeOH 98:2) ^{1}H NMR ($CDCl_3$, 300 MHz) δ = 4.74–4.76 (d, 2H, OCH_2), 5.22–5.39 (2dd, 2H, CH_2), 5.92–6.05 (m, 1H, CH), 6.92 + 7.20 (2 bs, 2H, NH + OH) 6.87–6.89 (m, 2H, Ar) 7.90–7.92 (d, H, Ar.) ^{13}C NMR ($CDCl_3$, 75 MHz) d = 65.9 (OCH_2), 113.4, 123.1, 131.5 and 154.9 (C_6H_4), 118.6 (CH*C*H_2), 132.8 (*C*HCH$_2$), 167.3 (COO).

Allyl 4-nitrosobenzoate (7)

Compound **7** was synthesized according to a procedure described in the literature.[23] The product was used immediately without further purification.

Allyl N-Fmoc-(4-aminomethyl)phenylazobenzoate (8)

Compound **8** was synthesized according to a procedure described in literature[17], except for the following. The reaction time was 16 h. The solvent was removed under reduced pressure and the resulting orange solid was dissolved in EtOAc and water. The organic layer was removed and the water layer was extracted with EtOAc (2 ×). During the extraction a slightly orange precipitate occurred. This precipitate was removed by filtration and the organic layers were combined, washed twice with brine, dried over Na_2SO_4 and filtered. The solvent was removed under reduced pressure and the resulting orange solid was purified by silica gel chromatography with CH_2Cl_2/MeOH 198:1 yielding 220 mg (0.42 mmol, 65%) of diazocompound **8** as an orange solid. R_f = 0.83 (CH_2Cl_2/MeOH 98:2). ^{1}H NMR ($CDCl_3$, 300 MHz) δ = 4.20–4.22 (t, 1H, CH Fmoc),

4.43–4.51 (2d, 4H, C*H*$_2$NH + CH2 Fmoc), 4.85–4.87 (d, 2H, COOC*H*$_2$CHCH$_2$), 5.25 (bs, 1H, NH), 5.29–5.46 (2dd, 2H, COOCH$_2$CHC*H*$_2$), 6.00–6.12 (m, 1H, COOCH$_2$C*H*CH$_2$), 7.24–7.60 (m, 6H, 2 ar + 4 Ar Fmoc), 7.74–7.77 (d, 2H, Ar Fmoc), 7.88–7.90 (d, 2H, Ar Fmoc), 7.92–7.95 (m, 4H, Ar), 8.19–8.22 (d, 2H, Ar). ^{13}C NMR ($CDCl_3$, 75 MHz) δ = 45.0 (CH_2NH), 47.6 (CH Fmoc), 66.1 (COO*C*H$_2$CHCH$_2$), 66.9 (CH2 Fmoc), 118.8 (COOCH$_2$CH*C*H$_2$), 120.2, 125.2, 127.3, 127.9, 141.6 and 144.1 (Ar Fmoc), 122.9, 128.4, 142.5 and 152.2 (*C*$_6$H$_4$CH$_2$NH), 123.7, 132.1, 132.3 and 155.4 (*C*$_6$H$_4$COO), 130.9 (COOCH$_2$*C*HCH$_2$), 156.4 (NHCOO), 165.9 (*C*OOCH$_2$CHCH$_2$).

N-Fmoc-(4-aminomethyl)phenylazobenzoic acid (Fmoc-AMPB-OH, 9)

Phenylsilane (56 µL, 0.46 mmol) was added to a solution of **8** (220 mg, 0.42 mmol) in THF (20 mL) and stirred under a nitrogen atmosphere. $Pd(PPh_3)_4$ (49.8 mg, 0.008 mmol) was added under an argon atmosphere and the reaction mixture was stirred for 2 h under a nitrogen atmosphere. The solvent was removed under reduced pressure and the resulting solid was dissolved in DMF and purified by silica gel chromatography with CH_2Cl_2/MeOH/CH_3COOH 97:2:1 yielding 180 mg (0.37 mmol, 90%) of Fmoc-AMPB-OH **9** as an orange solid. R_f = 0.65 (CH_2Cl_2/MeOH 95:5). ^{1}H NMR (DMSO-d$_6$, 300 MHz) δ = 4.25 (d, 2H, C*H*$_2$NH), 4.28–4.30 (d, 1H, CH Fmoc), 4.38–4.40 (d, 2H, CH_2 Fmoc), 7.31–7.36 (t, 2H, Ar), 7.40–7.46 (t, 4H, Ar Fmoc), 7.70–7.72 (d, 2H, Ar Fmoc), 7.89–7.97 (m, 6H, 4 Ar + 2 Ar Fmoc), 8.12–8.15 (d, 2H, Ar). ^{13}C NMR (DMSO-d$_6$, 75 MHz) δ = 43.5 (CH_2NH), 46.8 (CH Fmoc), 65.3 (CH_2 Fmoc), 120.1, 125.1, 127.0, 127.6, 140.8 and 144.3 (Ar Fmoc), 122.5, 127.4, 143.8 and 155.9 (*C*$_6$H$_4$CH$_2$NH), 122.9, 130.6, 132.7 and 154.3 (*C*$_6$H$_4$COOH), 156.4 (NHCOO), 166.7 (COOH).

Peptide 1

Peptide **1** was assembled on Tentagel®-Rink-NH-Fmoc resin (0.65 g, 0.15 mmol, loading 0.23 mmol/g) using standard Fmoc/tBu chemistry. The Fmoc protecting group was removed using 20% piperidine in NMP (3 × 8 mL, each 8 min) followed by washing steps with NMP (3 × 8 mL, each 2 min), CH_2Cl_2 (3 × 8 mL, each 2 min) and NMP (3 × 8 mL, each 2 min). The amino acid coupling mixtures were prepared by dissolving 4 equivalents of amino acid (0.60 mmol), 4 equivalents of HOBt and HBTU and 8 equivalents of DiPEA in NMP (10 mL) and coupled during a coupling time of 60 min. The resin was washed with NMP (3 × 8 mL, each 1 min) and CH_2Cl_2 (3 × 8 mL,

each 1 min) after every coupling step, followed by Fmoc deprotection. The coupling steps and deprotection steps were monitored using the Kaisertest.[24] When the Fmoc deprotection was not complete, the deprotection steps were repeated. The amino acid building blocks Fmoc-Leu-OH, Fmoc-Thr(tBu)-OH, Fmoc-Glu(OtBu)-OH, Fmoc-Tyr(OP(OBn)OH)-OH, Fmoc-Gly-OH, Fmoc-AMPB-OH (**9**), Fmoc-Gly-OH, Fmoc-Leu-OH, Fmoc-Gly-OH, Fmoc-Thr(tBu)-OH, and Fmoc-Tyr(OP(OBn)OH)-OH were subsequently coupled. For the coupling of Fmoc-Tyr(OP(OBn)OH)-OH, 2 equivalents of amino acid, 2 equivalents of the coupling reagents HATU and HOAt, and 5 equivalents of DiPEA were used. For the coupling of Fmoc-AMPB-OH also 2 equivalents of amino acid and 2 equivalents of the coupling reagents HATU and HOAt were used and 4 equivalents of DiPEA. After the first Fmoc-Tyr(OP(OBn)OH)-OH coupling an extra washing step (2 × 8 mL, each 10 min) with a mixture of 1 M TFA/1.1 M DiPEA in NMP was performed after each Fmoc deprotection step. This was done to replace the piperidine counterion of Tyr(OP(OBn)O^-) for protonated DiPEA. When all the coupling steps were completed the peptide was acetylated using a capping solution of Ac_2O (4.72 mL, 42.7 mmol), DiPEA (2.18 mL, 22.8 mmol), and HOBt (0.23 g, 1.7 mmol) in 100 mL of NMP for 2 × 20 min. The peptide was cleaved from the resin and the side chains were deprotected with a solution of TFA/H_2O/TIS (95/2.5/2.5) for 3 h. The resin was removed from the solution by filtration. The peptide was precipitated with MTBE/hexane 1:1 v/v at -20 °C and lyophilized from CH_3CN/H_2O 1:1 v/v yielding 141 mg (0.093 mmol, 62%) of the crude peptide. The peptide was purified by preparative HPLC. About half (62.4 mg) of the crude peptide was purified yielding 9.7 mg of **1**. If all of the crude peptide was purified with the same yield, the overall yield would have been 21.3 mg (16%).

HPLC retention times: **1b** 9.8 min, **1a** 10.4 min.

HRMS (ESI): $[M+Na]^+$ calculated 1533.547, found 1533.664; $[M+2Na]^{2+}$ calculated 778.268, found 778.366.

Surface plasmon resonance

Peptide **1** (1.02 mg, 0.675 μmol) was dissolved in HBS buffer (675 μL) to obtain a stock solution with a concentration of 1 mM. A series of samples was prepared in HBS buffer containing 50 nM Syk tSH2 and **1** with concentrations ranging from 0 to 3750 nM. The sensor chip was immobilized with the native ITAM peptide as described.[7] Competition experiments were performed with the trans isomer **1a** and with the isomer mixture

containing the maximum percentage of cis isomer **1b**. For this 240 µL samples were irradiated with visible light for complete conversion to the trans isomer **1a**. Then, half of the sample was injected into the SPR apparatus. The other half of the sample was irradiated with UV light of 366 nm to obtain the maximum percentage of cis conformer **1b** and subjected to the SPR assay under exclusion of light. K_D values have been derived from the competition experiments as was earlier described.[20] The intrinsic affinity of **1b** ($K_{A,cis} = 1/K_{D,cis}$) is derived by applying Eq. 1, in which K_{obs} is the observed association constant, f is the fraction of **1** in the cis isomer, and $K_{A,trans}$ is the affinity assayed for the pure trans conformer.

$$K_{A,obs} = f \cdot K_{A,cis} + (1-f)K_{A,trans} \quad (1)$$

To monitor the effect of conversion of **1b** to **1a** on binding in real time, experiments were performed with *in situ* irradiation in the SPR instrument. The isomer mixture **1a/1b** was first irradiated with 366 nm light to obtain a maximum percentage of cis isomer. Then the sample was injected into the SPR cuvette under exclusion of light. On reaching binding equilibrium the sample in the SPR cuvette was irradiated with visible light for conversion to trans isomer **1a**, and the change in SPR signal was recorded.

References

1. De Mol, N.J., Catalina, M.I., Dekker, F.J., Fischer, M.J.E., Heck, A.J., Liskamp, R.M.J., Protein flexibility and ligand rigidity: a thermodynamic and kinetic study of ITAM-based ligand binding to Syk tandem SH2, *ChemBioChem*, **2005**, 6, 2261-2270.
2. Kumaran, S., Grucza, R.A., Waksman, G., The tandem Src homology 2 domain of the Syk kinase: a molecular device that adapts to interphosphotyrosine distances, *Proc. Natl. Acad. Sci. U.S.A.*, **2003**, 100, 14828-14833.
3. Sada, K., Yamamura, H., Protein-tyrosine kinases and adaptor proteins in FcεRI-mediated signaling in mast cells, *Curr. Mol. Med.*, **2003**, 3, 85-94.
4. Simon, M., Vanes, L., Geahlen, R.L., Tybulewicz, V.L.J., Distinct roles for the linker region tyrosines of Syk in FcεRI signaling in primary mast cells, *J. Biol. Chem.*, **2005**, 280, 4510-4517.
5. Siraganian, R.P., Zhang, J., Suzuki, K., Sada, K., Protein tyrosine kinase Syk in mast cell signaling, *Mol. Immun.*, **2001**, 38, 1229-1233.
6. Colgan, J., Rothman, P., Manipulation of signaling to control allergic inflammation, *Curr. Opin. Allergy Clin. Immunol.*, **2007**, 7, 51-56.
7. Dekker, F.J., de Mol, N.J., van Ameijde, J., Fischer, M.J.E., Ruijtenbeek, R., Redegeld, F.A.M., Liskamp, R.M.J., Replacement of the intervening amino acid sequence of a Syk-binding diphosphopeptide by a nonpeptide spacer with preservation of high affinity, *ChemBioChem*, **2002**, 3, 238-242.

8. Dekker, F.J., de Mol, N.J., Fischer, M.J.E., Liskamp, R.M.J., Amino propynyl benzoic acid building block in rigid spacers of divalent ligands binding to the Syk SH2 domains with equally high affinity as the natural ligand, *Bioorg. Med. Chem. Lett.*, **2003**, 13, 1241-1244.
9. Catalina, M.I., Fischer, M.J.E., Dekker, F.J., Liskamp, R.M.J., Heck, A.J.R., Binding of a diphosphorylated-ITAM peptide to spleen tyrosine kinase (Syk) induces distal conformational changes: a hydrogen exchange mass spectrometry study, *J. Am. Soc. Mass. Spectrom.*, **2005**, 16, 1039-1051.
10. Ulysse, L., Cubillos, J., Chmielewski, J., Photoregulation of cyclic peptide conformation, *J. Am. Chem. Soc.*, **1995**, 117, 8466-8467.
11. Renner, C., Moroder, L., Azobenzene as conformational switch in model peptides, *ChemBioChem*, **2006**, 7, 868-878.
12. Renner, C., Kusebauch, U., Loeweneck, M., Milbradt, A.G., Moroder, L., Azobenzene as photoresponsive conformational switch in cyclic peptides, *J. Peptide Res.*, **2005**, 65, 4-14.
13. Futterer, K., Wong, J., Grucza, R.A., Chan, A.C., Waksman, G., Structural basis for Syk tyrosine kinase ubiquity in signal transduction pathways revealed by the crystal structure of its regulatory SH2 domains bound to a dually phosphorylated ITAM peptide, *J. Mol. Biol.*, **1998**, 281, 523-537.
14. Park, S.B., Standaert, R.F., A photoregulated ligand for the nuclear import receptor Karyopherin α, *Bioorg. Med. Chem.*, **2001**, 9, 3215-3223.
15. Standaert, R.F., Park, S.B., Abc amino acids: design, synthesis, and properties of new photoelastic amino acids, *J. Org. Chem.*, **2006**, 71, 7952-7966.
16. Behrendt, R., Schenk, M., Musiol, H.-J., Moroder, L., Photomodulation of conformational states. Synthesis of cyclic peptides with backbone-azobenzene moieties, *J. Peptide Sci.*, **1999**, 5, 519-529.
17. Ulysse, L., Chmielewski, J., The synthesis of a light-switchable amino acid for inclusion into conformationally mobile peptides, *Bioorg. Med. Chem. Lett.*, **1994**, 4, 2145-2146.
18. Aemissegger, A., Hilvert, D., Synthesis and application of an azobenzene amino acid as a light-switchable turn element in polypeptides, *Nat. Protocols*, **2007**, 2, 161-167.
19. Rovero, P., Pegoraro, S., Vigano, S., Amato, C., Vaccari, L., Balestreri, E., Felicioli, R., Solid-phase synthesis and dimerization of an azobenzene-containing peptide as photoisomerizable proteinase-inhibitor, *Lett. Pept. Sci.*, **1995**, 2, 27-32.
20. De Mol, N.J., Gillies, M.B., Fischer, M.J.E., Experimental and calculated shift in pK_a upon binding of phosphotyrosine peptide to the SH2 domain of $p56^{lck}$, *Bioorg. Med. Chem.*, **2002**, 10, 1477-1482.
21. Ruijtenbeek, R., Kruijtzer, J.A.W., van de Wiel, W., Fischer, M.J.E., Fluck, M., Redegeld, F.A.M., Liskamp, R.M.J., Nijkamp, F.P., Peptoid-peptide hybrids that bind Syk SH2 domains involved in signal transduction, *ChemBioChem*, **2001**, 2, 171-179.
22. Nakayama, K., Endo, M., Majima, T., A hydrophilic azobenzene-bearing amino acid for photochemical control of a restriction enzyme BamHI, *Bioconjugate Chem.*, **2005**, 16, 1360-1366.
23. Park, S.B., Standaert, R.F., α,α-Difluorophosphonomethyl azobenzene derivatives as photo-regulated phosphoamino acid analogs. 1. Design and synthesis, *Tetrahedron Lett.*, **1999**, 40, 6557-6560.
24. Kaiser, E., Colescott, R.L., Bossinger, C.D., Cook, P.I., Color test for detection of free terminal amino groups in the solid-phase synthesis of peptides, *Anal. Biochem.*, **1970**, 34, 595-598.

Chapter 3

Switching between low and high affinity for the Syk tandem SH2 domain by irradiation of azobenzene-containing ITAM peptidomimetics

Parts of this chapter have been published:

Kuil, J., van Wandelen, L.T.M., de Mol, N.J., Liskamp, R.M.J., Switching between low and high affinity for the Syk tandem SH2 domain by irradiation of azobenzene containing ITAM peptidomimetics, *J. Pept. Sci.*, **2009**, 15, 685-691

Abstract

Spleen tyrosine kinase (Syk) plays an essential role in IgE receptor signaling (FcεRI), which leads to mast cell degranulation. Divalent binding of the tandem SH2 domain (tSH2) of Syk to the intracellular ITAM motif of FcεRI activates the kinase domain of Syk and thereby initiates cell degranulation. The inter SH2 domain distance in Syk tSH2 might be important for Syk kinase activation. In this study photoswitchable ITAM peptidomimetics containing an azobenzene moiety were synthesized. Irradiation of these constructs changes the distance between the two SH2 binding epitopes and therefore, they may be used as photoswitches. The affinity of the cis – and trans isomer for tSH2 was assayed with SPR. The ITAM peptidomimetic with the smallest linker displayed the largest difference in affinity between the two isomers (at least 100-fold) and the affinity of the cis isomer was comparable to monovalent binding. The ITAM mimics with larger photoswitchable linkers displayed modest differences. These results indicate that Syk tSH2 is able to adapt the inter SH2 domain distance to ligands larger than native ITAM, but not to smaller ones.

Introduction

The incorporation of photoswitches (in particular azobenzene) into peptides for the modulation of the conformation and/or bioactivity has been given increasing attention.[1-5] Azobenzene is frequently used because of its fast and fully reversible photoisomerization. One noteworthy disadvantage of azobenzene is that 100% cis, unlike 100% trans, cannot be obtained.

A particularly interesting system for using the azobenzene photoswitch is the divalent ITAM – Syk tandem SH2 domain interaction. ITAM (Immunoreceptor Tyrosine based Activation Motif) is present, among others, in the β- and γ-chain of the multimeric ($\alpha\beta\gamma_2$) high affinity IgE receptor (FcεRI).[6-8] Once this receptor is stimulated by IgE and antigen binding, γ-ITAM is diphosphorylated (γ-dpITAM). After that, the Spleen tyrosine kinase (Syk) is recruited to the membrane by binding with its two SH2 domains (tandem SH2 domain, tSH2) to γ-dpITAM. This results in a conformational change and activation of the kinase domain of Syk.[9] Syk activation eventually leads to mast cell degranulation and overstimulation of this cascade leads to allergic reactions. Because the ITAM – Syk tSH2 interaction is essential for this signaling pathway,[10,11] inhibitors of this interaction are potential anti-allergic agents.

The ITAM sequence consists of Tyr-Xxx-Xxx-(Leu/Ile)-$(Xxx)_{n=6-8}$-Tyr-Xxx-Xxx-(Leu/Ile), in which Xxx can be any amino acid.[12] The underlined residues comprise the binding epitopes for Syk tSH2, when tyrosine is phosphorylated. The intervening residues $(Xxx)_{n=6-8}$ (in γ-ITAM n = 7) are not essential for binding and can be replaced by a rigid linker without significant loss of binding affinity.[13]

In a previous study we showed that the intervening amino acids can also be replaced by the (4-aminomethyl)phenylazobenzoic acid (AMPB) photoswitch and two additional glycine residues with largely preservation of the binding affinity when in trans configuration.[14] The binding affinity of the photostationary state containing a maximal amount of cis isomer was two times lower. In this photostationary state still 40% trans was present; therefore, the intrinsic affinity of the cis isomer was even lower.[14] Although the difference in binding affinity was significant, a larger difference is needed for applicability in a cellular system, ideally switching from an inactive to an active divalent binding ligand. Therefore, in the present study the design of new photoswitchable ligands for Syk tSH2 was aimed at optimizing the difference in binding affinity between the cis – and trans isomer. To accomplish this, two strategies were

explored. On the one hand, the linker in the previously reported ITAM mimic was shortened and rigidified. On the other hand, also two photoswitchable ligands were designed to bind Syk tSH2 with the highest affinity in the cis configuration. This was done because in the photostationary state with maximal cis always a significant amount of trans will be present. Therefore, when trans is the active isomer, the difference between trans and the 'inactive' state of maximal cis, will be limited by the presence of trans. This problem is not present when the cis isomer binds with the highest affinity, because it is possible to obtain 100% trans isomer.

Results and discussion

Design

In the crystal structure of Syk tSH2 complexed with ITAM, the length of the seven intervening residues in ITAM, which are not essential for binding, was found to be 14.1-16.4 Å.[15] To approach this range, in our previous study two glycine residues were added to AMPB to obtain a linker of 18.6 Å in trans configuration (compound **1**, Figure 1 and Table 1).[14] The binding affinity of the trans isomer of compound **1** for Syk tSH2 was 10-fold less than that of native γ-ITAM (K_D = 65 nM and 5.6 nM, respectively).[14,16] The linker in cis configuration (7.2 Å) was still long enough to bind divalently to both SH2 domains of Syk tSH2, resulting in an affinity (K_D 100% cis was calculated to be 860 nM) which is significantly better than that of a monovalent interaction (K_D = 27 μM).[14,17]

Now, a series of ITAM mimics (**2**-**4**) with large differences in linker lengths was designed, aiming at enlarging the difference in binding affinity between the cis – and trans isomer (Figure 1 and Table 1).

ITAM mimic **2**, like **1**, was designed to bind Syk tSH2 with high affinity in the trans configuration. Compound **2** has a linker lacking the two glycine residues, i.e. AMPB, which makes it smaller and more rigid than compound **1**. According to literature data AMPB is 12.0 Å in trans configuration and 6.2 Å in cis configuration.[18,19] To validate the molecular simulation experiments, used for estimating the linker lengths of the other photoswitchable peptides, the linker of **2** in both configurations, i.e. trans-AMPB and cis-AMPB, was minimized using simulated annealing, which yielded similar distances (12.3 Å and 6.1 Å, respectively).

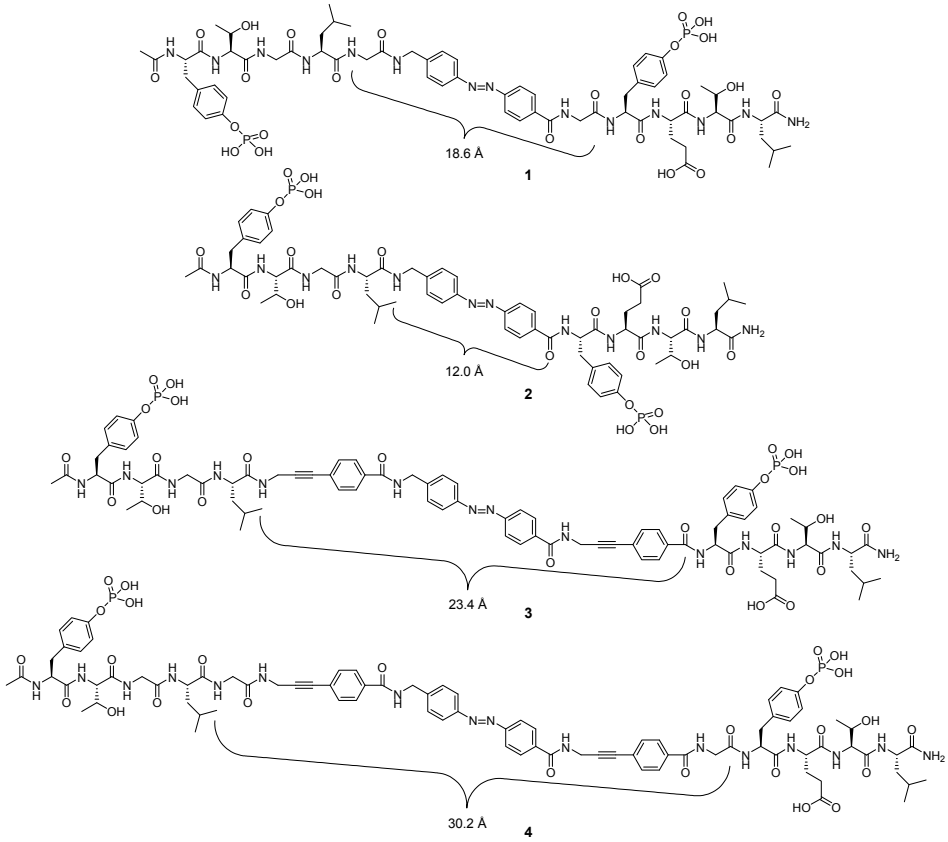

Figure 1. Photoswitchable ITAM mimics. Compound **1** was previously prepared and assayed. Peptidomimetic **2** was newly designed and possesses a smaller and more rigid linker than **1**. Compounds **3** and **4** were newly designed to obtain a higher affinity for the cis isomer. The indicated distances are between the SH2 binding epitopes when azobenzene is in the trans configuration.

For compounds **3** and **4** the other strategy was applied: they were designed to bind Syk tSH2 with high affinity in the cis configuration. In compound **3** a rigid amino propynyl benzoic acid building block was introduced on either side of AMBP and in compound **4** also a glycine residue was added to each side of the linker. The rigidity of the building blocks should keep the two SH2 epitopes at distance. The length of the linker in cis configuration was estimated for compound **3** to be 11.0 Å and for compound **4** to be 17.8 Å. Both these numbers are nearby the range of 14.1-16.4 Å

found in the crystal structure. The linkers of **3** and **4** in trans configuration, which were estimated to be respectively 23.4 Å and 30.2 Å, are well out of this range.

Table 1. The distances between the SH2 binding epitopes, measured from the N-terminal nitrogen atom to the C-terminal carbon atom of the linkers, in the cis – and trans configuration. The distances in the linker in compound **2**, which is AMPB, were obtained from literature.[18,19] The distances in the other photoswitchable compounds were estimated from simulated annealing. The distance in native ITAM was obtained from the crystal structure.[15]

Compound	Distance between SH2 binding epitopes (Å)	
	trans	cis
1	18.6	7.2
2	12.0	6.2
3	23.4	11.0
4	30.2	17.8
native ITAM	14.1 – 16.4	

Synthesis and switching of ITAM mimics

The synthesis of the Fmoc-AMPB-OH building block, as well as the synthesis of the rigid amino propynyl benzoic acid building block have been earlier described.[13,14] The peptides were assembled on the solid phase using Fmoc peptide chemistry. The orange solids obtained after the syntheses were subjected to preparative HPLC. The yields for the compounds **3** and **4** were low, due to uncompleted Alloc deprotections after incorporation of the alkyne-containing rigid building blocks and their low solubility in aqueous solutions, which made the purification by HPLC troublesome. Nevertheless, sufficient amounts of all peptides were obtained.

Then UV-VIS spectra of the peptides were recorded by dissolving a small amount of peptide in water. First the spectrum of 100% trans was measured. After this the sample was irradiated with 366 nm light for 120 s to obtain the photostationary state with maximal amount of cis isomer and the spectrum was immediately recorded (Figure 2). The peak at 335 nm, caused by trans π-π^* transitions in AMPB, dropped after UV irradiation in the spectra of all the photoswitchable peptidomimetics. In the spectra of compounds **3** and **4** also a peak at 268 nm was present, which was caused by the rigid building block.

To establish the percentage cis isomer present in the photostationary state with maximal cis, compound **2** was irradiated with UV light and an analytical HPLC spectrum was directly measured with a UV detector operating at the isosbestic point of 287 nm (Figure 3). By comparison of the obtained HPLC trace with the HPLC trace made after purification, which contained mostly trans-**2**, it was clear that the first peak could be assigned to cis-**2** and the second peak to trans-**2**. From the integration of both peaks it could be calculated that 66% cis isomer was present after UV irradiation. A close value of 64% cis was obtained from the amide signals in the ^{1}H-NMR spectra. A similar value was previously found for compound **1** (60%) and this value was also reported by others.[20] The amount of cis present after UV irradiation for compounds **3** and **4** was assumed to be approximately the same as for compound **2**.

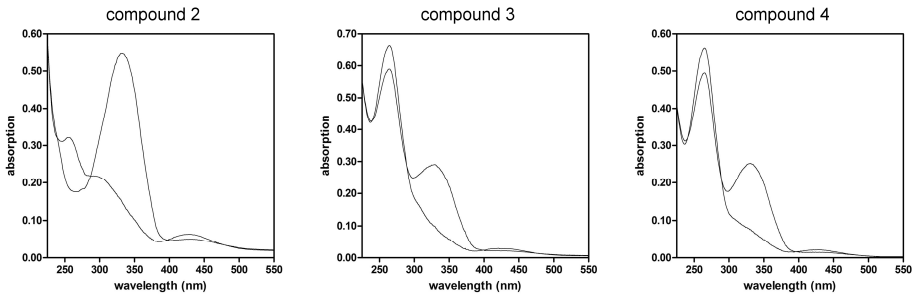

Figure 2. UV-VIS spectra of compounds **2**-**4** in water. The photoswitchable ITAM mimics **2**-**4** had a maximum at approximately 335 nm in trans configuration. In the photostationary state with maximal amount of cis isomer this maximum was substantially decreased (lower curves).

Binding studies

The interaction of the peptidomimetics with Syk tSH2 was assayed with surface plasmon resonance (SPR). The sensor chip was immobilized with native ITAM as was described previously.[21] Then the affinity of Syk tSH2 for the immobilized ITAM peptide determined by the addition of different concentrations Syk tSH2 and the equilibrium signal was fitted to a Langmuir binding isotherm. The K_D value for binding to the chip (K_C) was found to be 7.8 nM, which is comparable to the 5.6 nM affinity found earlier.[16] Then concentration ranges of the photoswitchable peptidomimetics in the presence of 25 nM Syk tSH2 were made for SPR competition experiments. Prior to addition, the samples were irradiated with visible light or UV light (366 nm) to obtain

the trans isomer or the maximal amount of cis isomer, respectively. After injection, the binding of tSH2 to the sensor chip was measured. From the obtained inhibition curves, the thermodynamic dissociation constants for the interaction in solution (K_D) were obtained by fitting to a competition model (Table 2).[14,22]

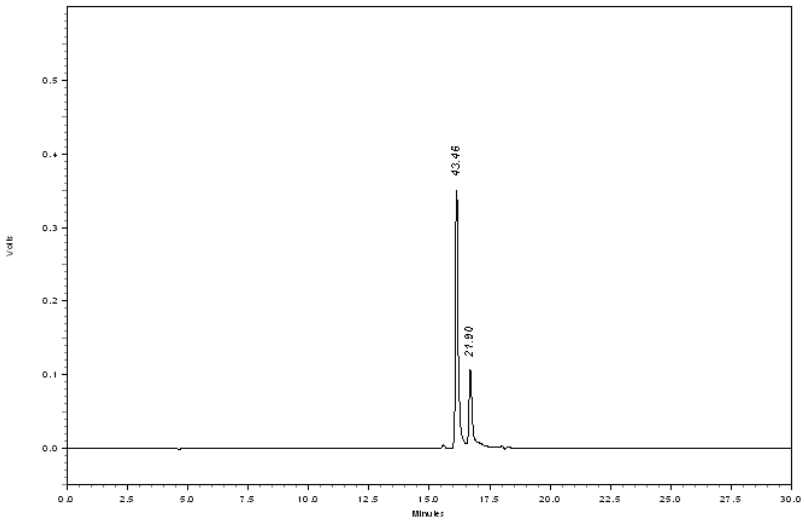

Figure 3. Analytical HPLC trace with UV detection at the isosbestic point of 287 nm of compound **2** after UV irradiation. The first peak is from cis-**2** and the second peak is from trans-**2**. The fraction of cis-**2** is: f = 43.46 / (43.46 + 21.90) = 0.66.

Table 2. Affinities of the cis – and trans isomer of the photoswitchable ITAM mimics for Syk tSH2 obtained from SPR competition experiments. $K_{D,obs}$ is the dissociation constant of the photostationary state with maximal cis isomer. $K_{D,cis}$ for compounds **2**-**4** was calculated with Eq. 1, assuming that the cis content of the UV irradiated samples was 66%, based on the percentage experimentally obtained for **2**.

Compound	trans	cis	
	$K_{D,trans}$ (nM)	$K_{D,obs}$ (nM)	$K_{D,cis}$ (nM)
1[14]	65 ± 8	146 ± 11	860
2	91 ± 10	332 ± 44	> 10 000
3	196 ± 35	161 ± 26	147
4	77 ± 13	56 ± 5	49

As an example, the inhibition curves of both isomers of compound **2** are shown in Figure 4. The trans isomer of compound **2** had a slightly lower affinity compared with compound **1** (Table 2). This was expected because the linker in compound **2** is considerable shorter than the native linker. Interestingly, the difference in binding affinity between the cis – and trans isomer is substantially larger for compound **2**. Actually, the threefold decrease in affinity between the photostationary state with maximal cis isomer and the trans isomer can be accounted for by the presence of approximately one-third of trans isomer. Therefore, the actual K_D value of 100% cis-**2** is much higher than trans-**2**, and can be estimated to be in the micromolar range or higher, indicating that cis-**2** was not interacting divalently. The affinity of a monovalent interaction amounts 27 μM.[17] Thus, the difference in affinity between the cis – and trans isomer of compound **2** is at least 100-fold.

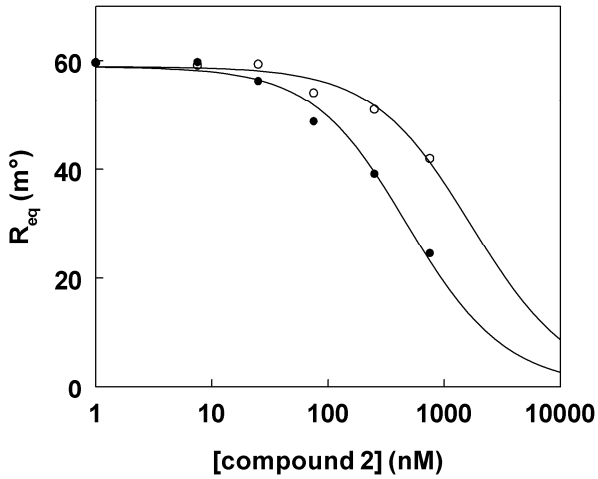

Figure 4. Inhibition curves of cis-2 (○) and trans-2 (●). The curves are fits according to a described model.[22]

In contrast to the large difference in affinity between cis-**2** and trans-**2**, the compounds **3** and **4**, containing extra rigid units, displayed much less differences. Cis-**3** did have a somewhat higher affinity for Syk tSH2 than trans-**3**, as designed, but the difference was rather small. Also for compound **4** the difference was very modest. Apparently Syk tSH2 is flexible enough to adapt to both isomers of compounds **3** and **4**.

This shows that a great variety of inter SH2 domain distances is possible, while retaining binding affinity. In addition, the similar affinity of cis-**4** (49 nM) and trans-**1** (65 nM) corresponds to the similar linker length, i.e. 17.8 Å and 18.6 Å, respectively.

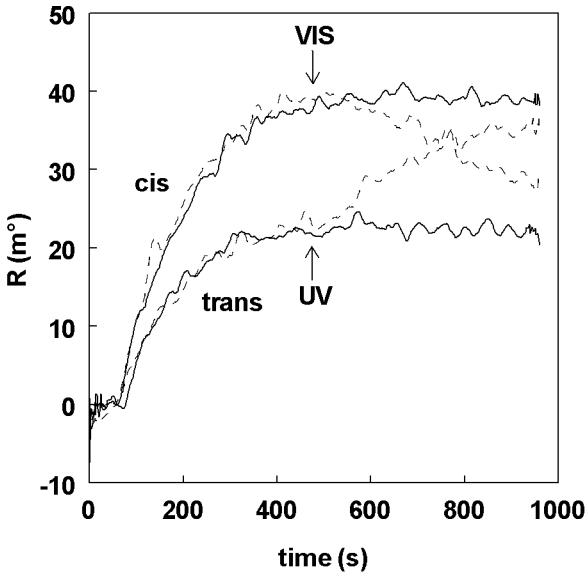

Figure 5. Real time SPR analysis of the effect of cis-trans isomerization of compound **2** on the extent of binding to Syk tSH2 by *in situ* UV (of trans-**2**) or VIS (of cis-**2**) irradiation. These signals are 'noisier' than usually observed, because they are single cell SPR signals without the correction for a reference cell signal.

Compound **2** was used to investigate the ability to isomerize during SPR experiments (Figure 5). First sensograms were recorded of 25 nM Syk tSH2 with either 750 nM trans-**2** or cis-**2**. After that, trans-**2** was injected and when equilibrium was reached, the SPR measuring cell was irradiated with 365 nm light. Due to the UV irradiation, the stronger binding trans-**2** was transformed to the weaker binding cis-**2**, which was less capable in competing with the immobilized ITAM for Syk tSH2 binding. Therefore, the SPR signal gradual increased towards the signal of cis-**2**.

Also the opposite was performed: the photostationary state (cis-**2**) was injected and after equilibrium the sample was irradiated with visible light, causing a decrease in SPR signal towards the signal of trans-**2**, displacing more Syk tSH2 from the sensor surface than cis-**2**.

These results show that it is possible to manipulate the binding of compound **2** during an experiment. Affinity for Syk tSH2 could be increased and decreased within an acceptable short time.

Conclusions

A series of photoswitchable ITAM mimics was prepared and the binding affinity of the cis – and trans isomer for Syk tSH2 was assayed with SPR. The smallest ITAM mimic (compound **2**) displayed a larger difference in binding affinity between the cis – and trans isomer, compared with our previously reported compound **1**.[14] The cis isomer of compound **2** could not bind Syk tSH2 divalently, indicating that the linker length is too small to bridge the smallest inter SH2 domain distance in Syk tSH2 (Figure 6). The affinity of trans-**2** for Syk tSH2 was only approximately 10-fold lower than that of native ITAM. However, azobenzene-containing compounds with trans as the active isomer are of limited use in biological experiments, because 100% cis cannot be reached. In other words, when the trans isomer is the active species, the difference in biological activity between the trans isomer and the photostationary state with maximal cis is always limited by the amount of trans present in the photostationary state with maximal cis.

To create azobenzene ligands which are applicable in biological assays, it is desirable that the cis isomer binds the target protein with the highest affinity. This is because it is possible to obtain 100% trans isomer without 'contamination' with the active cis isomer. ITAM mimics **3** and **4** were designed with this strategy in mind. However, the difference in binding affinity between the two isomers of both ITAM mimics was surprisingly small. This result is quite remarkable and can be explained by the relatively large flexibility of Syk tSH2. However, it should be emphasized that the small differences in binding affinity for compounds **3** and **4** does not mean that these are reflected in the bioactivity.

In Syk and in Zap-70, the other member of the Syk family kinases, the inter SH2 domain distance plays probably a key role in kinase activation.[9,23,24] Crystal structures of Zap-70 tSH2 show that the inter SH2 domain distance is larger when there is no ligand present, compared with tSH2 bound to native ITAM.[25,26] In the crystal structure of the inactive full-length Zap-70, the SH2-SH2 linker is in close contact with the kinase domain.[23] Changing the inter SH2 domain distance will strongly effect the

conformation of the SH2-SH2 linker[27] (Figure 6) and this could be relevant for kinase activation.[23,24] For Syk kinase no crystal structure of the complete protein is available yet. However, based on the comparable function and architecture of the Syk and Zap-70 kinases, similar activation mechanisms may apply. This could mean that the trans isomer of compound **3** and/or **4** maintains Syk in an inactive state, by keeping the SH2 domains far apart from each other, and that the cis isomer activates kinase activity. To verify this hypothesis, the effect of these compounds on Syk kinase activity should be established in the future.

Apart from the discussion about the bioactivity of compounds **3** and **4**, it can be concluded that the ITAM mimics **3** and **4**, which were designed to bind Syk tSH2 with higher affinity in the cis configuration, did not display large differences in affinity. The reason for this is the large flexibility of Syk tSH2. Nevertheless, for other, less flexible proteins, this strategy could yield ligands with a large difference in binding affinity between the trans isomer and the photostationary state with a maximal amount of cis isomer.

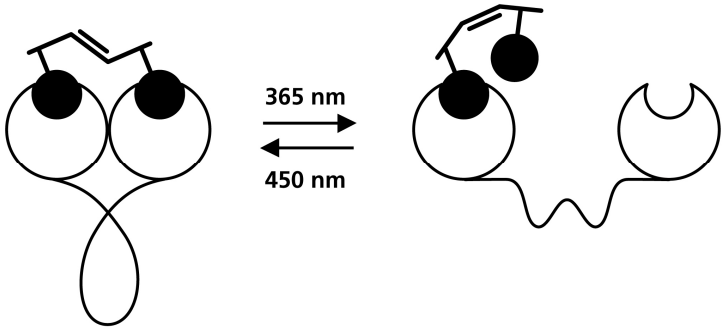

Figure 6. Syk tSH2 binds trans-**2** divalently (left) and cis-**2** monovalently (right). By irradiation of the sample with UV – or visible light, it is possible to switch between a mono- and divalent ligand for Syk tSH2 within an acceptable short time.

Experimental section

Molecular simulations

For all calculations YASARA (http://www.yasara.org) was used. PDB files of the linkers of compounds **1**-**4** were made using ChemDraw and Chem3D. These files were loaded in YASARA and a simulation cell, in which each axis was extended 5.0 Å from the molecule, was defined. The Amber99 forcefield was used and the temperature control was step-10 annealing, starting from 298 K and every 10 simulation steps the velocity of all atoms was reduced to 90%. Within approximately 2500 fs the temperature of 0 K was reached and the atoms almost did not move anymore. To be sure, the simulation was continued until 10000 fs was reached. All linkers were modeled as their N-terminal acetamide and C-terminal amide derivatives. All distances were measured from the N-terminal nitrogen atom to the C-terminal carbon atom after completion of the simulation of 10000 fs.

Synthesis

Chemicals were obtained from commercial sources and used without further purification. Solvents, which were used for the solid phase peptide synthesis, were stored over 4 Å molecular sieves, except for MeOH, which was stored over 3 Å molecular sieves. The reactions were performed at room temperature unless stated otherwise.

The syntheses of peptidomimetic **1** and the building blocks Fmoc-AMPB-OH and Alloc-4-(3-aminoprop-1-ynyl)benzoic acid were described previously.[13,14]

Peptidomimetics **2**-**4** were assembled on Tentagel®-Rink-NH-Fmoc resin (each 625 mg, 0.15 mmol, loading 0.24 mmol/g) using standard Fmoc/tBu chemistry. The Fmoc protecting group was removed using 20% piperidine in NMP (3 × 8 mL, each 8 min) followed by washing steps with NMP (3 × 8 mL, each 2 min), CH_2Cl_2 (3 × 8 mL, each 2 min) and NMP (3 × 8 mL, each 2 min). The Alloc protecting group was removed using 0.25 equivalents of $Pd(PPh_3)_4$ and 10 equivalents of anilinium para-toluene sulfinate in MeOH/THF (1:1) (2 × 8 mL, each 60 min). After Alloc deprotection the resin was washed with 0.1% sodium diethyldithiocarbamate in NMP (1 × 8 mL, 2 min), NMP (3 × 8 mL, each 2 min), CH_2Cl_2 (3 × 8 mL, each 2 min) and NMP (3 × 8 mL, each 2 min). The amino acid coupling mixtures were prepared by dissolving 4 equivalents of amino

acid, 4 equivalents of HOBt and HBTU and 8 equivalents of DiPEA in NMP and coupled during a coupling time of 60 minutes. The resin was washed with NMP (3 × 8 mL, each 1 min) and CH_2Cl_2 (3 × 8 mL, each 1 min) after every coupling step. The coupling steps and deprotection steps were monitored using the Kaisertest.[28] When the Fmoc deprotection was not complete, the deprotection steps were repeated. Fmoc-Tyr(OP(OBn)OH)-OH was coupled overnight using 2 equivalents of amino acid, 2 equivalents of the coupling reagents HOBt and HBTU and 5 equivalents of DiPEA. Alloc-4-(3-aminoprop-1-ynyl)benzoic acid was also coupled overnight using 2 equivalents of amino acid and 2 equivalents of the coupling reagents HOBt and HBTU and 4 equivalents of DiPEA. After the first Fmoc-Tyr(OP(OBn)OH)-OH coupling an extra washing step (2 × 8 mL, each 10 min) with a mixture of 1 M TFA/1.1 M DiPEA in NMP was performed after each Fmoc deprotection step. This was done to replace the piperidine counter ion of Tyr(OP(OBn)O^-) for protonated DiPEA. When all the coupling steps were completed the peptides were acetylated using a capping solution of Ac_2O (4.72 mL, 42.7 mmol), DiPEA (2.18 mL, 22.8 mmol) and HOBt (0.23 g, 1.7 mmol) in 100 mL of NMP for 2 × 20 min. The peptides were cleaved from the resin and the side chains were deprotected with TFA/H_2O/TIS (95/3.5/1.5) for 3 h. The resin was removed from the solution by filtration and the peptides were precipitated with MTBE/hexane 1:1 v/v at -20 °C and lyophilized from CH_3CN/H_2O 1:1 v/v yielding 181.8 mg of mimic **2**, 163.8 mg of **3** and 110.2 mg of **4**. The peptides were purified by preparative HPLC and analyzed by analytical HPLC and mass spectrometry. For the preparative HPLC a Gilson system with a UV detector operating at 220 and 254 nm was used. An Alltech Prosphere C18 300 Å 10 µm (250 × 22 mm) column and a gradient of 100% buffer A (0.1% TFA in H_2O/CH_3CN 95:5) to 100% buffer B (0.1% TFA in H_2O/CH_3CN 5:95) in 60 minutes was used for **3** and **4** and an Alltech Alltima C8 100 Å 10 µm (250 × 22 mm) column and a gradient of 100% buffer A to 100% buffer B in 100 minutes was used for **2**. Analytical HPLC was measured on a Shimadzu HPLC system with a UV detector operating at 220 and 254 nm. For the analytical HPLC a gradient from 100% buffer A (15 mM TEA in H_2O titrated at pH 6 with 85% H_3PO_4) to 100% buffer B (buffer A/CH_3CN 1:9) in 20 minutes was used. An Alltech Prosphere C18 300 Å 5 µm (250 × 4.6 mm) column was used for **3** and **4** and an Alltech Adsorbosphere XL C8 90 Å 5 µm (250 × 4.6 mm) column was used for **2**. The fractions containing pure product were lyophilized yielding orange fluffy solids. For **2** 90 mg was purified

yielding 27.2 mg of pure product. For **3** 50 mg was purified yielding 1.1 mg of pure product. For **4** 50 mg was purified yielding 1.0 mg of pure product.

^{1}H NMR spectra of compound **2** were recorded on a Varian Inova 500 MHz spectrometer in H_2O/D_2O 9:1 using dioxane as an internal reference.

HRMS (ESI) of **2**: $[M+H]^+$ calculated 1397.5220, found 1397.4916; $[M+Na]^+$ calculated 1419.5040, found 1419.4063; $[M+2H]^{2+}$ calculated 699.2649, found 699.2689; $[M+H+Na]^{2+}$ calculated 710.2559, found 710.2312; $[M+2Na]^{2+}$ calculated 721.2469, found 721.2332.

LC-MS (ESI) of **3**: $[M+H]^+$ calculated 1711.63, found 1711.63; $[M+Na]^+$ calculated 1733.61, found 1733.71.

LC-MS (ESI) of **4**: $[M+H]^+$ calculated 1825.67, found 1825.54.

Photoisomerization

Photoisomerization was performed using a visible light emitting lamp (Schott/Paes KL-1500) in combination with a glass plate to filter the UV light or a 6 W 366 nm handheld TLC lamp (Konrad Benda).[18,19] During the real time SPR analysis of cis-trans isomerization a 1 W/cm^2 365 nm UV LED lamp (LED-100, Lightning Enterprises, Limington, USA) was used instead of the TLC lamp, because the TLC lamp did not fit into the SPR apparatus.

UV-VIS spectra were recorded with an UV1 spectrophotometer (Thermo Electron Corporation).

Syk protein expression

Fusion clones of the gluthathione S-transferase (GST) Syk tSH2 domain were kindly provided by Prof. Gabriel Waksman (Washington University, St. Louis, MI).[15] The Escherichia coli strain BL21 contained the pGEX-KT vector with amino acids 10–273 of human Syk, enabling thrombin cleavage of the GST moiety. Isolation procedures were previously described.[16]

Surface plasmon resonance assays

SPR measurements were performed on a double channel IBISII SPR instrument (Eco Chemie, Utrecht, The Netherlands) equipped with a CM 5 sensor chip (GE Healthcare, Biacore, Uppsala, Sweden).

The sensor chip was immobilized with the native ITAM peptide as was described earlier.[21] The affinity of Syk tSH2 for the immobilized ITAM peptide (K_C) was determined by addition of Syk tSH2 in a concentration range of 0 to 100 nM in HBS buffer. The K_C value was calculated by fitting the equilibrium signals to a Langmuir binding isotherm.

Stock solutions of the peptide mimics **2**-**4** with a concentration of 1 mM in HBS buffer were prepared. A series of samples was prepared in HBS buffer containing 25 nM Syk tSH2 and a photoswitchable peptide mimic in various concentrations. First, competition experiments were performed with the trans isomer. For this, 240 μL of a sample was irradiated with visible light for conversion to the trans isomer. Then, half of the sample was injected into the SPR apparatus. The other half of the sample was irradiated with UV light of 366 nm to obtain the maximum percentage of cis isomer, and subjected to the SPR assay under strict exclusion of light. K_D values have been derived from the competition experiments as was earlier described.[22]

The intrinsic affinity of the cis isomer ($K_{A,cis} = 1/K_{D,cis}$) was derived by applying Eq. 1, in which $K_{A,obs}$ is the observed association constant of a sample with maximal amount of cis isomer, f is the fraction of compound in cis configuration and $K_{A,trans}$ is the affinity assayed for the pure trans isomer.

$$K_{A,obs} = f \cdot K_{A,cis} + (1-f)K_{A,trans} \quad (1)$$

To monitor the effect of isomerization of compound **2** on binding in real time, experiments were performed with *in situ* irradiation in the SPR instrument. A solution containing 25 nM Syk tSH2 and 750 nM compound **2** in HBS buffer was prepared and the sensograms of trans-**2** and cis-**2** were recorded. Then Syk tSH2 – trans-**2** was injected again and after 400 s the sample in the SPR cuvette was irradiated with UV light and the change in SPR signal was continuously recorded. Lastly, Syk tSH2 – cis-**2** was injected into the SPR cuvette under exclusion of light. After 400 s the sample in the SPR cuvette was irradiated with visible light for conversion to the trans isomer, while the change in SPR signal was recorded.

Acknowledgements

Esther Pronker is kindly acknowledged for the SPR competition experiments of compounds **3** and **4**. We thank Kees Versluis (Department of Biomolecular Mass Spectrometry, Utrecht University) for recording the high-resolution mass spectrum of compound **2**.

References

1. Gorostiza, P., Isacoff, E.Y., Optical switches for remote and noninvasive control of cell signaling, *Science*, **2008**, 322, 395-399.
2. Renner, C., Moroder, L., Azobenzene as conformational switch in model peptides, *ChemBioChem*, **2006**, 7, 868-878.
3. Mayer, G., Heckel, A., Biologically active molecules with a "light switch", *Angew. Chem. Int. Ed.*, **2006**, 45, 4900-4921.
4. Ulysse, L., Cubillos, J., Chmielewski, J., Photoregulation of cyclic peptide conformation, *J. Am. Chem. Soc.*, **1995**, 117, 8466-8467.
5. Aemissegger, A., Hilvert, D., Synthesis and application of an azobenzene amino acid as a light-switchable turn element in polypeptides, *Nat. Protocols*, **2007**, 2, 161-167.
6. Singh, R., Masuda, E.S., Spleen tyrosine kinase (Syk) biology, inhibitors and therapeutic applications, *Annu. Rep. Med. Chem.*, **2007**, 42, 379-391.
7. Gilfillan, A.M., Tkaczyk, C., Integrated signalling pathways for mast-cell activation, *Nat. Rev. Immunol.*, **2006**, 6, 218-230.
8. Kraft, S., Kinet, J.-P., New developments in FcεRI regulation, function and inhibition, *Nat. Rev. Immunol.*, **2007**, 7, 365-378.
9. Siraganian, R.P., Zhang, J., Suzuki, K., Sada, K., Protein tyrosine kinase Syk in mast cell signaling, *Mol. Immunol.*, **2001**, 38, 1229-1233.
10. Turner, M., Schweighoffer, E., Colucci, F., Di Santo, J.P., Tybulewicz, V.L., Tyrosine kinase SYK: essential functions for immunoreceptor signaling, *Immunol. Today*, **2000**, 21, 148-154.
11. Zhang, J., Swaim, W.D., Berenstein, E.H., Siraganian, R.P., Syk protein tyrosine kinase is essential for the high affinity IgE receptor-induced morphological changes in mast cells., *J. Allergy Clin. Immunol.*, **1997**, 99, 379-379.
12. Isakov, N., ITIMs and ITAMs - The Yin and Yang of antigen and Fc receptor-linked signaling machinery, *Immunol. Res.*, **1997**, 16, 85-100.
13. Dekker, F.J., de Mol, N.J., Fischer, M.J.E., Liskamp, R.M.J., Amino propynyl benzoic acid building block in rigid spacers of divalent ligands binding to the Syk SH2 domains with equally high affinity as the natural ligand, *Bioorg. Med. Chem. Lett.*, **2003**, 13, 1241-1244.
14. Kuil, J., van Wandelen, L.T.M., de Mol, N.J., Liskamp, R.M.J., A photoswitchable ITAM peptidomimetic: Synthesis and real time surface plasmon resonance (SPR) analysis of the effects of cis-trans isomerization on binding, *Bioorg. Med. Chem.*, **2008**, 16, 1393-1399.
15. Futterer, K., Wong, J., Grucza, R.A., Chan, A.C., Waksman, G., Structural basis for Syk tyrosine kinase ubiquity in signal transduction pathways revealed by the crystal structure of its regulatory SH2 domains bound to a dually phosphorylated ITAM peptide, *J. Mol. Biol.*, **1998**, 281, 523-537.

16. De Mol, N.J., Catalina, M.I., Dekker, F.J., Fischer, M.J.E., Heck, A.J., Liskamp, R.M.J., Protein flexibility and ligand rigidity: a thermodynamic and kinetic study of ITAM-based ligand binding to Syk tandem SH2, *ChemBioChem*, **2005**, 6, 2261-2270.
17. Ruijtenbeek, R., Kruijtzer, J.A.W., van de Wiel, W., Fischer, M.J.E., Fluck, M., Redegeld, F.A.M., Liskamp, R.M.J., Nijkamp, F.P., Peptoid-peptide hybrids that bind Syk SH2 domains involved in signal transduction, *ChemBioChem*, **2001**, 2, 171-179.
18. Park, S.B., Standaert, R.F., A photoregulated ligand for the nuclear import receptor Karyopherin α, *Bioorg. Med. Chem.*, **2001**, 9, 3215-3223.
19. Standaert, R.F., Park, S.B., Abc amino acids: design, synthesis, and properties of new photoelastic amino acids, *J. Org. Chem.*, **2006**, 71, 7952-7966.
20. Rovero, P., Pegoraro, S., Vigano, S., Amato, C., Vaccari, L., Balestreri, E., Felicioli, R., Solid-phase synthesis and dimerization of an azobenzene-containing peptide as photoisomerizable proteinase-inhibitor, *Lett. Pept. Sci.*, **1995**, 2, 27-32.
21. Dekker, F.J., de Mol, N.J., van Ameijde, J., Fischer, M.J.E., Ruijtenbeek, R., Redegeld, F.A.M., Liskamp, R.M.J., Replacement of the intervening amino acid sequence of a Syk-binding diphosphopeptide by a nonpeptide spacer with preservation of high affinity, *ChemBioChem*, **2002**, 3, 238-242.
22. De Mol, N.J., Gillies, M.B., Fischer, M.J.E., Experimental and calculated shift in pK_a upon binding of phosphotyrosine peptide to the SH2 domain of $p56^{lck}$, *Bioorg. Med. Chem.*, **2002**, 10, 1477-1482.
23. Deindl, S., Kadlecek, T.A., Brdicka, T., Cao, X., Weiss, A., Kuriyan, J., Structural basis for the inhibition of tyrosine kinase activity of ZAP-70, *Cell*, **2007**, 129, 735-746.
24. Au-Yeung, B.B., Deindl, S., Hsu, L.Y., Palacios, E.H., Levin, S.E., Kuriyan, J., Weiss, A., The structure, regulation, and function of ZAP-70, *Immunol. Rev.*, **2009**, 228, 41-57.
25. Folmer, R.H.A., Geschwindner, S., Xue, Y., Crystal structure and NMR studies of the apo SH2 domains of ZAP-70: two bikes rather than a tandem, *Biochemistry*, **2002**, 41, 14176-14184.
26. Hatada, M.H., Lu, X.D., Laird, E.R., Green, J., Morgenstern, J.P., Lou, M.Z., Marr, C.S., Phillips, T.B., Ram, M.K., Theriault, K., Zoller, M.J., Karas, J.L., Molecular-basis for interaction of the protein-tyrosine kinase Zap-70 with the T-cell receptor, *Nature*, **1995**, 377, 32-38.
27. Catalina, M.I., Fischer, M.J.E., Dekker, F.J., Liskamp, R.M.J., Heck, A.J.R., Binding of a diphosphorylated-ITAM peptide to spleen tyrosine kinase (Syk) induces distal conformational changes: a hydrogen exchange mass spectrometry study, *J. Am. Soc. Mass. Spectrom.*, **2005**, 16, 1039-1051.
28. Kaiser, E., Colescott, R.L., Bossinger, C.D., Cook, P.I., Color test for detection of free terminal amino groups in the solid-phase synthesis of peptides, *Anal. Biochem.*, **1970**, 34, 595-598.

Chapter 4

ITAM-derived phosphopeptide-containing dendrimers as multivalent ligands for Syk tandem SH2 domain

Parts of this chapter have been published:

Kuil, J., Branderhorst, H.M., Pieters, R.J., de Mol, N.J., Liskamp, R.M.J., ITAM-derived phosphopeptide-containing dendrimers as multivalent ligands for Syk tandem SH2 domain, *Org. Biomol. Chem.*, **2009**, 7, 4088-4094

Abstract

Spleen tyrosine kinase (Syk) is activated when its tandem SH2 domain (tSH2) binds to a diphosphorylated ITAM motif of e.g. the FcεRI receptor. In this divalent interaction each SH2 domain binds to a phosphotyrosine-containing tetrapeptide motif in ITAM. One of those tetrapeptide sequences was synthesized and conjugated to dendrimers via 'click' chemistry to create a series of functional phosphopeptide-containing dendrimers ranging from a monovalent to an octavalent dendrimer. The affinity of the functionalized dendrimers for Syk tSH2 has been assayed in SPR competition experiments. Both the tetra- and octavalent dendrimer had an affinity in the high nanomolar range, which is approximately a 100-fold enhancement compared to the monovalent tetrapeptide, indicating a multivalency effect.

Introduction

Multivalency can enhance binding affinity in peptide-protein and in carbohydrate-protein interactions to a great extent.[1-8] The simplest form of a multivalent interaction is a divalent interaction as is exemplified by the interaction between ITAM (Immunoreceptor Tyrosine based Activation Motif) and the tandem SH2 domain (tSH2) of the Syk kinase (Figure 1A).[9-13] This interaction is essential in the IgE receptor signaling pathway.[14-17] γ-ITAM is part of the intracellular domain of the γ-chain of the multimeric ($\alpha\beta\gamma_2$) high affinity IgE receptor (FcεRI). Once this receptor is stimulated by IgE binding, γ-ITAM is diphosphorylated at two tyrosine residues leading to 'γ-dpITAM'. The tSH2 domain of Syk can then bind to γ-dpITAM, which results in activation of the Syk kinase domain. The resulting kinase activity initiates an intracellular cascade which ends with mast cell degranulation.[15] Overstimulation of this cascade leads to allergic responses and therefore interference with this peptide-protein interaction can be relevant for therapeutic purposes.

In the divalent ITAM – Syk tSH2 interaction, the two monovalent interactions are not identical. Both the binding epitopes of γ-dpITAM as well as the two SH2 domains of Syk are slightly different. In the ITAM sequence, pTyr-Thr-Gly-Leu-Asn-Thr-Arg-Ser-Gln-Glu-Thr-pTyr-Glu-Thr-Leu (the SH2 binding epitopes are underlined), two out of four residues of both SH2 epitopes are not identical. The phosphorylated tyrosine and the leucine residue, which are identical, are most important for binding. Likewise, the two SH2 domains in Syk tSH2 are not identical, but there is a considerable amount of similarity: 35% of the sequences of the murine Syk SH2 domains are identical, 63% is identical or conserved and 75% is identical, conserved or semi-conserved (Figure 1B).[18]

The affinity of a monovalent phosphorylated ITAM-tetrapeptide for Syk tSH2 is approximately 1000-fold lower than that of dpITAM.[10-12] Thus, for high affinity both phosphotyrosine epitopes are needed and they should be connected to each other as in native ITAM. Several linkers have been designed to create high-affinity ITAM mimics, of which two (**5** and **6**) are depicted in Figure 2.[11,12] Both compounds showed distinct multivalency effects and compound **5** had even similar affinity for Syk tSH2 as native ITAM. The fact that Syk tSH2 binds ITAM-based ligands with varying distances between the SH2 binding epitopes with high affinity indicates that this protein possesses a considerable degree of flexibility. With this in mind, we wanted to explore the possibility to incorporate completely different linkers between the two binding epitopes,

while still retaining acceptable binding affinity. For this, multivalent dendrimeric scaffolds were very appropriate.

Dendrimers are often successfully applied as multivalent ligands for proteins.[19-23] In this study our versatile amino acid based dendrimers were used (Scheme 1) outfitted with alkyne moieties suitable for ligand attachment by 'click' chemistry.[24,25] Monovalent up to octavalent dendrimers were functionalized with ITAM-phosphotetrapeptide **7**, yielding ligands with various valencies and various lengths between the SH2 binding epitopes. The affinity for Syk tSH2 of the functionalized dendrimers has been assayed in SPR competition experiments.

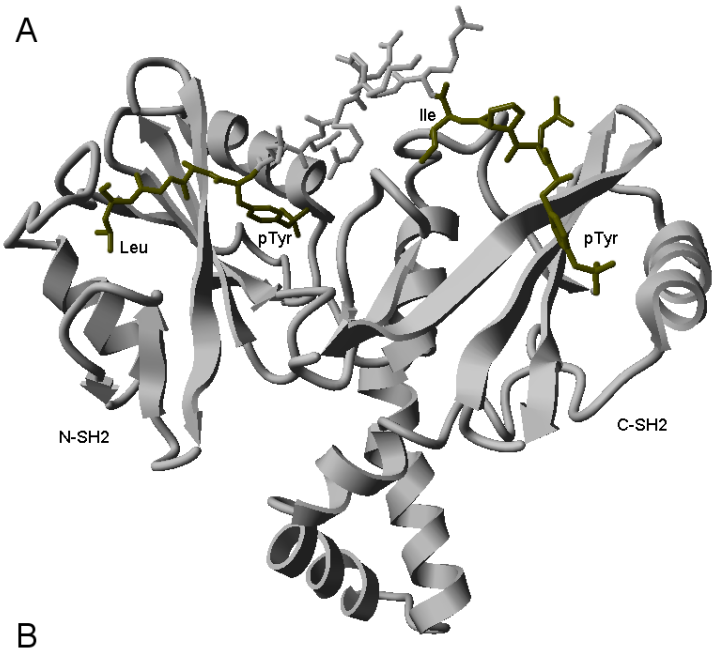

Figure 1. Syk tSH2. A: Crystal structure of Syk tSH2 complexed with ITAM, derived from the CD3ε chain of the T cell receptor.[9] The two tetrapeptidic epitopes of ITAM are shown in black. The N-terminal ITAM epitope binds Syk C-SH2 and the C-terminal ITAM epitope binds Syk N-SH2. B: Alignment of the murine SH2 domains of Syk. * identical residues; : conserved residues; . semi-conserved residues.

Results and discussion

Design

The design of multivalent ligands for Syk tSH2 started with the selection of one of the two tetrapeptidic epitopes of ITAM. The C-terminal epitope (C-ITAM: pTyr-Glu-Thr-Leu) binds Syk N-SH2 and the N-terminal epitope (N-ITAM: pTyr-Thr-Gly-Leu) binds Syk C-SH2 (Figure 1A).[9] The full-length ITAM phosphopeptide with only phosphorylation of the C-terminal tyrosine residue binds Syk tSH2 with a slightly higher affinity than when the N-terminal tyrosine residue is phosphorylated (K_D = 1.3 μM and 7.2 μM, respectively).[26] Furthermore, C-ITAM binds Syk C-SH2 with somewhat higher affinity than N-ITAM does (IC_{50} = 25 μM and 48 μM, respectively).[27] Therefore, the C-ITAM phosphopeptide was chosen for attachment to the dendrimers. In addition, the C-ITAM phosphopeptide incorporated in e.g. diphosphopeptide divalent molecular constructs **5** and **6** has been used in previous studies to improve the monovalent interaction (Figure 2).[10-12]

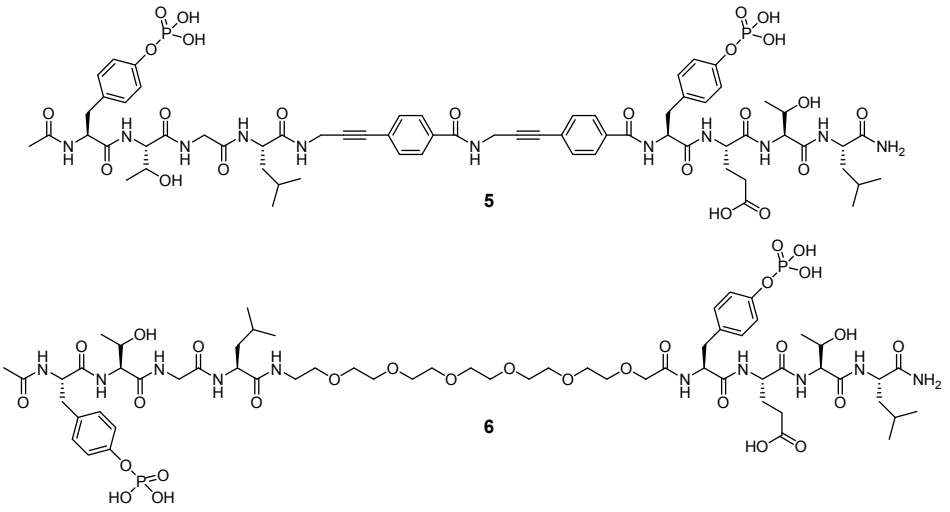

Figure 2. Previous prepared Syk tSH2 ligands containing C-ITAM.[12] The affinity for Syk tSH2 of compound **5** and **6** is, respectively, a 1000-fold and a 100-fold higher than C-ITAM.

Synthesis

The tetrapeptide (pTyr-Glu-Thr-Leu) was attached to dendrimers with a different number of alkyne endgroups via 'click' chemistry, that is the copper(I) catalyzed [3 + 2] cycloaddition between azides and alkynes.[21,25,28-30] Consequently, an azide functionality had to be introduced into the peptide. Furthermore, a spacer between the peptide and the dendrimers was introduced to provide sufficient space for bridging both SH2 domains in Syk tSH2 and therefore the clickable phosphopeptide **7** (Scheme 1) containing a 6-azidohexanoic acid spacer was prepared.

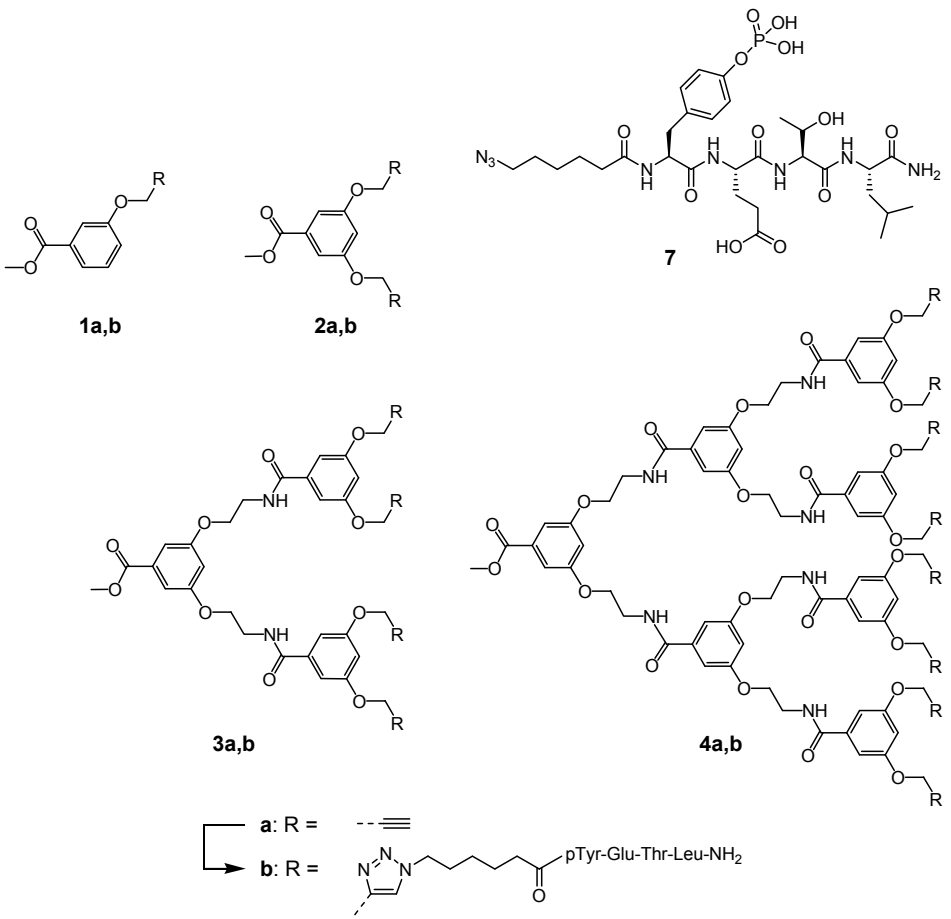

Scheme 1. Synthesis of the dendrimers functionalized with phosphopeptide **7**. General reaction conditions: 1.5 equiv **7** per arm, 0.5 equiv $CuSO_4 \cdot 5H_2O$ and 0.5 equiv sodium ascorbate per arm in DMF/H_2O, 80 ºC, microwave heating, 20 min. Yields: **1b** 94%, **2b** 53%, **3b** 50%, **4b** 56%.

Phosphopeptide **7** was assembled on the solid phase and the synthesis of the dendrimers has been described previously.[25] The dendrimers were subsequently functionalized with the azidophosphopeptide using 'click' chemistry (Scheme 1). To ensure completion of the reaction, 1.5 equivalent of phosphopeptide per arm was added. All reactions were complete after 20 min using microwave heating. The yield of monovalent structure **1b,** after RP-HPLC purification, was very good (94%). The yields, after purification of the other dendrimers **2b**, **3b** and especially **4b**, were very satisfactory.

Binding studies

The binding of the dendrimers to Syk tSH2 was examined using surface plasmon resonance (SPR) as was described previously.[11] Native γ-dpITAM containing a N-terminal 6-aminohexanoic acid spacer was immobilized on a SPR sensor chip. First, the affinity of Syk tSH2 for the immobilized native ITAM peptide was determined by addition of different concentrations of Syk tSH2 and the equilibrium signal was fitted to a Langmuir binding isotherm (Figure 3A). The K_D value for binding to the chip (K_C) was found to be 7.8 nM, which is comparable to the 5.6 nM affinity found earlier.[31] Then SPR competition experiments were performed by adding different concentrations of the phosphopeptide-containing dendrimers in the presence of 25 nM Syk tSH2 to evaluate the affinity of the compounds for Syk tSH2. From the obtained inhibition curves the dissociation constants were calculated by fitting to a competition model yielding thermodynamic binding constants in solution (K_S) (Figure 3B and Table 1).[32]

The affinity of monovalent phosphopeptide construct **1b** for Syk tSH2 is 20 μM. This is very similar to the K_D value of Ac-pTyr-Glu-Thr-Leu-NH_2, which is 27 μM.[10] Divalent compound **2b** shows a very modest increase in affinity (K_S = 6.5 μM), which is explained by the two-fold increase in binding sites and is still indicative of a monovalent interaction. The fact that **2b** is still monovalently bound can be rationalized by the fact that the orientation of the two epitopes with respect to each other is inverted in **2b** compared with ITAM. This also explains why this divalent construct is significantly less active than the earlier reported divalent constructs **5** and **6**. Thus, compound **2b** might be considered as H_2N-Leu-Thr-Glu-pTyr-dendrimer-pTyr-Glu-Thr-Leu-NH_2, whereas the ITAM sequence is pTyr-Thr-Gly-Leu-$(Xxx)_7$-pTyr-Glu-Thr-Leu. The space between both phosphotyrosine-containing epitopes is apparently not enough to allow repositioning and truly divalent binding.

The tetravalent phosphopeptide-containing dendrimer **3b** did bind with a significantly higher affinity than **1b**, showing a distinct multivalency effect. The K_S value was 252 nM, which is 79 times lower than the value for the monovalent dendrimer **1b**. This means that the relative potency of **3b** per peptide is 20. Octavalent phosphopeptide-containing **4b** displayed a similar affinity as phosphopeptide-containing **3b**. Because of this, the relative potency per peptide is lower, although the affinity for tSH2 is slightly higher than that of **3b**. The similar potency of dendrimer **3b** and **4b** might indicate that upon binding of one Syk tSH2 protein, there is no space left to bind a second Syk tSH2.

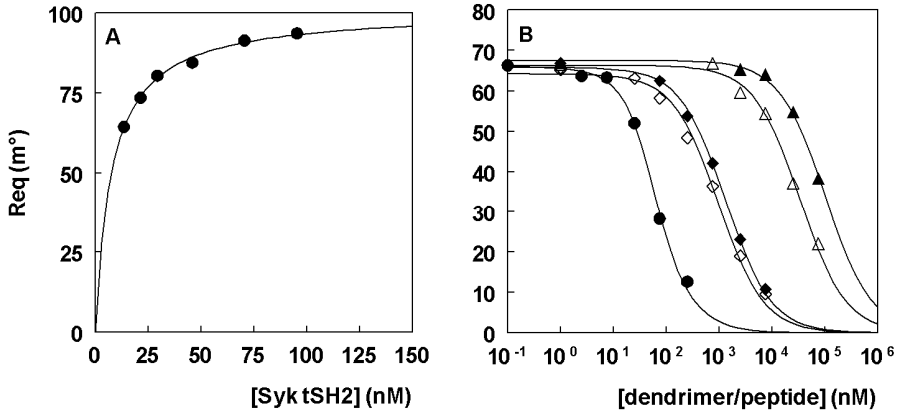

Figure 3. A: SPR determination of the affinity of Syk tSH2 for immobilized γ-dpITAM phosphopeptide on the sensor surface (K_C). Data of equilibrium signals are fitted with a Langmuir binding isotherm. B: SPR competition experiments in the presence of 25 nM Syk tSH2. Data are fitted with a competition model yielding the affinity in solution (K_S) as described.[32] The inhibition curves represent γ-dpITAM (●), **1b** (▲), **2b** (Δ), **3b** (♦) and **4b** (◊).

Table 1. Affinities of the phosphopeptide-containing dendrimers and two reference peptides for Syk tSH2 from SPR competition experiments (K_S values).

Compound	Valency	K_S (nM)	Relative potency (per peptide)
Ac-pTyr-Glu-Thr-Leu-NH_2[10]	1	27 000	-
native ITAM	2	8.3 ± 0.7	-
1b	1	19 810 ± 1168	1 (1)
2b	2	6 518 ± 565	3.0 (1.5)
3b	4	252 ± 16	79 (20)
4b	8	183 ± 17	108 (14)

The tetra- and octavalent phosphopeptide-containing dendrimers **3b** and **4b** had similar affinities for Syk tSH2 as previously synthesized ITAM mimic **6**.[12] However, none of these dendrimers had a similar affinity as the native γ-dpITAM peptide or ITAM mimic **5**. A possible explanation for this lower affinity might be that the orientation of the two SH2 epitopes in the dendrimers is not optimal for binding, as was discussed above for **2b**. All phosphopeptide epitopes were N-terminally conjugated to the alkyne-containing dendrimers, whereas in native ITAM and in the mimics **5** and **6** the N-terminus of one epitope (C-ITAM) was connected to the C-terminus of the other epitope (N-ITAM) (Figure 4). Hence, to mimic ITAM ultimately better, it might be preferable to functionalize the dendrimers with a mixture of epitopes possessing N-terminal – and C-terminal containing azides. However, this would yield mixtures of phosphopeptide-containing dendrimers, which are difficult to characterize. Furthermore, the aim of this study was to prepare relative simple phosphodendrimers with high-affinity for Syk tSH2. Therefore, we chose to attach all peptidic epitopes N-terminally, which resulted in pure compounds that could be fully characterized and displayed considerable multivalency effects.

In addition to divalent binding via a chelation mechanism[2], addressed above, also other mechanisms of multivalent binding may take place, such as statistical rebinding.[5,33,34] This effect is caused by an overall slower off-rate of the multivalent ligand due to the close proximity of, in this case, other phospho-epitopes, which can replace the bound epitope when released from one of the SH2 domains. Comparing **3b** to **4b**, in **4b** more phospho-epitopes are available (Figure 4), which could lead to

enhanced rebinding. However, no marked increased in affinity is observed, which might indicate that these additional epitopes are not within reach of an SH2 domain from which a bound epitope is released.

Because chelation was probably the predominant factor of the enhanced binding affinity, it is important that the dendrimers are large enough to bridge the distance between the two SH2 domains of Syk tSH2. When no ligand is present, tSH2 probably has an extended conformation in which the two SH2 domains are more apart from each other (left cartoon in Figure 4).[31] The SH2 domains move closer to one another upon binding of the native ITAM sequence.[31] It was expected that the distance between the alkyne endgroups in the dendrimers was not sufficiently large to bridge the two SH2 domains of Syk tSH2. Therefore, a flexible 6-azidohexanoic acid spacer was introduced between the dendrimeric scaffold and the SH2 binding epitopes for providing enough length and flexibility to adapt the construct to the correct shape for binding. Clearly, this was not the case for divalent compound **2b**. In the tetra – and octavalent dendrimers **3b** and **4b**, however, there is sufficient space for bridging the two SH2 domains, indicated by the strongly increased affinity. The fact that **3b** and **4b** had similar affinities for Syk tSH2 indicates that in the larger **4b** inter SH2 binding distances are not improved compared to **3b**.

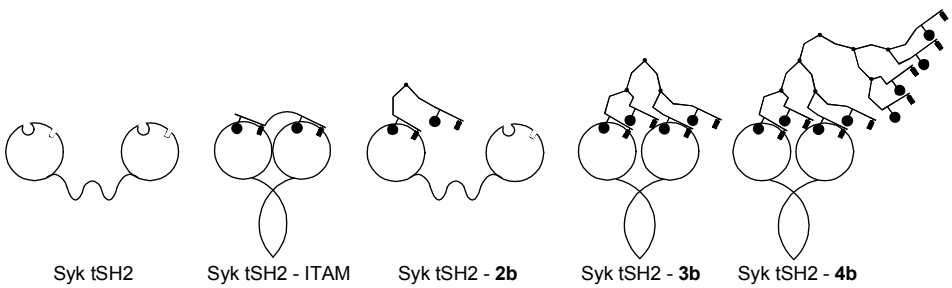

Figure 4. Models of possible binding to Syk tSH2. When Syk tSH2 is unbound, then the SH2 domains are more apart from each other (left cartoon).[31] Ligands, which can bind divalently, such as ITAM, **3b** and **4b**, are likely capable to bring the SH2 domains closer to one another,[31] which could be important for Syk kinase activation, as has been suggested for the closely related Zap-70 kinase.[35,36] The black circles represent the side-chains of pTyr and the black rectangles represent the side-chains of Leu.

The lower affinities of the dendrimers compared with native ITAM showed that the dendrimeric phosphopeptide ligands cannot fully adapt their orientation for optimal binding to Syk tSH2 and vice versa. Hence, despite the fact that Syk tSH2 is a relatively flexible protein,[31] complete adjustment of its conformation for a proper alignment with the tetra- and octavalent compounds seems not possible.

The dendrimeric scaffolds are possibly not the only reason for the fact that the dendrimers cannot fully adapt their orientation for Syk tSH2 binding. Another reason for the lower affinity than native ITAM might be that in ITAM both SH2 domains bind their preferred optimal sequence of four amino acid residues. In the case of the phosphodendrimers, C-SH2 has to bind to a non-native sequence, as was discussed in the design. Although the effect of the absence of the native C-SH2 ligand is probably minor, it is possible that dendrimers containing both C-ITAM and N-ITAM epitopes will bind Syk tSH2 with higher affinity.

Conclusions

An azide-containing phosphopeptide ligand for binding to Syk N-SH2 was synthesized and efficiently coupled by a copper(I) catalyzed [3 + 2] cycloaddition ('click') reaction to different generations of alkyne-containing dendrimers. The affinity of the resulting phosphopeptide-containing dendrimers for Syk tSH2 was determined by SPR in competition assays. The affinity of the monovalent construct **1b** and the divalent phosphopeptide-containing dendrimer **2b** was in the same order of magnitude as the phosphopeptide itself. The tetra- and octavalent phosphopeptide-containing dendrimers **3b** and **4b** showed indeed a multivalency effect and they both had K_D values in a range comparable to previously synthesized ITAM mimics.[11-13] The affinity might be improved further by using multivalent phosphopeptide dendrimeric constructs containing both C-terminally and N-terminally linked phosphopeptides to dendrimers, which is under present investigation.

Experimental section

General

All chemicals were obtained from commercial sources and used without further purification. Solvents, which were used for the solid phase peptide synthesis, were stored over 4 Å molecular sieves. The reactions were performed at room temperature unless stated otherwise. The reactions were monitored and the R_f values were determined by thin layer chromatography (TLC). The TLC plates were obtained from Merck and were coated with silica gel 60 F-254 (0.25 mm). The spots were visualized by UV light and Cl_2-TDM *(N,N,N',N',*-tetramethyl-4,4'-diaminodiphenylmethane) staining. Solvents were removed under reduced pressure at a temperature of 40 ºC. Column chromatography was performed with Silicycle UltraPure silica gels, SiliaFlash (pore size 60 Å, particle size distribution 40-63 μm).

^{1}H NMR spectra were measured on a Varian Mercury plus 300 MHz spectrometer or a Varian Inova 500 MHz spectrometer and the chemical shifts are given in ppm (δ) relative to TMS, except for **7** (MeOH) and for **1b** and **2b** (dioxane). ^{13}C NMR spectra were measured on a Varian Mercury plus 75 MHz spectrometer and the chemical shifts are given in ppm (δ) relative to $CDCl_3$. The ^{13}C NMR spectra were measured using the attached proton test (APT). Microwave reactions were carried out in a Biotage Initiator microwave oven. The microwave power was limited by temperature control once the desired temperature was reached. A sealed vessel of 0.5-2 mL was used. The crude peptide and dendrimers were analyzed with an analytical Shimadzu HPLC system with a UV detector operating at 220 and 254 nm using an Alltech Alltima C8 90 Å 5 μm (250 × 4.6 mm) column. For analytical HPLC a gradient of 100% buffer A (15 mM TEA in H_2O titrated at pH 6 with 85% H_3PO_4) to 100% buffer B (buffer A/CH_3CN 1:9) in 20 min was used. For preparative HPLC a Gilson system with a UV detector operating at 220 and 254 nm equipped with an Alltech Alltima C8 100 Å 10 μm (250 × 22 mm) column was used. A gradient of 100% buffer A (0.1% TFA in H_2O/CH_3CN 95:5) to 100% buffer B (0.1% TFA in H_2O/CH_3CN 5:95) in 100 min was used unless otherwise stated. The purity of the preparative HPLC fractions was assessed with analytical HPLC using the same conditions as stated above.

SPR measurements were performed on a double channel IBISII SPR instrument (Eco Chemie, Utrecht, The Netherlands) equipped with a CM 5 sensor chip (BIAcore AB, Uppsala, Sweden).

6-azidohexanoic acid

6-bromohexanoic acid (1.95 g, 10 mmol) and NaN_3 (3.25 g, 50 mmol) were added to 100 mL of DMF and the mixture was stirred overnight at 100 ºC. DMF was evaporated and EtOAc was added. The organic phase was washed with 1 M $KHSO_4$ (3 ×) and brine, dried over Na_2SO_4, filtered and concentrated yielding 1.57 g of 6-azidohexanoic acid as a brown oil in quantitative yield. The product was used without further purification. R_f = 0.44 (0.5% CH_3COOH in CH_2Cl_2/MeOH 95:5). ^1H NMR ($CDCl_3$, 300 MHz) δ = 1.41-1.49 (m, 2H, CH_2), 1.58-1.73 (m, 4H, 2 CH_2), 2.34-2.41 (m, 2H, C*H*$_2$COOH), 3.29 (t, 2H, N_3CH_2), 11.28 (bs, 1H, COOH). ^{13}C NMR ($CDCl_3$, 75 MHz) δ = 23.8, 27.6, 32.3, 33.4, 33.8, (5 CH_2), 179.6 (COOH).

Azido phosphopeptide 7

The peptide was manually assembled on Tentagel®-Rink-NH-Fmoc resin (1.92 g, 0.50 mmol, loading 0.26 mmol/g) using standard Fmoc/tBu chemistry. The Fmoc protecting group was removed using 20% piperidine in NMP (3 × 20 mL, each 8 min) followed by washing with NMP (3 × 20 mL, each 2 min), CH_2Cl_2 (3 × 20 mL, each 2 min) and NMP (3 × 20 mL, each 2 min). The amino acid coupling mixtures were prepared by dissolving 4 equivalents of amino acid (2.0 mmol), 4 equivalents of HOBt and HBTU and 8 equivalents of DiPEA in NMP (20 mL) and coupled during a coupling time of 60 minutes. The resin was washed with NMP (3 × 20 mL, each 1 min) and CH_2Cl_2 (3 × 20 mL, each 1 min) after every coupling step. The coupling steps and deprotection steps were monitored using the Kaisertest.[37] The amino acid building blocks Fmoc-Leu-OH, Fmoc-Thr(tBu)-OH, Fmoc-Glu(OtBu)-OH, Fmoc-Tyr(OP(OBn)OH)-OH and 6-azidohexanoic acid were subsequently coupled. Fmoc-Tyr(OP(OBn)OH)-OH was coupled overnight using 2 equivalents of amino acid, 2 equivalents of the coupling reagents HBTU and HOBt and 5 equivalents of DiPEA. After the Fmoc-Tyr(OP(OBn)OH)-OH coupling an extra washing step (2 × 20 mL, each 10 min) with a mixture of 1 M TFA/1.1 M DiPEA in NMP was performed after the Fmoc deprotection step. This was done to replace the piperidine counter ion of Tyr(OP(OBn)O$^-$) for protonated DiPEA. When all the coupling steps and deprotection steps were completed the peptide was cleaved from the resin and the side chains were deprotected with a solution of TFA/H_2O/TIS (95/2.5/2.5) for 3 h. The resin was removed from the solution by filtration. The peptide was precipitated with MTBE/hexane 1:1 v/v at -20 °C and lyophilized from CH_3CN/H_2O 1:1 v/v yielding 260 mg of the crude peptide. 150 mg of

the peptide was purified by preparative HPLC. A gradient of 100% buffer A to 100% buffer B in 40 minutes was used. The product was obtained after pooling and lyophilization as a fluffy white solid (71.2 mg).
HRMS (ESI): $[M+H]^+$ calculated 743.3129, found 743.3163.
^{1}H NMR (D_2O, 300 MHz) δ = 0.91, 0.97 (2d, 6H, 2 CH_3 Leu), 1.25 (d, 3H, Thr CH_3), 1.26-1.30 (m, 2H, Azhx CH_2), 1.50-1.62 (m, 4H, Azhx 2 CH_2), 1.66-1.76 (m, 3H, Leu β CH_2 and δ CH), 1.97-2.14 (m, 2H, Glu β CH_2), 2.27 (t, 2H, Azhx CH_2), 2.44 (dd, 2H, Glu δ CH_2), 2.94-3.17 (m, 2H, pTyr β CH_2), 3.30 (t, 2H, Azhx CH_2), 4.19-4.23 (m, 1H, Thr β CH), 4.34 (d, 1H, Thr α CH), 4.38-4.44 (m, 2H, Leu α CH, Glu α CH), 4.59 (dd, 1H, pTyr α CH), 7.16, 7.25 (2d, 4H, ar pTyr).

Dendrimer 1a, 2a, 3a, 4a
The synthesis of these dendrimers was described earlier.[25,30]

Phosphopeptide containing dendrimer 1b
A solution of **1a** (2.85 mg, 15 μmol), **7** (16.71 mg, 22.5 μmol), $CuSO_4.5H_2O$ (1.87 mg, 7.5 μmol) and sodium ascorbate (1.49 mg, 7.5 μmol) in 1 mL of DMF and 100 μL of H_2O was heated under microwave irradiation at 80 °C for 20 min. Analytical HPLC showed complete consumption of **1a**. The mixture was concentrated and subjected to purification by preparative HPLC. The product was obtained after lyophilization as a fluffy white solid (13.1 mg, 94%).
HRMS (ESI): $[M+Na]^+$ calculated 955.3657, found 955.3717.
^{1}H NMR (D_2O, 500 MHz) δ = 0.84, 0.90 (2d, 6H, 2 CH_3 Leu), 0.93-0.98 (m, 2H, Azhx CH_2), 1.20 (d, 3H, Thr CH_3), 1.43 (bs, 2H, Azhx CH_2), 1.56-1.67 (m, 3H, Leu β CH_2 and δ CH), 1.80 (bs, 2H, Azhx CH_2), 1.89-2.08 (m, 2H, Glu β CH_2), 2.14 (bs, 2H, Azhx CH_2), 2.37 (bs, 2H, Glu δ CH_2), 2.90-3.05 (m, 2H, pTyr β CH_2), 3.90 (s, 3H, CH_3OOC), 4.17 (m, 1H, Thr β CH), 4.29 (m, 1H, Thr α CH), 4.38 (m, 1H, Leu α CH), 4.55 (m, 1H, Glu α CH), 4.66 (bd, 1H, pTyr α CH), 4.78 (bs, 4H, Azhx CH_2 and CH_2CCH), 7.07, 7.14 (2d, 4H, Ar pTyr), 7.29, 7.45, 7.63 (3m, 4H, Ar), 8.08 (s, 1H, $CH_{triazole}$), 8.25, 8.29, 8.36, 8.39 (4d, 4H, 4 NH).

Phosphopeptide containing dendrimer 2b
A solution of **2a** (1.83 mg, 7.5 μmol), **7** (16.71 mg, 22.5 μmol), $CuSO_4.5H_2O$ (1.87 mg, 7.5 μmol) and sodium ascorbate (1.49 mg, 7.5 μmol) in 1 mL of DMF and 100 μL of

H_2O was heated under microwave irradiation at 80 °C for 20 min. Analytical HPLC showed complete consumption of **2a**. The mixture was concentrated and subjected to purification by preparative HPLC. The product was obtained after lyophilization as a fluffy white solid (6.9 mg, 53%).

HRMS (ESI): $[M+H]^+$ calculated 1729.6916, found 1729.5875; $[M+Na]^+$ calculated 1751.6735, found 1751.6201; $[M+2H]^{2+}$ calculated 865.3497, found 865.324; $[M+H+Na]^{2+}$ calculated 876.3407, found 876.2612; $[M+2Na]^{2+}$ calculated 887.3317, found 887.2672.

^{1}H NMR (D_2O, 500 MHz) δ = 0.83, 0.88 (2d, 12H, 4 CH_3 Leu), 0.94 (m, 4H, 2 Azhx CH_2), 1.20 (s, 6H, 2 Thr CH_3), 1.42 (bs, 4H, 2 Azhx CH_2), 1.55-1.66 (m, 6H, 2 Leu β CH_2 and δ CH), 1.78 (bs, 4H, 2 Azhx CH_2), 1.89-2.06 (m, 4H, 2 Glu β CH_2), 2.13 (bs, 4H, 2 Azhx CH_2), 2.36 (bs, 4H, 2 Glu δ CH_2), 2.89-3.01 (m, 4H, 2 pTyr β CH_2), 3.89 (s, 3H, CH_3OOC), 4.17 (m, 2H, 2 Thr β CH), 4.29 (m, 2H, 2 Thr α CH), 4.37 (m, 2H, 2 Leu α CH), 4.56 (m, 2H, 2 Glu α CH), 4.68 (bd, 2H, 2 pTyr α CH), 4.81 (bs, 8H, 2 Azhx CH_2 and 2 C*H*$_2$CCH), 6.89 (s, 4H, 2 NH_2), 7.06, 7.09 (2d, 8H, 2 Ar pTyr), 7.16, 7.27, 7.64 (3m, 3H, Ar), 8.06 (s, 2H, 2 $CH_{triazole}$), 8.22, 8.27, 8.36, 8.37 (4d, 8H, 8 NH).

Phosphopeptide containing dendrimer 3b

A solution of **3a** (2.55 mg, 3.75 μmol), **7** (16.71 mg, 22.5 μmol), $CuSO_4.5H_2O$ (1.87 mg, 7.5 μmol) and sodium ascorbate (1.49 mg, 7.5 μmol) in 1 mL of DMF and 100 μL of H_2O was heated under microwave irradiation at 80 °C for 20 min. Analytical HPLC showed complete consumption of **3a**. The mixture was concentrated and subjected to purification by preparative HPLC. The product was obtained after lyophilization as a fluffy white solid (6.8 mg, 50%).

HRMS (ESI): $[M+H+Na]^{2+}$ calculated 1837.298, found 1837.514.

^{1}H NMR (DMSO-d_6, 300 MHz) δ = 0.82, 0.86 (2d, 24H, 8 CH_3 Leu), 1.04 (d, 12H, 4 Thr CH_3), 1.07-1.18 (m, 8H, 4 Azhx CH_2), 1.39-1.53 (m, 16H, 8 Azhx CH_2), 1.56-1.65 (m, 4H, 4 Leu δ CH), 1.73-1.83 (m, 8H, 4 Leu β CH_2), 1.91-2.09 (m, 16H, 4 Glu β CH_2 and 4 Azhx CH_2), 2.24-2.32 (m, 8H, 4 Glu δ CH_2), 2.69-2.73, 2.95-2.99 (2m, 8H, 4 pTyr β CH_2), 3.85 (s, 3H, CH_3OOC), 4.00 (t, 4H, 2 OCH_2CH_2NH), 4.18-4.33 (m, 28H, 4 Thr β CH and 4 Thr α CH and 4 Leu α CH and 4 Glu α CH and 4 Azhx CH_2 and 2 O*CH*$_2$CH$_2$NH), 4.51 (m, 4H, 4 pTyr α CH), 5.17 (s, 8H, 4 C*H*$_2$CCH), 6.92 (s, 8H, 4 NH_2), 7.04 (d, 8H, Ar pTyr), 7.18-7.27 (m, 17H, Ar pTyr and Ar), 7.72 (d, 4H, 4 Thr

NH), 7.75 (d, 4H, 4 Leu NH), 8.04 (d, 4H, 4 pTyr NH), 8.22 (s, 4H, 4 $CH_{triazole}$), 8.24 (d, 4H, 4 Glu NH), 9.01 (bs, 2H, 2 OCH_2CH_2NH).

Phosphopeptide containing dendrimer 4b

A solution of **4a** (2.90 mg, 1.875 μmol), **7** (16.71 mg, 22.5 μmol), $CuSO_4.5H_2O$ (1.87 mg, 7.5 μmol) and sodium ascorbate (1.49 mg, 7.5 μmol) in 1 mL of DMF and 100 μL of H_2O was heated under microwave irradiation at 80 °C for 20 min. Analytical HPLC showed complete consumption of **4a**. The mixture was concentrated and subjected to purification by preparative HPLC. The product was obtained after lyophilization as a fluffy white solid (7.9 mg, 56%).

HRMS (ESI): $[M+4H]^{4+}$ calculated 1873.353, found 1873.312; $[M+3H+Na]^{4+}$ calculated 1879.101, found 1879.177; $[M+4H+Na]^{5+}$ calculated 1503.482, found 1503.581.

^{1}H NMR (DMSO-d_6, 300 MHz) δ = 0.81, 0.86 (2d, 48H, 16 CH_3 Leu), 1.03 (d, 24H, 8 Thr CH_3), 1.07-1.12 (m, 16H, 8 Azhx CH_2), 1.39-1.49 (m, 32H, 16 Azhx CH_2), 1.55-1.62 (m, 8H, 8 Leu δ CH), 1.72-1.77 (m, 16H, 8 Leu β CH_2), 1.91-2.03 (m, 32H, 8 Glu β CH_2 and 8 Azhx CH_2), 2.24-2.29 (m, 16H, 8 Glu δ CH_2), 2.69-2.73, 2.95-2.99 (2m, 16H, 8 pTyr β CH_2), 3.79 (s, 3H, CH_3OOC), 4.00-4.02 (m, 12H, 6 OCH_2CH_2NH), 4.14-4.36 (m, 60H, 8 Thr β CH and 8 Thr α CH and 8 Leu α CH and 8 Glu α CH and 8 Azhx CH_2 and 6 OCH_2CH_2NH), 4.51 (m, 8H, 8 pTyr α CH), 5.15 (s, 16H, 8 CH_2CCH), 6.90 (s, 16H, 8 NH_2), 7.04 (d, 16H, Ar pTyr), 7.15-7.27 (m, 37H, Ar pTyr and Ar), 7.75 (d, 8H, 8 Thr NH), 7.83 (d, 8H, 8 Leu NH), 8.04 (d, 8H, 8 pTyr NH), 8.21 (s, 8H, 8 $CH_{triazole}$), 8.24 (d, 8H, 8 Glu NH), 8.68 (bs, 6H, 6 OCH_2CH_2NH).

SPR binding studies

Stock solutions of dendrimers **1b**, **2b**, **3b** and **4b** with a concentration of 1 mM in HEPES buffered saline (HBS) buffer were prepared. For **3b** and **4b** 17% DMSO was present in this stock solution to keep the compounds dissolved. The sensor chip was immobilized with the native γ-dpITAM peptide as was described earlier.[11] The affinity of Syk tSH2 for the immobilized ITAM peptide was determined by addition of Syk tSH2 in a concentration range of 0 to 100 nM in HBS buffer. The K_C value was calculated by fitting the equilibrium signals to a Langmuir binding isotherm.

Competition experiments were performed with different concentrations of the phosphopeptide-containing dendrimers in the presence of 25 nM Syk tSH2 in HBS buffer. K_S values were calculated according to described procedures.[32]

References

1. Mammen, M., Choi, S.K., Whitesides, G.M., Polyvalent interactions in biological systems: Implications for design and use of multivalent ligands and inhibitors, *Angew. Chem. Int. Ed.*, **1998**, 37, 2755-2794.
2. Lundquist, J.J., Toone, E.J., The cluster glycoside effect, *Chem. Rev.*, **2002**, 102, 555-578.
3. Kitov, P.I., Bundle, D.R., On the nature of the multivalency effect: A thermodynamic model, *J. Am. Chem. Soc.*, **2003**, 125, 16271-16284.
4. Reczek, J.J., Kennedy, A.A., Halbert, B.T., Urbach, A.R., Multivalent recognition of peptides by modular self-assembled receptors, *J. Am. Chem. Soc.*, **2009**, 131, 2408-2415.
5. Kiessling, L.L., Gestwicki, J.E., Strong, L.E., Synthetic multivalent ligands as probes of signal transduction, *Angew. Chem. Int. Ed.*, **2006**, 45, 2348-2368.
6. Rao, J.H., Lahiri, J., Isaacs, L., Weis, R.M., Whitesides, G.M., A trivalent system from vancomycin·D-Ala-D-Ala with higher affinity than avidin·biotin, *Science*, **1998**, 280, 708-711.
7. Badjic, J.D., Nelson, A., Cantrill, S.J., Turnbull, W.B., Stoddart, J.F., Multivalency and cooperativity in supramolecular chemistry, *Acc. Chem. Res.*, **2005**, 38, 723-732.
8. Robinson, J.A., Design of protein-protein interaction inhibitors based on protein epitope mimetics, *ChemBioChem*, **2009**, 10, 971-973.
9. Futterer, K., Wong, J., Grucza, R.A., Chan, A.C., Waksman, G., Structural basis for Syk tyrosine kinase ubiquity in signal transduction pathways revealed by the crystal structure of its regulatory SH2 domains bound to a dually phosphorylated ITAM peptide, *J. Mol. Biol.*, **1998**, 281, 523-537.
10. Ruijtenbeek, R., Kruijtzer, J.A.W., van de Wiel, W., Fischer, M.J.E., Fluck, M., Redegeld, F.A.M., Liskamp, R.M.J., Nijkamp, F.P., Peptoid-peptide hybrids that bind Syk SH2 domains involved in signal transduction, *ChemBioChem*, **2001**, 2, 171-179.
11. Dekker, F.J., de Mol, N.J., van Ameijde, J., Fischer, M.J.E., Ruijtenbeek, R., Redegeld, F.A.M., Liskamp, R.M.J., Replacement of the intervening amino acid sequence of a Syk-binding diphosphopeptide by a nonpeptide spacer with preservation of high affinity, *ChemBioChem*, **2002**, 3, 238-242.
12. Dekker, F.J., de Mol, N.J., Fischer, M.J.E., Liskamp, R.M.J., Amino propynyl benzoic acid building block in rigid spacers of divalent ligands binding to the Syk SH2 domains with equally high affinity as the natural ligand, *Bioorg. Med. Chem. Lett.*, **2003**, 13, 1241-1244.
13. Kuil, J., van Wandelen, L.T.M., de Mol, N.J., Liskamp, R.M.J., A photoswitchable ITAM peptidomimetic: Synthesis and real time surface plasmon resonance (SPR) analysis of the effects of cis-trans isomerization on binding, *Bioorg. Med. Chem.*, **2008**, 16, 1393-1399.
14. Gilfillan, A.M., Tkaczyk, C., Integrated signalling pathways for mast-cell activation, *Nat. Rev. Immunol.*, **2006**, 6, 218-230.
15. Kraft, S., Kinet, J.-P., New developments in FcεRI regulation, function and inhibition, *Nat. Rev. Immunol.*, **2007**, 7, 365-378.
16. Siraganian, R.P., Zhang, J., Suzuki, K., Sada, K., Protein tyrosine kinase Syk in mast cell signaling, *Mol. Immun.*, **2001**, 38, 1229-1233.
17. Bradding, P., Novel approaches to the inhibition of mast cells in allergic disease, *Clin. Exp. Allergy*, **2008**, 38, 704-708.
18. http://www.ebi.ac.uk/Tools/clustalw2/index.html

19. Niederhafner, P., Sebestik, J., Jezek, J., Peptide dendrimers, *J. Pept. Sci.*, **2005**, 11, 757-788.
20. Pieters, R.J., Rijkers, D.T.S., Liskamp, R.M.J., Application of the 1,3-dipolar cycloaddition reaction in chemical biology: Approaches toward multivalent carbohydrates and peptides and peptide-based polymers, *QSAR Comb. Sci.*, **2007**, 26, 1181-1190.
21. Branderhorst, H.M., Liskamp, R.M.J., Visser, G.M., Pieters, R.J., Strong inhibition of cholera toxin binding by galactose dendrimers, *Chem. Commun.*, **2007**, 5043-5045.
22. van Baal, I., Malda, H., Synowsky, S.A., van Dongen, J.L.J., Hackeng, T.M., Merkx, M., Meijer, E.W., Multivalent peptide and protein dendrimers using native chemical ligation, *Angew. Chem. Int. Ed.*, **2005**, 44, 5052-5057.
23. Lee, C.C., MacKay, J.A., Frechet, J.M.J., Szoka, F.C., Designing dendrimers for biological applications, *Nat. Biotechnol.*, **2005**, 23, 1517-1526.
24. Mulders, S.J.E., Brouwer, A.J., Van der Meer, P.G.J., Liskamp, R.M.J., Synthesis of a novel amino acid based dendrimer, *Tetrahedron Lett.*, **1997**, 38, 631-634.
25. Rijkers, D.T.S., van Esse, G.W., Merkx, R., Brouwer, A.J., Jacobs, H.J.F., Pieters, R.J., Liskamp, R.M.J., Efficient microwave-assisted synthesis of multivalent dendrimeric peptides using cycloaddition reaction (click) chemistry, *Chem. Commun.*, **2005**, 4581-4583.
26. Grucza, R.A., Bradshaw, J.M., Mitaxov, V., Waksman, G., Role of electrostatic interactions in SH2 domain recognition: Salt-dependence of tyrosyl-phosphorylated peptide binding to the tandem SH2 domain of the Syk kinase and the single SH2 domain of the Src kinase, *Biochemistry*, **2000**, 39, 10072-10081.
27. Narula, S.S., Yuan, R.W., Adams, S.E., Green, O.M., Green, J., Philips, T.B., Zydowskyt, L.D., Botfield, M.C., Hatada, M., Laird, E.R., Zoller, M.J., Karas, J.L., Dalgarnol, D.C., Solution structure of the C-terminal SH2 domain of the human tyrosine kinase Syk complexed with a phosphotyrosine pentapeptide, *Structure*, **1995**, 3, 1061-1073.
28. Rostovtsev, V.V., Green, L.G., Fokin, V.V., Sharpless, K.B., A stepwise Huisgen cycloaddition process: Copper(I)-catalyzed regioselective "ligation" of azides and terminal alkynes, *Angew. Chem. Int. Ed.*, **2002**, 41, 2596-2599.
29. Tornoe, C.W., Christensen, C., Meldal, M., Peptidotriazoles on solid phase: [1,2,3]-triazoles by regiospecific copper(I)-catalyzed 1,3-dipolar cycloadditions of terminal alkynes to azides, *J. Org. Chem.*, **2002**, 67, 3057-3064.
30. Joosten, J.A.F., Tholen, N.T.H., El Maate, F.A., Brouwer, A.J., van Esse, G.W., Rijkers, D.T.S., Liskamp, R.M.J., Pieters, R.J., High-yielding microwave-assisted synthesis of triazole-linked glycodendrimers by copper-catalyzed [3+2] cycloaddition, *Eur. J. Org. Chem.*, **2005**, 3182-3185.
31. De Mol, N.J., Catalina, M.I., Dekker, F.J., Fischer, M.J.E., Heck, A.J., Liskamp, R.M.J., Protein flexibility and ligand rigidity: a thermodynamic and kinetic study of ITAM-based ligand binding to Syk tandem SH2, *ChemBioChem*, **2005**, 6, 2261-2270.
32. De Mol, N.J., Gillies, M.B., Fischer, M.J.E., Experimental and calculated shift in pK_a upon binding of phosphotyrosine peptide to the SH2 domain of $p56^{lck}$, *Bioorg. Med. Chem.*, **2002**, 10, 1477-1482.
33. Pieters, R.J., Maximising multivalency effects in protein-carbohydrate interactions, *Org. Biomol. Chem.*, **2009**, 7, 2013-2025.
34. Wolfenden, M.L., Cloninger, M.J., Carbohydrate-functionalized dendrimers to investigate the predictable tunability of multivalent interactions, *Bioconjugate Chem.*, **2006**, 17, 958-966.
35. Deindl, S., Kadlecek, T.A., Brdicka, T., Cao, X., Weiss, A., Kuriyan, J., Structural basis for the inhibition of tyrosine kinase activity of ZAP-70, *Cell*, **2007**, 129, 735-746.
36. Au-Yeung, B.B., Deindl, S., Hsu, L.Y., Palacios, E.H., Levin, S.E., Kuriyan, J., Weiss, A., The structure, regulation, and function of ZAP-70, *Immunol. Rev.*, **2009**, 228, 41-57.
37. Kaiser, E., Colescott, R.L., Bossinger, C.D., Cook, P.I., Color test for detection of free terminal amino groups in the solid-phase synthesis of peptides, *Anal. Biochem.*, **1970**, 34, 595-598.

Chapter 5

A proteomics pull-down approach to study proteins binding to non-, mono- and diphosphorylated γ-ITAM mimics

Abstract

Stimulation of the multimeric (αβγ2) high-affinity IgE receptor (FcεRI) initiates signal transduction cascades which leads to mast cell degranulation. One of the first intracellular events of this cascade is the diphosphorylation of the ITAM motifs on intracellular part of the β- and γ-chains of FcεRI. SH2 domain containing proteins (e.g. Syk kinase) are recruited to the phosphorylated ITAMs and thereby activated, which is essential for cell degranulation. To evaluate the binding partners of γ-ITAM in a cell lysate, a pull-down assay was developed. Four rigid γ-ITAM mimics, containing no, one or two phosphorylated tyrosines, were synthesized. For the preparation of those peptides, synthesis routes for a rigid amino propynyl benzoic acid building block and an ethyleneglycol spacer were developed. The rigid γ-ITAM mimics and the diphosphorylated native γ-ITAM were immobilized on agarose beads. The beads were incubated with cell lysate of RBL-2H3 cells and the bound proteins were eluted with native γ-ITAM. Beads immobilized with diphosphorylated native γ-ITAM or the diphosphorylated rigid ITAM mimic could efficiently pull-down Syk tSH2 from a cell lysate spiked with 0.1% Syk tSH2. However, incubation of the different beads with lysate gave considerable aspecific binding. Further optimization of the protocol is required to reduce the aspecific binding.

Introduction

IgE and antigen binding to the tetrameric ($\alpha\beta\gamma_2$) high affinity IgE receptor (FcεRI) on mast cells stimulate signal transduction processes and induces cell degranulation.[1-3] When IgE binds to the extracellular domain of the α-chain, the tyrosine kinase Lyn is activated and it phosphorylates the receptor intracellularly on tyrosines of the Immunoreceptor Tyrosine based Activation Motifs (ITAMs).[2,3] ITAM is present on the β- and γ-chains and the sequence comprises Tyr-Xxx-Xxx-(Leu/Ile)-$(Xxx)_{n=6-8}$-Tyr-Xxx-Xxx-(Leu/Ile), in which Xxx can be any amino acid (in γ-ITAM n = 7). After the phosphorylation, the two underlined parts in the ITAM sequence function as binding epitopes for SH2 domains. The diphosphorylated γ-ITAM (γ-dpITAM) recruits the Spleen tyrosine kinase (Syk) to the receptor. Apart from the kinase domain, Syk also has two tandemly arranged SH2 domains (tSH2) and is therefore able to bind γ-dpITAM divalently. Upon binding, the conformation of Syk changes and its kinase domain is activated.[4] This activation eventually leads to cell degranulation and release of mediators.

In addition to Syk, there are also other proteins (e.g. Lyn) which bind to γ-dpITAM.[2] For better understanding of the IgE receptor signaling cascade, it is important to identify all the proteins capable of binding to the phosphotyrosines of γ-dpITAM. For this an affinity pull-down approach was designed with different γ-ITAM peptides as ligands. Pull-down experiments, in combination with the identification of proteins binding to the immobilized compound, are important proteomics tools.[5-9]

Recently, an interesting example of a pull-down experiment with phosphopeptides was described in a paper of Soto-Cruz et al., in which different β-ITAMs derived from FcεRI were immobilized on beads.[10] The used sequence of β-ITAM was **YEEL**HVYSPI**YSAL**, in which the two bold sequences are the binding epitopes for Syk tSH2, when the tyrosine residues are phosphorylated. Soto-Cruz et al. used all combinations of non-, mono-, di- and tri-tyrosine-phosphorylated peptides. They found that, besides Syk, also Grb2, Shc, SHIP and SHP-1 were able to bind to phosphorylated β-ITAMs.

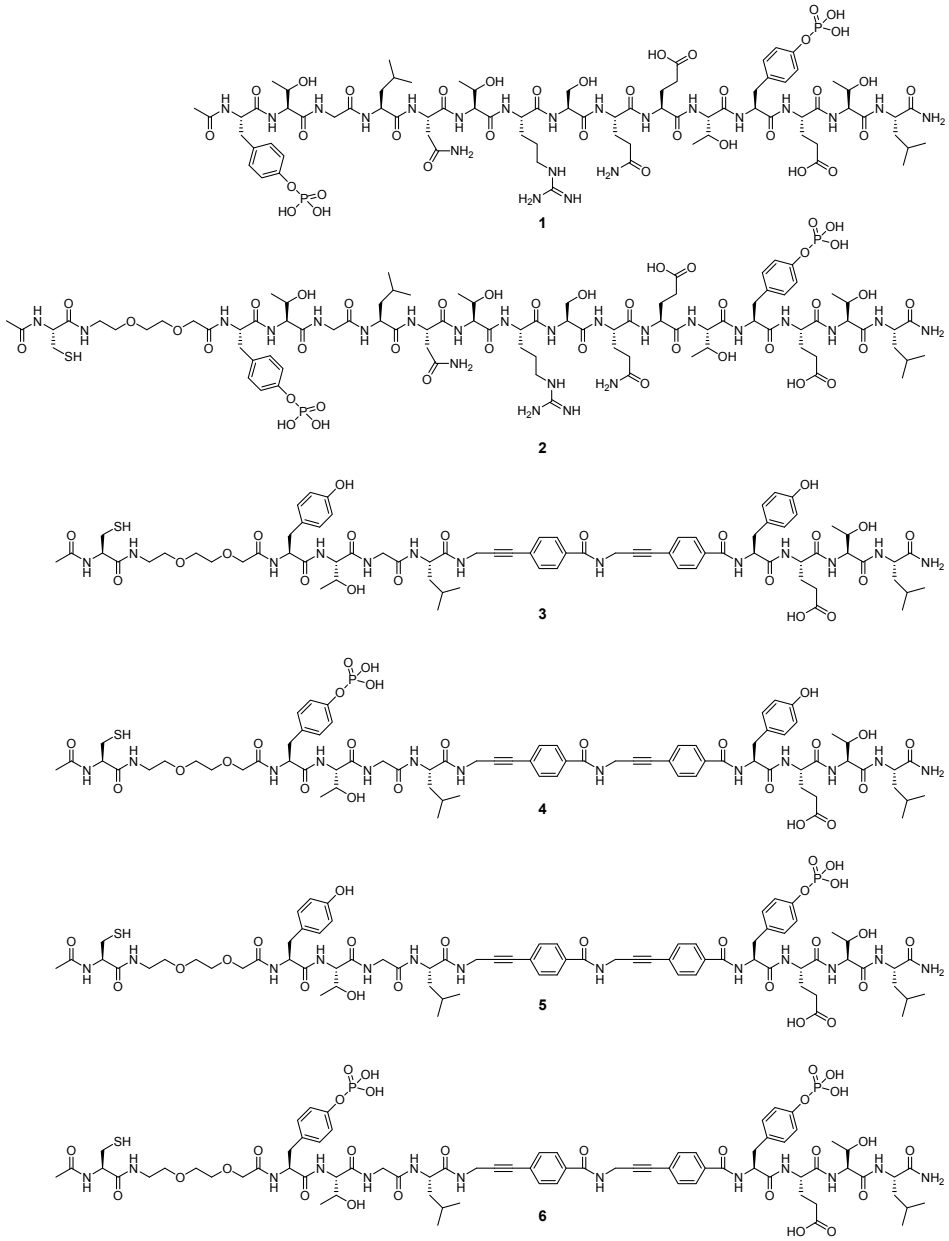

Figure 1. Overview of all peptides used for immobilization on beads (**2**-**6**) and for specific elution (**1**). They comprise native γ-ITAM (**1** and **2**) and nonphosphorylated (**3**), monophosphorylated (**4** and **5**), and diphosphorylated (**6**) ITAM mimics.

Although β- and γ-ITAM sequences are fairly similar, they possess different functions in IgE receptor signaling: β-ITAM phosphorylation plays a role in amplifying the signal from IgE binding, whereas γ-ITAM is responsible for the primary onset of signal transduction leading to degranulation.[2,3] These functional differences arise from their structural differences. β-ITAM has six residues between the two SH2 binding epitopes and γ-ITAM has seven intervening residues. Furthermore, β-ITAM possesses a third non-canonical tyrosine residue between the two SH2 binding epitopes, which can be phosphorylated *in vivo*.[11]

Until now, the binding partners of γ-ITAM have not been established. A pull-down assay was set up with γ-dpITAM (**2**) and γ-ITAM mimics as immobilized ligands. We explored ITAM mimics with one (**4** and **5**) and two (**6**) phosphorylated tyrosines and a nonphosphorylated (**3**) ITAM mimic, as a control (Figure 1). In those ITAM mimics the seven residues between the two SH2 binding epitopes were replaced by a rigid linker. This linker consisted of two amino propynyl benzoic acid building blocks.[12] A modified synthesis route to the rigid building block is shown in Scheme 1. Furthermore, a spacer between the ITAM sequence and the cysteine residue, used for attachment to the beads, was introduced to ensure that ITAM is accessible for protein binding. For this, an ethyleneglycol spacer was chosen, for which also a synthesis route is given (Scheme 2).

Results and discussion

Synthesis of building blocks

The linker between the SH2 binding epitopes in the rigid γ-ITAM mimic consisted of two rigid building blocks. This rigid building block was synthesized according to a slightly adapted procedure of the previously described synthesis route (Scheme 1).[12] First propargylamine was protected with a Boc group and then compound **7** was coupled to unprotected 4-iodobenzoic acid by means of a Sonogashira coupling.[13] For this cross coupling reaction the $Pd(OAc)_2$ catalyst was used instead of the more oxygen sensitive $Pd(PPh_3)_4$.[14] The reaction was completed after 10 minutes of microwave (mw) heating and straightforward work-up yielded the desired compound **8** in a reasonable yield. The Boc group was removed by acid treatment and replaced by an Alloc group, which is compatible with Fmoc/tBu peptide synthesis. The protection of the amine with an Fmoc group yields an insoluble compound and therefore the Alloc group was used.

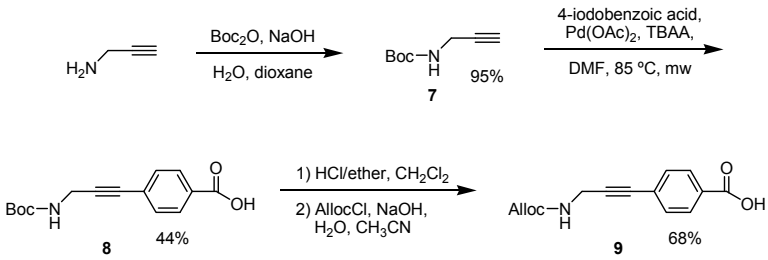

Scheme 1. Synthesis of the rigid building block **9**.

Also the synthesis of the ethyleneglycol spacer was optimized (Scheme 2).[15,16] The Fmoc protected spacer can be widely applied in peptide synthesis and is compatible with normal Fmoc/tBu solid phase peptide synthesis. Therefore, a reliable, fast and high-yielding synthesis route is desirable.

First 2(2-aminoethoxy)ethanol was protected with a trityl group (Scheme 2). Then the protected compound **10** was used in a substitution reaction with tert-butyl bromoacetate using NaH for the deprotonation of the hydroxyl functionality and NaI as a catalyst. After addition of the reagents, the reaction did not reach completion, as observed by TLC, and therefore, the reagents were added twice more. This procedure yielded the spacer **11** with two acid labile protecting groups in 67% yield, which was higher than when in one portion a large excess of reagents was added, which resulted in more side products. The use of the trityl group was crucial in the alkylation reaction, because it ensured that the amine was not partially deprotonated, which was the case when Boc was used as a protecting group, resulting in lower yields. Both the trityl and tert-butyl group were removed with TFA and the liberated amine was protected with an Fmoc-group, yielding building block **12** in an overall yield of 54%.

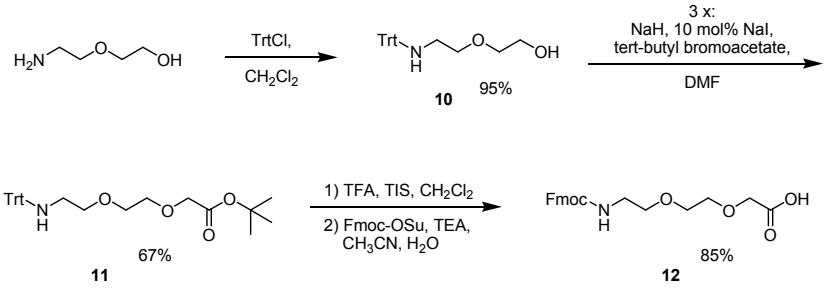

Scheme 2. Synthesis of the Fmoc-protected ethyleneglycol spacer **12**.

Peptide synthesis and pull-down strategy

The synthesis and purification of the rigid ITAM mimics was essentially the same as described previously.[12] For Alloc deprotection $Pd(PPh_3)_4$ was used as a catalyst. The Kaisertest was used to monitor all coupling and deprotection steps.[17] However, this ninhydrin-based test was inadequate for following the Alloc deprotection, because the test was already convincingly positive when only a small amount was deprotected. HPLC proved to be a better option for monitoring the Alloc deprotection.

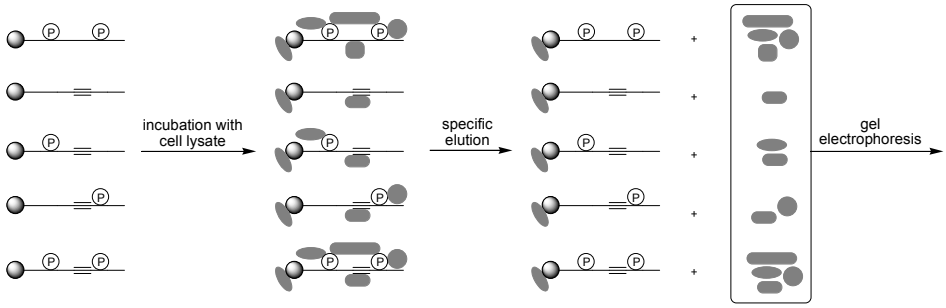

Figure 2. Pull-down strategy. The immobilized peptides (left) where incubated with lysate and the bound proteins (middle) were eluted with native γ-dpITAM (**1**). The elutes were subjected to gel electrophoresis (right).

The strategy to investigate the role of the individual phosphate groups in γ-ITAM – protein interactions is illustrated in Figure 2. First the thiol-containing γ-ITAM peptides were immobilized on beads. Then the beads were incubated with a lysate of RBL-2H3 cells. These cells have the FcεRI signaling cascade and are often used as a model for studying mast cell degranulation.[18] After this, the interacting proteins were eluted with native γ-dpITAM (**1**). This should theoretically furnish only the proteins binding to the γ-ITAM peptides, and not proteins binding aspecifically to the beads. The eluted fractions were analyzed with gel electrophoresis.

Loading of the beads

The peptides were immobilized on SulfoLink agarose beads containing iodoacetamide end groups. After overnight coupling, the supernatant was removed and the absorption of the supernatant was measured at 280 nm to determine the amount of

not coupled peptide. Using a calibration curve of known concentrations of peptide, the amount of still free and, therefore also, coupled peptide could be calculated (Figure 3). Typically the loading was about 0.9 mg peptide/mL beads. Since the SulfoLink agarose beads have a coupling capacity of approximately 1 mg thiol-containing peptide per mL, the obtained 0.9 mg/mL was satisfactory.

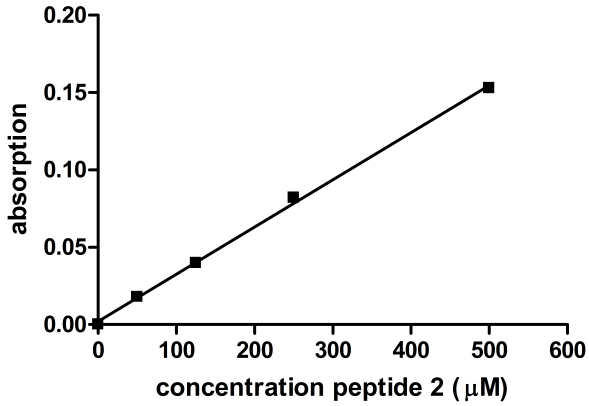

Figure 3. Calibration curve of peptide **2** at 280 nm. The amount of still free peptide **2** was calculated using this curve. By subtraction from the used amount of peptide the loading of the beads was determined.

Tuning the elution conditions

For evaluation of the elution conditions, beads loaded with native γ-dpITAM **2** were used. The beads were incubated with 4 mg of protein from lysed RBL-2H3 cells. The proteins were obtained from non-stimulated RBL-2H3 cells, which were collected as described in the experimental section. The cell lysate was spiked with 4 μg of Syk tSH2, which was 0.1% of the total protein content. After incubation the bound proteins were eluted with increasing concentrations of γ-dpITAM (**1**). The fractions were put on gel and analyzed with coomassie – and silver staining (Figure 4). Syk tSH2 (MW = 29 kDa) eluted already at 16 μM of γ-dpITAM. Also two bands around 70 kDa were observed and one of these might be full-length Syk (MW = 72 kDa), which is present in RBL-2H3 cells. Elution appeared to be nearly complete upon elution with 40 μM of **1**.

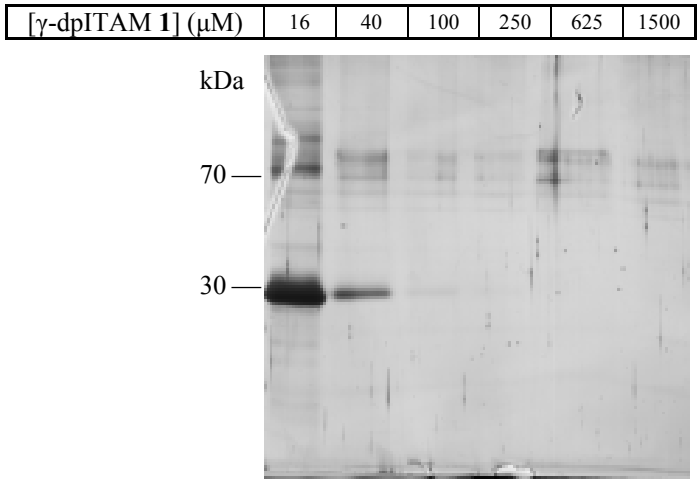

Figure 4. Optimizing the elution conditions for the pull-down assay. Beads were functionalized with diphosphorylated native γ-ITAM **2** and incubated with a RBL-2H3 cell lysate. The bound proteins were eluted with increasing concentrations of ITAM peptide **1**, as shown at the top. The elutes were concentrated and subjected to gel electrophoresis. The gel shown here is silver stained.

Pull-down experiments with nonphosphorylated and diphosphorylated rigid ITAM peptides

Now that the elution conditions were established, the different γ-ITAMs could be compared. First, the nonphosphorylated peptide **3** and the diphosphorylated peptide **6** were used. Beads immobilized with one of the peptides were incubated with either plain lysate or lysate spiked with 2 μg Syk tSH2 (0.1% of total protein content). The results of the experiment evidently showed that diphosphorylated peptide **6** could efficiently pull-down tSH2, whereas nonphosphorylated peptide **3** could not (Figure 5). Furthermore, peptide **6** was also capable of binding more other, especially high MW, proteins. Again, a band around 72 kDa was present in the two lanes of diphosphorylated peptide **6**. In the lane of diphosphorylated peptide **6**, in which the lysate was spiked with tSH2, the 72 kDa band is less intense than that in the lane of peptide **6** without tSH2. This could indicate that tSH2 competed with full-length Syk for binding to immobilized diphosphorylated **6**. Furthermore, also some 'non-specific' binders were observed, particularly a protein at 45 kDa.

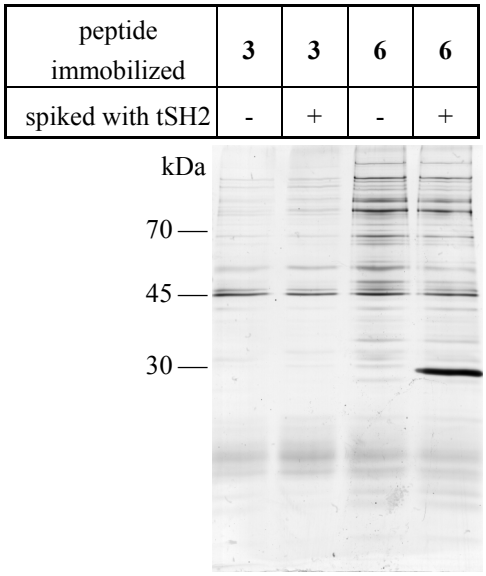

Figure 5. Comparison of pulled-down proteins of the nonphosphorylated (**3**) and the diphosphorylated (**6**) γ-ITAM mimic. In both cases RBL-2H3 cell lysate was spiked with 0.1% Syk tSH2 (based on total protein content) as indicated.

Pull-down experiments with all peptides

Now that it was established that the protocol worked properly for peptide **3** and **6**, peptides **2**-**6** were immobilized and experiments were performed without the positive control of spiking the lysate with tSH2. Cysteine was included as a negative control. Each immobilized peptide and cysteine was incubated with 3.1 mg of lysate. After washing steps, the bound proteins were eluted with 16 μM native γ-ITAM (**1**) and subjected to gel electrophoresis.

The first striking observation was that already many bands were present in the lane of the cysteine beads (Figure 6). Between incubation and elution, five washings steps were carried out, making it unlikely that the bands represented unbound proteins. Apparently many bound proteins were eluted even by the mild specific elution conditions using 16 μM native γ-ITAM (**1**). Another remarkable feature was that the intensity of the bands of the monophosphorylated peptides **4** and **5** was higher compared with the diphosphorylated peptides **2** and **6**. However, this experiment was only carried out once, and therefore, definitive conclusions cannot be drawn. The bands at 35 and 60 kDa were only present in the lanes of the monophosphorylated peptides. Possibly the proteins in these bands possess one SH2 or phosphotyrosine binding (PTB) domain.

Although the results from this first experiment were interesting, optimization of the protocol is clearly required for more definitive and meaningful conclusions.

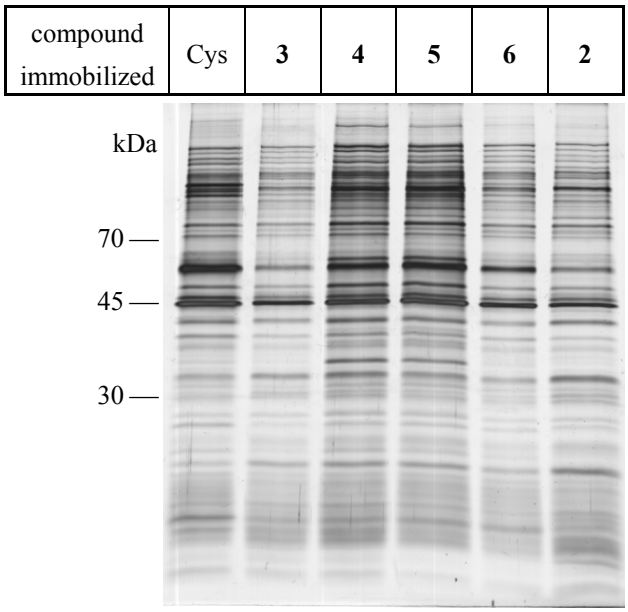

Figure 6. Silver stained gel of a pull-down experiment with all peptides and cysteine as negative control.

Conclusions

Six ITAM peptides were successfully synthesized and purified. The diphosphorylated γ-ITAM peptide **2** and ITAM mimic **6** were able to pull-down Syk tSH2 from a cell lysate spiked with 0.1% Syk tSH2. Unfortunately, comparison between the proteins binding to the different peptides was difficult, due to high background signals. Even beads loaded with cysteine could pull-down many proteins. Before analyzing the identity of pulled-down proteins, the protocol has to be improved further to yield gels with less aspecific binding. Improvements could include more washing steps, preincubation of the lysate with 'naked' beads and/or the use of other beads and buffers. Eventually, those gels might be subjected to in-gel digestion and LC-MS/MS analysis to identify the proteins capable of binding to the immobilized (phospho)peptides. When conditions for the pull-down experiments are optimized, also

lysate of stimulated cells should be included to indentify differences in protein binding between stimulated – and non-stimulated cells.

Experimental section

General

All chemicals were obtained from commercial sources and used without further purification. Solvents, which were used for the solid phase peptide synthesis, were stored over 4 Å molecular sieves, except for MeOH, which was stored over 3 Å molecular sieves. The reactions were performed at room temperature unless stated otherwise. The reactions were monitored and the R_f values were determined by thin layer chromatography (TLC). The TLC plates were obtained from Merck and were coated with silica gel 60 F-254 (0.25 mm). The spots were visualized by UV light and Cl_2-TDM *(N,N,N',N'*,-tetramethyl-4,4'-diaminodiphenylmethane) and ninhydrin staining. Solvents were removed under reduced pressure at a temperature of 40 ºC. Column chromatography was performed with Silicycle UltraPure silica gels, SiliaFlash (pore size 60 Å, particle size distribution 40-63 μm).

^{1}H NMR spectra were measured on a Varian Mercury plus 300 MHz spectrometer and the chemical shifts are given in ppm (δ) relative to TMS, expect for **8** and **9** (MeOH). ^{13}C NMR spectra were measured on a Varian Mercury plus 75 MHz spectrometer and the chemical shifts are given in ppm (δ) relative to $CDCl_3$ or CD_3OD. The ^{13}C NMR spectra were measured using the attached proton test (APT). Microwave reactions were carried out in a Biotage Initiator microwave oven. The microwave power was limited by temperature control once the desired temperature was reached. A sealed vessel of 10-20 mL was used.

Analytical HPLC was measured on a Shimadzu HPLC system with a UV detector operating at 220 and 254 nm and in some cases also an evaporative light scattering detector (PL-ELS 1000, Polymer Laboratories) was used. A gradient from 100% buffer A (15 mM TEA in H_2O titrated at pH 6 with 85% H_3PO_4) to 100% buffer B (buffer A/CH_3CN 1:9) in 20 min was used. For the preparative HPLC a Gilson system with a UV detector operating at 220 and 254 nm and an Applied Biosystems workstation with a UV detector operating at 214 nm were used. A gradient of 100% buffer A (0.1% TFA in H_2O/CH_3CN 95:5) to 100% buffer B (0.1% TFA in H_2O/CH_3CN 5:95) was applied.

N-Boc-propargylamine (7)

Propargylamine.HCl (4.58 g, 50 mmol) was dissolved in 1 M NaOH (55 mL) and dioxane (50 mL) and cooled to 0 ºC. Boc_2O (10.91 g, 50 mmol) was added and the mixture was stirred overnight at r.t. Dioxane was evaporated. EtOAc was added and the organic phase was washed with 5% $NaHCO_3$ (2 ×), 5% citric acid (2 ×) and brine, dried over Na_2SO_4, filtered and concentrated. The product was purified with silica gel column chromatography (EtOAc/hexane 1:4) yielding 7.34 g (47.3 mmol, 95%) of **7** as a white solid. R_f = 0.44 (EtOAc/hexane 1:4). ^{1}H NMR ($CDCl_3$, 300 MHz) δ = 1.46 (s, 9H, tBu), 2.23 (s, 1H, CH≡C), 3.92 (bs, 2H, CH_2N), 4.90 (bs, 1H, NH). ^{13}C NMR ($CDCl_3$, 75 MHz) δ = 28.3 (3 CH_3), 30.3 (CH_2), 71.1 (CH), 79.9, 80.1 (C tBu, CH≡*C*), 155.2 (CO).

N-Boc-4-(3-(3-aminoprop-1-ynyl)benzoic acid (8)

A solution of amine **7** (930 mg, 6 mmol), 4-iodobenzoic acid (1.24 g, 5 mmol), tert-butyl ammonium acetate (3.77 g, 12.5 mmol) and $Pd(OAc)_2$ (22 mg, 0.10 mmol) in 7.5 of mL DMF was heated under microwave irradiation at 85 °C for 10 min. The mixture was acidified with 5% citric acid and EtOAc was added. The organic phase was washed with 5% citric acid (2 ×) and brine, dried over Na_2SO_4, filtered and concentrated. The product was purified by silica gel column chromatography (0.5% CH_3COOH in EtOAc/hexane 1:2) yielding 610 mg (2.22 mmol, 44%) of **8** as a white solid. R_f = 0.22 (0.5% CH_3COOH in EtOAc/hexane 1:2). ^{1}H NMR (CD_3OD, 300 MHz) δ = 1.46 (s, 9H, tBu), 4.07 (s, 2H, CH_2N), 4.96 (bs, 2H, NH COOH), 7.50 (d, 2H, Ar), 7.97 (d, 2H, Ar). ^{13}C NMR (CD_3OD, 75 MHz) δ = 28.7 (3 CH_3), 31.4 (CH_2), 82.3 (C tBu, C≡*C*-CH_2), 90.1 (*C*≡C-CH_2), 129.0, 130.7, 131.5, 132.6 (Ar), 169.1 (2 CO).

N-Alloc-4-(3-(3-aminoprop-1-ynyl)benzoic acid (9)

Carboxylic acid **8** (610 mg, 2.22 mmol) was dissolved in 20 mL of CH_2Cl_2 and 5 mL of a saturated solution of HCl in ether was added. The mixture was stirred for 2 hours and the solvents were evaporated. The HCl salt was dissolved in 6 mL of 1 M NaOH and 6 mL of CH_3CN and cooled to 0 ºC. Allylchloroformate (319 µL, 3 mmol) was added, the mixture was stirred for 4 hours at r.t. and after that CH_3CN was evaporated. EtOAc was added and the organic phase was washed with 1 M $KHSO_4$ (3 ×) and brine, dried over Na_2SO_4, filtered and concentrated. The product was purified with silica gel column chromatography (0.5% CH_3COOH in EtOAc/hexane 1:2) yielding 390 mg (1.50 mmol, 68%) of Alloc protected derivative **9** as a white solid. R_f = 0.16 (0.5% CH_3COOH in

EtOAc/hexane 1:2). ^{1}H NMR (CD_3OD, 300 MHz) δ = 4.15 (s, 2H, CH_2N), 4.57 (d, 2H, $COOCH_2CHCH_2$), 4.97 (bs, 2H, NH COOH), 5.18-5.35 (m, 2H, $COOCH_2CHCH_2$), 5.90-6.00 (m, 1H, $COOCH_2CHCH_2$), 7.49 (d, 2H, Ar), 7.97 (d, 2H, Ar). ^{13}C NMR (CD_3OD, 75 MHz) δ = 31.8 (CH_2NH), 66.7 ($COOCH_2CHCH_2$), 82.5 ($C\equiv C\text{-}CH_2$), 89.8 ($C\equiv C\text{-}CH_2$), 117.7 ($COOCH_2CHCH_2$), 128.9, 130.7, 131.5, 132.6 (Ar), 134.3 ($COOCH_2CHCH_2$) 169.1 (2 CO).

N-trityl-2-(2-aminoethoxy)ethanol (10)

Tritylchloride (13.94 g, 50 mmol) and TEA (10.45 mL, 75 mmol) were added to 2(2-aminoethoxy)ethanol (5.01 mL, 50 mmol) in 100 mL of CH_2Cl_2 and the mixture was stirred overnight. The reaction mixture was washed with 5% $NaHCO_3$, H_2O and brine, dried over Na_2SO_4, filtered and concentrated. The product was purified by silica gel column chromatography (CH_2Cl_2/MeOH 97:3) yielding 16.50 g (47.5 mmol, 95%) of Trityl protected amine **10** as a white solid. R_f = 0.62 (CH_2Cl_2/MeOH 95:5). ^{1}H NMR ($CDCl_3$, 300 MHz) δ = 2.15 (s, 2H, NH + OH), 2.36 (t, 2H, $NHCH_2$), 3.48, 3.60, 3.68 (3t, 6H, 3 CH_2), 7.17-7.20, 7.26-7.29, 7.47-7.48 (3m, 15H, trityl). ^{13}C NMR ($CDCl_3$, 75 MHz) δ = 43.6 ($NHCH_2$), 62.1 (CH_2OH), 71.0, 71.5, 72.1 ($NHCH_2CH_2$, CH_2CH_2OH, C trityl), 126.6, 128.1, 128.9, 146.2 (Ar).

tert-butyl N-trityl-2-(2-(2-aminoethoxy)ethoxy)acetate (11)

Trityl protected amine **10** (255 mg, 0.734 mmol) was dissolved in 5 mL of dry DMF and after 15 min of stirring under a nitrogen atmosphere an oil dispersion of 60% NaH (35 mg, 0.881 mmol) was added. After 15 min of stirring under a nitrogen atmosphere tert-butyl bromoacetate (130 µL, 0.881 mmol) and NaI (13 mg, 0.0881 mmol) were added. After 30 min the same quantities of NaH, tert-butyl bromoacetate and NaI were added and the mixture was stirred for 30 min under a nitrogen atmosphere. This was repeated a third time and then water was added and the mixture was extracted three times with EtOAc. The combined organic layers were dried over Na_2SO_4, filtered and concentrated. The product was purified with silica gel column chromatography (EtOAc/hexane first 1:5, then 1:4 and 1:3) yielding 226 mg (0.490 mmol, 67%) of compound **11** as a colorless oil. R_f = 0.85 (CH_2Cl_2/MeOH 95:5). ^{1}H NMR ($CDCl_3$, 300 MHz) δ = 1.45 (s, 9H, tBu), 2.04 (s, 1H, NH), 2.35 (t, 2H, $NHCH_2$), 3.56, 3.61, 3.66 (3t, 6H, 3 CH_2), 3.99 (s, 2H, CH_2COO), 7.14-7.19, 7.23-7.28, 7.46-7.49 (3m, 15H, trityl).

^{13}C NMR ($CDCl_3$, 75 MHz) δ = 28.4 (CH_3), 43.3 ($NHCH_2$), 69.3, 70.5, 70.9, 71.0, 71.7, (4 CH_2, C trityl), 126.5, 128.0, 128.9, 146.4 (Ar), 169.9 (CO).

N-Fmoc-2-(2-(2-aminoethoxy)ethoxy)acetic acid (12)

Trityl protected compound **11** (9.51, 20.6 mmol) was dissolved in 15 mL of CH_2Cl_2 and 8.64 mL (42 mmol) of TIS. TFA (50 mL) was added and the reaction mixture was stirred for 3 hours and the solvents were removed under reduced pressure. The TFA salt was dissolved in 75 mL of H_2O and TEA was added until pH = 9. Fmoc-OSu (7.08 g, 21 mmol) in 75 mL of CH_3CN was added and the mixture was stirred for 1 hour maintaining the pH at 9 with TEA. The CH_3CN was evaporated and the aqueous phase was acidified with 1 M $KHSO_4$ and extracted three times with EtOAc. The combined organic layers were washed with brine, dried over Na_2SO_4, filtered and concentrated. The product was purified with silica gel column chromatography (CH_2Cl_2/MeOH 96:4) yielding 6.75 g (17.5 mmol, 85%) of **12** as a white solid. The product was lyophilized from CH_3CN/H_2O to obtain a white powder. R_f = 0.10 (CH_2Cl_2/MeOH 96:4). ^{1}H NMR ($CDCl_3$, 300 MHz) δ = 3.41 (t, 2H, NHC*H*$_2$), 3.60 (t, 2H, NHCH$_2$C*H*$_2$), 3.66 (t, 2H, NHCH$_2$CH$_2$OC*H*$_2$), 3.74 (t, 2H, NHCH$_2$CH$_2$OCH$_2$C*H*$_2$), 4.16 (s, 2H, C*H*$_2$CO), 4.22 (t, 1H, CH Fmoc), 4.40 (d, 2H, CH_2 Fmoc), 5.29 (s, 1H, NH), 7.26-7.42 (m, 4H, Ar Fmoc), 7.60 (d, 2H, Ar Fmoc), 7.75 (d, 2H, 2 Ar Fmoc), 8.62 (bs, 1H, COOH). ^{13}C NMR ($CDCl_3$, 75 MHz) δ = 40.8 ($NHCH_2$), 47.2 (CH Fmoc), 66.5 (CH_2 Fmoc), 68.5, 69.8, 70.2, 71.2 (4 CH_2), 119.9, 125.1, 127.0, 127.7, 141.3 and 143.9 (Ar Fmoc), 156.3 (CONH), 173.1 (COOH).

Peptides 1 and 2

Peptides **1** and **2** were manually assembled on Tentagel®-Rink-NH-Fmoc resin (for peptide **1** 208 mg, 0.05 mmol, loading 0.24 mmol/g and for peptide **2** 834 mg, 0.20 mmol loading 0.24 mmol/g) using standard Fmoc/tBu chemistry. The Fmoc protecting group was removed using 20% piperidine in NMP (3 × 15 mL for each gram of resin, each 8 min) followed by washing steps with NMP (3 × 15 mL for each gram of resin, each 2 min), CH_2Cl_2 (3 × 15 mL for each gram of resin, each 2 min) and NMP (3 × 15 mL for each gram of resin, each 2 min). The amino acid coupling mixtures were prepared by dissolving 4 equivalents of amino acid, 4 equivalents of HOBt and HBTU and 8 equivalents of DiPEA in NMP (15 mL for each gram of resin) and coupled during a coupling time of 60 minutes. The resin was washed with NMP (3 × 15 mL for each

gram of resin, each 1 min) and CH_2Cl_2 (3 × 15 mL for each gram of resin, each 1 min) after every coupling step, followed by Fmoc deprotection. The coupling steps and deprotection steps were monitored using the Kaisertest.[17] When the Fmoc deprotection was not complete, the deprotection steps were repeated. Amino acid building blocks Fmoc-Leu-OH, Fmoc-Thr(tBu)-OH, Fmoc-Glu(OtBu)-OH, Fmoc-Tyr(OP(OBn)OH)-OH, Fmoc-Thr(tBu)-OH, Fmoc-Glu(OtBu)-OH, Fmoc-Gln(Trt)-OH, Fmoc-Ser(tBu)-OH, Fmoc-Arg(Pbf)-OH, Fmoc-Thr(tBu)-OH, Fmoc-Asn(Trt)-OH, Fmoc-Leu-OH, Fmoc-Gly-OH, Fmoc-Thr(tBu)-OH and Fmoc-Tyr(OP(OBn)OH)-OH were subsequently coupled. For peptide **2**, N-Fmoc-2-(2-(2-aminoethoxy)ethoxy)acetic acid (**12**) and Fmoc-Cys(Trt)-OH were also coupled to the peptide chain. For the coupling of Fmoc-Tyr(OP(OBn)OH)-OH, 2 equivalents of amino acid, 2 equivalents of the coupling reagents HATU and HOAt and 5 equivalents of DiPEA were used. After the first Fmoc-Tyr(OP(OBn)OH)-OH coupling an extra washing step (2 × 15 mL for each gram of resin, each 10 min) with a mixture of 1 M TFA/1.1 M DiPEA in NMP was performed after each Fmoc deprotection step. This was done to replace the piperidinium counter ion of Tyr(OP(OBn)O^-) for protonated DiPEA. When all the coupling steps and deprotection steps were completed the peptides were acetylated using a capping solution of Ac_2O (4.72 mL, 42.7 mmol), DiPEA (2.18 mL, 22.8 mmol) and HOBt (0.23 g, 1.7 mmol) in 100 mL of NMP for 2 × 30 min. The peptides were cleaved from the resin and the side chains were deprotected with a solution of TFA/H_2O/TIS (92.5/5/2.5) for peptide **1** and TFA/H_2O/TIS/EDT (90/5/2.5/2.5) for peptide **2** for 3 h. The resins were removed from the solution by filtration. The peptides were precipitated with MTBE/hexane 1:1 v/v at -20 °C and lyophilized from CH_3CN/H_2O 1:1 v/v yielding 133 mg of crude peptide **1** and 421 mg of crude peptide **2**. 50 mg of both peptides was purified by preparative HPLC using an Alltech Adsorbosphere XL C8 90 Å 10 µm (250 × 22 mm) column. A gradient of 100% buffer A to 100% buffer B in 40 minutes was used for both peptides. The fractions were analyzed with analytical HPLC using an Alltech Alltima C8 5 µm (250 × 4.6 mm) column. After pooling and lyophilization 17.5 mg of pure peptide **1** and 9.9 mg of pure peptide **2** were obtained.

HRMS (ESI) of **1**: $[M+H]^+$ calculated 1976.8044, found 1977.2501; $[M+Na]^+$ calculated 1998.7864, found 1999.3105.

HRMS (ESI) of **2**: $[M+H]^+$ calculated 2224.8906, found 2225.6975; $[M+Na]^+$ calculated 2246.8726, found 2247.6765; $[M+H+Na]^{2+}$ calculated 1123.9381, found 1124.2335.

Peptides 3, 4, 5 and 6

Peptides **3**-**6** were manually assembled on Tentagel®-Rink-NH-Fmoc resin (each 0.77 g, 0.20 mmol, loading 0.26 mmol/g) according to the procedures used for peptide **1** and **2**. Amino acid building blocks Fmoc-Leu-OH, Fmoc-Thr(tBu)-OH, Fmoc-Glu(OtBu)-OH, Fmoc-Tyr(OP(OBn)OH)-OH or Fmoc-Tyr(tBu)-OH, *N*-Alloc-4-(3-(3-aminoprop-1-ynyl)benzoic acid (**9**), N-Alloc-4-(3-(3-aminoprop-1-ynyl)benzoic acid (**9**), Fmoc-Leu-OH, Fmoc-Gly-OH, Fmoc-Thr(tBu)-OH, Fmoc-Tyr(OP(OBn)OH)-OH or Fmoc-Tyr(tBu)-OH, N-Fmoc-2-(2-(2-aminoethoxy)ethoxy)acetic acid (**12**) and Fmoc-Cys(Trt)-OH were subsequently coupled. When all coupling steps and deprotection steps were completed the peptides were acetylated using capping solution. The peptides were cleaved from the resin and the side chains were deprotected with a solution of TFA/H_2O/TIS/EDT (90/5/2.5/2.5) for 3 h. After lyophilization from CH_3CN/H_2O 1:1 v/v 135 mg of crude peptide **3**, 140 mg of crude peptide **4**, 179 mg of crude peptide **5** and 163 mg of crude peptide **6** were obtained. A quantity of 50 mg of each peptide was purified by preparative HPLC using an Alltech Adsorbosphere XL C8 90 Å 10 µm (250 × 22 mm) column for peptides **3**, **4** and **5** and an Alltech Alltima C8 100 Å 10 µm (250 × 22 mm) column for peptide **6**. A gradient of 100% buffer A to 100% buffer B in 40 minutes was used for peptides **3**, **4** and **5** and a gradient of 90 minutes was used for peptide **6**. The fractions were analyzed with analytical HPLC using an Alltech Alltima C8 5 µm (250 × 4.6 mm) column for peptides **3** and **4** and an Alltech Adsorbosphere XL C8 90 Å 5 µm (250 × 4.6 mm) column for peptides **5** and **6**. After pooling and lyophilization 4.8 mg of pure peptide **3**, 5.8 mg of pure peptide **4**, 8.9 mg of pure peptide **5** and 16.2 mg of pure peptide **6** were obtained.

HRMS (ESI) of **3**: $[M+H]^+$ calculated 1562.6877, found 1563.0153; $[M+Na]^+$ calculated 1584.6697, found 1584.8419; $[M+2H]^{2+}$ calculated 781.8478, found 782.0435; $[M+H+Na]^{2+}$ calculated 792.8382, found 792.5547; $[M+2Na]^{2+}$ calculated 803.8292, found 804.0493.

HRMS (ESI) of **4**: $[M+H]^+$ calculated 1642.6541, found 1643.0800; $[M+Na]^+$ calculated 1664.6361, found 1664.9752; $[M+2H]^{2+}$ calculated 821.831, found 822.0479; $[M+H+Na]^{2+}$ calculated 832.8214, found 833.0208; $[M+2Na]^{2+}$ calculated 843.8123, found 844.0172.

HRMS (ESI) of **5**: $[M+H]^+$ calculated 1642.6541, found 1643.0115; $[M+Na]^+$ calculated 1664.6361, found 1664.9752; $[M+2H]^{2+}$ calculated 821.831, found 821.9995;

$[M+H+Na]^{2+}$ calculated 832.8214, found 833.0208; $[M+2Na]^{2+}$ calculated 843.8123, found 843.9681.
HRMS (ESI) of **6**: $[M+Na]^{+}$ calculated 1744.6019, found 1744.9742; $[M+2Na]^{2+}$ calculated 883.7955, found 884.0009.

Cell culture

RBL-2H3 cells were cultured in 25, 75 and 225 cm^2 flasks in RPMI 1640 medium with L-glutamine, supplemented with 10% heat-inactivated fetal calf serum, 100 U/mL penicillin, 100 µg/mL streptomycin in a humidified atmosphere of 5% CO_2 at 37 ºC. For serial passage and cell collecting, the cells were detached with trypsin (0.05%) and ethylenediaminetetraacetic acid (EDTA) (0.02%) for 10 minutes at 37 °C. After trypsinization cells were resuspended in medium for further use. For cell collecting for the preparation of lysate, the cells were transferred into tubes and centrifuged for 5 min at 300 rpm at 4 °C. The supernatant was removed and the cells were washed (2 ×) with ice-cold PBS. The cells were stored at -80 °C.

Loading of the beads

SulfoLink Coupling Gel (Pierce Biotechnology) was washed (4 × three times the volume of the beads) with coupling buffer (5 mM EDTA-Na_2 in 50 mM Tris, pH = 8.5) and incubated overnight with 0.5 mM peptide in coupling buffer at 6 °C, using the same volume as the beads. Then the beads were washed (3 ×) with coupling buffer and the unreacted iodoacetamide functionalities of the beads were blocked by incubation with 50 mM cysteine in coupling buffer for 2 hours at 6 °C, using the same volume as the beads. The beads were washed (3 × three times the volume of the beads) with 1 M NaCl. The loading efficiency was calculated by determination of the amount of unreacted peptide using a spectrophotometer (UV1, Thermo Electron Corporation) operating at 280 nm. Typical loading was about 0.9 mg peptide/mL beads. The beads were stored in PBS containing 0.5% NaN_3.

Pull-down experiments

Cells were mechanically lyzed for 2 minutes at 4 °C in binding buffer (PBS with 200 mM sucrose and 5 mM $MgCl_2$, pH = 7.4) using a small pestle and a small tube. The obtained suspension was centrifuged for 5 min at 14000 rpm at 4 °C. The supernatant was collected and the protein content was determined using a Bradford assay.[19] The

immobilized beads were washed (4 ×) with binding buffer and incubated with the lysate for 2 hours at 6 °C. The beads were washed (5 ×) with binding buffer and the proteins were eluted with 4 × 50 µL of 16 mM native γ-ITAM (**1**) in binding buffer. The combined fractions were concentrated by centrifugation of an Eppendorf tube with a cut-off filter of 5 kDa and were subjected to gel electrophoresis using a 12% SDS-PAGE gel. The proteins in the gels were visualized with coomassie blue and silver staining.

Acknowledgements

Poupak Dadvar is kindly acknowledged for her assistance with the pull-down experiments.

References

1. Singh, R., Masuda, E.S., Spleen tyrosine kinase (Syk) biology, inhibitors and therapeutic applications, *Annu. Rep. Med. Chem.*, **2007**, 42, 379-391.
2. Gilfillan, A.M., Tkaczyk, C., Integrated signalling pathways for mast-cell activation, *Nat. Rev. Immunol.*, **2006**, 6, 218-230.
3. Kraft, S., Kinet, J.-P., New developments in FcεRI regulation, function and inhibition, *Nat. Rev. Immunol.*, **2007**, 7, 365-378.
4. Siraganian, R.P., Zhang, J., Suzuki, K., Sada, K., Protein tyrosine kinase Syk in mast cell signaling, *Mol. Immunol.*, **2001**, 38, 1229-1233.
5. Pandey, A., Mann, M., Proteomics to study genes and genomes, *Nature*, **2000**, 405, 837-846.
6. Blagoev, B., Kratchmarova, I., Ong, S.E., Nielsen, M., Foster, L.J., Mann, M., A proteomics strategy to elucidate functional protein-protein interactions applied to EGF signaling, *Nat. Biotechol.*, **2003**, 21, 315-318.
7. Schulze, W.X., Mann, M., A novel proteomic screen for peptide-protein interactions, *J. Biol. Chem.*, **2004**, 279, 10756-10764.
8. Hinsby, A.M., Olsen, J.V., Mann, M., Tyrosine phosphoproteomics of fibroblast growth factor signaling - A role for insulin receptor substrate-4, *J. Biol. Chem.*, **2004**, 279, 46438-46447.
9. Zhou, F., Galan, J., Geahlen, R.L., Tao, W.A., A novel quantitative proteomics strategy to study phosphorylation-dependent peptide-protein interactions, *J. Proteome Res.*, **2007**, 6, 133-140.
10. Soto-Cruz, I., Oliver, J.M., Ortega, E., Analysis of proteins binding to the ITAM motif of the beta-subunit of the high-affinity receptor for IgE (FcεRI), *J. Recept. Sig. Transd.*, **2007**, 27, 67-81.
11. Pribluda, V.S., Pribluda, C., Metzger, H., Biochemical evidence that the phosphorylated tyrosines, serines, and threonines on the aggregated high affinity receptor for IgE are in the immunoreceptor tyrosine-based activation motifs, *J. Biol. Chem.*, **1997**, 272, 11185-11192.

12. Dekker, F.J., de Mol, N.J., Fischer, M.J.E., Liskamp, R.M.J., Amino propynyl benzoic acid building block in rigid spacers of divalent ligands binding to the Syk SH2 domains with equally high affinity as the natural ligand, *Bioorg. Med. Chem. Lett.*, **2003**, 13, 1241-1244.
13. Sonogashira, K., Tohda, Y., Hagihara, N., A convenient synthesis of acetylenes: catalytic substitutions of acetylenic hydrogen with bromoalkenes, iodoarenes and bromopyridines, *Tetrahedron Lett.*, **1975**, 16, 4467-4470.
14. Urgaonkar, S., Verkade, J.G., Ligand-, copper-, and amine-free Sonogashira reaction of aryl iodides and bromides with terminal alkynes, *J. Org. Chem.*, **2004**, 69, 5752-5755.
15. Dekker, F.J., de Mol, N.J., van Ameijde, J., Fischer, M.J.E., Ruijtenbeek, R., Redegeld, F.A.M., Liskamp, R.M.J., Replacement of the intervening amino acid sequence of a Syk-binding diphosphopeptide by a nonpeptide spacer with preservation of high affinity, *ChemBioChem*, **2002**, 3, 238-242.
16. Koskinen, A.M.P., Vale, T., Vihavainen, S., Hakala, J.M.L., Synthesis of α-helix substituted analogs of calcitonin gene-related peptide, *Bioorg. Med. Chem. Lett.*, **1995**, 5, 513-518.
17. Kaiser, E., Colescott, R.L., Bossinger, C.D., Cook, P.I., Color test for detection of free terminal amino groups in the solid-phase synthesis of peptides, *Anal. Biochem.*, **1970**, 34, 595-598.
18. Isersky, C., Metzger, H., Buell, D.N., Cell cycle-associated changes in receptors for IgE during growth and differentiation of a rat basophilic leukemia cell line, *J. Exp. Med.*, **1975**, 141, 1147-1162.
19. Bradford, M.M., A rapid and sensitive method for the quantitation of microgram quantities of protein utilizing the principle of protein-dye binding, *Anal. Biochem.*, **1976**, 72, 248-254.

Chapter 6

Cell permeable ITAM constructs for the modulation of mediator release in mast cells

Kuil, J., Fischer, M.J.E., de Mol, N.J., Liskamp, R.M.J., Cell permeable ITAM constructs for the modulation of mediator release in mast cells, *manuscript in preparation*

Abstract

Spleen tyrosine kinase (Syk) is essential for high affinity IgE receptor (FcεRI) mediated mast cell degranulation. Once FcεRI is stimulated, intracellular ITAM motifs of the receptor are diphosphorylated (dpITAM) and Syk is recruited to the receptor by binding of the Syk tandem SH2 domain to dpITAM, resulting in activation of Syk and, eventually, degranulation.

To investigate intracellular effects of ITAM mimics, constructs were synthesized with ITAM mimics conjugated to different cell penetrating peptides, i.e. Tat, TP10, octa-Arg and K(Myr)KKK, or a lipophilic C_{12}-chain. In most constructs the cargo and carrier were linked to each other through a disulfide bridge, which is convenient for combining different cargos with different carriers and has the advantage that the cargo and the carrier may be separated by reduction of the disulfide once it is intracellularly. The ability of these ITAM constructs to penetrate into RBL-2H3 cells was assessed using flow cytometry. TP10 and octa-Arg were found to be the most efficient carriers for this cell type. Fluorescence microscopy showed that the octa-Arg-SS-Flu-ITAM construct was present in various parts of the cells, although it was not homogeneously distributed. In addition, cell penetrating constructs without fluorescent labels were synthesized to examine degranulation in RBL-2H3 cells. Octa-Arg-SS-ITAM stimulated the mediator release up to 140%, indicating that ITAM mimics may have the ability to activate non-receptor bound Syk.

Introduction

The first event in IgE receptor signaling in mast cells is IgE and antigen binding to the multimeric ($\alpha\beta\gamma_2$) high affinity IgE receptor (FcεRI), resulting in aggregation and stimulation of the receptor.[1-5] The β- and γ-chains of this FcεRI receptor contain a specific intracellular sequence called the Immunoreceptor Tyrosine based Activation Motif (ITAM). The ITAM sequence consists of Tyr-Xxx-Xxx-(Leu/Ile)-$(Xxx)_{n=6-8}$-Tyr-Xxx-Xxx-(Leu/Ile), in which Xxx can be any amino acid. Once FcεRI is stimulated, γ-ITAM is diphosphorylated leading to 'γ-dpITAM' and the underlined residues become binding epitopes for SH2 domains. An SH2 domain containing protein that binds diphosphorylated γ-ITAM (γ-dpITAM) is Spleen tyrosine kinase (Syk). Syk consists of a kinase domain and two SH2 domains in tandem (tSH2). Syk is recruited to the cell membrane by binding to γ-dpITAM, resulting in a conformational change of Syk and activation of its kinase domain.[3] Then Syk transfers the signal further, which eventually leads to cell degranulation and mediator release. Therefore, Syk is essential for degranulation. Overstimulation of this cascade leads to allergic responses, and therefore it is interesting to inhibit the ITAM – Syk interaction as a potential target for anti-allergic therapy.

Although there is much knowledge about the functioning of Syk,[6,7] the process of conformational change and kinase activation, which includes phosphorylation of Syk on multiple sites, is not fully understood. For example, the aggregation of FcεRI receptors in lipid rafts could also be important for ITAM phosphorylation and Syk activation.[8]

In this study, the effect of a rigid, very potent ITAM mimic on mast cell degranulation was evaluated (Figure 1). In this ITAM mimic, the seven intervening amino acid residues between the SH2 binding epitopes were replaced by a rigid linker without affecting the binding affinity.[6,9] As a model for mast cells, rat basophilic leukemia (RBL-2H3) cells were used. These cells, having the IgE receptor signaling cascade, are widely studied as a model of secretory mucosal type mast cells.[10,11]

Because the ITAM mimic, which is a charged, diphosphorylated peptide mimic, was most likely not capable of penetrating through the RBL-2H3 cell membrane, cell penetrating peptides (CPPs) or a liphophilic carrier were coupled to it. CPPs are often used to transport cargo into cells, allowing to study cellular processes and protein-protein interactions in cells.[12-15] There is a large number of examples present in the literature of successful cell penetration, although it is still not possible to decide

rationally which CPP to use, because cellular uptake is also dependent on the cargo, the cell type and the experimental settings.[15,16] For example, the translocation of negatively charged cargo (e.g. phosphopeptides) into cells is relatively difficult because of repulsion by the negative charges on cell membranes.[17-19] In fact, a negatively charged peptide fused to a polyarginine CPP can efficiently block cellular association and uptake.[20]

Because ITAM has three negatively charged residues, it was expected that cell penetration would be challenging. Therefore several cell penetrating carriers were selected to create a diverse set of constructs for studying cell penetration. Fluorescently labeled cell permeable constructs were synthesized and subjected to flow cytometry, to quantify the cell labeling. Then the cellular distribution of the most effective constructs was evaluated with fluorescence microscopy. Finally, constructs without a fluorescent label were also synthesized and their biological activity was evaluated in RBL-2H3 cells.

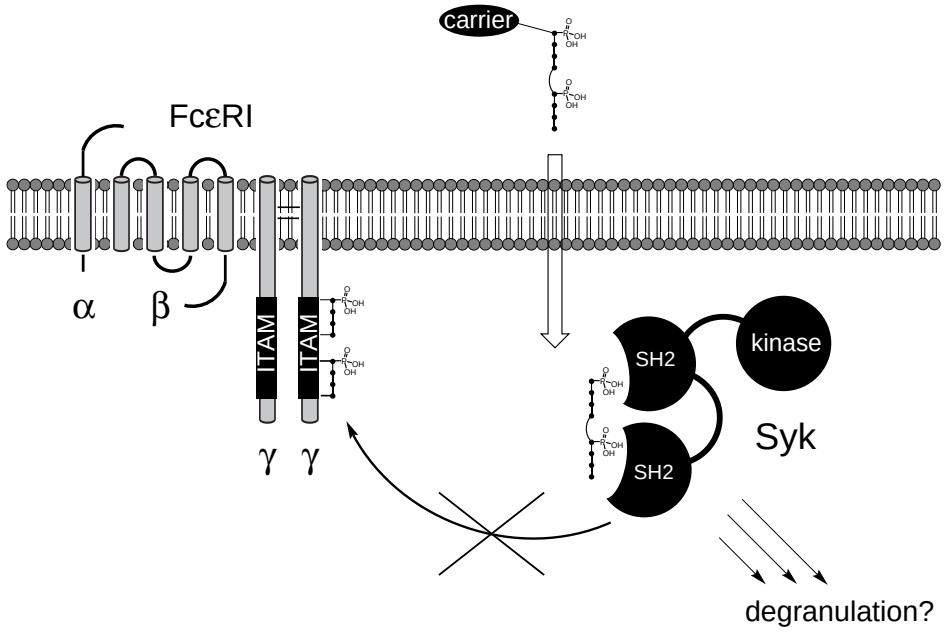

Figure 1. Schematic overview of intervention in the FcεRIγ – Syk interaction, making use of a cell penetrating carrier coupled to an ITAM mimic.

Results and discussion

Selection of different cargos and carriers

Several carriers were selected to evaluate which would be most suitable (Figure 2). The Tat peptide was included, because it is the most frequently studied CPP.[21-24] Moreover, it has been reported that Tat is able to penetrate into RBL cells.[25]

Transportan 10 (TP10), a deletion analog of transportan, is the only CPP which has been thoroughly studied for the delivery of peptides into RBL-2H3 cells.[26,27] In contrast to several other CPPs, TP10, consisting of 21 amino acid residues, possesses only 5 positive charges and no arginine residues.

Furthermore, a polyarginine containing peptide was selected. Octa-arginine was chosen as a polyarginine CPP, since it is a commonly used peptide which is able to penetrate many different cell types.[28-30]

A lipophilic alkyl chain was selected, because it has been shown that modification of peptides with a simple alkyl or fatty acid chain (e.g. myristoylation) allows cellular uptake.[31,32] Here, a C_{12} alkyl chain was chosen as an equivalent of a fatty acid chain.[33] Finally, a combination of cationic residues and an alkyl chain was selected. For this, a peptide containing four lysine residues and a myristyl group on one of the lysine side-chains was chosen (K(Myr)KKK).[25]

The cargo was composed of an ITAM mimic with two rigid amino propynyl benzoic acid building blocks replacing the seven intervening residues between the SH2 binding epitopes (Figure 2).[6,9] This rigid ITAM mimic has similar affinity for Syk tSH2 as the native peptide[6,9] and is expected to be less prone to enzymatic degradation. Fluorescein was attached to the N-terminus of the ITAM mimic to allow detection in flow cytometry and fluorescence microscopy.

Since it was expected that the two phosphotyrosine residues as well as the glutamate residue in the ITAM mimic would have an adverse effect on the intracellular delivery, a fluorescein moiety was also used as cargo as a control for the ability of the carriers to achieve the desired transport.

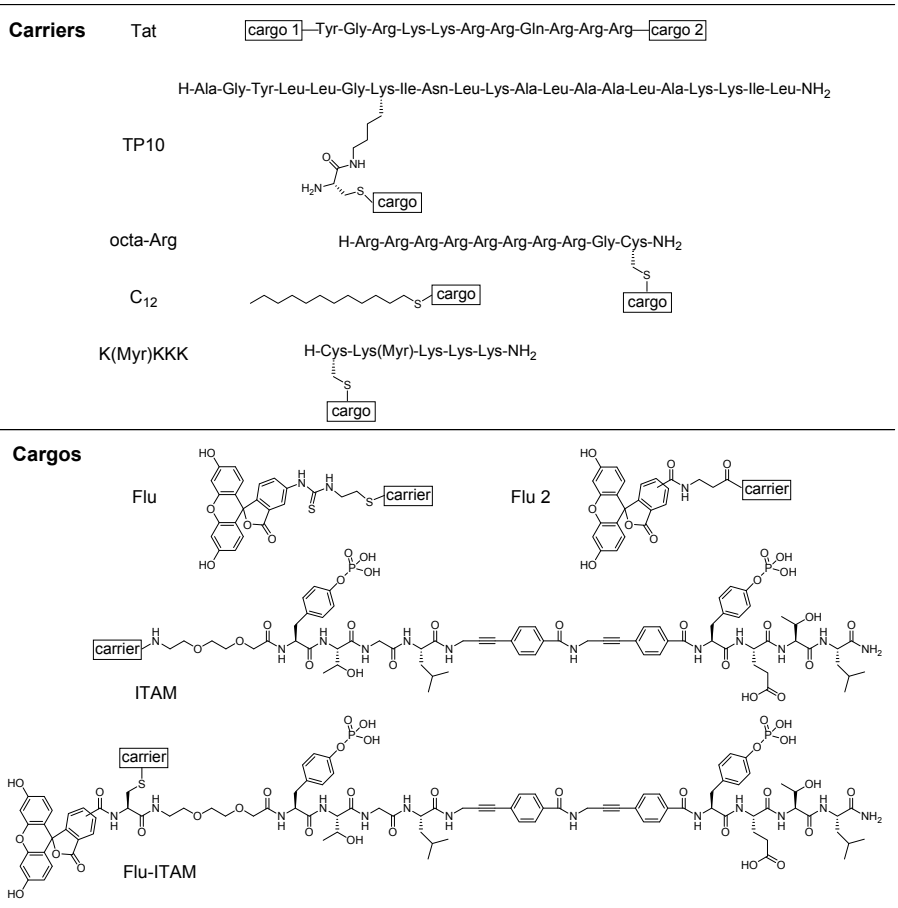

Constructs

Carrier	Cargo	Construct abbreviation
Tat	cargo 1 = Flu 2, cargo 2 = NH_2	Flu-Tat (**18**)
Tat	cargo 1 = Flu 2, cargo 2 = ITAM	Flu-Tat-ITAM (**19**)
TP10 (**4**)	Flu (**11**)	TP10-SS-Flu (**20**)
TP10 (**4**)	Flu-ITAM (**12**)	TP10-SS-Flu-ITAM (**21**)
octa-Arg (**6**)	Flu (**11**)	octa-Arg-SS-Flu (**22**)
octa-Arg (**5**)	Flu-ITAM (**13**)	octa-Arg-SS-Flu-ITAM (**23**)
C_{12} (**7**)	Flu (**11**)	C_{12}-SS-Flu (**24**)
C_{12} (**7**)	Flu-ITAM (**12**)	C_{12}-SS-Flu-ITAM (**25**)
K(Myr)KKK (**9**)	Flu-ITAM (**13**)	K(Myr)KKK-SS-Flu-ITAM (**26**)

Figure 2. Overview of all cell permeable constructs used in this study for flow cytometry analysis and fluorescence microscopy. Flu-Tat (**18**) and Flu-Tat-ITAM (**19**) were completely synthesized on the solid phase and therefore the cargo was attached to the carrier via an amide bond. TP10, octa-Arg, C_{12} and K(Myr)KKK were connected to the cargo via a disulfide bond. Abbreviations: Flu: fluorescein, SS: disulfide bond, Myr: myristate.

Synthesis of the fluorescein-labeled constructs for flow cytometry and fluorescence microscopy

The two modified Tat peptides, Flu-Tat (**18**) and Flu-Tat-ITAM (**19**), were completely synthesized on the solid phase. A short ethyleneglycol spacer was incorporated between Tat and ITAM in the Flu-Tat-ITAM construct **19** (Figure 2). In both Tat peptides a β-alanine residue was attached to the N-terminus prior to the coupling of 5(6)-carboxyfluorescein.

The other carriers were attached to the cargos via a disulfide bond. The advantage of a disulfide bond is that it easily allows to combine different carriers with different cargos. Another advantage is that a disulfide bond may be gradually cleaved inside cells and after that the carrier can no longer possibly interfere with the bioactivity of the cargo.[34]

For mixed disulfide formation the thiol group of either the carrier or the cargo had to be activated using 2,2'-dithiobis(5-nitropyridine), which yields a para-nitro-2-pyridinesulfenyl activated thiol moiety. The activation was performed during peptide cleavage from the resin[35] or after purification of the peptide.[36-38]

As an illustrative example, the synthesis of TP10-SS-Flu-ITAM (**21**) is shown (Scheme 1). The synthesis of the other constructs was essentially identical and details regarding all syntheses are given in the experimental section. For optimal intracellular delivery TP10 should be connected via the side-chain of Lys7 to the cargo.[39] A known strategy for the attachment of the cargo to TP10 via a disulfide bond, is the introduction of a cysteine residue attached to Lys7.[26,27] The Boc-Cys(Npys)-OH building block is frequently used for yielding directly the cysteine activated TP10. However, the 3-nitro-2-pyridinesulfenyl group is base labile and will be cleaved during Fmoc deprotection. Therefore, an activated cysteine residue has to be introduced after completion of the assembly of the peptide. Because this strategy can be troublesome, instead the Fmoc-Lys(Boc-Cys(Trt))-OH building block (**2**) was incorporated during the solid phase peptide synthesis, which was prepared from Fmoc-Lys-OH and Boc-Cys(Trt)-OSu (**1**). After cleavage from the resin the thiol of the cysteine residue was directly activated using 2,2'-dithiobis(5-nitropyridine) (Scheme 1).[35] The activated TP10 carrier (TP10-Cys(pNpys), **4**) was purified by RP-HPLC.

The ITAM cargo **12** containing a cysteine and an N-terminal fluorescein was synthesized on the solid phase. The synthesis of the used acetylene-containing rigid

building block has been described previously.[9] A short ethyleneglycol spacer was incorporated into the sequence between the ITAM mimic and the cysteine residue, ensuring that the ITAM mimic is fully accessible for Syk binding. After the synthesis also this peptide was purified by RP-HPLC.

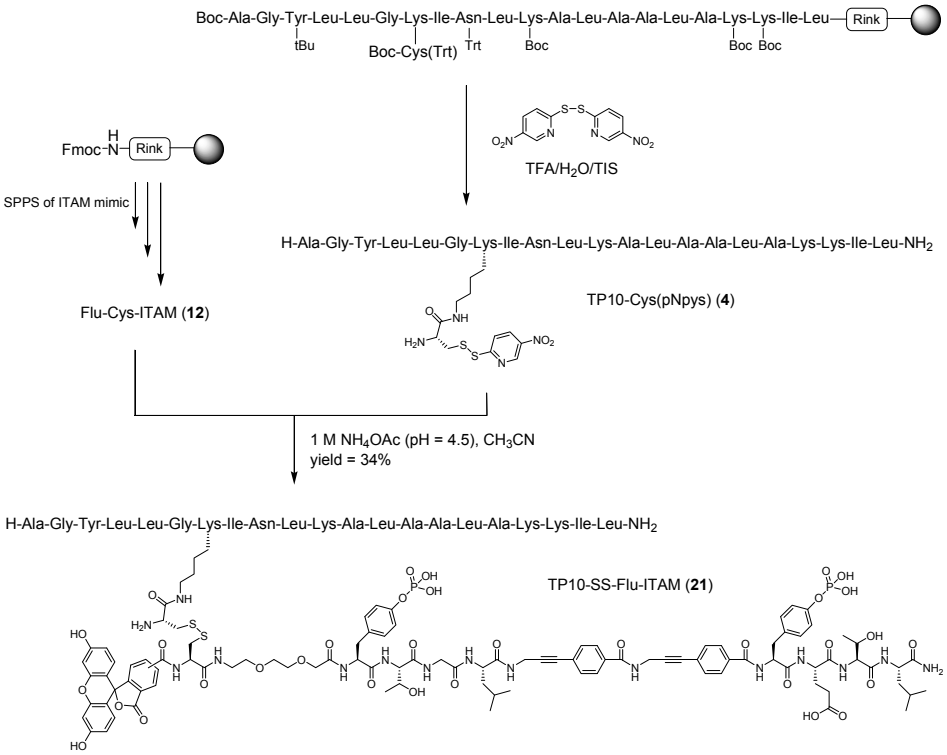

Scheme 1. Synthesis of TP10-SS-Flu-ITAM (**21**). The TP10-carrier was first prepared on the resin with the Fmoc-Lys(Boc-Cys(Trt))-OH building block (**2**) incorporated into the sequence (seventh residue from the N-terminus). During cleavage and deprotection the cysteine was activated, yielding TP10-Cys(pNpys) (**4**). This carrier was conjugated to cargo Flu-ITAM (**12**) to yield the cell penetrating construct **21**.

ITAM peptide **12** was reacted with the thiol activated TP10 (TP10-Cys(pNpys), **4**) under slightly acidic conditions to prevent homodimer formation of the free thiol (Scheme 1).[38] Within a few minutes a yellow color of the released 5-nitropyridine-2-thiol appeared. After the conjugation, the construct was purified by RP-HPLC and analyzed by analytical RP-HPLC and mass spectrometry. Similar strategies were

applied for the synthesis of the other carrier-SS-Flu and carrier-SS-Flu-ITAM constructs.

Flow cytometry

Flow cytometry analysis was performed to quantify the cell labeling of the different constructs. First, the incubation conditions were established. The RBL-2H3 cells, which are adherent cells, were incubated with the constructs before or after detachment with trypsin. The histograms, displaying the amount cell labeling, were comparable for both incubation conditions. However, the percentage of non-viable cells was lower when cells were incubated before detachment, as observed from the Forward Scatter and Side Scatter (data not shown). Therefore, incubation of the RBL-2H3 cells with the constructs was carried out when they were still attached to a 12 wells plate. After incubation, the cells were washed, detached with trypsin, washed and analyzed with flow cytometry (Figure 3). The trypsinization step after the incubation also prevents over-estimation of the amount of construct present in the cells, since it has been shown that treatment of cells with trypsin reduces the amount of plasma membrane bound constructs by digestion of the CPP and/or membrane proteins.[15] For flow cytometry analysis the cells were gated on Forward Scatter and Side Scatter and approximately 10,000 viable cells were analyzed by making histograms with the amount of fluorescence on the X-axis and the number of cells on the Y-axis. Untreated cells are in each histogram included as a reference (Figure 3).

Cells incubated with the negative controls carboxyfluorescein and the fluorescein-containing ITAM mimic without a carrier (Flu-ITAM, **17**) showed no significant increase in fluorescence compared to the untreated cells even at 25 μM (data shown for 3 and 10 μM). Surprisingly, also Flu-Tat (**18**) and Flu-Tat-ITAM (**19**) did not label the cells significantly more than Flu-ITAM (**17**). This is contradictory to results published by Nelson et al., although they used the shorter Tat(49-57) peptide in combination with RBL-2H3 cells.[25] Furthermore, by Flu-Tat (**18**) and, especially, by Tat-Flu-ITAM (**19**) it seems that two populations of cells were present: one population with almost no cell labeling and one population with some labeling (Figure 3). The geometric mean for all cells for both Tat-constructs is, however, comparable with that of the negative control **17**.

TP10, on the other hand, showed a large degree of cell labeling, irrespective of the cargo (Figure 3). Also octa-Arg-SS-Flu (**22**) was capable of efficiently labeling the

RBL-2H3 cells. The labeling with octa-Arg-SS-Flu-ITAM (**23**) was, especially for the 10 μM concentration, only slightly less than octa-Arg-SS-Flu. The lipid C_{12}-SS-Flu construct **24** displayed the highest levels of cell labeling with a geometric mean of 264.03 (for the untreated cells it was 2.87). This is probably due to the fact that this compound is relatively small and hydrophobic. In C_{12}-SS-Flu-ITAM (**25**), the relative hydrophilic ITAM mimic had a diminishing effect on cell labeling, showing the same amount of fluorescent loading as for the negative control Flu-ITAM (**17**). The combination of a small cationic peptide and an alkyl chain (K(Myr)KKK, **26**) was moderately effective in cell labeling.

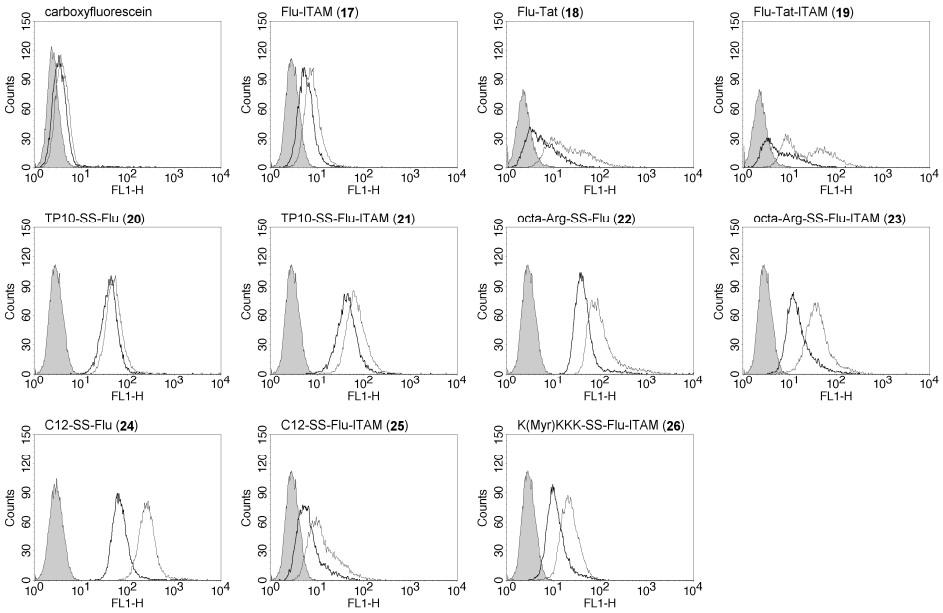

Figure 3. Flow cytometry analysis of the cellular uptake of the fluorescein labeled constructs into RBL-2H3 cells. Each graph presents untreated cells (trace filled with grey), 3 μM compound (bold trace) and 10 μM compound (plain trace). The x-axis represents the fluorescence intensity and the y-axis the number of cells.

Fluorescence microscopy

Fluorescence microscopy was performed to evaluate the intracellular distribution of constructs in the cells. Because of the promising flow cytometry results, the distribution of TP10-SS-Flu-ITAM (**21**), octa-Arg-SS-Flu-ITAM (**23**) and C_{12}-SS-Flu (**24**) inside

RBL-2H3 cells was assessed. The cells were incubated with 10 µM of a construct followed by washing steps. The viable cells were directly analyzed while still adherent.

Unexpectedly, cells incubated with TP10-SS-Flu-ITAM (**21**) showed almost no intracellular fluorescence under the microscope (Figure 4), although the incubation conditions were very similar compared to those used for the flow cytometry experiments, except that in these experiments cells were detached by incubation with trypsin. The incubation was also performed with medium without fetal calf serum, but also then no intracellular fluorescence was detected. Maybe the TP10-SS-Flu-ITAM construct was present in the endosomes and there the fluorescence is reduced due to the low pH, although this was not hampering the detection with flow cytometry experiments.

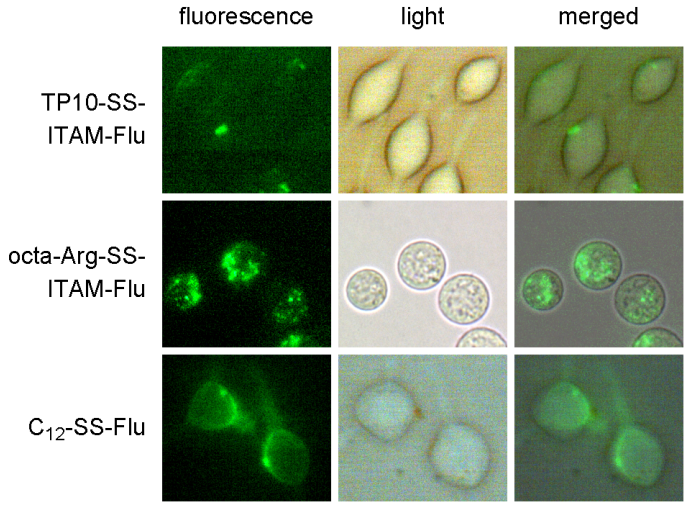

Figure 4. The uptake and distribution of C_{12}-SS-Flu (**24**), TP10-SS-ITAM-Flu (**21**) and octa-Arg-SS-ITAM-Flu (**23**) in RBL-2H3 cells. The cells were incubated with 10 µM compound for 1 hour at 37 ºC. After washing steps the viable cells were immediately analyzed with fluorescence microscopy.

Octa-Arg-SS-Flu-ITAM (**23**) could be visualized inside the RBL-2H3 cells with fluorescence microscopy. The octa-Arg construct was not homogeneously distributed and present in various parts of the cells.

Fluorescence microscopy showed that C_{12}-SS-Flu (**24**) was retained in the cell membrane (Figure 4), being unable to penetrate into the cytosol. Apparently, the C_{12}-chain could not deliver the fluorescein cargo intracellularly. Possible explanations for

this are the absence or too slow flip-flop mechanism[40] to allow cellular uptake, or, alternatively, the lipophilic compound does flip-flop, but the disulfide bond is not cleaved inside the cytosol, leading to accumulation of fluorescence at the cell membrane.

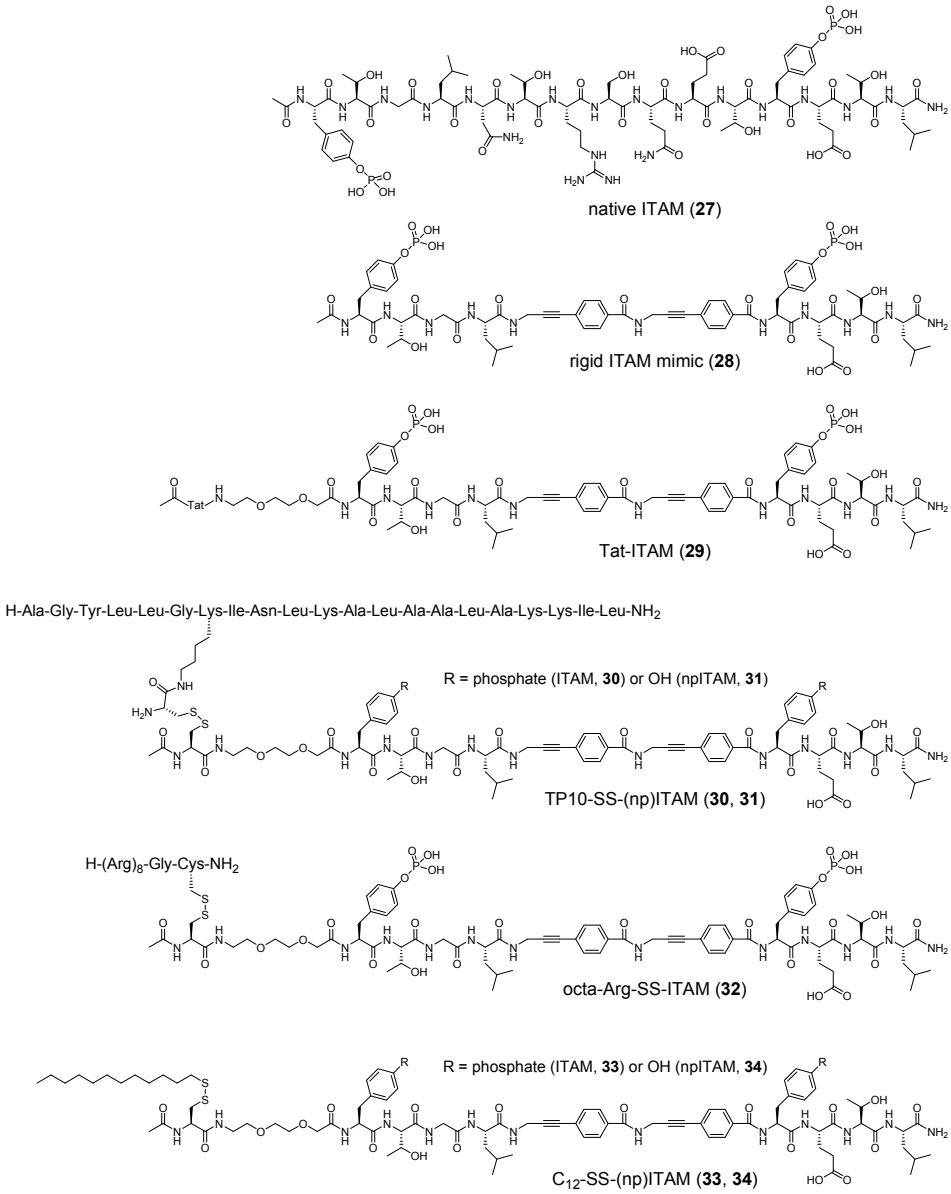

Figure 5. Native ITAM (**27**), the rigid ITAM mimic **28** and cell penetrating constructs **29 - 34** used for the evaluation of the bioactivity.

Synthesis of non-fluorescent labeled constructs

After establishing the cellular uptake and distribution using the fluorescently labeled derivatives, the bioactivity of the most promising penetrating molecular constructs had to be evaluated. For this purpose the fluorescent label needed for visualization by flow cytometry or fluorescent microscopy was now omitted in the molecular constructs and ITAM constructs with carriers Tat, TP10, octa-Arg and C_{12} were synthesized (Figure 5). Furthermore, a TP10 and a C_{12} construct with a nonphosphorylated ITAM mimic (npITAM) were synthesized as negative controls. The used synthetic strategy was analogous to that used for the fluorescently labeled constructs and is described in detail in the experimental section.

Table 1. Affinities of native ITAM, the rigid ITAM mimic and the cell permeable constructs for Syk tSH2 from SPR competition experiments.

Compound	K_D (nM)
native ITAM (**27**)	8.3 ± 0.7
rigid ITAM mimic (**28**)	5.3 ± 0.5
Tat-ITAM (**29**)	283 ± 21
TP10-SS-ITAM (**30**)	11.7 ± 3.2
octa-Arg-SS-ITAM (**32**)	29.7 ± 5.4
C_{12}-SS-ITAM (**33**)	26.6 ± 2.4
C_{12}-SS-npITAM (**34**)	> 100 000

Affinity of cell penetrating ITAM constructs for Syk tSH2

Before assessing the effect of the constructs on IgE receptor mediated signaling in RBL-2H3 cells, first the affinity of the constructs for Syk tSH2 as well as the cytotoxicity was determined. The binding affinity was established with surface plasmon resonance (SPR) competition experiments, as described earlier.[41] The K_D values of native ITAM (**27**) and rigid ITAM mimic (**28**) were virtually identical to the previously reported values (Table 1 and Figure 6).[6,9] The affinities of TP10-SS-ITAM (**30**), octa-Arg-SS-ITAM (**32**) and C_{12}-SS-ITAM (**33**) for Syk tSH2 were similar to the affinity of the rigid ITAM mimic without a carrier (**28**). The only diphosphorylated construct with a significant lower affinity was Tat-ITAM (**29**). Possibly, the positively charged residues in the Tat sequence bind to the two phosphate groups of ITAM, which reduces

the accessibility of the phosphotyrosines for SH2 binding. The nonphosphorylated C_{12}-SS-npITAM (**34**) control construct showed no binding.

From the SPR data it can be concluded that all diphosphorylated constructs, except Tat-ITAM (**29**), bind Syk tSH2 without significant interference by the carrier part.

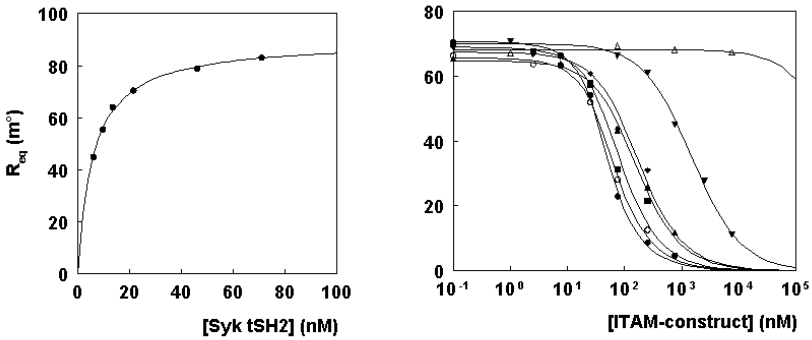

Figure 6. A: SPR determination of the affinity of Syk tSH2 for immobilized γ-dpITAM phosphopeptide on the sensor surface. Data of equilibrium signals are fitted with a Langmuir binding isotherm. B: SPR competition experiments in the presence of 25 nM Syk tSH2. Data are fitted with a competition model yielding the affinity in solution (K_D) as described.[42] The inhibition curves represent native ITAM **27** (○), rigid ITAM mimic **28** (●), Tat-ITAM **29** (▼), TP10-SS-ITAM **30** (■), octa-Arg-SS-ITAM **32** (♦), C_{12}-SS-ITAM **33** (▲) and C_{12}-SS-npITAM **34** (Δ).

Viability assays

The cytotoxicity of the constructs was determined using an XTT viability assay[43] to exclude any artifacts in the bioactivity assay (vide infra) due to toxicity. The XTT assay determines the viability of living cells from their mitochondrial dehydrogenases, which convert XTT into the corresponding UV active orange formazan. Cells in 96-wells plates were incubated with different concentrations of the ITAM constructs **29**-**33** for 1 hour, which is the maximum incubation time used in all other cell experiments. After incubation the amount of viable cells was determined with an XTT assay (Figure 7). It was found that concentrations of 10 μM and lower of all constructs are not toxic. At 20 μM all constructs showed some toxicity and therefore 10 μM was the highest concentration used in the β-hexosaminidase release degranulation bioactivity assay.

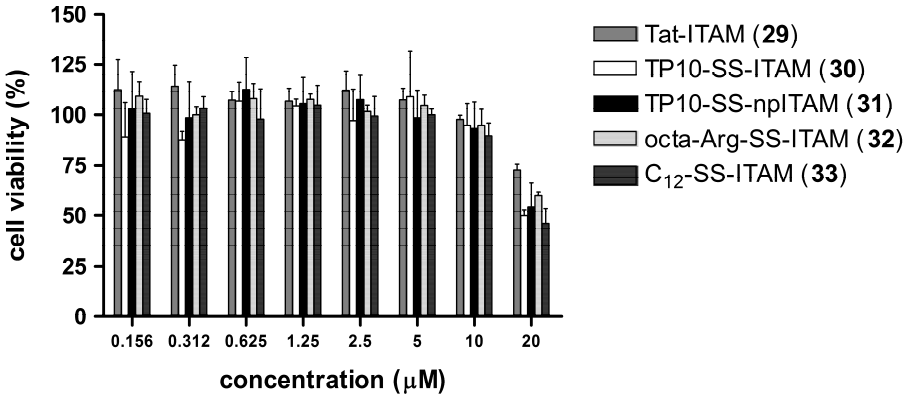

Figure 7. Cell viability of RBL-2H3 cells in the presence of different concentrations of cell penetrating constructs. RBL-2H3 cells were incubated with 0 – 20 μM construct for 1 hour under cell culture conditions prior to performing the XTT assays. Cell viability is expressed as the percentage of viable cells relative to untreated controls. Data are from experiments performed in quadruplicate and represent one of two independent experiments. The bars represent average ± SD.

Effect of cell penetrating ITAM constructs on degranulation

The effect of the cell penetrating constructs on RBL-2H3 degranulation was established by a β-hexosaminidase release assay.[44] In a typical experiment, first anti-DNP-IgE in medium was added to RBL-2H3 cells in a 96-wells plate. After 1 hour of incubation, the medium was aspirated and compounds were added in different concentrations. After 20 min of incubation, DNP_{30}-HSA was added to cross-link and stimulate the FcεRI receptors. Then the cells were allowed to degranulate for 30 min, releasing mediators such as β-hexosaminidase. Next the supernatant was collected, the cells were lyzed and the lysate was also collected. The amount of β-hexosaminidase present in the supernatant and the lysate was determined by the addition of the substrate 4-methyl umbelliferyl-N-acetyl-β-D-glucosaminide. This substrate can be cleaved by β-hexosaminidase, liberating the fluorescent 4-methyl umbelliferone.

First, the amount of β-hexosaminidase release was established without addition of constructs. The percentage of this control release compared to the total amount of β-hexosaminidase was 41%, which is indicative for viable, competent cells.[45] This amount was approximately obtained from all release assays and for every separate experiment the obtained control release was defined as 100%. Furthermore, the basal release of

non-stimulated cells, which were treated with plain medium and plain buffer instead of, respectively, anti-DNP-IgE and DNP_{30}-HSA, was defined as 0%.

The effect of Tat-ITAM (**29**) on β-hexosaminidase release could not be established, because too much DMSO was needed the keep the construct in solution. For the release assay a maximum of only 0.25% DMSO was tolerated, whereas the XTT assay allowed higher concentrations of DMSO. Nonetheless, no effect on degranulation was expected for this construct, as flow cytometry analysis indicated no binding. The low solubility of Tat-ITAM (**29**) is probably due to formation of intramolecular salt-bridges by the positively charged amino acid residues in the Tat sequence with the negatively charged phosphotyrosine residues. This intramolecular collapse might also explain the low affinity for Syk tSH2 (Table 1), because the phosphotyrosine residues are then not accessible for SH2 binding. Be this as it may, this intramolecular collapse was probably not the cause of the low cellular uptake, since also Flu-Tat (**18**) did not penetrate into the RBL-2H3 cells.

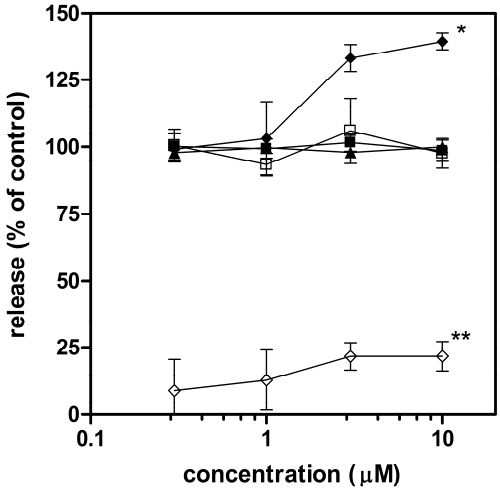

Figure 8. Effect of the cell penetrating ITAM constructs on β-hexosaminidase release upon FcεRI induced stimulation of RBL-2H3 cells. The β-hexosaminidase release was expressed as percentage of the controls, which were not treated with a construct. Data are from experiments performed in quadruplicate and represent one of at least two independent experiments. The bars represent average ± SD. The curves represent TP10-SS-ITAM **30** (■), TP10-SS-npITAM **31** (□), octa-Arg-SS-ITAM **32** (♦) and C_{12}-SS-ITAM **33** (▲). The lower curve (◊) represents the effect of octa-Arg-SS-ITAM **32** on non-stimulated cells.

TP10-SS-ITAM (**30**), as well as the nonphosphorylated negative control TP10-SS-npITAM (**31**), showed no effect on β-hexosaminidase release up to 10 μM (Figure 8). Fluorescence microscopy also showed almost no cellular uptake of these constructs. However, flow cytometry showed that TP10-SS-Flu-ITAM (**21**) and TP10-SS-Flu (**20**) could efficiently label the RBL-2H3 cells. It has been observed before that results of a functional assay do not always correlate with flow cytometry data.[46,47]

In addition, the C_{12}-SS-ITAM construct **33** displayed, as was expected from the flow cytometry data, no effect on β-hexosaminidase release (Figure 8). However, the octa-Arg-SS-ITAM construct **32** stimulated this release in a concentration dependent manner. The increase in mediator release relative to the control release of untreated stimulated cells caused by **32** was significant for both 3 and 10 μM **32**, with p-values for both of $p < 0.05$ (* in Figure 8). The increase of the degranulation by 10 μM octa-Arg-SS-ITAM (**32**) in stimulated cells was 140% compared with untreated stimulated cells. It was also investigated whether the cell permeable ITAM mimic **32** could initiate release in non-stimulated cells. For the non-stimulated cells a slight increase was observed, but the effect was less pronounced. The increase in degranulation of the non-stimulated cells compared to the control release in non-stimulated cells was significant for 3 and 10 μM (for both $p < 0.05$, ** in Figure 8). However, the increase in release of 3 and 10 μM **32** compared to 0.3 and 1 μM **32** was not significant in non-stimulated cells.

Conclusions

This is, to our best knowledge, the first paper describing the delivery of synthetic ITAM peptide mimics into Syk containing cells as well as evaluation of their effect on the signal transduction cascade leading to mediator release. Although large differences in behavior of the cell penetrating ITAM constructs have been observed in flow cytometry, fluorescence microscopy showed only significant uptake of octa-Arg-SS-Flu-ITAM (**23**) into the RBL-2H3 cells. Moreover, the octa-Arg-SS-ITAM construct **32** was also the only compound capable of influencing the mediator release: it stimulated the release in a concentration dependent fashion, implying that this ITAM construct activated Syk kinase. Possibly, the resulting activated kinase, when bound to the ITAM construct, is not present in the membrane compartment where the natural occurring ITAM sequences are present as part of the FcεRI γ-chain (Figure 1).

Although our original aim was to develop SH2 binders leading to inhibition of mediator release, we seem to have discovered a cell penetrating ITAM peptidomimetic construct capable of stimulation of mediator release. The full-length crystal structure of the closely related Zap-70 kinase might give a clue how binding of tSH2 to ITAM may affect kinase activaty.[48] In this structure the inactive form of Zap-70 shows a close contact between the SH2-SH2 linker of tSH2 and the catalytic domain. This interaction helps to keep the kinase in the inactive state. ITAM engagement leads to a conformational change involving the distance and position of the SH2 domains and the SH2-SH2 linker between them. Although the structure of full-length Syk kinase is not yet known in such detail,[49] we propose that a similar mechanism is also involved in the activation of the Syk kinase.

In the regulation of Syk activity, next to the conformational change in the Syk tSH2 domain, also other processes are involved, such as phosphorylation of the tSH2-kinase linker. These other processes only take place in stimulated cells, i.e. cells treated with anti-DNP-IgE and DNP_{30}-HSA. This explains that the octa-Arg-SS-ITAM peptidomimetic construct **32** was capable of stimulating kinase activity in stimulated RBL-2H3 cells and that it did not increase degranulation noticeably in non-stimulated cells.

This biological mechanism offers in principle the possibility to design ITAM mimics with linkers between the SH2 binding epitopes of varying length and rigidity, in order to keep the kinase in the active state using a short linker and, possibly, keep the kinase in the inactive state by a larger linker. Our previous work demonstrated that the Syk tSH2 domain adapts to a large variation in the ITAM-linker length[9,41,50] and some of these linkers may lead to ITAM peptidomimetic constructs capable of inhibition of mediator release.

Experimental section

General remarks concerning the syntheses

All chemicals were obtained from commercial sources and used without further purification. Solvents, which were used for the solid phase peptide synthesis, were stored over 4 Å molecular sieves, except for MeOH, which was stored over 3 Å molecular sieves. Reactions were performed at room temperature unless stated

otherwise. Monitoring took place and R_f values were determined by thin layer chromatography (TLC). The TLC plates were obtained from Merck and were coated with silica gel 60 F254 (0.25 mm). Spots were visualized by UV light and by ninhydrin and Cl_2-TDM (*N*,*N*,*N'*,*N'*,-tetramethyl-4,4'-diaminodiphenylmethane) staining. Solvents were removed under reduced pressure at a temperature of 40 ºC. Column chromatography was performed with Silicycle UltraPure silica gels, SiliaFlash (pore size 60 Å, particle size distribution 40-63 μm).

^{1}H NMR spectra were measured on a Varian Mercury plus 300 MHz spectrometer and chemical shifts are given in ppm (δ) relative to TMS. ^{13}C NMR spectra were measured on a Varian Mercury plus 75 MHz spectrometer and chemical shifts are given in ppm (δ) relative to $CDCl_3$, DMSO-d_6, or CD_3OD. The ^{13}C NMR spectra were measured using the attached proton test (APT).

General procedure for solid phase peptide synthesis

All peptides were manually assembled on Tentagel®-Rink-NH-Fmoc resin using standard Fmoc/tBu chemistry. The Fmoc protecting group was removed using 20% piperidine in NMP (3 × 10 mL for each gram of resin, each 8 min) followed by washing steps with NMP (3 × 10 mL for each gram of resin, each 2 min), CH_2Cl_2 (3 × 10 mL for each gram of resin, each 2 min) and NMP (3 × 10 mL for each gram of resin, each 2 min). The Alloc protecting group was removed using 0.25 equivalents of $Pd(PPh_3)_4$ and 10 equivalents of anilinium para-toluene sulfinate in MeOH/THF (1:1) (2 × 10 mL for each gram of resin, each 60 min). After Alloc deprotection the resin was washed with 0.1% sodium diethyldithiocarbamate in NMP (1 × 10 mL for each gram of resin for 2 min), NMP (3 × 10 mL for each gram of resin, each 2 min), CH_2Cl_2 (3 × 10 mL for each gram of resin, each 3 min) and NMP (3 × 10 mL for each gram of resin, each 2 min). The amino acid coupling mixtures were prepared by dissolving 4 equivalents of amino acid, 4 equivalents of HOBt and HBTU and 8 equivalents of DiPEA in NMP and coupled during a coupling time of 60 minutes. Using the same coupling conditions 5(6)-carboxyfluorescein was coupled overnight. The resin was washed with NMP (3 × 10 mL for each gram of resin, each 1 min) and CH_2Cl_2 (3 × 10 mL for each gram of resin, each 1 min) after every coupling step. The coupling steps and deprotection steps were monitored using the Kaisertest.[51] When the Fmoc deprotection was not complete, the deprotection step was repeated. Fmoc-Tyr(OP(OBn)OH)-OH was coupled overnight using 2 equivalents of amino acid, 2 equivalents of the coupling reagents HOBt and

HBTU and 5 equivalents of DiPEA. Alloc-4-(3-aminoprop-1-ynyl)benzoic acid was also coupled overnight using 2 equivalents of amino acid and 2 equivalents of the coupling reagents HOBt and HBTU and 4 equivalents of DiPEA. After the first Fmoc-Tyr(OP(OBn)OH)-OH coupling an additional washing step (2 × 10 mL for each gram of resin, each 10 min) with a mixture of 1 M TFA/1.1 M DiPEA in NMP was performed after each Fmoc deprotection step in order to replace the piperidinium counter ion of Tyr(OP(OBn)O^-) by protonated DiPEA. Peptides containing an N-terminal carboxyfluorescein were subjected to the standard Fmoc deprotection protocol (3 × 10 mL of 20% piperidine in NMP for each gram of resin, each 8 min) after carboxyfluorescein coupling. This was necessary to remove any carboxyfluorescein residues, which were coupled to the phenolic hydroxy groups of the carboxyfluorescein residue already attached to the peptide chain.[52] When all coupling steps were completed acetylation was carried out using a capping solution of Ac_2O (4.72 mL, 42.7 mmol), DiPEA (2.18 mL, 22.8 mmol) and HOBt (0.23 g, 1.7 mmol) in 100 mL of NMP for 2 × 30 min to give acetylated peptides **15-17** and **29**. The peptides were cleaved from the resin and the side chains were deprotected with various cleavage cocktails, as indicated for each peptide, for 3 h. The resin was removed from the solution by filtration and the peptides were precipitated with MTBE/hexane 1:1 v/v at -20 °C and lyophilized from CH_3CN/H_2O 1:1 v/v yielding the crude peptides. The peptides were purified by preparative HPLC and analyzed by analytical HPLC and mass spectrometry. For the preparative HPLC a Gilson system with a UV detector operating at 220 and 254 nm or an Applied Biosystems workstation with a UV detector operating at 214 nm were employed with different gradients, which are indicated for each compound below. Analytical HPLC was measured on a Shimadzu HPLC system with a UV detector operating at 220 and 254 nm and for some peptides also an evaporative light scattering detector (PL-ELS 1000, Polymer Laboratories) was used with a gradient from 100% buffer A to 100% buffer B in 20 min. Two buffer combinations were used for all HPLC runs. The buffer combination for all preparative HPLC runs and for some analytical HPLC runs, as indicated for each compound, was the 'standard TFA buffers': buffer A (0.1% TFA in H_2O/CH_3CN 95:5) and buffer B (0.1% TFA in H_2O/CH_3CN 5:95). The buffer combination for the analytical HPLC of most of the phosphotyrosine containing compounds, as indicated for each compound, was 'the TEAP buffers': buffer A (15 mM TEA in H_2O titrated at pH 6 with 85% H_3PO_4) and buffer B (buffer A/CH_3CN 1:9).

Native ITAM (27), rigid ITAM mimic (28) and Alloc-4-(3-aminoprop-1-ynyl)benzoic acid

The synthesis of the native ITAM peptide (**27**) and the rigid ITAM mimic (**28**) as well as the synthesis of the rigid building block Alloc-4-(3-aminoprop-1-ynyl)benzoic acid has been described earlier by us.[9]

Synthesis of the carriers

Boc-Cys(Trt)-OSu (1)

N-hydroxysuccinimide (1.38 g, 12 mmol) was added to Boc-Cys(Trt)-OH (11.4 mmol, 5.27 g) in 200 mL of CH_3CN. The mixture was cooled to 0 ºC and DCC (2.35 g, 11.4 mmol) was added. The mixture was stirred overnight at r.t. and it was filtered and concentrated. The product was crystallized from 2-propanol yielding 4.97 g (8.86 mmol, 78%) of **1** as white crystals. R_f = 0.61 (EtOAc/hexane 1:1). ^{1}H NMR ($CDCl_3$, 300 MHz) δ = 1.43 (s, 9H, tBu), 2.66 (d, 2H, β CH_2), 2.79 (s, 4H, 2 CH_2), 4.33 (t, 1H, CH), 4.87 (d, 1H, NH), 7.20-7.46 (m, 15H, trityl). ^{13}C NMR ($CDCl_3$, 75 MHz) δ = 25.5 (2 CH_2), 28.2 (3 CH_3), 33.6 (β CH_2), 51.1 (CH), 67.4 (C trityl), 80.6 (C tBu), 127.0, 128.2, 129.5, 144.1 (Ar), 154.5 (CO Boc), 166.8 (COO), 168.3 (2 CO).

Fmoc-Lys(Boc-Cys(Trt))-OH (2)

TFA (20 mL) and CH_2Cl_2 (20 mL) were added to Fmoc-Lys(Boc)-OH (2.34 g, 5.0 mmol) and the mixture was stirred for 1 hour and concentrated. DMF (20 mL) and 100 mL of CH_3CN were added to the resulting TFA salt. DiPEA (2.97 mL, 18 mmol) and Boc-Cys(Trt)-OSu (**1**) (2.52 g, 4.5 mmol) were added and the mixture was stirred overnight. The solvents were evaporated and the residue was dissolved in EtOAc. The solution was washed with 5% citric acid (3 ×) and brine (3 ×), dried over Na_2SO_4, filtered and concentrated. The product was purified by silica gel column chromatography (0.5% CH_3COOH in EtOAc/hexane 2:1) yielding 2.50 g (3.07 mmol, 68%) of Fmoc-Lys(Boc-Cys(Trt))-OH (**2**) as a white foam. R_f = 0.34 (0.5% CH_3COOH in EtOAc/hexane 2:1). ^{1}H NMR ($CDCl_3$, 300 MHz) δ = 1.39 (s, 9H, tBu), 1.41-1.47 (m, 4H, Lys γ δ CH_2), 2.29-2.68 (m, 2H, Cys β CH_2), 3.17 (bs, 2H, Lys ε CH_2), 3.80 (bs, 1H, Cys α CH), 4.18 (t, 1H, Lys α CH), 4.31-4.42 (m, 3H, CH, CH_2 Fmoc), 5.06 (d, 1H, Cys NH), 5.72 (d, 1H, Lys NH), 6.21 (d, 1H, Lys εCH_2-N*H*), 7.16-7.39 (m, 19H, 15 trityl, 4 Ar Fmoc), 7.58, 7.74 (2d, 4H, Ar Fmoc). ^{13}C NMR ($CDCl_3$, 75 MHz) δ = 21.9

(Lys γ CH_2), 28.3 (3 CH_3), 28.6 (Lys δ CH2), 31.4 (Lys β CH_2), 33.8 (Cys β CH_2), 38.7 (Lys ε CH_2), 47.1 (CH Fmoc), 53.6 (2 α CH), 67.1, 67.2 (C trityl, CH_2 Fmoc), 80.3 (C tBu), 119.9, 125.2, 127.1, 127.7, 141.3, 143.8 (Ar Fmoc), 126.9, 128.0, 129.6, 144.4 (Ar trityl), 155.7, 156.2 (CO Boc, Fmoc), 170.9 (CO Cys), 174.8 (COOH).

TP10-Cys (3) and TP10-Cys(pNpys) (4)

These peptides were assembled on Tentagel®-Rink-NH-Fmoc resin. For **3** 641 mg of resin (0.17 mmol, loading 0.26 mmol/g) and for **4** 321 mg of resin, (0.08 mmol, loading 0.26 mmol/g) was used. The appropriate Fmoc-amino acid building blocks including dipeptide **2** were included in the solid phase peptide synthesis (see general procedure). TFA/H_2O/TIS/EDT (90/5/2.5/2.5) was used for cleavage and deprotection yielding **3** and 2,2'-dithiobis(5-nitropyridine) (1298 mg, 0.42 mmol) in TFA/H_2O/TIS (92.5/5/2.5) was used for cleavage and deprotection yielding **4**. Lyophilization from CH_3CN/H_2O 1:1 v/v gave 338 mg of crude **3**, of which 250 mg was purified, and 335 mg of crude **4**. Purification was achieved by preparative HPLC using an Alltech Alltima C8 100 Å 10 μm (250 × 22 mm) column. Gradients of 100% buffer A to 100% buffer B in 90 minutes for **3** and in 80 minutes for **4** were used. The fractions were analyzed by analytical HPLC using an Alltech Alltima C8 5 μm (250 × 4.6 mm) column and the standard TFA buffers. 111.2 mg of pure **3** and 77.7 mg of pure **4** were obtained after pooling and lyophilization as white fluffy solids.

HRMS (ESI) of **3**: $[M+2H]^{2+}$ calculated 1142.7193, found 1142.7195; $[M+3H]^{3+}$ calculated 762.1488, found 762.1577.

MS (MALDI-TOF) of **4**: $[M+H]^+$ calculated 2438.415, found 2438.500; $[M+Na]^+$ calculated 2460.397, found 2460.321.

Octa-Arg-Cys (5)

This peptide was assembled on Tentagel®-Rink-NH-Fmoc resin (962 mg, 0.25 mmol, loading 0.26 mmol/g). The amino acid building blocks Fmoc-Cys(Trt)-OH, Fmoc-Gly-OH and Fmoc-Arg(Pbf)-OH (8 ×) were subsequently coupled. TFA/H_2O/TIS/EDT (90/5/2.5/2.5) was used for cleavage and deprotection. After lyophilization from CH_3CN/H_2O 1:1 v/v 371 mg of the crude peptide was obtained, of which 200 mg was purified by preparative HPLC using an Alltech Alltima C8 100 Å 10 μm (250 × 22 mm) column. A gradient of 100% buffer A to 100% buffer B in 60 minutes was used. The fractions were analyzed by analytical HPLC using an Alltech Alltima C8 5 μm (250 ×

4.6 mm) column and the standard TFA buffers. 113.3 mg of the pure compound was obtained after pooling and lyophilization as a white fluffy solid.
HRMS (ESI): $[M+2H]^{2+}$ calculated 713.9409, found 713.9344; $[M+3H]^{3+}$ calculated 476.2965, found 476.3069.

Octa-Arg-Cys(pNpys) (6)

Octa-Arg-Cys **5** (23.5 mg, 10 μmol) in 3 mL of H_2O was added to 2,2'-dithiobis(5-nitropyridine) (15.5 mg, 50 μmol) dissolved in 1 mL of TFA. The mixture was stirred for 3 hours and then evaporated to dryness. The product was obtained by preparative HPLC using an Alltech Alltima C8 100 Å 10 μm (250 × 22 mm) column. A gradient of 100% buffer A to 100% buffer B in 60 minutes was used. The fractions were analyzed by analytical HPLC using an Alltech Alltima C8 5 μm (250 × 4.6 mm) column and the standard TFA buffers. Pure **6** was obtained after pooling and lyophilization (14.1 mg, 54%) as a white fluffy solid.

C_{12}-S-pNpys (7)

To a solution of 2,2'-dithiobis(5-nitropyridine) (776 mg, 2.5 mmol) in 15 mL of TFA/DCM 1:1, 1-dodecanethiol (120 μL, 0.5 mmol) was added dropwise and the mixture was stirred for 1 hour. The solvents were evaporated and **7** was obtained after silica gel column chromatography (hexane, then EtOAc/hexane 1:3) in quantitative yield as a yellow solid. R_f = 0.86 (EtOAc/hexane 1:3). ^{1}H NMR ($CDCl_3$, 300 MHz) δ = 0.82 (t, 3H, CH_3), 120 (bs, 16H, CH_2), 1.35 (bs, 2H, CH_2CH_3),1.63-1.72 (m, 2H, SCH_2CH_2) 2.79 (t, 2H, SCH_2), 7.88 (d, 1H, Ar), 8.36 (d, 1H, Ar), 9.20 (s, 1H, Ar). ^{13}C NMR ($CDCl_3$, 75 MHz) δ = 14.0 (CH_3), 22.6 (CH_2CH_3), 28.4-29.5 (8 CH_2), 31.8 (SCH_2CH_2), 39.3 (SCH_2), 118.9, 131.4, 141.8, 144.9, 169.3 (Ar).

Fmoc-Lys(Myr)-OH (8)

To a solution of myristic acid (1.60 g, 7.0 mmol) in 10 mL of DMF and 100 mL of CH_3CN, N-hydroxysuccinimide (863 mg, 7.5 mmol) was added. After cooling to 0 ºC DCC (1.44 g, 7.0 mmol) was added. The mixture was then stirred overnight at r.t. Filtration and concentration afforded Myr-OSu.
Fmoc-Lys(Boc)-OH (2.34 g, 5.0 mmol) was dissolved in 20 mL of TFA and 20 mL of CH_2Cl_2. The mixture was stirred for 3 hours followed by concentration and 25 mL of DMF and 100 mL of CH_3CN were added to the TFA salt. After neutralization with

TEA, additional TEA (826 µL, 5.0 mmol) and Myr-OSu were added and stirring was continued for 3 hours. The solvents were evaporated and the product was dissolved in EtOAc. The solution was washed with 1 M $KHSO_4$ (3 ×) and brine (1 ×), dried over Na_2SO_4, filtered and concentrated. The product was purified by silica gel column chromatography (0.5% CH_3COOH in EtOAc/hexane 2:1) yielding 2.01 g (3.65 mmol, 73%) of **8** as a white foam. R_f = 0.16 (0.5% CH_3COOH in EtOAc/hexane 2:1). ^1H NMR (DMSO, 300 MHz) δ = 0.85 (t, 3H, CH_3), 1.14-1.28 (m, 22H, 10 CH_2 myristoyl and Lys γ CH_2), 1.36 (m, 2H, Lys δ CH_2), 1.46 (t, 2H, myristoyl β CH_2), 1.56-1.77 (m, 2H, Lys β CH_2), 2.02 (t, 2H, myristoyl α CH_2), 3.03 (t, 2H, Lys ε CH_2), 3.87-3.91 (m, 1H, CH Fmoc), 4.22-4.28 (m, 3H, Lys α CH, CH_2 Fmoc), 7.30-7.44 (m, 4H, Ar Fmoc), 7.58-7.61 (m, 2H, 2 NH), 7.73, 7.89 (2d, 4H, Ar Fmoc). ^{13}C NMR (DMSO, 75 MHz) δ = 19.4 (CH_3), 27.5 (Lys δ CH_2), 28.5 (CH_2CH_3), 30.8 (myristoyl β CH_2), 34.1-34.4 (myristoyl 9 CH_2), 35.9 (Lys δ CH_2), 36.7 (Lys β CH_2), 40.9 (myristoyl α CH_2), 43.5 (Lys ε CH_2), 52.1 (CH Fmoc), 59.2 (Lys α CH), 71.1 (CH_2 Fmoc), 125.5, 130.7, 132.5, 133.1, 146.2, 149.3 (Ar Fmoc), 161.6 (CO Fmoc), 177.4 (myristoyl CO), 179.4 (COOH).

Cys-K(Myr)KKK (9)

This peptide was assembled on Tentagel®-Rink-NH-Fmoc resin (1.02 g, 0.25 mmol, loading 0.24 mmol/g). The amino acid building blocks Fmoc-Lys(Boc)-OH, Fmoc-Lys(Boc)-OH, Fmoc-Lys(Boc)-OH, **8**, and Fmoc-Cys(Trt)-OH were subsequently coupled. TFA/H_2O/TIS/EDT (90/5/2.5/2.5) was used for cleavage and deprotection of the peptide. After lyophilization from CH_3CN/H_2O 1:1 v/v 239 mg of the crude peptide was obtained, of which 100 mg was purified by preparative HPLC using an Alltech Alltima C8 100 Å 10 µm (250 × 22 mm) column. A gradient of 100% buffer A to 100% buffer B in 60 minutes was used. The fractions were analyzed by analytical HPLC using an Alltech Alltima C8 5 µm (250 × 4.6 mm) column and the standard TFA buffers. 70.0 mg of the pure compound was obtained after pooling and lyophilization as a white fluffy solid.

MS (ESI): $[M+H]^+$ calculated 843.62, found 843.65; $[M+2H]^{2+}$ calculated 422.32, found 422.35.

Synthesis of the cargos

2-(tritylthio)ethanamine (10)[53]

Tritrylchloride (3.63 g, 13.0 mmol) was added to a solution of cysteamine.HCl (1.00 g, 8.80 mmol) in 50 mL of DMF/CH_2Cl_2 1:1 and the mixture was stirred for 2 hours. The solvents were evaporated and the product was purified by silica gel column chromatography (CH_2Cl_2/EtOAc 9:1, then CH_2Cl_2/MeOH 4:1) yielding 2.35 g (7.36 mmol, 84%) of **10** as a pale yellow solid. R_f = 0.68 (CH_2Cl_2/MeOH 4:1). ^{1}H NMR ($CDCl_3$, 300 MHz) δ = 1.50 (s, 2H, NH_2), 2.28 (t, 2H, SCH_2), 2.50 (t, 2H, NHCH_2), 7.11-7.24, 7.39-7.44 (2m, 15H, trityl). ^{13}C NMR ($CDCl_3$, 75 MHz) δ = 35.6 (CH_2S), 40.5 ($NHCH_2$), 66.2 (C trityl), 126.3, 127.5, 129.2 144.5 (Ar).

Fluorescein-CH_2-CH_2-S(Trt) (11)

Cysteamine derivative **10** (160 mg, 0.50 mmol) in 1 mL of DMF was added to fluorescein isothiocyanate isomer 1 (195 mg, 0.50 mmol) in 6 mL of DMF and the mixture was stirred for 2 hours. Then the DMF was evaporated and the product was purified by silica gel column chromatography (CH_2Cl_2/MeOH 95:5) yielding 319 mg (0.45 mmol, 90%) of thiocarbamate **11** as an orange solid. R_f = 0.13 (CH_2Cl_2/MeOH 95:5). ^{1}H NMR (DMSO, 300 MHz) δ = 2.42 (t, 2H, SCH_2), 3.50 (d, 2H, NHCH_2), 6.54-6.68 (m, 6H, Ar fluorescein), 7.17 (d, 1H, Ar fluorescein), 7.22-7.36 (m, 15H, trityl), 7.71 (d, 1H, Ar fluorescein), 8.23 (s, 1H, Ar fluorescein), 10.01 (bs, 2H, OH). ^{13}C NMR (DMSO, 75 MHz) δ = 30.8 (SCH_2), 42.3 ($NHCH_2$), 66.0 (C trityl), 102.2, 109.7, 112.6, 116.7, 124.1, 126.4, 127.7, 128.6, 141.1, 147.2, 151.9, 159.5 (Ar fluorescein), 126.8, 128.1, 129.1, 144.4 (Ar trityl), 168.5 (CO), 180.4 (CS).

Flu-Cys-ITAM (12) and Flu-Cys(pNpys)-ITAM (13)

These peptides were assembled on Tentagel®-Rink-NH-Fmoc resin (each 1.02 g, 0.25 mmol, loading 0.24 mmol/g). The following amino acid building blocks were subsequently coupled: Fmoc-Leu-OH, Fmoc-Thr(tBu)-OH, Fmoc-Glu(OtBu)-OH, Fmoc-Tyr(OP(OBn)OH)-OH, Alloc-4-(3-aminoprop-1-ynyl)benzoic acid, Alloc-4-(3-aminoprop-1-ynyl)benzoic acid, Fmoc-Leu-OH, Fmoc-Gly-OH, Fmoc-Thr(tBu)-OH, Fmoc-Tyr(OP(OBn)OH)-OH, Fmoc-2-(2-(2-aminoethoxy)ethoxy)acetic acid, Fmoc-Cys(Trt)-OH. After coupling of 5(6)-carboxyfluorescein, TFA/H_2O/TIS/EDT (90/5/2.5/2.5) was used for cleavage and deprotection of **12**. 2,2'-dithiobis(5-

nitropyridine) (388 mg, 1.25 mmol) in TFA/H_2O/TIS (92.5/5/2.5) was used for cleavage and deprotection of **13**. After lyophilization from CH_3CN/H_2O 1:1 v/v 298 mg of crude **12** and 457 mg of crude **13** were obtained. The peptides were purified by preparative HPLC using an Alltech Alltima C8 100 Å 10 µm (250 × 22 mm) column. A gradient of 100% buffer A to 100% buffer B in 100 minutes was used for both peptides. The fractions were analyzed by analytical HPLC using an Alltech Alltima C8 5 µm (250 × 4.6 mm) column and the TEAP buffers. 40.8 mg of pure **12** was obtained and 14.2 mg of pure **13** was obtained, starting from 228 mg crude peptide **13**, both as yellow fluffy solids after pooling and lyophilization.
HRMS (ESI) of **12**: $[M+H]^+$ calculated 2038.6576, found 2038.6373.
MS (MALDI-TOF, negative mode) of **13**: $[M-H]^-$ calculated 2192.101, found 2192.105.

Ac-Cys-ITAM (14), Ac-Cys(pNpys)-ITAM (15) and Ac-Cys-npITAM (16)
These peptides were assembled on Tentagel®-Rink-NH-Fmoc resin (**14**: 865 mg, 0.225 mmol, loading 0.26 mmol/g; **15**: 417 mg, 0.10 mmol, loading 0.24 mmol/g; **16**: 769 mg, 0.20 mmol, loading 0.26 mmol/g). The amino acid building blocks were identical to those used for the synthesis of **12** and **13**. After removal of the last Fmoc group, the N-terminus was acetylated with capping solution. TFA/H_2O/TIS/EDT (90/5/2.5/2.5) was used for cleavage and deprotection of peptides **14** and **16**. For **15** 2,2'-dithiobis(5-nitropyridine) (155 mg, 0.50 mmol) in TFA/H_2O/TIS (95.5/5/2.5) was used. After lyophilization from CH_3CN/H_2O 1:1 v/v 163 mg of crude **14**, 177 mg of crude **15** and 135 mg of crude **16** were obtained. The peptides were purified by preparative HPLC using an Alltech Adsorbosphere XL C8 90 Å 10 µm (250 × 22 mm) column for **14** and **16** and an Alltech Alltima C8 100 Å 10 µm (250 × 22 mm) column for **15**. A gradient of 100% buffer A to 100% buffer B in 40 minutes was used for **14** and **16** and a gradient of 100 minutes was used for **15**. The fractions were analyzed by analytical HPLC using an Alltech Adsorbosphere XL C8 90 Å 5 µm (250 × 4.6 mm) column and the standard TFA buffers for **14** and **16** and an Alltech Alltima C8 5 µm (250 × 4.6 mm) column and the TEAP buffers for **15**. 40.1 mg of pure **14**, 4.8 mg of pure **15** (only 80 mg was purified of **15**) and 15.5 mg of pure **16** were obtained after pooling and lyophilization as white fluffy solids.
HRMS (ESI) of **14**: $[M+Na]^+$ calculated 1744.6019, found 1744.9742; $[M+2Na]^{2+}$ calculated 883.7955, found 884.0009.
MS (ESI, negative mode) of **15**: $[M-H]^-$ calculated 1875.84, found 1876.25.

HRMS (ESI) of **16**: $[M+H]^+$ calculated 1562.6877, found 1563.0153; $[M+Na]^+$ calculated 1664.6361, found 1664.9752; $[M+2H]^{2+}$ calculated 821.831, found 822.0479; $[M+H+Na]^{2+}$ calculated 832.8214, found 833.0208; $[M+2Na]^{2+}$ calculated 843.8123, found 844.0172.

Flu-ITAM (17)

This peptide was assembled on Tentagel®-Rink-NH-Fmoc resin (417 mg, 0.10 mmol, loading 0.24 mmol/g). The amino acid building blocks were identical to those used for the synthesis of **12** and **13** excepting Fmoc-Cys(Trt)OH. After coupling of 5(6)-carboxyfluorescein TFA/H_2O/TIS/EDT (90/5/2.5/2.5) was used for cleavage and deprotection of the peptide. Lyophilization from CH_3CN/H_2O 1:1 v/v gave 148 mg of the crude peptide, of which 50 mg was purified by preparative HPLC using an Alltech Alltima C8 100 Å 10 μm (250 × 22 mm) column. A gradient of 100% buffer A to 100% buffer B in 100 minutes was used. The fractions were analyzed by analytical HPLC using an Alltech Alltima C8 5 μm (250 × 4.6 mm) column and the TEAP buffers and 9.4 mg of the pure compound was obtained after pooling and lyophilization as a yellow fluffy solid.

HRMS (ESI): $[M+H]^+$ calculated 1935.6484, found 1935.6533; $[M+2H]^{2+}$ calculated 968.3281, found 968.2862.

Synthesis of carrier-fluorescein constructs

Flu-Tat (18)

This peptide was assembled on Tentagel®-Rink-NH-Fmoc resin (1.04 g, 0.25 mmol, loading 0.24 mmol/g). The amino acid building blocks Fmoc-Arg(Pbf)-OH, Fmoc-Arg(Pbf)-OH, Fmoc-Arg(Pbf)-OH, Fmoc-Gln(Trt)-OH, Fmoc-Arg(Pbf)-OH, Fmoc-Arg(Pbf)-OH, Fmoc-Lys(Boc)-OH, Fmoc-Lys(Boc)-OH, Fmoc-Arg(Pbf)-OH, Fmoc-Gly-OH, Fmoc-Tyr(tBu)-OH, Fmoc-βalanine-OH and 5(6)-carboxyfluorescein were subsequently coupled. TFA/H_2O/TIS (92.5/5/2.5) was used for cleavage and deprotection of the peptide. After lyophilization from CH_3CN/H_2O 1:1 v/v 394 mg of the crude peptide was obtained, of which 51 mg was purified by preparative HPLC using an Alltech Adsorbosphere XL C8 90 Å 10 μm (250 × 22 mm) column. A gradient of 100% buffer A to 100% buffer B in 40 minutes was used. The fractions were analyzed by analytical HPLC using an Alltech Adsorbosphere XL C8 90 Å 5 μm (250 ×

4.6 mm) column and the standard TFA buffers and 9.6 mg of the pure peptide was obtained as a yellow fluffy solid after pooling and lyophilization.
HRMS (ESI): $[M+2H]^{2+}$ calculated 995.0343, found 995.2886; $[M+3H]^{3+}$ calculated 663.6328, found 663.4452; $[M+4H]^{4+}$ calculated 497.9844, found 497.8207.

TP10-SS-Flu (20)

TFA (2 mL), TIS (5 µL) and CH_2Cl_2 (1 mL) were added to **11** (5.4 mg, 7.6 µmol) and the mixture was stirred for 2 hours. After evaporation of the volatiles, TP10-Cys(pNpys) (**4**) (23 mg, 7.6 µmol) dissolved in 1 mL of CH_3CN and 2 mL of 1 M NH_4OAc (pH 4.5) was added. Stirring was continued overnight and then the solvents were evaporated followed by purification of the product by preparative HPLC using an Alltech Alltima C8 100 Å 10 µm (250 × 22 mm) column. A gradient of 100% buffer A to 100% buffer B in 90 minutes was used. The fractions were analyzed by analytical HPLC using an Alltech Alltima C8 5 µm (250 × 4.6 mm) column and the standard TFA buffers. The product was obtained as a yellow fluffy solid (4.2 mg, 17%) after pooling and lyophilization.
HRMS (ESI): $[M+2H]^{2+}$ calculated 1375.7322, found 1375.2452; $[M+3H]^{3+}$ calculated 917.4908, found 917.0551.

Octa-Arg-SS-Flu (22)

A mixture of TFA (2 mL), TIS (5 µL) and CH_2Cl_2 (1 mL) was added to **11** (3.8 mg, 5.4 µmol), the resulting solution was stirred for 2 hours and after that the volatiles were evaporated. Octa-Arg-Cys(pNpys) (**6**) (14.1 mg, 5.4 µmol) in 4 mL of 1 M NH_4OAc (pH 4.5) was added and the mixture was stirred overnight. The solvents were evaporated and the product was purified by preparative HPLC using an Alltech Alltima C8 100 Å 10 µm (250 × 22 mm) column. A gradient of 100% buffer A to 100% buffer B in 100 minutes was used. The fractions were analyzed by analytical HPLC using an Alltech Alltima C8 5 µm (250 × 4.6 mm) column and the standard TFA buffers. After pooling and lyophilization of the appropriate fractions the product was obtained as a yellow fluffy solid (7.7 mg, 55%).
HRMS (ESI): $[M+3H]^{3+}$ calculated 630.9799, found 630.9855; $[M+4H]^{4+}$ calculated 473.4869, found 473.5040.

C_{12}-SS-Flu (24)

A mixture of TFA (2 mL), TIS (40 µL) and H_2O (40 µL) was added to **11** (35 mg, 50 µmol), the mixture was stirred for 4 hours and the solvents were evaporated. C_{12}-S-pNpys (**7**) (18 mg, 50 µmol) in 2 mL of THF and 2 mL of 1 M NH_4OAc (pH 4.5) was added and the mixture was stirred overnight. The solvents were evaporated and the product was purified by silica gel column chromatography (CH_2Cl_2/MeOH 92.5:7.5) and lyophilized from CH_3CN/H_2O 1:1 yielding 14.1 mg (21 µmol, 42%) of the product as an orange powder. R_f = 0.49 (CH_2Cl_2/MeOH 9:1). ^{1}H NMR (CD_3OD, 300 MHz) δ = 0.88 (t, 3H, CH_3), 1.27 (bs, 16H, CH_2), 1.37-1.40 (m, 2H, CH_3CH_2), 1.67-1.72 (m, 2H, SCH_2CH_2), 2.74 (t, 3H, SCH_2), 2.99 (t, 2H, $NHCH_2CH_2$), 3.93 (t, 2H, $NHCH_2$), 6.52 (d, 2H, Ar), 6.55-6.68 (m, 4H, Ar), 7.14 (d, 1H, Ar), 7.78 (dd, 1H, Ar), 8.17 (d, 1H, Ar). ^{13}C NMR (CD_3OD, 75 MHz) δ = 14.5 (CH_3), 23.7 (CH_3CH_2), 29.5 (SH_3CH_2), 30.2-30.7 (7 CH_2), 33.1 ($CH_3CH_2CH_2$), 37.8 ($NHCH_2CH_2$), 39.8 (SCH_2), 44.6 ($NHCH_2$), 79.1 (C fluorescein), 103.5, 111.5, 113.6, 120.0, 125.7, 129.1, 130.3, 131.9, 142.3, 150.1 154.2, 161.5 (Ar), 171.1 (CO), 183.0 (CS).

Synthesis of carrier-(fluorescein-)ITAM constructs

Flu-Tat-ITAM (19)

This peptide was assembled on Tentagel®-Rink-NH-Fmoc resin (739 mg, 0.17 mmol, loading 0.23 mmol/g). The appropriate amino acid building blocks were subsequently coupled. TFA/H_2O/TIS/EDT (90/5/2.5/2.5) was used for cleavage and deprotection of the peptide. After lyophilization from CH_3CN/H_2O 1:1 v/v 133 mg of the crude peptide was obtained. 17 mg of the peptide was purified by preparative HPLC using an Alltech Prosphere C4 300 Å 10 µm (250 × 22 mm) column. A gradient of 100% buffer A to 100% buffer B in 40 minutes was used. The fractions were analyzed by analytical HPLC using an Alltech Prosphere C4 300 Å 5 µm (250 × 4.6 mm) column and the standard TFA buffers. 4.3 mg of the pure compound was obtained after pooling and lyophilization as a yellow fluffy solid.

HRMS (ESI): $[M+2H]^{2+}$ calculated 1775.3047, found 1775.4950; $[M+3H]^{3+}$ calculated 1184.4453, found 1184.0286.

Tat-ITAM (29)

This peptide was assembled on Tentagel®-Rink-NH-Fmoc resin (626 mg, 0.144 mmol, loading 0.23 mmol/g). The amino acid building blocks were identical to those used for the synthesis of **19**, except the last two building blocks, i.e. Fmoc-βalanine-OH and 5(6)-carboxyfluorescein, which were not coupled. After deprotection of the last Fmoc group, the N-terminus was acetylated with capping solution. TFA/H_2O/TIS/EDT (90/5/2.5/2.5) was used for cleavage and deprotection of the peptide. After lyophilization from CH_3CN/H_2O 1:1 v/v 183 mg of the crude peptide was obtained. 26 mg of the peptide was purified by preparative HPLC using an Alltech Prosphere C4 300 Å 10 µm (250 × 22 mm) column. A gradient of 100% buffer A to 100% buffer B in 40 minutes was used. The fractions were analyzed by analytical HPLC using an Alltech Prosphere C4 300 Å 5 µm (250 × 4.6 mm) column and the standard TFA buffers. 4.3 mg of the pure compound was obtained after pooling and lyophilization as a white fluffy solid.

HRMS (ESI): $[M+2H]^{2+}$ calculated 1581.3125, found 1581.4844; $[M+3H]^{3+}$ calculated 1054.6566, found 1054.6653; $[M+4H]^{4+}$ calculated 791.2578, found 791.4642; $[M+5H]^{5+}$ calculated 633.2344, found 633.3635.

General procedure for hetero disulfide formation[38]

CH_3CN and 1 M NH_4OAc (pH 4.5) were added (approximately 1:1 v/v) to the free thiol (1 eq) and the pNpys activated thiol (1 eq). The mixture was stirred overnight and lyophilized. The product was purified and preparative, Alltech Alltima C8 100 Å 10 µm (250 × 22 mm or 250 × 10 mm), HPLC columns were used unless otherwise stated. A gradient of 100% buffer A to 100% buffer B in 100 minutes was applied. The fractions were analyzed by analytical HPLC using an Alltech Alltima C8 5 µm (250 × 4.6 mm) column and the appropriate fractions were pooled and lyophilized.

TP10-SS-Flu-ITAM (21)

The general disulfide formation procedure was applied at 3 µmol scale using TP10-Cys(pNpys) (**4**) and Flu-Cys-ITAM (**12**). For analytical HPLC the standard TFA buffers were used. The product was obtained as a yellow fluffy solid (4.4 mg, 34%). HRMS (ESI): $[M+2H]^{2+}$ calculated 2161.9592, found 2161.8464; $[M+3H]^{3+}$ calculated 1440.6935, found 1440.8491; $[M+4H]^{4+}$ calculated 1080.7721, found 1080.9844.

Octa-Arg-SS-Flu-ITAM (23)

The general disulfide formation procedure was applied at 1.3 μmol scale using octa-Arg-Cys (**5**) and Flu-Cys(pNpys)-ITAM (**13**). For analytical HPLC the standard TFA buffers were used. The product was obtained as a yellow fluffy solid (1.9 mg, 32%). MS (MALDI-TOF): $[M+H]^+$ calculated 3462.508, found 3462.239.

C_{12}-SS-Flu-ITAM (25)

The general disulfide formation procedure was applied at 3 μmol scale using C_{12}-S-pNpys (**7**) and Flu-Cys-ITAM (**12**). For analytical HPLC the TEAP buffers were used. The product was obtained as a yellow fluffy solid (1.3 mg, 27%). HRMS (ESI): $[M+2H]^{2+}$ calculated 1119.9126, found 1119.8400; $[M+H+2Na]^{3+}$ calculated 762.1228, found 762.2044.

K(Myr)KKK-SS-Flu-ITAM (26)

The general disulfide formation procedure was applied at 1.6 μmol scale using K(Myr)KKK-Cys (**9**) and Flu-Cys(pNpys)-ITAM (**13**). For analytical HPLC the standard TFA buffers were used. The product was obtained as a yellow fluffy solid (0.3 mg, 6%). MS (MALDI-TOF): $[M+H]^+$ calculated 2879.256, found 2879.723.

TP10-SS-ITAM (30)

The general disulfide formation procedure was applied at 2.5 μmol scale using TP10-Cys (**3**) and Ac-Cys(pNpys)-ITAM (**15**), except that the reaction time was 1 hour. For analytical HPLC the standard TFA buffers were used. The product was obtained as a white fluffy solid (2.1 mg, 21%). MS (MALDI-TOF): $[M+H]^+$ calculated 4004.028, found 4004.219.

TP10-SS-npITAM (31)

The general disulfide formation procedure was applied at 2.4 μmol scale using TP10-Cys(pNpys) (**4**) and Ac-Cys-npITAM (**16**). For analytical HPLC the standard TFA buffers were used. The product was obtained as a white fluffy solid (2.8 mg, 30%). HRMS (ESI): $[M+2H]^{2+}$ calculated 1923.8445, found 1923.6176; $[M+3H]^{3+}$ calculated 1282.8990, found 1282.6471; $[M+4H]^{4+}$ calculated 962.4262, found 962.2748.

Octa-Arg-SS-ITAM (32)

The general disulfide formation procedure was applied at 1.4 µmol scale using octa-Arg-Cys(pNpys) (**6**) and Ac-Cys-ITAM (**14**). For preparative HPLC an Alltech Prosphere C4 300 Å 5 µm (250 × 10 mm) column was used and for analytical HPLC the standard TFA buffers were used. The product was obtained as a white fluffy solid (1.6 mg, 27%). MS (MALDI-TOF): $[M+H]^+$ calculated 3146.471, found 3146.305.

C_{12}-SS-ITAM (33)

The general disulfide formation procedure was applied at 3.3 µmol scale using C_{12}-S-pNpys (**7**) and Ac-Cys-ITAM (**14**). For analytical HPLC the TEAP buffers were used. The product was obtained as a white fluffy solid (1.1 mg, 17%). HRMS (ESI): $[M+H]^+$ calculated 1922.7803, found 1922.8661; $[M+Na]^+$ calculated 1944.7622, found 1944.8240; $[M+2H]^{2+}$ calculated 961.8941, found 961.8193; $[M+H+Na]^{2+}$ calculated 972.885, found 972.8207; $[M+2Na]^{2+}$ calculated 983.8760, found 983.8316; $[M+H+K]^{2+}$ calculated 980.8720, found 980.8080.

C_{12}-SS-npITAM (34)

The general disulfide formation procedure was applied at 2.6 µmol scale using C_{12}-S-pNpys (**7**) and Ac-Cys-npITAM (**16**). For analytical HPLC the standard TFA buffers were used. The product was obtained as a white fluffy solid (1.4 mg, 31%). HRMS (ESI): $[M+H]^+$ calculated 1762.8476, found 1762.6885, $[M+Na]^+$ calculated 1784.8296, found 1784.6439, $[M+2H]^{2+}$ calculated 881.9277, found 881.8311; $[M+H+Na]^{2+}$ calculated 892.9187, found 892.8214; $[M+2Na]^{2+}$ calculated 903.9097, found 903.8288, $[M+H+K]^{2+}$ calculated 900.9057, found 900.7785.

Cell culture and stock solutions

RBL-2H3 cells were cultured in 25, 75 and 225 cm^2 cell culture flasks in RPMI 1640 with L-glutamine, supplemented with 10% heat-inactivated fetal calf serum, 100 U/mL penicillin and 100 µg/mL streptomycin in a humidified atmosphere of 5% CO_2 at 37 ºC. For serial passage and experiments, the cells were detached with trypsin (0.05%) and ethylenediaminetetraacetic acid (EDTA) (0.02%) for 10 minutes at 37 °C. After trypsinization cells were resuspended in medium for further use.

Stock solutions of the compounds with a concentration of 1 mM in H_2O/DMSO 9:1 were prepared and used for all experiments, except for Tat-ITAM (**29**), of which a stock solution of 1 mM in H_2O/DMSO 1:1 was prepared.

Flow cytometry

RBL-2H3 cells were plated in 12-wells plates overnight resulting in a confluency of ± 50%. The medium was aspirated and compounds **17**-**26** and 5(6)-carboxyfluorescein were added in different concentrations in complete RPMI 1640 medium. The cells were incubated for 1 hour at 37 °C. The cells were washed with PBS, detached with trypsin/EDTA and resuspended in complete medium. The cells were transferred into tubes and centrifuged for 5 min at 300 rpm at 4 °C. The supernatant was removed and the cells were washed with ice-cold PBS. Finally the cells were resuspended in 250 µL ice-cold PBS and fluorescence was measured using a BD (Becton Dickinson) FACSCalibur flow cytometer. Live cells were gated on Forward Scatter and Side Scatter and approximately 10,000 viable cells were analyzed.

Fluorescence microscopy

RBL-2H3 cells were plated on 30-mm glass-bottom culture dishes (MatTek Corp.) and cultured overnight in complete medium to allow the cells to adhere. The medium was removed and the cells were incubated for 1 hour at 37 ºC with 1 mL of complete medium containing 10 µM compound. The medium was discarded, and the cells were washed 2 × 2 min with 2 mL of PBS and 1 × 2 min with 2 mL of D-MEM/F-12 without phenol red, antibiotics or serum (imaging medium). Imaging medium was added and the cells were immediately analyzed with fluorescence microscopy using a Nikon Eclipse TE2000-U microscope.

SPR competition experiments

SPR measurements were performed on a double channel IBISII SPR instrument (Eco Chemie, Utrecht, The Netherlands) equipped with a CM 5 sensor chip (BIAcore AB, Uppsala, Sweden). Native γ-dpITAM peptide containing a 6-aminohexanoic acid spacer was immobilized on the sensor chip as was described earlier.[41] Competition experiments were performed with different concentrations of compound in the presence of 25 nM Syk tSH2 in HBS buffer. K_D values for the affinity in solution were calculated according to described procedures.[42]

Cell viability assay

RBL-2H3 cells were plated in 96-wells plates in complete RPMI 1640 medium and cultured overnight. The cells were incubated with different concentrations of construct in complete RPMI 1640 medium (100 μL in each well) for 1 hour under tissue culture conditions. Cell viability was assessed using XTT assays.[43] Briefly, the medium was discarded and 160 μL complete medium was added to each well. Then 40 μL of 1 mg/mL XTT (sodium 3'-[1-(phenylaminocarbonyl)-3,4-tetrazolium]-bis(4-methoxy-6-nitro)benzene sulfonic acid hydrate) and 25 μM PMS (phenazine methosulfate) in plain RPMI 1640 was added and the cells were incubated for 2 hours under cell tissue conditions. The absorbance was measured at 450 nm with a reference wavelength of 690 nm using a BioTek μQuant microplate spectrophotometer.

β-hexosaminidase release assay

The assay was essentially identical to the assay described earlier.[44] Briefly, RBL-2H3 cells were plated in 96-wells plates in complete RPMI 1640 medium and cultured overnight. The cells were sensitized with a monoclonal IgE directed against the dinitrophenyl hapten (anti-DNP-IgE, 0.2 μg/mL) for 1 hour in complete RPMI 1640 medium. After sensitization, the cells were washed (2 × 50 μL) with a Tyrode's salt buffer (137 mM NaC1, 2.7 mM KCl, 0.31 mM NaH_2PO_4, 12 mM $NaHCO_3$, 1.8 mM $CaC1_2$, 0.5 mM $MgC1_2$, 10 mM Hepes, 5.6 mM glucose, 0.1% bovine serum albumin, pH 7.2) and 50 μL of the Tyrode's salt buffer was added. After 10 min, constructs (50 μL in Tyrode's salt buffer) were added in different concentrations and the cells were incubated for 20 min. Exocytosis was triggered by the addition of DNP-albumin conjugate (DNP_{30}-HSA, 25 μL, 0.1 μg/mL) followed by incubation for 30 min. Supernatant (50 μL of each well) was collected. The remaining buffer was removed and the cells were treated with 125 μL 1% Triton-X-100 in Tyrode's salt buffer for 5 min and 50 μL of the lysate was also collected.

To the collected samples 50 μL of 4-methyl umbelliferyl-N-acetyl-β-D-glucosaminide (160 μM) in citrate buffer (0.1 M, pH 4.5) was added and the samples were incubated for one hour at 37 °C. The enzymatic reaction was stopped by adding 100 μL ice-cold glycine buffer (0.2 M, pH 10.7). The fluorescence was measured in a well plate reader at excitation and emission wavelengths of 360 nm and 452 nm, respectively (BMG LABTECH FLUOstar OPTIMA), and was quantitated using 4-methyl umbelliferone as a standard.

Acknowledgements

Linda Quarles van Ufford is kindly acknowledged for her assistance with the cell culturing. Dr. Marjan Fretz is acknowledged for her help with the flow cytometry and the fluorescence microscopy experiments.

References and notes

1. Gilfillan, A.M., Tkaczyk, C., Integrated signalling pathways for mast-cell activation, *Nat. Rev. Immunol.*, **2006**, 6, 218-230.
2. Kraft, S., Kinet, J.-P., New developments in FcεRI regulation, function and inhibition, *Nat. Rev. Immunol.*, **2007**, 7, 365-378.
3. Siraganian, R.P., Zhang, J., Suzuki, K., Sada, K., Protein tyrosine kinase Syk in mast cell signaling, *Mol. Immunol.*, **2001**, 38, 1229–1233.
4. Bradding, P., Novel approaches to the inhibition of mast cells in allergic disease, *Clin. Exp. Allergy*, **2008**, 38, 704-708.
5. Colgan, J., Rothman, P., Manipulation of signaling to control allergic inflammation, *Curr. Opin. Allergy Clin. Immunol.*, **2007**, 7, 51-56.
6. De Mol, N.J., Catalina, M.I., Dekker, F.J., Fischer, M.J.E., Heck, A.J., Liskamp, R.M.J., Protein flexibility and ligand rigidity: a thermodynamic and kinetic study of ITAM-based ligand binding to Syk tandem SH2, *ChemBioChem*, **2005**, 6, 2261-2270.
7. Kumaran, S., Grucza, R.A., Waksman, G., The tandem Src homology 2 domain of the Syk kinase: a molecular device that adapts to interphosphotyrosine distances, *Proc. Natl. Acad. Sci. U.S.A.*, **2003**, 100, 14828-14833.
8. Draber, P., Draberova, L., Lipid rafts in mast cell signaling, *Mol. Immunol.*, **2002**, 38, 1247-1252.
9. Dekker, F.J., de Mol, N.J., Fischer, M.J.E., Liskamp, R.M.J., Amino propynyl benzoic acid building block in rigid spacers of divalent ligands binding to the Syk SH2 domains with equally high affinity as the natural ligand, *Bioorg. Med. Chem. Lett.*, **2003**, 13, 1241-1244.
10. Isersky, C., Metzger, H., Buell, D.N., Cell cycle-associated changes in receptors for IgE during growth and differentiation of a rat basophilic leukemia cell line, *J. Exp. Med.*, **1975**, 141, 1147-1162.
11. Mousli, M., Bueb, J.L., Bronner, C., Rouot, B., Landry, Y., G-protein activation: a receptor-independent mode of action for cationic amphiphilic neuropeptides and venom peptides, *Trends Pharmacol. Sci.*, **1990**, 11, 358-362.
12. Fischer, R., Fotin-Mleczek, M., Hufnagel, H., Brock, R., Break on through to the other side - Biophysics and cell biology shed light on cell-penetrating peptides, *ChemBioChem*, **2005**, 6, 2126 – 2142.
13. Stewart, K.M., Horton, K.L., Kelley, S.O., Cell-penetrating peptides as delivery vehicles for biology and medicine, *Org. Biomol. Chem.*, **2008**, 6, 2242-2255.
14. Jones, S.W., Christison, R., Bundell, K., Voyce, C.J., Brockbank, S.M.V., Newham, P., Lindsay, M.A., Characterisation of cell-penetrating peptide-mediated peptide delivery, *Br. J. Pharmacol.*, **2005**, 145, 1093-1102.
15. Mueller, J., Kretzschmar, I., Volkmer, R., Boisguerin, P., Comparison of cellular uptake using 22 cell-penetrating peptides in 4 different cell lines, *Bioconjugate Chem.*, **2008**, 19, 2363-2374.

16. Maiolo, J.R., Ferrer, M., Ottinger, E.A., Effects of cargo molecules on the cellular uptake of arginine-rich cell-penetrating peptides, *Biochim. Biophys. Acta - Biomem.*, **2005**, 1712, 161-172.
17. Dunican, D.J., Doherty, P., Designing cell-permeant phosphopeptides to modulate intracellular signaling pathways, *Biopolymers*, **2001**, 60, 45-60.
18. Kertesz, A., Varadi, G., Toth, G.K., Fajka-Boja, R., Monostori, E., Sarmay, G., Optimization of the cellular import of functionally active SH2-domain-interacting phosphopeptides, *Cell. Mol. Life Sci.*, **2006**, 63, 2682-2693.
19. Ye, G.F., Nam, N.H., Kumar, A., Saleh, A., Shenoy, D.B., Amiji, M.M., Lin, X.F., Sun, G.Q., Parang, K., Synthesis and evaluation of tripodal peptide analogues for cellular delivery of phosphopeptides, *J. Med. Chem.*, **2007**, 50, 3604-3617.
20. Jiang, T., Olson, E.S., Nguyen, Q.T., Roy, M., Jennings, P.A., Tsien, R.Y., Tumor imaging by means of proteolytic activation of cell-penetrating peptides, *Proc. Natl. Acad. Sci. U.S.A.*, **2004**, 101, 17867-17872.
21. Mishra, A., Gordon, V.D., Yang, L.H., Coridan, R., Wong, G.C.L., HIV TAT forms pores in membranes by inducing saddle-splay curvature: Potential role of bidentate hydrogen bonding, *Angew. Chem. Int. Ed.*, **2008**, 47, 2986-2989.
22. Gump, J.M., Dowdy, S.F., TAT transduction: the molecular mechanism and therapeutic prospects, *Trends Mol. Med.*, **2007**, 13, 443-448.
23. Zhao, M., Weissleder, R., Intracellular cargo delivery using TAT peptide and derivatives, *Med. Res. Rev.*, **2004**, 24, 1-12.
24. Kaplan, I.M., Wadia, J.S., Dowdy, S.F., Cationic TAT peptide transduction domain enters cells by macropinocytosis, *J. Controlled Release*, **2005**, 102, 247-253.
25. Nelson, A.R., Borland, L., Allbritton, N.L., Sims, C.E., Myristoyl-based transport of peptides into living cell, *Biochemistry*, **2007**, 46, 14771-14781.
26. Jones, S., Farquhar, M., Martin, A., Howl, J., Intracellular translocation of the decapeptide carboxyl terminal of $G_i3\alpha$ induces the dual phosphorylation of p42/p44 MAP kinases, *Biochim. Biophys. Acta - Mol. Cell Res.*, **2005**, 1745, 207-214.
27. Howl, J., Jones, S., Farquhar, M., Intracellular delivery of bioactive peptides to RBL-2H3 cells induces beta-hexosaminidase secretion and phospholipase D activation, *ChemBioChem*, **2003**, 4, 1312-1316.
28. Fretz, M.M., Penning, N.A., Al-Taei, S., Futaki, S., Takeuchi, T., Nakase, I., Storm, G., Jones, A.T., Temperature-, concentration- and cholesterol-dependent translocation of L- and D-octa-arginine across the plasma and nuclear membrane of $CD34^+$ leukaemia cells, *Biochem. J.*, **2007**, 403, 335-342.
29. Fuchs, S.M., Raines, R.T., Pathway for polyarginine entry into mammalian cell, *Biochemistry*, **2004**, 43, 2438-2444.
30. Mitchell, D.J., Kim, D.T., Steinman, L., Fathman, C.G., Rothbard, J.B., Polyarginine enters cells more efficiently than other polycationic homopolymers, *J. Pept. Res.*, **2000**, 56, 318-325.
31. Gras-Masse, M., Lipid vector for the delivery of peptides towards intracellular pharmacological targets, *J. Mol. Recog.*, **2003**, 16, 234-239.
32. Eichholtz, T., Debont, D.B.A., Dewidt, J., Liskamp, R.M.J., Ploegh, H.L., A myristoylated pseudosubstrate peptide, a novel protein-kinase-C inhibitor, *J. Biol. Chem.*, **1993**, 268, 1982-1986.
33. Carrigan, C.N., Imperiali, B., The engineering of membrane-permeable peptides, *Anal. Biochem.*, **2005**, 341, 290-298.
34. Saito, G., Swanson, J.A., Lee, K.D., Drug delivery strategy utilizing conjugation via reversible disulfide linkages: role and site of cellular reducing activities, *Adv. Drud Delivery Rev.*, **2003**, 55, 199-215.
35. Ghosh, A.K., Fan, E., A novel method for sequence independent incorporation of activated/protected cysteine in Fmoc solid phase peptide synthesis, *Tetrahedron Lett.*, **2000**, 41, 165-168.

36. Matsueda, R., Kimura, T., Kaiser, E.T., Matsueda, G.R., 3-nitro-2-pyridinesulfenyl group for protection and activation of the thiol function of cysteine, *Chem. Lett.*, **1981**, 737-740.
37. Matsueda, R., Higashida, S., Ridge, R.J., Matsueda, G.R., Activation of conventional S-protecting groups of cysteine by conversion into the 3-nitro-2-pyridinesulfenyl (Npys) group, *Chem. Lett.*, **1982**, 921-924.
38. Rabanal, F., DeGrado, W.F., Dutton, P.L., Use of 2,2'-dithiobis(5-nitropyridine) for the heterodimerization of cysteine containing peptides. Introduction of the 5-nitro-2-pyridinesulfenyl group, *Tetrahedron Lett.*, **1996**, 37, 1347-1350.
39. El-Andaloussi, S., Jarver, P., Johansson, H.J., Langel, U., Cargo-dependent cytotoxicity and delivery efficacy of cell-penetrating peptides: a comparative study, *Biochem. J.*, **2007**, 407, 285-292.
40. Kol, M.A., de Kroon, A.I.P.M., Killian, J.A., de Kruijff, B., Transbilayer movement of phospholipids in biogenic membranes, *Biochemistry*, **2004**, 43, 2673-2681.
41. Dekker, F.J., de Mol, N.J., van Ameijde, J., Fischer, M.J.E., Ruijtenbeek, R., Redegeld, F.A.M., Liskamp, R.M.J., Replacement of the intervening amino acid sequence of a Syk-binding diphosphopeptide by a nonpeptide spacer with preservation of high affinity, *ChemBioChem*, **2002**, 3, 238-242.
42. De Mol, N.J., Gillies, M.B., Fischer, M.J.E., Experimental and calculated shift in pK_a upon binding of phosphotyrosine peptide to the SH2 domain of $p56^{lck}$, *Bioorg. Med. Chem.*, **2002**, 10, 1477-1482.
43. Scudiero, D.A., Shoemaker, R.H., Paull, K.D., Monks, A., Tierney, S., Nofziger, T.H., Currens, M.J., Seniff, D., Boyd, M.R., Evaluation of a soluble tetrazolium formazan assay for cell-growth and drug sensitivity in culture using human and other tumor-cell lines, *Cancer Res.*, **1988**, 48, 4827-4833.
44. Fischer, M.J.E., Paulussen, J.J.C., Horbach, D.A., Roelofsen, E.P.W., Vanmiltenburg, J.C., Demol, N.J., Janssen, L.H.M., Inhibition of mediator release in RBL-2H3 cells by some H_1-antagonist derived antiallergic drugs: Relation to lipophilicity and membrane effects, *Inflamm. Res.*, **1995**, 44, 92-97.
45. Naal, R.M.Z.G., Tabb, J., Holowka, D., Baird, B., In situ measurement of degranulation as a biosensor based on RBL-2H3 mast cells, *Biosens. Bioelectron.*, **2004**, 20, 791-796.
46. Lundin, P., Johansson, H., Guterstam, P., Holm, T., Hansen, M., Langel, U., El Andaloussi, S., Distinct uptake routes of cell-penetrating peptide conjugates, *Bioconjugate Chem.*, **2008**, 19, 2535-2542.
47. Lundberg, P., El-Andaloussi, S., Sutlu, T., Johansson, H., Langel, U., Delivery of short interfering RNA using endosomolytic cell-penetrating peptides, *FASEB J.*, **2007**, 21, 2664-2671.
48. Deindl, S., Kadlecek, T.A., Brdicka, T., Cao, X., Weiss, A., Kuriyan, J., Structural basis for the inhibition of tyrosine kinase activity of ZAP-70, *Cell*, **2007**, 129, 735-746.
49. The only high resolution structures of Syk domains are: C-SH2 complexed with a phosphopentapeptide (PDB entry code 1csz), tSH2 complexed with ITAM (PDB entry code 1a81) and the kinase domain (PDB entry code 1xba).
50. Kuil, J., van Wandelen, L.T.M., de Mol, N.J., Liskamp, R.M.J., A photoswitchable ITAM peptidomimetic: Synthesis and real time surface plasmon resonance (SPR) analysis of the effects of cis-trans isomerization on binding, *Bioorg. Med. Chem.*, **2008**, 16, 1393-1399.
51. Kaiser, E., Colescott, R.L., Bossinger, C.D., Cook, P.I., Color test for detection of free terminal amino groups in the solid-phase synthesis of peptides, *Anal. Biochem.*, **1970**, 34, 595-598.
52. Fischer, R., Mader, O., Jung, G., Brock, R., Extending the applicability of carboxyfluorescein in solid-phase synthesis, *Bioconjugate Chem.*, **2003**, 14, 653-660.
53. Halkes, K.M., de Souza, A.C., Maljaars, C.E.P., Gerwig, G.J., Kamerling, J.P., A facile method for the preparation of gold glyconanoparticles from free oligosaccharides and their applicability in carbohydrate-protein interaction studies, *Eur. J. Org. Chem.*, **2005**, 3650-3659.

Chapter 7

Allosteric regulation of Syk kinase activity induced by a conformational change of its tandem SH2 domain: Effects of rigid ITAM mimics studied by a flow-through microarray technique

Kuil, J., Ruijtenbeek, R., de Mol, N.J., Liskamp, R.M.J., Allosteric regulation of Syk kinase activity induced by a conformational change of its tandem SH2 domain: Effects of rigid ITAM mimics studied by a flow-through microarray technique, *manuscript in preparation*

Abstract

Spleen tyrosine kinase (Syk) is a protein involved in signal transduction of immune receptors. It consists of two tandemly arranged SH2 domains (tSH2) and a kinase domain. Activation of Syk is initiated when tSH2 binds to a diphosphorylated ITAM motif, which is intracellularly present on e.g. the high-affinity IgE receptor (FcεRI). Effects of ITAM mimics on constitutively active Syk were studied using a flow-through microarray technique (PamStation®). The microarrays existed of 144 peptides, known to be substrates for protein tyrosine kinases. It was found that Syk activity is slightly increased by the native ITAM peptide. A rigid ITAM mimic with approximately the same distance between the two SH2 binding epitopes had generally a slight inhibiting effect on kinase activity. However, a rigid ITAM mimic with a larger distance between the binding epitopes was capable at inhibiting phosphorylation of the substrates present on the arrays. This is the first demonstration that allosteric changes in tSH2 regulate Syk kinase activity. This may initiate the development of selective Syk inhibitors, based on pushing both SH2 domains in tSH2 further apart from each other by ITAM mimics with rigid linkers of appropriate length.

Introduction

The Spleen tyrosine kinase (Syk) family of nonreceptor tyrosine kinases consists of two proteins found in immune cells: Syk and Zap-70.[1,2] Both proteins comprises two SH2 domains in tandem (tSH2) and a kinase domain. Furthermore, a SH2-SH2 linker (interdomain A) and a tSH2-kinase linker (interdomain B) are present.

Syk is essential in IgE receptor signaling, in which it is activated by binding to an Immunoreceptor Tyrosine based Activation Motif (ITAM).[3-9] ITAM is present on the intracellular domains of the β- and γ-chains of the high affinity IgE receptor (FcεRI). FcεRI consists of an α-, β- and two γ-chains and is present in for instance mast cells and basophils. The ITAM consensus sequence consists of Tyr-Xxx-Xxx-(Leu/Ile)-$(Xxx)_{n=6-8}$-Tyr-Xxx-Xxx-(Leu/Ile), in which Xxx can be any amino acid. The underlined residues comprise the binding epitopes for Syk tSH2, when tyrosine is phosphorylated. Once FcεRI is stimulated by IgE binding and receptor cross-linking, γ-ITAM is diphosphorylated (γ-dpITAM). Syk is recruited to the cell membrane by binding to γ-dpITAM with its tSH2 domain, and subsequently a conformational change of Syk and activation of its kinase domain is the result.[7] Syk transfers the signal further by phosphorylation of e.g. the Linker for Activation of T-cells family (LAT) and the Non T cell Activation Linker (NTAL) proteins, which eventually leads to cell degranulation.[8,9] Overstimulation of this cascade leads to allergic responses and therefore Syk inhibitors are potential anti-allergic drugs. Furthermore, Syk is also a potential target for treatment of breast cancer, leukemia, thrombus development on damaged endothelium or atherosclerotic plaques leading to e.g. stroke.[10,11]

We have found that the intervening residues $(Xxx)_{n=6-8}$ (in γ-ITAM n = 7) were not essential for binding of γ-ITAM to Syk tSH2.[3,12,13] Those residues could be replaced by various linkers while retaining high binding affinity. An ITAM peptidomimetic with a rigid linker consisting of two amino propynyl benzoic acid building blocks (compound **2** in Figure 1) has comparable binding affinity for Syk tSH2 as the native ITAM peptide.[3,13]

A binding model for the γ-dpITAM – Syk tSH2 interaction was proposed based on our previously reported kinetic data.[3] According to this model, first one SH2 domain binds one phosphotyrosine (pTyr) residue and then the other SH2 domain binds the second pTyr residue. To enable binding of the latter, the SH2 domains have to move closer to each other by means of a conformational change in the SH2-SH2 linker. It is

assumed that this change in SH2-SH2 distance allosterically regulates Syk kinase activity. This hypothesis was corroborated by the crystal structure of the closely related full-length inactive Zap-70 protein.[2,14] The structure of tSH2 in this Zap-70 structure is very similar to that observed in the uncomplexed tSH2,[15] with the SH2 domains further apart from each other than when bound to diphosphorylated ITAM. In the inactive Zap-70 structure the inter SH2 linker is in close contact with the tSH2-kinase linker and the kinase domain.[2,14] Changing the inter-SH2 distance could cause conformational changes in the tSH2-kinase linker and the activation loop of the kinase domain. Consequently, various phosphorylation sites in the tSH2-kinase linker and the activation loop become accessible for kinases, leading to activation of Zap-70.

We have studied the interaction of ITAM and ITAM mimics with Syk tSH2.[3,13,16] It is observed that the tSH2 domain is very flexible and can easily adapt to ITAM mimics with varying distance between the SH2 binding epitopes, retaining high affinity.[16] The aim of the present study is to investigate whether changing the inter SH2 distance affects Syk kinase activity. For this ITAM mimics were designed which possessed rigid linkers between the SH2 binding epitopes, replacing the seven intervening residues. One of these compounds (**2** in Figure 1) has been studied before.[3,13] The linker in compound **2** had approximately the same length as in native ITAM **1** and had a comparable affinity for Syk tSH2. To study effects of increase in inter SH2 distance, an ITAM peptidomimetic with a longer rigid linker was designed (compound **3**).

The affinity of ITAM mimics **2** and **3** for Syk tSH2 was determined by SPR experiments. The effect of native γ-ITAM (**1**) as well as mimics **2** and **3** on Syk kinase activity was assessed with a recently developed flow-though peptide microarray system (PamStation®). Each array exists of 144 protein tyrosine kinase (PTK) substrates.[17-20] Each of the substrates consisted of 13 amino acid residues and contained at least one tyrosine. Unlike most other microarray systems,[21,22] in the PamStation system the analyte solution can be pumped up and down through the microarrays, because they are on porous aluminium oxide, resulting in excellent mixing. A fluorescently labeled antibody, i.e. the phosphotyrosine antibody PY20, is used to detect tyrosine phosphorylation on the arrays. The degree of phosphorylation can be determined and quantified by taking a picture of the array with a CCD camera and inferred from the degree of fluorescence on the spots.

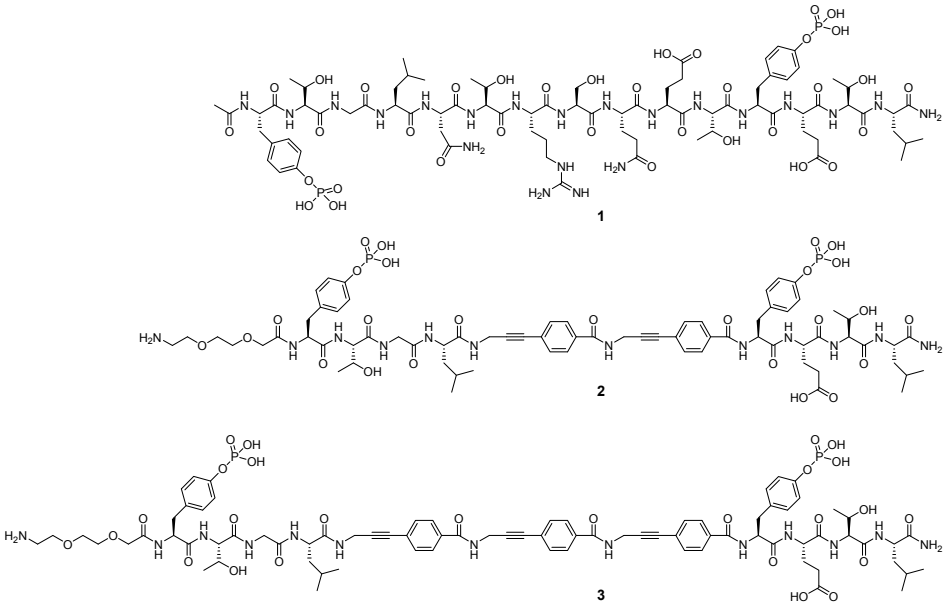

Figure 1. Native γ-ITAM (**1**) and rigid ITAM mimics **2** and **3**. The rigid ITAM mimics are provided with an ethyleneglycol spacer for immobilization on an SPR surface.

Results and discussion

Design and synthesis

The length of the seven intervening residues when ITAM is bound to Syk tSH2 is 14.1–16.4 Å according to the crystal structure.[23] The length of the rigid linker in compound **2**, containing two amino propynyl benzoic acid building blocks was estimated with molecular simulations and amounts to 14.5 Å, which is nicely in the range of the ITAM peptides in the crystal structure. To examine the effect of larger ITAM mimics on binding and kinase activity, also a mimic with three rigid building blocks was designed (compound **3**). The length of this linker was also estimated with molecular simulations and amounts 20.7 Å, which is significantly longer than in native ITAM.

The synthesis of the required rigid amino propynyl benzoic acid building block and native ITAM **1** has been described previously.[13] The synthesis and purification of ITAM

mimics **2** and **3** was essentially identical to that of the rigid ITAM mimic described earlier.[13]

SPR binding studies

The affinity for Syk tSH2 was established by SPR experiments. The affinity of native ITAM **1** for Syk tSH2 has been determined previously (Table 1). To assay the binding affinity by direct SPR measurements, compounds **2** and **3** were immobilized on an SPR sensor chip and the affinity for Syk tSH2 was determined by the addition of 0 – 200 nM Syk tSH2 (Figure 2, Table 1). The observed affinity of **2** was similar to that determined previously with SPR competition experiments.[3] Interestingly, ITAM mimic **3** had almost the same affinity for Syk tSH2. The fact that Syk tSH2 can bind ITAM mimics with different linker lengths with high affinity has been observed earlier by us.[12,13,16]

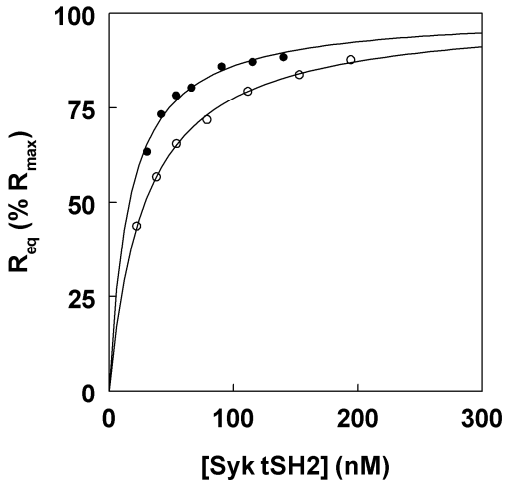

Figure 2. Direct SPR affinity assay of compounds **2** and **3**. Compounds **2** (●) and **3** (○) were immobilized on a SPR sensor chip. On the y-axis the amount of binding at equilibrium is expressed as percentage of the maximal binding capacity of each surface. The curves represent the fits with a Langmuir binding isotherm.[24]

Table 1. Affinities of compounds **1-3** for Syk tSH2 obtained from SPR experiments.

Compound	K_D (nM)
native ITAM **1**[3]	5.6
rigid ITAM mimic **2**	16.1 ± 1.4
rigid ITAM mimic **3**	28.9 ± 0.9

Microarray based kinase assay

On each microarray 144 PTK substrates were immobilized. One peptide, present on position 1-12 (row 1, column 12), was already phosphorylated and functioned as a positive control. Syk was purchased as an active kinase. Initial microarray experiments were carried out without ITAM, to establish the experimental conditions and the substrate preference of Syk. First the arrays were blocked with BSA, to diminish aspecific binding of e.g. Syk or the phosphotyrosine-antibody. Then an analyte solution containing Syk, ATP and BSA in Abl buffer (kinase buffer) was added and the solution was pumped up and down through the arrays for 30 minutes (60 pump-cycles), which resulted in tyrosine phosphorylation of some of the immobilized peptides.

In principle this flow-through microarray technology enables monitoring of the phosphorylation in real time. To do so, a fluorescent phosphotyrosine antibody has to be added to the kinase solution. When the kinase phosphorylates an immobilized peptide, the antibody will immediately bind to it and this can be followed in real time with a CCD camera. Unfortunately, in this specific case it was not possible to obtain kinetic data in this way, because the anti-phosphotyrosine antibody would also bind to the used ITAM ligands, resulting in a decrease in sensitivity. Therefore, all experiments were performed as endpoint assays. After Syk had been allowed to phosphorylate the particular peptide substrates, the arrays were thoroughly washed with kinase buffer and PBS (pH = 9) to ensure the removal of any remaining bound ITAM ligand.

Then, the PY20-FITC phosphotyrosine-antibody was added and the amount of phosphorylation was visualized with a CCD camera. An example of a CCD-picture is shown in Figure 3. As can be seen, several peptides were phosphorylated by Syk. The same procedure was also performed without the addition of ATP, to establish the amount of basal signal not resulting from peptide conversion but due to aspecific binding of the phosphotyrosine antibody or of phosphorylated Syk protein that is also detected by the antibody. This aspecific binding was substantial for a number of

immobilized peptides. The peptide on position 10-3 (RET 1022-1034), for example, displayed one of the highest levels of fluorescence intensity after the experiments with Syk and ATP (Figure 3). However, phosphorylation was not the cause of the high signal, since subtraction of the aspecific binding by the antibody yielded only a modest amount of phosphorylation. Therefore, the aspecific binding by the antibody was subtracted from the signals in each single spot, which gave a more realistic view of the phosphorylation data.

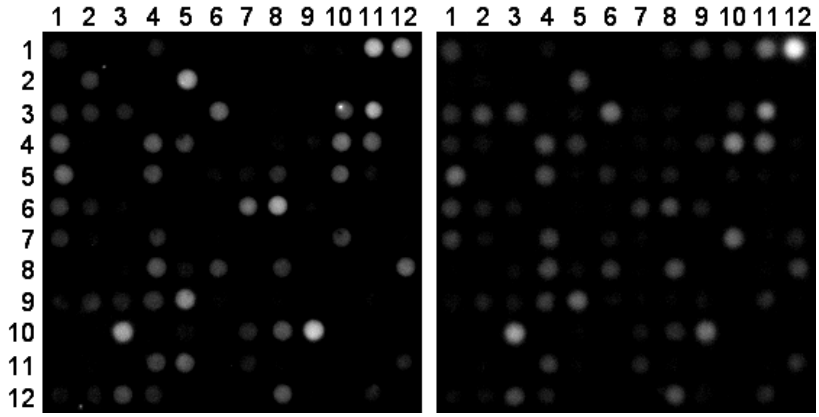

Figure 3. Typical images of microarrays after an experiment with 28 nM of Syk and 10 μM of ATP (left) or with 28 nM of Syk without ATP (right), both without the addition of an ITAM ligand.

After subtraction of the control signals, a list of the top 25 phosphorylated peptides was prepared and is shown in Table 2. In this Table potential substrates of Syk are presented. Before discussing this in more detail, it should be highlighted here that biological interpretation of peptide microarray data is complicated because the phosphorylation sites on proteins are represented on the microarray not by complete proteins, but by peptides, which is of course an artificial condition. In a cell, substrate recognition and preference by a kinase is the result of cellular localisation, the folding of the substrate protein, protein (domain) interactions and sequence preference. Only the latter is partially mimicked in a peptide microarray experiment. Nonetheless, peptide phosphorylation as detected on the chip is a valid starting point for further explorations and generates hypotheses that can be tested.

Table 2. Top 25 list of the immobilized peptides phosphorylated by Syk.

Position on the array (row and column)	Protein name	Abbreviation and position of sequence in the protein	UniProt Accession No.	Peptide sequence
1-4	Annexin A1	ANXA1 14-26	P04083	IENEEQE**Y**VQTVK
1-11	Platelet-derived growth factor subunit B	PDGFB 1014-1028	P01127	PNEGDND**Y**IIPLPDP
2-2	E3 ubiquitin-protein ligase CBL	CBL 693-705	P22681	EGEEDTE**Y**MTPSS
2-5	B-cell antigen receptor complex-associated protein alpha chain	CD79A 181-193	P11912	E**Y**EDENL**Y**EGLNL
3-1	Embryonal Fyn-associated substrate	EFS 246-258	O43281	GGTDEGI**Y**DVPLL
3-10	Gamma-enolase	ENOG 37-49	P09104	SGASTGI**Y**EALEL
3-11	Ephrin type-A receptor 1	EPHA1 774-786	P21709	LDDFDGT**Y**ETQGG
4-1	Ephrin type-A receptor 2	EPHA2 765-777	P29317	EDDPEAT**Y**TTSGG
4-4	Ephrin type-A receptor 7	EPHA7 607-619	Q15375	T**Y**IDPET**Y**EDPNR
4-5	Ephrin type-B receptor 1	EPHB1 771-783	P54762	DDTSDPT**Y**TSSLG
4-11	Receptor tyrosine-protein kinase erbB-2	ERBB2 870-882	P04626	LDIDETE**Y**HADGG
5-1	Receptor tyrosine-protein kinase erbB-4	ERBB4 1277-1289	Q15303	IVAENPE**Y**LSEFS
5-4	Protein tyrosine kinase 2 beta	FAK2 572-584	Q14289	R**Y**IEDED**YY**KASV
5-8	Fibroblast growth factor receptor 2	FGFR2 762-774	P21802	TLTTNEE**Y**LDLSQ
5-10	Fibroblast growth factor receptor 3	FGFR3 753-765	P22607	TVTSTDE**Y**LDLSA
5-11	Tyrosine-protein kinase FRK	FRK 380-392	P42685	KVDNEDI**Y**ESRHE
6-7	Linker for activation of T-cells family member 1	LAT 194-206	O43561	MESIDD**Y**VNVPES
6-8	Linker for activation of T-cells family member 1	LAT 249-261	O43561	EEGAPD**Y**ENLQEL
8-4	Phosphatidylinositol 3-kinase regulatory subunit alpha	P85A 600-612	27986	NENTEDQ**Y**SLVED
8-12	Beta-type platelet-derived growth factor receptor	PGFRB 572-584	P09619	VSSDGHE**Y**I**Y**VDP
9-5	1-phosphatidylinositol-4,5-bisphosphate phosphodiesterase gamma-1	PLCG1 764-776	P19174	IGTAEPD**Y**GAL**Y**E
10-8	Src substrate protein p85	SRC8_CHICK 476-488	Q01406	E**Y**EPETV**Y**EVAGA
10-9	Src substrate protein p85	SRC8_CHICK 492-504	Q14247	**Y**QAEENT**Y**DE**Y**EN
11-5	Troponin T, slow skeletal muscle	TNNT1 2-14	P13805	SDTEEQE**Y**EEEQP
11-12	Vascular endothelial growth factor receptor 1	VEGFR1 1235-1247	P17948	ATSMFDD**Y**QGDSS

Three interesting phosphorylation events on the microarray are discussed here. A peptide which was phosphorylated by Syk was EYEDENLYEGLNL (position 2-5). This peptide is derived from the B-cell antigen receptor complex-associated protein alpha chain (UniProt Accession No. P11912). Syk is known to play an important role in B-cells.[25] This peptide partly contains the intracellular ITAM sequence of the B cell receptor.[26] The immobilized peptide, shown in italics below, possesses the N-terminal SH2 binding epitope of ITAM, which is shown in bold: *EYEDENL**YEGLNL***DDCSMYEDI. This suggests that Syk is capable of phosphorylating this ITAM motif on the α-chain of the B cell receptor.

The phosphorylated peptides MESIDDYVNVPES (position 6-7) and EEGAPDYENLQEL (position 6-8) are also noteworthy and are both derived from LAT. LAT is a 262 amino acid membrane protein (UniProt Accession No. O43561), possessing one transmembrane domain, a short extracellular domain (4 residues) and a large intracellular domain.[27] LAT is phosphorylated on tyrosines by Syk, after activation of Syk by e.g. FcεRI stimulation.[8,9,27] The phosphotyrosine residues on LAT function as docking sites for proteins such as Grb2, PLC-γ1 and PI3K.[27]

So far, phosphorylation by Syk of these sites in LAT has not been found experimentally. It is known that Zap-70 phosphorylates at least five tyrosine residues in LAT, i.e. Tyr 156, Tyr161, Tyr200, Tyr220 and Tyr255.[28] It is likely that Syk phosphorylates at least Tyr200 and Tyr220, as they are docking sites for Grb2 when phosphorylated. The results of the microarray experiments suggest that Tyr200 of LAT protein can probably be phosphorylated by Syk. The LAT peptide containing Tyr255 was also phosphorylated, suggesting that Tyr255 is a substrate of Syk too.

Effect of ITAM peptides 1-3 on Syk kinase activity

Using the above discussed endpoint assay, in which in the final step anti-phosphotyrosine antibody was added, the effects of ITAM ligands **1-3** on Syk activity was now studied (Figure 4). Native γ-ITAM **1** stimulated Syk kinase activity for most substrates, although for many substrates this stimulation was small.

As a control, Syk was also exposed to a nonphosphorylated ITAM peptide (compound **4**). This peptide had, in general, no influence on the phosphorylation activity of Syk (data not shown).

ITAM mimic **2**, which had a linker of almost the same length as in native γ-ITAM, had minor effects on kinase activity (Figure 4). Some peptides were more

phosphorylated but most were slightly less phosphorylated. For all top-25 peptides the amount of phosphorylation was less when compound **2** was present in comparison with native γ-ITAM ligand **1**.

A much more pronounced effect on Syk kinase activity was shown by the longer ITAM mimic **3**, which inhibited phosphorylation of all 25 peptides (Figure 4). Several peptides were not phosphorylated at all when **3** was added, whereas others were significantly less phosphorylated. Also the phosphorylation of the peptide derived from the B-cell antigen receptor complex (CD79A 181-193) and the two peptides derived from LAT (LAT 194-206 and LAT 249-261) was strongly inhibited by **3**.

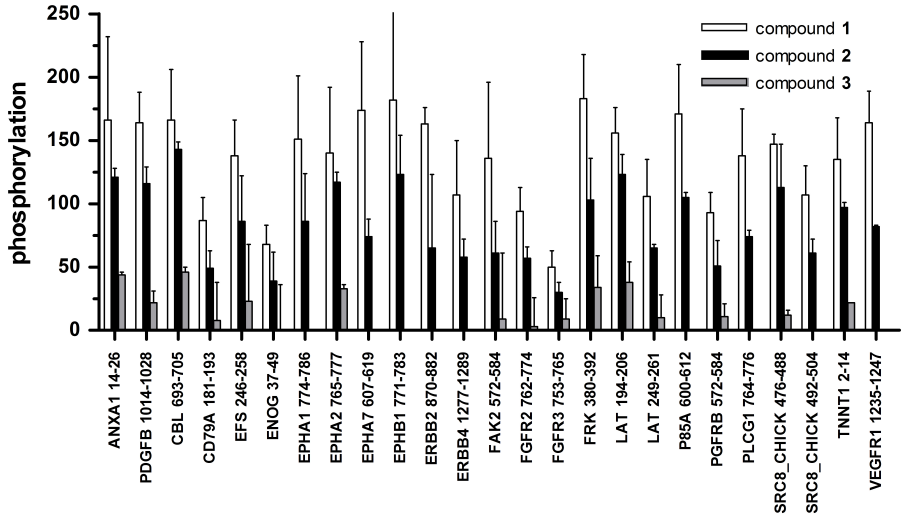

Figure 4. Effect of ITAM peptides on Syk kinase activity. Peptide phosphorylation of Syk without a ligand was defined as 100. Compounds **1-3** were added in a 100-fold excess to ensure Syk binding. The substrates in the array are indicated by abbreviation (see Table 2). Data shown are mean values from duplo experiments. The bars represent average ± SD.

It has been postulated for Zap-70 that the tSH2 domain is more than a docking device: ITAM binding changes the orientation of the SH2 domains, leading to a large conformational change in tSH2.[2,14] A schematic representation showing the proposed effects of ITAM binding on Syk kinase activity is shown in Figure 5. We have observed earlier that binding by the native ITAM derived ligand **1** of Syk tSH2 resulted in fixation of the SH2 domains close the one another.[3] This fixation reduced the dynamics

of the SH2-SH2 linker.[29] The results presented here demonstrate for the first time that forcing the SH2 domains at a larger distance inhibits the kinase activity. This suggests that fixation of the SH2 domains apart from each other forces the SH2-SH2 linker into its inactive state, which results in inhibition of kinase activity in an allosteric manner (Figure 5).

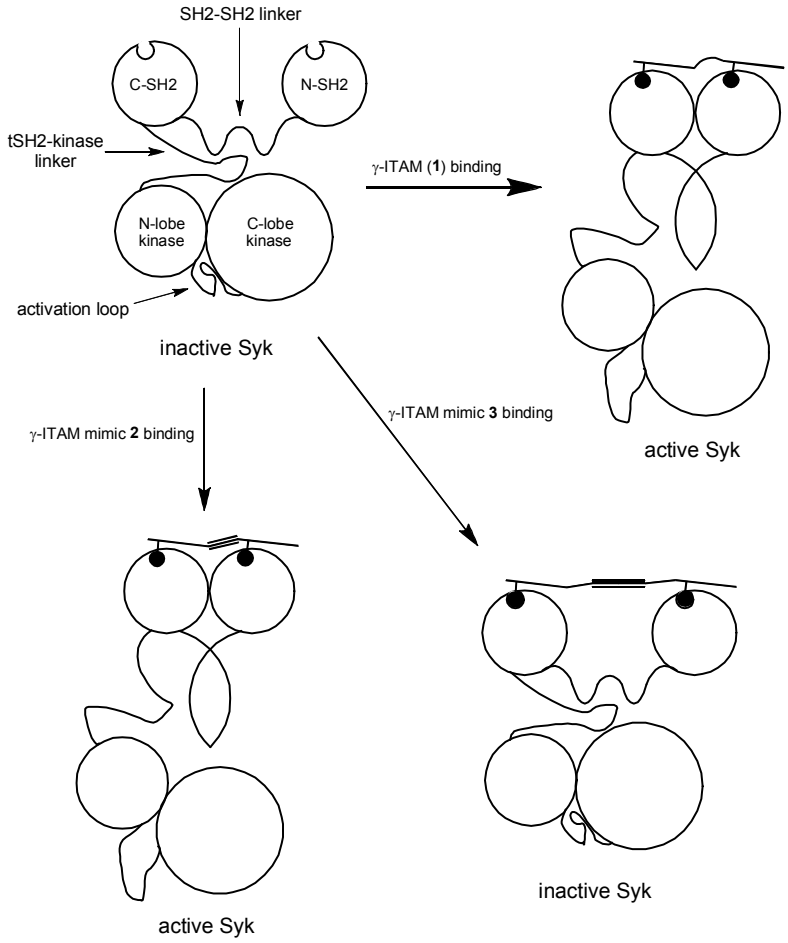

Figure 5. Schematic models of the effects of the ITAM peptides on Syk kinase activity. Native γ-ITAM **1** and rigid ITAM mimic **2** bring the SH2 domains closer to each other, which results in conformational changes in the SH2-SH2 linker, the tSH2-kinase linker and in the activation loop of the kinase domain, resulting in kinase activation. Probably these changes are accompanied by phosphorylation on tyrosine residues in the tSH2-kinase linker and in the activation loop of the kinase domain, as in Zap-70.[2,14] ITAM mimic **3** probably maintains Syk in an inactive state by keeping the SH2 domains apart.

Conclusions

Changing the inter SH2 distance can regulate Syk kinase activity in an allosteric manner. Native γ-ITAM and mimic **2**, which possessed a linker of similar length, had minor, although opposite effects on Syk kinase activity. ITAM mimic **3**, with the SH2 binding epitopes further apart from each other, inhibited Syk kinase activity significantly. These results are the first experimental evidence that Syk kinase activity can be allosterically inhibited by forcing the SH2 domains further apart. It is attractive to explore this finding in the design of new selective Syk inhibitors based on ITAM mimics having a rigid scaffold for keeping the SH2 binding epitopes apart.

Experimental section

General

All chemicals were obtained from commercial sources and used without further purification. Solvents, which were used for the solid phase peptide synthesis, were stored over 4 Å molecular sieves, except for MeOH, which was stored over 3 Å molecular sieves. The reactions were performed at room temperature unless stated otherwise.

Molecular simulations

For calculations of the distance between the SH2 binding epitopes in the ITAM mimics YASARA (http://www.yasara.org) was used. PDB files of the two rigid linkers of compounds **2** and **3** were made using ChemDraw and Chem3D. These files were loaded in YASARA and a simulation cell, in which each axis was extended 5.0 Å from the molecule, was defined. The Amber99 forcefield was used and the temperature control was step-10 annealing, starting from 298 K and every 10 simulation steps the velocity of all atoms was reduced to 90%. Within approximately 2500 fs the temperature of 0 K was reached and the atoms almost did not move anymore. To be sure, the simulation was continued until 10000 fs was reached. The linkers were modeled as their N-terminal acetamide and C-terminal amide derivatives. The distances were measured from the N-terminal nitrogen atom to the C-terminal carbon atom after completion of the simulation of 10000 fs.

HPLC

Analytical HPLC was measured on a Shimadzu HPLC system with a UV detector operating at 220 and 254 nm and in some cases also an evaporative light scattering detector (PL-ELS 1000, Polymer Laboratories) was used. For analytical HPLC an Alltech Prosphere C4 300 Å 5 µm (250 × 4.6 mm) column (compounds **2**-**3**) or an Alltech Alltima C8 5 µm (250 × 4.6 mm) column (compound **4**) was used, employing a gradient from 100% buffer A (15 mM TEA in H_2O titrated at pH 6 with 85% H_3PO_4) to 100% buffer B (buffer A/CH_3CN 1:9) in 20 min. For preparative HPLC a Gilson system with a UV detector operating at 220 and 254 nm and an Applied Biosystems workstation with a UV detector operating at 214 nm both equipped with an Alltech Prosphere C4 300 Å 10 µm (250 × 22 mm) column (compounds **2**-**3**) or an Alltech Adsorbosphere XL C8 90 Å 10 µm (250 × 22 mm) column (compound **4**) were used. In both systems a gradient of 100% buffer A (0.1% TFA in H_2O/CH_3CN 95:5) to 100% buffer B (0.1% TFA in H_2O/CH_3CN 5:95) in 40 min was applied.

N-Alloc-4-(3-(3-aminoprop-1-ynyl)benzoic acid

The synthesis of N-Alloc-4-(3-(3-aminoprop-1-ynyl)benzoic acid has been described previously.[13]

Compound 1

The synthesis of peptide **1**, which is derived from native γ-ITAM, has been described previously.[12]

Compounds 2 and 3

The peptidomimetics were manually assembled on Tentagel®-Rink-NH-Fmoc resin (both 192 mg, 0.05 mmol, loading 0.26 mmol/g) using standard Fmoc/tBu chemistry. The Fmoc protecting group was removed using 20% piperidine in NMP (3 × 4 mL, each 8 min) followed by washing steps with NMP (3 × 4 mL, each 2 min), CH_2Cl_2 (3 × 4 mL, each 2 min) and NMP (3 × 4 mL, each 2 min). The Alloc protecting group was removed using 0.25 equivalents of $Pd(PPh_3)_4$ and 10 equivalents of anilinium para-toluene sulfinate in MeOH/THF (1:1) (2 × 4 mL, each 60 min). After Alloc deprotection the resin was washed with 0.1% sodium diethyldithiocarbamate in NMP (1 × 4 mL, 2 min), NMP (3 × 4 mL, each 2 min), CH_2Cl_2 (3 × 4 mL, each 2 min) and NMP (3 × 4 mL, each 2 min). The amino acid coupling mixtures were prepared by dissolving 4

equivalents of amino acid, 4 equivalents of HOBt and HBTU and 8 equivalents of DiPEA in NMP and coupled during a coupling time of 60 minutes. The resin was washed with NMP (3 × 4 mL, each 1 min) and CH_2Cl_2 (3 × 4 mL, each 1 min) after every coupling step. The coupling steps and deprotection steps were monitored using the Kaisertest.[30] When the Fmoc deprotection was not complete, the deprotection step was repeated. The amino acid building blocks Fmoc-Leu-OH, Fmoc-Thr(tBu)-OH, Fmoc-Glu(OtBu)-OH, Fmoc-Tyr(OP(OBn)OH)-OH, N-Alloc-4-(3-(3-aminoprop-1-ynyl)benzoic acid, N-Alloc-4-(3-(3-aminoprop-1-ynyl)benzoic acid (for **3** another N-Alloc-4-(3-(3-aminoprop-1-ynyl)benzoic acid was coupled), Fmoc-Leu-OH, Fmoc-Gly-OH, Fmoc-Thr(tBu)-OH, Fmoc-Tyr(OP(OBn)OH)-OH and N-Fmoc-2-(2-(2-aminoethoxy)ethoxy)acetic acid were subsequently coupled. Fmoc-Tyr(OP(OBn)OH)-OH was coupled overnight using 2 equivalents of amino acid, 2 equivalents of the coupling reagents HOBt and HBTU and 5 equivalents of DiPEA. N-Alloc-4-(3-(3-aminoprop-1-ynyl)benzoic acid was also coupled overnight using 2 equivalents of amino acid and 2 equivalents of the coupling reagents HOBt and HBTU and 4 equivalents of DiPEA. After the first Fmoc-Tyr(OP(OBn)OH)-OH coupling an extra washing step (2 × 4 mL, each 10 min) with a mixture of 1 M TFA/1.1 M DiPEA in NMP was performed after each Fmoc deprotection step. This was done to replace the piperidinium counter ion of Tyr(OP(OBn)O^-) for protonated DiPEA. The peptides were cleaved from the resin and the side chains were deprotected with TFA/H_2O/TIS/EDT (90/5/2.5/2.5) for 3 h. The resin was removed from the solution by filtration and the peptides were precipitated with MTBE/hexane 1:1 v/v at -20 °C and lyophilized from CH_3CN/H_2O 1:1 v/v yielding 47 mg of crude **2** and 43 mg of crude **3**. The peptides were purified by preparative HPLC and analyzed by analytical HPLC and mass spectrometry. 5.0 mg of pure **2** and 1.1 mg of pure **3** was obtained after pooling and lyophilization.
MS (ESI) of **2**: $[M+H]^+$ calculated 1577.60, found 1577.65
MS (MALDI-TOF) of **3**: $[M+H]^+$ calculated 1734.654, found 1734.785; $[M+Na]^+$ calculated 1756.635, found 1756.714.

Compound 4

The peptidomimetic was manually assembled on Tentagel®-Rink-NH-Fmoc resin (0.77 g, 0.20 mmol, loading 0.26 mmol/g) according to the same procedures as for compounds **2** and **3**. The amino acid building blocks Fmoc-Leu-OH, Fmoc-Thr(tBu)-OH, Fmoc-Glu(OtBu)-OH, Fmoc-Tyr(tBu)-OH, N-Alloc-4-(3-(3-aminoprop-1-

ynyl)benzoic acid, N-Alloc-4-(3-(3-aminoprop-1-ynyl)benzoic acid, Fmoc-Leu-OH, Fmoc-Gly-OH, Fmoc-Thr(tBu)-OH, Fmoc-Tyr(tBu)-OH, N-Fmoc-2-(2-(2-aminoethoxy)ethoxy)acetic acid and Fmoc-Cys(Trt)-OH were subsequently coupled. When all the coupling steps and deprotection steps were completed the peptidomimetic was acetylated using a capping solution of Ac_2O (4.72 mL, 42.7 mmol), DiPEA (2.18 mL, 22.8 mmol) and HOBt (0.23 g, 1.7 mmol) in 100 mL of NMP for 2 × 30 min. The peptidomimetic was cleaved from the resin and the side chains were deprotected with a solution of TFA/H_2O/TIS/EDT (90/5/2.5/2.5) for 3 h. After lyophilization from CH_3CN/H_2O 1:1 v/v 135 mg of crude peptidomimetic was obtained. 50 mg of the peptidomimetic was purified by preparative HPLC and analyzed by analytical HPLC and mass spectrometry. 4.8 mg of pure compound was obtained after pooling and lyophilization.

HRMS (ESI) of **4**: $[M+H]^+$ calculated 1562.6877, found 1563.0153; $[M+Na]^+$ calculated 1584.6697, found 1584.8419; $[M+2H]^{2+}$ calculated 781.8478, found 782.0435; $[M+H+Na]^{2+}$ calculated 792.8382, found 792.5547; $[M+2Na]^{2+}$ calculated 803.8292, found 804.0493.

Syk protein expression

Fusion clones of the gluthathione S-transferase (GST) Syk tSH2 domain were kindly provided by Prof. Gabriel Waksman (Washington University, St. Louis, MI).[23] The Escherichia coli strain BL21 contained the pGEX-KT vector with amino acids 10–273 of human Syk, enabling thrombin cleavage of the GST moiety. Isolation procedures have been described previously.[3]

SPR binding studies

SPR measurements were performed on a double channel IBISII SPR instrument (Eco Chemie, Utrecht, The Netherlands) equipped with a CM 5 sensor chip (BIAcore AB, Uppsala, Sweden). ITAM mimics **2** or **3** were immobilized through their free N-terminal amine on the ethyleneglycol spacer as was previously described.[12] The affinity of Syk tSH2 for the immobilized ITAM mimic was determined by addition of Syk tSH2 in a concentration range of 0 to 200 nM in HBS buffer. The K_D value was calculated by fitting the equilibrium signals to a Langmuir binding isotherm.[24]

Microarray experiments

Microarray experiments were performed on a PamStation®12 instrument (PamGene B.V., 's Hertogenbosch, The Netherlands). PamChips® with four protein tyrosine kinase (PTK) arrays on each chip were used. Each array contained 144 spots and each spot contained one peptide sequence consisting of 13 amino acid residues. One peptide, present on position 1-12 (row 1, column 12), possessed a phosphorylated tyrosine residue, and is a positive control. The other 143 peptides possessed at least one tyrosine residue and all peptides were derived from proteins known to be substrates for PTKs. Experiments on temperature-controlled (30 ºC) peptide arrays were preformed by pumping the sample up and down through the 3-dimensional porous chip.

Before running the experiment the arrays were blocked using a solution for each array of 0.2 mg/mL BSA (New England Biolabs, Ipswich, USA) in 25 µL of Abl buffer (50 mM Tris/HCl pH = 7.5, 10 mM $MgCl_2$, 1 mM EGTA, 2 mM DTT, 0.01% Brij35) (New England Biolabs, Ipswich, USA) for 15 minutes. Then the arrays were washed (2 × 1 min) with 25 µL of Abl buffer. The arrays were subsequently treated for 30 minutes with a solution of 25 µL of Abl buffer containing 28 nM full-length Syk (Millipore, Billerica, USA), 0.02 mg/mL BSA and for some arrays also 10 µM ATP and/or 2.8 µM of ITAM mimic, after which the arrays were washed (2 × 1 min) with 25 µL of Abl buffer. The chips were removed from the apparatus and they were washed twice with 500 mL of PBS buffer (pH = 9) for 30 minutes each. After this, the chips were placed back into the PamStation, washed (2 × 1 min) with 25 µL of Abl buffer and blocked again with BSA, using the same procedure as described above. Finally, the arrays were washed (3 × 1 min) with 25 µL of Abl buffer and 12.5 µg/mL anti-phosphotyrosine antibody PY20-FITC (Exalpha Biologicals, Shirley, USA) in 25 µL of Abl buffer was added. After 9 minutes of pumping, the solution was aspirated, 25 µL of Abl buffer was added and images of the arrays were taken using a CCD camera. Images were analyzed by BioNavigator software (PamGene B.V., 's Hertogenbosch, The Netherlands). The fluorescent intensities were expressed as arbitrary units.

Acknowledgements

Erwin Schoof M.Sc. is kindly acknowledged for the SPR experiments with compounds **2** and **3**.

References

1. Arias-Palomo, E., Recuero-Checa, M.A., Bustelo, X.R., Llorca, O., 3D structure of Syk kinase determined by single-particle electron microscopy, *Biochim. Biophys. Acta - Proteins and Proteomics*, **2007**, 1774, 1493-1499.
2. Au-Yeung, B.B., Deindl, S., Hsu, L.Y., Palacios, E.H., Levin, S.E., Kuriyan, J., Weiss, A., The structure, regulation, and function of ZAP-70, *Immunol. Rev.*, **2009**, 228, 41-57.
3. De Mol, N.J., Catalina, M.I., Dekker, F.J., Fischer, M.J.E., Heck, A.J., Liskamp, R.M.J., Protein flexibility and ligand rigidity: a thermodynamic and kinetic study of ITAM-based ligand binding to Syk tandem SH2, *ChemBioChem*, **2005**, 6, 2261-2270.
4. Kumaran, S., Grucza, R.A., Waksman, G., The tandem Src homology 2 domain of the Syk kinase: a molecular device that adapts to interphosphotyrosine distances, *Proc. Natl. Acad. Sci. U.S.A.*, **2003**, 100, 14828–14833.
5. Sada, K., Yamamura, H., Protein-tyrosine kinases and adaptor proteins in FcεRI-mediated signaling in mast cells, *Curr. Mol. Med.*, **2003**, 3, 85-94.
6. Simon, M., Vanes, L., Geahlen, R.L., Tybulewicz, V.L.J., Distinct roles for the linker region tyrosines of Syk in FcεRI signaling in primary mast cells, *J. Biol. Chem.*, **2005**, 280, 4510–4517.
7. Siraganian, R.P., Zhang, J., Suzuki, K., Sada, K., Protein tyrosine kinase Syk in mast cell signaling, *Mol. Immun.*, **2001**, 38, 1229–1233.
8. Gilfillan, A.M., Tkaczyk, C., Integrated signalling pathways for mast-cell activation, *Nat. Rev. Immunol.*, **2006**, 6, 218-230.
9. Kraft, S., Kinet, J.-P., New developments in FcεRI regulation, function and inhibition, *Nat. Rev. Immunol.*, **2007**, 7, 365-378.
10. Navara, C.S., The spleen tyrosine kinase (Syk) in human disease, implications for design of tyrosine kinase inhibitor based therapy, *Curr. Pharm. Design*, **2004**, 10, 1739-1744.
11. Gobessi, S., Laurenti, L., Longo, P.G., Carsetti, L., Berno, V., Sica, S., Leone, G., Efremov, D.G., Inhibition of constitutive and BCR-induced Syk activation downregulates Mcl-1 and induces apoptosis in chronic lymphocytic leukemia B cells, *Leukemia*, **2009**, 23, 686-697.
12. Dekker, F.J., de Mol, N.J., van Ameijde, J., Fischer, M.J.E., Ruijtenbeek, R., Redegeld, F.A.M., Liskamp, R.M.J., Replacement of the intervening amino acid sequence of a Syk-binding diphosphopeptide by a nonpeptide spacer with preservation of high affinity, *ChemBioChem*, **2002**, 3, 238-242.
13. Dekker, F.J., de Mol, N.J., Fischer, M.J.E., Liskamp, R.M.J., Amino propynyl benzoic acid building block in rigid spacers of divalent ligands binding to the Syk SH2 domains with equally high affinity as the natural ligand, *Bioorg. Med. Chem. Lett.*, **2003**, 13, 1241-1244.
14. Deindl, S., Kadlecek, T.A., Brdicka, T., Cao, X., Weiss, A., Kuriyan, J., Structural basis for the inhibition of tyrosine kinase activity of ZAP-70, *Cell*, **2007**, 129, 735-746.
15. Folmer, R.H.A., Geschwindner, S., Xue, Y., Crystal structure and NMR studies of the apo SH2 domains of ZAP-70: two bikes rather than a tandem, *Biochemistry*, **2002**, 41, 14176-14184.
16. Kuil, J., van Wandelen, L.T.M., de Mol, N.J., Liskamp, R.M.J., A photoswitchable ITAM peptidomimetic: Synthesis and real time surface plasmon resonance (SPR) analysis of the effects of cis-trans isomerization on binding, *Bioorg. Med. Chem.*, **2008**, 16, 1393-1399.
17. Hilhorst, R., Houkes, L., van den Berg, A., Ruijtenbeek, R., Peptide microarrays for detailed, high-throughput substrate identification, kinetic characterization, and inhibition studies on protein kinase A, *Anal. Biochem.*, **2009**, 387, 150-161.
18. van Beuningen, R., Pijnenburg, D.D., Melchers, D.D., Hilhorst, R.R., Boender, P.J., van de Berg, A.A., Ruijtenbeek, R.R., Use of flow-through peptide microarrays in cell-lysate, kinase and inhibitor screens., *Clin. Cancer Res.*, **2005**, 11, 9026s-9026s.

19. van Beuningen, R., van Damme, H., Boender, P., Bastiaensen, N., Chan, A., Kievits, T., Fast and specific hybridization using flow-through microarrays on porous metal oxide, *Clin. Chem*, **2001**, 47, 1931-1933.
20. Lemeer, S., Ruijtenbeek, R., Pinkse, M.W.H., Jopling, C., Heck, A.J.R., den Hertog, J., Slijper, M., Endogenous phosphotyrosine signaling in zebrafish embryos, *Mol. Cell. Proteom.*, **2007**, 6, 2088-2099.
21. Schutkowski, M., Reineke, U., Reimer, U., Peptide arrays for kinase profiling, *ChemBioChem*, **2005**, 6, 513-521.
22. Cretich, M., Damin, F., Pirri, G., Chiari, M., Protein and peptide arrays: Recent trends and new directions, *Biomol. Eng.*, **2006**, 23, 77-88.
23. Futterer, K., Wong, J., Grucza, R.A., Chan, A.C., Waksman, G., Structural basis for Syk tyrosine kinase ubiquity in signal transduction pathways revealed by the crystal structure of its regulatory SH2 domains bound to a dually phosphorylated ITAM peptide, *J. Mol. Biol.*, **1998**, 281, 523-537.
24. De Mol, N.J., Gillies, M.B., Fischer, M.J.E., Experimental and calculated shift in pK_a upon binding of phosphotyrosine peptide to the SH2 domain of $p56^{lck}$, *Bioorg. Med. Chem.*, **2002**, 10, 1477-1482.
25. Carsetti, L., Laurenti, L., Gobessi, S., Longo, P.G., Leone, G., Efremov, D.G., Phosphorylation of the activation loop tyrosines is required for sustained Syk signaling and growth factor-independent B-cell proliferation, *Cell. Signal.*, **2009**, 21, 1187-1194.
26. Humphrey, M.B., Lanier, L.L., Nakamura, M.C., Role of ITAM-containing adapter proteins and their receptors in the immune system and bone, *Immunol. Rev.*, **2005**, 208, 50-65.
27. Zhang, W.G., Sloan-Lancaster, J., Kitchen, J., Trible, R.P., Samelson, L.E., LAT: The ZAP-70 tyrosine kinase substrate that links T cell receptor to cellular activation, *Cell*, **1998**, 92, 83-92.
28. Paz, P.E., Wang, S.J., Clarke, H., Lu, X.B., Stokoe, D., Abo, A., Mapping the Zap-70 phosphorylation sites on LAT (linker for activation of T cells) required for recruitment and activation of signalling proteins in T cells, *Biochem. J.*, **2001**, 356, 461-471.
29. Catalina, I., Fischer, M.J.E., Dekker, F.J., Liskamp, R.M.J., Heck, A.J.R., Binding of a diphosphorylated-ITAM peptide to spleen tyrosine kinase (Syk) induces distal conformational changes: a hydrogen exchange mass spectrometry study, *J. Am. Soc. Mass. Spectrom.*, **2005**, 16, 1039–1051.
30. Kaiser, E., Colescott, R.L., Bossinger, C.D., Cook, P.I., Color test for detection of free terminal amino groups in the solid-phase synthesis of peptides, *Anal. Biochem.*, **1970**, 34, 595-598.

Chapter 8

Summary and perspectives

Summary

The Spleen tyrosine kinase (Syk) is a 72 kDa cytosolic protein and consists of two tandemly arranged SH2 domains (tSH2) in addition to a kinase domain. Syk is present in most hematopoietic cells such as basophiles, mast cells and lymphocytes. It is also widely expressed in non-hematopoietic cells like fibroblasts, epithelial cells, breast tissue cells, hepatocytes, neuronal cells and vascular endothelial cells.

Syk plays a role in several signaling pathways, including B-cell receptor signaling, cell-cell adhesion and immunoreceptor signaling. Here, the focus was on the high affinity IgE receptor (FcεRI) signaling pathway in mast cells and basophils, in which Syk is essential. FcεRI consists of an α-, β- and two γ-chains. The β- and γ-chains contain a specific intracellular sequence called the Immunoreceptor Tyrosine based Activation Motif (ITAM). The ITAM sequence consists of Tyr-Xxx-Xxx-(Leu/Ile)-$(Xxx)_{n=6-8}$-Tyr-Xxx-Xxx-(Leu/Ile), in which Xxx can be any amino acid. The underlined residues comprise the binding epitopes for Syk tSH2, when tyrosine is phosphorylated. Upon IgE stimulation of the receptor, the ITAM motif becomes diphosphorylated (γ-dpITAM). After this, Syk is recruited to the membrane by binding to γ-dpITAM. This results in a conformational change of Syk, kinase activation and, finally, cell degranulation and release of mediators. Overstimulation of this pathway leads to allergic responses and therefore Syk is an interesting target for potential anti-allergic therapy. Besides its role in inflammatory and autoimmune disorders, Syk is also linked to leukemia and breast cancer, i.e. Syk is absent in malignant breast cancer cells.

ITAM binding of Syk is proposed to cause fixation of the SH2 domains closer to each other. This fixation is accompanied with a conformational change in the SH2-SH2 linker. It is assumed that this change in the conformation of the SH2-SH2 linker allosterically regulates Syk kinase activity. This activation model was the main hypothesis on which the research described in this thesis was based.

The intervening residues $(Xxx)_{n=6-8}$ in ITAM (in γ-ITAM n = 7) are not essential for binding to Syk tSH2 and can be replaced by different linkers. Dekker et al. prepared ITAM mimics with a tetraethyleneglycol –, hexaethyleneglycol –, rigid – and semi-rigid linker. The ITAM mimic with the rigid linker, consisting of two amino propynyl benzoic acid building blocks, had similar affinity for Syk tSH2 as native ITAM. This rigid ITAM mimic was the starting point of the research described in this thesis.

Photoswitchable ITAM mimics

In **chapter 2** the synthesis of a photoswitchable peptidomimetic ligand for Syk tSH2 is described. In this ligand an azobenzene moiety and two glycine residues replaced the seven intervening residues in ITAM. An ITAM mimic with such a photoswitchable linker may regulate the distance between the two phosphotyrosine containing ITAM sequences, which bind to tSH2. Different affinities of the cis – and trans isomer of the ligand were found by surface plasmon resonance (SPR). The trans isomer had 2.2-fold more affinity than the photostationary state with maximal cis. By *in situ* irradiation during SPR measurements the effect of the cis – trans isomerization on binding could be monitored in real time.

Elaborating further on this result, in **chapter 3** the preparation of three other azobenzene containing photoswitchable ITAM peptidomimetics is described. The aim of the synthesis of this series of compounds was to enhance the difference in binding affinity between the cis – and trans isomer. One ITAM mimic possessed a smaller linker and the other two had larger linkers, resulting in a series with large differences in linker length. The ITAM peptidomimetic with the smallest linker displayed the largest difference in affinity between the two isomers (at least 100-fold) and the affinity of the cis isomer was comparable to monovalent binding. The ITAM mimics with larger photoswitchable linkers displayed modest differences. These results indicate that Syk tSH2 is able to adapt the inter SH2 domain distance to ligands larger than native ITAM, but not to smaller ones.

ITAM-derived phosphopeptide-containing dendrimers

The interaction between ITAM and Syk tSH2 is divalent, which is the simplest form of a multivalent interaction. Dendrimers are often used as multivalent ligands and in **chapter 4** their use as high-affinity Syk tSH2 ligands was explored. In the divalent ITAM – tSH2 interaction each SH2 domain binds to a phosphotyrosine-containing tetrapeptide motif in ITAM. One of those tetrapeptide sequences was synthesized and conjugated to dendrimers via ‘click’ chemistry to create a series of functional phosphopeptide-containing dendrimers ranging from a monovalent to an octavalent dendrimer. The affinity of the functionalized dendrimers for Syk tSH2 has been assayed in SPR competition experiments. Both the tetra- and octavalent dendrimer had an affinity in the high nanomolar range, which is approximately a 100-fold enhancement compared with the monovalent tetrapeptide, indicating a multivalency effect.

Affinity pull-down experiments with ITAMs

In **chapter 5** the evaluation of the binding partners of γ-ITAM and rigid ITAM mimics in a cell lysate is described. Four rigid γ-ITAM mimics containing no, one or two phosphorylated tyrosines were synthesized. For the preparation of those peptidomimetics, synthesis routes for the rigid amino propynyl benzoic acid building block and for an ethyleneglycol spacer were adapted. After the synthesis, the rigid γ-ITAM mimics and the diphosphorylated native γ-ITAM were immobilized on agarose beads. The beads were incubated with cell lysate of RBL-2H3 cells and the bound proteins were eluted with native γ-ITAM. Beads immobilized with diphosphorylated native γ-ITAM or the diphosphorylated rigid ITAM mimic could efficiently fish out Syk tSH2 from a cell lysate spiked with 0.1% Syk tSH2. However, incubation of the different beads with lysate gave considerable aspecific binding. Further optimization of the protocol is required to reduce the aspecific binding.

Cell penetrating ITAM constructs

In **chapter 6** the investigation to the intracellular effects of the rigid ITAM mimic is described. This ITAM mimic, which is a negatively charged peptidomimetic, is most likely not capable of cell penetration. Therefore, cell permeable moieties were coupled to the ITAM mimic to allow the study of its intracellular effects. Constructs were synthesized in which the ITAM mimic was conjugated to different cell penetrating peptides, i.e. Tat, TP10, octa-Arg and K(Myr)KKK, or a lipophilic C_{12}-chain. In most constructs the cargo and carrier were linked to each other through a disulfide bridge, which is convenient for combining different cargos with different carriers and has the advantage that the cargo and the carrier may be separated by reduction of the disulfide once it is intracellularly. The ability of these ITAM constructs to penetrate into RBL-2H3 cells was assessed using flow cytometry. TP10 and octa-Arg were found to be the most efficient carriers for this cell type. Fluorescence microscopy showed that the octa-Arg-SS-Flu-ITAM construct was present in various parts of the cells, although it was not homogeneously distributed. In addition, cell penetrating constructs without fluorescent labels were synthesized to examine degranulation in RBL-2H3 cells. Octa-Arg-SS-ITAM stimulated the mediator release up to 140%, indicating that ITAM mimics may have the ability to activate non-receptor bound Syk.

Microarray experiments to assay effects of ITAMs on Syk kinase actvity

In **chapter 7** the effects of ITAM mimics on constitutively active Syk were studied using a flow-through microarray technique (PamStation®). The microarrays existed of 144 peptides, known to be substrates for protein tyrosine kinases. It was found that Syk activity is slightly increased by the native ITAM peptide. A rigid ITAM mimic with approximately the same distance between the two SH2 binding epitopes had generally a slight inhibiting effect on kinase activity. However, a rigid ITAM mimic with a larger distance between the binding epitopes was capable at inhibiting phosphorylation of almost all substrates present on the arrays. This is the first demonstration that allosteric changes in tSH2 regulate Syk kinase activity. This may initiate the development of selective Syk inhibitors, based on pushing both SH2 domains in tSH2 further apart from each other by ITAM mimics with rigid linkers of appropriate length.

Perspectives

The research described in this thesis mainly involved the ITAM – Syk tSH2 interaction and the resulting implications for Syk kinase activation. Different tSH2 ligands were prepared en tested for affinity and activity.

SPR binding studies were essential in the investigations. This is exemplified in chapters 2-3, where different affinities for the cis – and trans isomers of the photoswitchable ITAM mimics were found with SPR. We concluded that Syk tSH2 could adapt to larger ligands than native ITAM, but not to considerable smaller ones. Although this was an important observation, we had no information concerning the relation between the binding mode and kinase activity. To test this, the photoswitchable ITAM mimics might be subjected to cellular – and microarray experiments.

Another improvement could include replacing azobenzene with another photoswitch, which can switch from 100% cis to 100% trans and visa versa. If this is synthetically feasible, then it would very interesting to prepare such an ITAM mimic, to conjugate this to a CCP and to test this construct in cells. It could yield a compound which can intracellularly switch Syk on and off.

Studying kinase activity was performed in two different settings: in living cells and with microarrays. With cell assays we found that the ITAM mimic containing two rigid units stimulated degranulation. This could be rationalized by the fact that the ITAM

mimic had approximately the same linker length as native ITAM. Maybe even more interesting were the results obtained from the microarray experiments: the ITAM mimic with three rigid units could efficiently inhibit kinase activity.

The three rigid units-containing ITAM mimic is an appealing starting point for further research. Microarray experiments could be expanded to obtain IC_{50} values. Furthermore, this promising Syk inhibitor should be tested in cells, as described in chapter 6. Octa-Arg seems the most appropriate CPP, because of the results obtained with the other ITAM mimic and because this CPP is relative hydrophilic. The hydrophobicity of the CPP-ITAM mimic construct could still be a problem: for cellular tests the CPP-ITAM mimic construct should dissolve in buffer up to 10 μM concentrations. However, this potential problem will most likely be solvable.

In conclusion, further investigations could include the combination of the research described in the different chapters of this thesis. During the development of cell permeable Syk inhibitors, the possibility of replacing the phosphate groups with phosphatase-resistant mimics might be considered. Moreover, this concept could be used to develop selective Zap-70 inhibitors. This would also further validate our Syk activation hypothesis.

Appendices

Nederlandse samenvatting

Het Spleen tyrosine kinase (Syk) is een 72 kDa cytosolisch eiwit en bestaat uit twee naast elkaar liggende SH2 domeinen en een kinase domein. Syk is aanwezig in de meeste bloedcellen, zoals basofielen, mestcellen en lymfocieten. Bovendien zit Syk in niet-bloedcellen zoals bindweefsel-, epitheel-, borstklier-, lever-, zenuw- en vaatwandcellen.

Syk speelt een rol in meerdere signaalpaden, waaronder het B-cel receptor pad, cel-cel adhesie en immunoreceptor paden. In dit onderzoek lag de focus op het IgE receptor (FcεRI) signaalpad in mestcellen en basofielen, waarin Syk essentieel is. FcεRI bestaat uit een α-, een β- en twee γ-ketens. De β- en γ-ketens hebben een specifiek intracellulaire sequentie die ITAM genoemd wordt. De ITAM sequentie bestaat uit Tyr-Xxx-Xxx-(Leu/Ile)-$(Xxx)_{n=6-8}$-Tyr-Xxx-Xxx-(Leu/Ile), waarin Xxx elk willekeurig aminozuur residue kan zijn. De onderstreepte residuen zijn de bindings epitopen voor Syk tSH2 als de tyrosines gefosforyleerd zijn. Door IgE stimulatie van de receptor wordt ITAM gedifosforyleerd (γ-dpITAM). Daarna wordt Syk naar het membraan gerecruiteerd door middel van binding aan γ-dpITAM. Dit resulteert in een conformationele verandering van Syk, kinase activatie en cel degranulatie, d.w.z. het vrijkomen van mediatoren. Overstimulatie van dit pad leidt tot allergische reacties en daarom is Syk een potentieel target voor anti-allergie therapie. Naast zijn rol in inflammatoire en auto-immuunziekten wordt Syk ook gelinkt aan leukemie en borstkanker, d.w.z. Syk is afwezig in borstkankercellen.

Er wordt verondersteld dat ITAM binding de SH2 domeinen van Syk dichter bij elkaar brengt. Dit gaat gepaard met een verandering in de conformatie van de SH2-SH2 linker. Aangenomen wordt dat deze conformationele verandering de Syk kinase activiteit reguleert. Dit activerings model was de belangrijkste hypothese waarop het onderzoek beschreven in dit proefschrift is gebaseerd.

De tussenliggende residuen $(Xxx)_{n=6-8}$ in ITAM (in γ-ITAM n = 7) zijn niet essentieel voor binding en kunnen worden vervangen door verschillende linkers. Dekker et al. hebben ITAM mimetica gemaakt met een tetraethyleenglycol –, hexaethyleenglycol –, rigide – en semi-rigide linker. Het ITAM mimeticum met de rigide linker, dat uit twee amino propynyl benzoëzuur bouwstenen bestond, had dezelfde affiniteit voor Syk tSH2 als ITAM zelf. Dit rigide ITAM mimeticum was het beginpunt van het onderzoek dat in dit proefschrift beschreven is.

Lichtschakelbare ITAM mimetica

In **hoofdstuk 2** is de synthese van een lichtschakelbaar peptidomimetisch ligand voor Syk tSH2 beschreven. In dit ligand vervingen een azobenzeen eenheid en twee glycine residuen de zeven tussenliggende residuen in ITAM. Een ITAM mimeticum met zo'n lichtschakelbare linker kan de afstand tussen de twee fosfotyrosine bevattende ITAM sequenties, die aan tSH2 binden, reguleren. Verschillende affiniteiten voor de cis – en de trans isomeer van het ligand werden gevonden met bindings experimenten m.b.v. SPR. De trans isomeer had 2,2 keer meer affiniteit dan de toestand waarin de meeste cis isomeer aanwezig was. Bovendien kon door het bestralen met zichtbaar light tijdens een SPR meting het effect van cis-trans isomerisatie op binding direct gevolgd worden.

Voortbordurend op dit resultaat is in **hoofdstuk 3** de synthese van drie andere azobenzeen-bevattende lichtschakelbare ITAM peptidomimetica beschreven. Het doel van de synthese van deze serie verbindingen was het vergroten van het verschil in bindings affiniteit tussen de cis – en trans isomeer. Eén ITAM mimeticum had een kleinere linker en de andere twee hadden grotere linkers, wat resulteerde in een serie met grote verschillen in linker lengte. Het ITAM peptidomimeticum met de kleinste linker had het grootste verschil in affiniteit tussen de twee isomeren (minstens 100 maal) en de affiniteit van de cis isomeer was vergelijkbaar met monovalente binding. De ITAM mimetica met grotere lichtschakelbare linkers hadden kleine verschillen tuseen de cis – trans isomeren. Deze resultaten laten zien dat Syk tSH2 de inter SH2 afstand kan aanpassen aan liganden die groter zijn dan het natieve ITAM, maar niet aan kleinere.

Fosfopeptide-bevattende dendrimeren

De interactie tussen ITAM en Syk tSH2 is divalent en dit is de eenvoudigste vorm van een multivalente interactie. Dendrimeren worden vaak gebruikt als multivalente liganden en in **hoofdstuk 4** is hun bruikbaarheid als hoge-affiniteits Syk tSH2 liganden onderzocht. In de divalente ITAM – tSH2 interactie bindt elk SH2 domein aan een fosfotyrosine-bevattende tetrapeptide-motief in ITAM. Eén van die tetrapeptides was gesynthetiseerd en geconjugeerd aan dendrimeren via 'click' chemie. Dit resulteerde in een serie van functionele fosfopeptide-bevattende dendrimeren variërend van een monovalent tot een octavalent dendrimeer. De affiniteit van de gefunctionaliseerde dendrimeren voor Syk tSH2 werd gemeten met SPR competitie experimenten. Zowel

het tetra- als het octavalente dendrimeer hadden een affiniteit in het hoge nanomolaire gebied, wat ongeveer een 100-voudige verbetering is ten opzichte van het monovalente tetrapeptide, duidend op een multivalentie effect.

Affiniteits 'uitvis' experimenten met ITAMs

In **hoofdstuk 5** wordt de evaluatie van de bindings partners van γ-ITAM en rigide ITAM mimetica in een cel lysaat beschreven. Vier rigide γ-ITAM mimetica met nul, één of twee gefosforyleerde tyrosines zijn gesynthetiseerd. Voor de synthese van deze peptidomimetica zijn synthese routes voor de rigide amino propynyl benzoëzuur bouwsteen en voor de ethyleenglycol spacer aangepast. Na de synthese werden de rigide γ-ITAM mimetica en het gedifosforyleerde originele γ-ITAM peptide op agarose bolletjes geïmmobiliseerd. Deze bolletjes werden daarna geïncubeerd met cel lysaat van RBL-2H3 cellen en de gebonden eiwitten werden geëlueerd met natief γ-ITAM. De bolletjes die met natief γ-ITAM of met het gedifosforyleerde ridige ITAM mimeticum waren geïmmobiliseerd konden Syk tSH2 efficient uit een cel lysaat, waarbij 0.1% Syk tSH2 was toegevoegd, vissen. Echter, incubatie van de verschillende bolletjes met lysaat gaf aanzienlijke aspecifieke binding. Verdere optimalisatie van het protocol is nodig om de aspecifieke binding te reduceren.

Cel penetrerende ITAM constructen

In **hoofdstuk 6** is het onderzoek naar de intracellulaire effecten van het rigide ITAM mimeticum beschreven. Het ITAM mimeticum, dat een negatief geladen peptidomimeticum is, is waarschijnlijk niet tot cel penetratie in staat. Daarom werden cel permeabele fragmenten gekoppeld aan het ITAM mimeticum om de studie van de intracellulaire effecten mogelijk te maken. Constructen waarin het ITAM mimeticum was gekoppeld aan verschillende cel penetrerende peptides, d.w.z. Tat, TP10, octa-Arg en K(Myr)KKK, of een lipofiele C_{12}-keten werden gesynthetiseerd. In de meeste constructen werden de ITAM-vracht en de 'carrier' aan elkaar gekoppeld d.m.v. een disulfide binding. Dit vergemakkelijkde het combineren van verschillende vrachten en carriers en had als voordeel dat de vracht van de carrier gescheiden kon worden d.m.v. reductie van de disulfide binding als het construct in de cel is. Het vermogen van deze ITAM constructen om in RBL-2H3 cellen, een model voor mestcellen, te penetreren werd onderzocht d.m.v. flow cytometry. TP10 en octa-Arg waren het meest effectief voor dit cel type. Fluorescentie microscopie liet zien dat het octa-Arg-SS-Flu-ITAM

construct aanwezig was in verschillende cel compartimenten, hoewel het niet homogeen verdeeld was. Bovendien zijn cel penetrerende constructen zonder fluorescente labels gesynthetiseerd om degranulatie in RBL-2H3 cellen te bestuderen. Octa-Arg-SS-ITAM stimuleerde het vrijkomen van mediatoren tot 140%, wat aangeeft dat ITAM mimetica niet-receptor gebonden Syk kunnen activeren.

Microarray experimenten om de effecten van ITAMs op Syk kinase activiteit te onderzoeken

In **hoofdstuk 7** zijn de effecten van ITAM mimetica op continue actief Syk bestudeerd met een 'flow-through microarray' techniek (PamStation®). Op de microarrays zaten 144 peptides waarvan bekend is dat het substraten zijn van tyrosine kinases. Het bleek dat de Syk activiteit een klein beetje verhoogd werd door het natieve ITAM peptide. Een rigide ITAM mimeticum met ongeveer dezelfde afstand tussen de twee SH2 bindings epitopen had in het algemeen een klein inhiberend effect op de kinase activiteit. Echter, een rigide ITAM mimeticum met een grotere afstand tussen de bindings epitopen was in staat om de fosforylatie van bijna alle substraten die aanwezig waren op de arrays te inhiberen. Dit is de eerste keer dat is aangetoond dat allosterische veranderingen in tSH2 de Syk kinase activiteit reguleert. Dit zou de ontwikkeling kunnen initiëren van selectieve Syk inhibitoren, gebaseerd op het uit elkaar duwen van beide SH2 domeinen in tSH2 door ITAM mimetica met rigide linkers van de juiste lengte.

List of abbreviations

Ac	acetyl
Ac_2O	acetic anhydride
Azhx	6-azidohexanoic acid
AMPB	(4-aminomethyl) phenylazobenzoic acid
Alloc	allyloxycarbonyl
Ar	aromatic
APT	attached proton test
BCR	B cell receptor for antigen
Boc	*tert*-Butyloxycarbonyl
BOP	benzotriazole-1-yl-oxy-tris-(dimethylamino)-phosphonium hexafluorophosphate
Bn	benzyl
br	broad
CPP	cell penetrating peptide
C-SH2	C-terminal SH2 domain of Syk
δ	chemical shift
d	doublet
DiPEA	N,N-diisopropylethylamine
DMF	dimethylformamide
DMSO	dimethylsulfoxide
DBU	1,8-diazabicyclo[5.4.0.]-undec-7-ene
DCC	N,N′-Dicyclohexylcarbodiimide
dpITAM	diphosphorylated ITAM
EDT	1,2-ethanedithiol
EDTA	ethylenediaminetetraacetic acid
EM	electron microscopy
equiv	equivalents
ESI	electrospray ionization
Et	ethyl
Et_2O	diethylether
EtOAc	ethyl acetate
EtOH	ethanol
FACS	Fluorescence-activated cell-sorting
FcεRI	high affinity IgE receptor (type I)
Fmoc	9-fluorenylmethyl-oxycarbonyl
GST	gluthatione-S-transferase
HATU	O-(7-azabenzotriazol-1-yl)-1,1,3,3-tetramethyluronium hexafluorophosphate
HBS	HEPES buffered saline
HBTU	2-(1H-benzotriazole-1-yl)-1,1,3,3-tetramethyluronium hexafluorophosphate
HEPES	4-(2-hydroxyethyl)-piperazine-1-ethane-sulfonic acid
HOAt	1-Hydroxy-7-azabenzotriazole
HOBt	1-hydroxybenzotriazole
HPLC	high performance liquid chromatography
HRMS	high resolution mass spectrometry
IC_{50}	50% inhibiting concentration
IgE	immunoglubulin E
ITAM	immunoreceptor tyrosine based activation motif
K_D	dissociation constant
LAT	linker for activation of T cells
LC-MS	liquid chromatography – mass spectrometry
m	multiplet

MALDI-TOF	matrix assisted laser desorption ionisation – time of flight
MeOH	methanol
MHz	megahertz
MS	mass spectrometry
MTBE	*tert*-butyl methyl ether
MW	molecular weight
Myr	myristate
m/z	mass to charge ratio
NHS	N-hydroxysuccinimide
NMP	N-methyl-2-pyrrolidone
NMR	nuclear magnetic resonance
npITAM	nonphosphorylated ITAM
N-SH2	N-terminal SH2 domain of Syk
NTAL	non T cell activation linker
PAGE	polyacrylamide-gel electrophoresis
Pbf	2,2,4,6,7-pentamethyl-dihydrobenzofuran-5-sulfonyl
PBS	phosphate buffered saline
PDB	protein data bank
pNpys	5-nitro-2-pyridinesulfenyl
ppm	parts per million
pTyr	L-phosphotyrosine
Rf	retardation factor
PTB	phosphotyrosine binding
PTK	protein tyrosine kinase
PTPase	protein tyrosine phosphatase
s	singlet
SD	standard deviation
SDS	sodium dodecyl sulphate
SH2	Src homology-2
SH3	Src homology-3
RBL-2H3	rat basophilic leukemia cells
SPR	surface plasmon resonance
Src	Rous sarcoma
Su	succinimidyl
Syk	spleen tyrosine kinase
t	triplet
Tat	human immunodeficiency virus transactivation protein
tBu	tert-butyl
TEA	triethylamine
TFA	trifluoroacetic acid
THF	tetrahydrofuran
TIS	triisopropylsilane
TLC	thin layer chromatography
TMS	trimethylsilane
TP10	transportan 10
Tris	2-amino-2-(hydroxymethyl) propane-1,3-diol
Trt	trityl
tSH2	tandem SH2 domain
UV	ultra violet
VIS	visible
XTT	sodium 3'-[1-(phenylaminocarbonyl)-3,4-tetrazolium]-bis(4-methoxy-6-nitro)benzene sulfonic acid hydrate
Zap-70	70 kDa zeta-associated protein

Abbrevations of amino acids

Ala	A	L-alanine
Arg	R	L-arginine
Asp	D	L-aspartic acid
Asn	N	L-asparagine
Cys	C	L-cysteine
Gln	Q	L-glutamine
Glu	E	L-glutamic acid
Gly	G	glycine
His	H	L-histidine
Ile	I	L-isoleucine
Leu	L	L-leucine
Lys	K	L-lysine
Met	M	L-methionine
Phe	F	L-phenylalanine
Pro	P	L-proline
Ser	S	L-serine
Thr	T	L-threonine
Trp	W	L-tryptophan
Tyr	Y	L-tyrosine
Val	V	L-valine
pTyr	pY	L-phosphotyrosine
Xxx	X	arbitrary amino acid

Curriculum vitae

Joeri Kuil werd op 28 november 1980 geboren in Amersfoort. Het VWO diploma werd in 1999 Cum Laude behaald aan s.g. De Amersfoortse Berg, waarna werd begonnen aan de studie Scheikunde aan de Universiteit Utrecht. In 2000 werd het propedeuse diploma Cum Laude behaald en werd de overstap gemaakt naar de Bachelor opleiding geneesmiddelchemie. In 2003 werd het Bachelor diploma Cum Laude behaald, terwijl in 2002 al werd begonnen met de master Drug Innovation. Tijdens de master opleiding werd een major project gedaan bij de vakgroep Medicinal Chemistry and Chemical Biology onder begeleiding van Dr. Dirk T.S. Rijkers en een minor project werd gedaan bij Altana Pharma onder begeleiding van Dr. Hans A.M. Christiaans. In 2004 werd het Master diploma Cum Laude behaald. In dat dezelfde jaar trad de auteur in dienst bij de vakgroep Medicinal Chemistry and Chemical Biology als assistent in opleiding (AIO) onder begeleiding van Dr. Nico J. de Mol en Prof. dr. Rob M.J. Liskamp. Het promotieonderzoek bestond uit het bestuderen van de ITAM – Syk tSH2 interactie en de activatie van Syk kinase d.m.v. ITAM binding. Het onderzoek had een multidisciplinair karakter bestaande uit o.a. organische – en peptide synthese, HPLC en biologische (cel) experimenten. De resultaten van het promotieonderzoek zijn ondermeer gepresenteerd op het 20th American Peptide Society Symposium (26-30 juni 2007, Montreal, Canada) en staan in dit proefschrift beschreven. Sinds mei 2009 is de auteur werkzaam als post doctoraal onderzoeker bij Het Nederlands Kanker Instituut – Antoni van Leeuwenhoek Ziekenhuis (NKI-AVL).

List of publications

- Kuil, J., Branderhorst, H.M., Pieters, R.J., de Mol, N.J., Liskamp, R.M.J., ITAM-derived phosphopeptide-containing dendrimers as multivalent ligands for Syk tandem SH2 domain, *Org. Biomol. Chem.*, **2009**, 7, 4088-4094
- Kuil, J., van Wandelen, L.T.M., de Mol, N.J., Liskamp, R.M.J., Switching between low and high affinity for the Syk tandem SH2 domain by irradiation of azobenzene containing ITAM peptidomimetics, *J. Pept. Sci.*, **2009**, 15, 685-691
- Kuil, J., van Wandelen, L.T.M., de Mol, N.J., Liskamp, R.M.J., A photoswitchable ITAM peptidomimetic: Synthesis and real time surface plasmon resonance (SPR) analysis of the effects of cis-trans isomerization on binding, *Bioorg. Med. Chem.*, **2008**, 16, 1393-1399
- Carvalho de Souza, A., Kuil, J., Maljaars, C.E.P., Halkes, K.M., Vliegenthart, J.F.G., Kamerling, J.P., Synthesis and conjugation of oligosaccharide analogues of fragments of the immunoreactive glycan part of the circulating anodic antigen of the parasite Schistosoma mansoni, *Org. Biomol. Chem.*, **2004**, 2, 2972-2987
- Kuil, J., Fischer, M.J.E., de Mol, N.J., Liskamp, R.M.J., Cell permeable ITAM constructs for the modulation of mediator release in mast cells, *manuscript in preparation*
- Kuil, J., Ruijtenbeek, R., de Mol, N.J., Liskamp, R.M.J., Allosteric regulation of Syk kinase activity induced by a conformational change of its tandem SH2 domain: Effects of rigid ITAM mimics studied by a flow-through microarray technique, *manuscript in preparation*

International symposia

- Kuil, J., van Wandelen, L.T.M., Dadvar, P., Fischer, M.J.E., de Mol, N.J., Liskamp, R.M.J., Peptidomimetic ligands for the tandem SH2 domain of the Syk protein involved in signal transduction (poster, abstract), 20th American Peptide Society Symposium, 26-30 June 2007, Montreal, Canada

Dankwoord

Nu mijn proefschrift (bijna) klaar is, mag ik nog één ding doen en dat is een dankwoord schrijven. Hoewel dit voor mij beslist niet het makkelijkste gedeelte is, is dit zeker nodig, aangezien vele mensen mij geholpen hebben. Allereerst wil ik graag mijn promotor Rob Liskamp bedanken. Rob, bedankt dat je me de kans hebt gegeven om een promotieonderzoek te doen in een groep waar zeer interessant en divers onderzoek wordt gedaan. Je hebt me veel vrijheid gegeven, maar ik kon wel altijd bij je terecht en dat was een zeer prettige combinatie. Je enthousiasme tijdens de SH2-overleggen was zeer motiverend.

Mijn co-promotor en directe begeleider, Nico de Mol, wil ik graag bedanken voor de dagelijkse begeleiding en het corrigeren van mijn manuscripten. Gedurende mijn promotie periode ging ik steeds meer biologische experimenten doen en parallel daaraan werd jouw aandeel in het onderzoek ook steeds groter. De overleggen die we hadden waren vaak leerzaam voor mij. Succes met het verdere Syk- en SH2-onderzoek. Ik hoop dat er nog vele mooie publicaties volgen!

Graag wil ik mijn voorgangers, Rob Ruijtenbeek en Frank Dekker, bedanken voor de fundamenten die jullie hebben gelegd voor dit onderzoek. Frank, zoals je ziet is het rigide ITAM mimeticum dat jij hebt gemaakt heel belangrijk geweest voor mijn onderzoek. Rob, ik wil je niet alleen bedanken voor het werk dat je hebt gedaan in je AIO periode, maar vooral ook voor de prettige samenwerking m.b.t. de PamStation experimenten.

Tijdens mijn onderzoek heb ik veel (cel) biologische technieken gebruikt die voor mij nieuw waren. Ik wil dan ook van deze gelegenheid gebruik maken de mensen die mij hierbij hebben geholpen te bedanken. Als eerste wil ik Marcel bedanken voor de introductie in de celkweek. Daarnaast wil ik ook Linda bedanken voor de prettige samenwerking.

Marjan Fretz wil ik hartelijk bedanken voor haar hulp met de FACS experimenten en de fluorescentie microscopie: zonder jouw hulp en kennis was het een stuk lastiger geweest. Verder wil ik ook de andere celkweekers van Biofarmacie bedanken voor de gezellige sfeer.

In het kader van samenwerken met andere vakgroepen wil ik Poupak Dadvar hartelijk bedanken voor het inwerken in de wondere wereld van de proteomics. Jammer dat het onderzoek niet heeft gebracht wat we er van tevoren van hadden gehoopt.

Ook wil ik graag de studenten die ik heb mogen begeleiden bedanken voor hun inzet en gezelligheid. Robert, dank voor je inzet tijdens je Bachelor stage. Loek, mede door jouw enthousiasme en inzet is het 'photoswitch project' een succes geworden. Veel succes met je eigen promotie! In het kader van het photoswitch project wil ik ook Esther Pronker bedanken voor de SPR metingen aan de rigide photoswitchable ITAM mimics. Verder wil ik Erwin Schoof bedanken voor zijn bijdrage aan de SPR metingen van de rigide ITAM mimics.

Hans Jacobs en Arwin wil ik bedanken voor de bestellingen e.d., Annemarie en Fatna voor het meten van LC-MS en Maldi spectra en Johan voor het meten van 500 MHz NMR spectra. Cees Versluis en Ronald van Ooijen, bedankt voor het meten van de hoge resolutie massa's. Ik wil Dirk bedanken voor zijn adviezen en voor de begeleiding toen ik nog student was bij Med Chem. Roland, bedankt voor de samenwerking m.b.t. het dendrimeren artikel. Natatia en Paula bedankt voor allerhande dingen die jullie hebben geregeld. Frouke, dank voor je geduld dat je had met het maken van de voorkant. Schrijfmaatjes Alex en Maarten en kamergenoot Jeroen bedankt voor het een stukje leuker maken van het schrijven. Van mijn huidige werk bij het NKI wil ik mijn collega's bedanken voor hun interesse. In het bijzonder wil ik Fijs van Leeuwen bedanken voor de ruimte die je me hebt gegeven voor het afronden van mijn proefschrift.

Uiteraard wil ik al mijn collega's bij Med Chem bedanken voor hun gezelligheid en adviezen. Met name de gezellige sfeer op het lab, de kerstdiners, de lab-uitjes en de profcoach competitie (Roda JK heeft zelfs één seizoen de Polymer Boys verslagen!) zullen me bijblijven.

In het bijzonder wil ik mijn labgenoten van Z617 bedanken. Hilbert, jij zorgde altijd voor vrolijkheid in het lab. We hebben samen veel gepraat tijdens het kolommen, extraheren, TLC-en e.d. over van alles en nog wat, waaronder ook regelmatig de chemie. Het dendrimeren hoofdstuk is hier een mooi product van.

In mijn eerst AIO-jaar was Z617 een echt koolhydraat lab met o.a. John J, Fatna en Jochem. Daar kwam later verandering in toen Ana en Tania op ons lab kwamen werken: allen bedankt voor de gezelligheid. Daarna kwamen Marjolein, Monique Mulder en Raymond, die ook voor een hele leuke sfeer zorgden. Veel succes met jullie projecten!

Dan is er nog één collega die ik in het bijzonder wil bedanken: Monique van Scherpenzeel. Doordat we beide op veel verschillende plekken werkten, spraken we niet eens zo veel met elkaar. Maar als we tijd hadden, was het altijd leuk om met je over (bio)chemie of andere dingen te praten. Leuk dat je paranimf wilt zijn!

Sander, bedankt dat je paranimf wilt zijn. Ik hoop dat het ook voor jou een leuke dag wordt. Ook wil ik Christiaan, Wilmar, Jorieke en Jochem bedanken voor jullie interesse.

Ten slotte wil ik mijn ouders bedanken voor de vrijheid en adviezen die jullie mij hebben gegeven. Mark, René, Tiny, Noël, Miriam en Arthur bedankt voor jullie interesse: ik ben benieuwd hoe ver jullie komen in het lezen van mijn proefschrift! Dit geldt natuurlijk niet voor jou, Mark: bedankt voor het nalezen van het manuscript.

Floor, bedankt dat je altijd wilde luisteren naar mijn verhalen over het werk en aanverwante zaken en bedankt dat jij de laatste maanden nooit gestrest werd van mijn ‘afrondende’ bezigheden. Op naar jouw promotie!

Joeri,
oktober 2009